Mathematical modeling, analysis of tumor-immune competitive systems and its control strategies

Thesis
submitted for the award of the Degree of

Doctor of Philosophy

in Science

by

Mrinmoy Sardar

Centre for Mathematical Biology and Ecology

Department of Mathematics

Jadavpur University

Kolkata - 700032, India

November, 2023

This thesis is dedicated to my parents
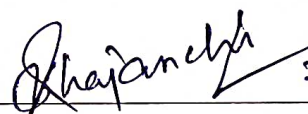*Duranta Sardar & Jaba Sardar*
and my teacher Pradyut Pal

Certificate from the supervisors

This is to certify that the thesis entitled "**Mathematical modeling, analysis of tumor-immune competitive systems and its control strategies**" submitted by Mrinmoy Sardar who got his name registered on 04th September, 2018 (Registration No. SMATH1213318, Index No. 133/18/Maths./26) for the award of Ph.D. (Science) degree of Jadavpur University, is absolutely based upon his own work under the supervision of Dr. Santosh Biswas and Dr. Subhas Khajanchi and that neither this thesis nor a part of it has been submitted for any degree/diploma or any academic award anywhere before.

21/11/2023

Dr. Santosh Biswas
Associate Professor
Department of Mathematics
Jadavpur University
188, Raja S.C. Mullick Road,
Kolkata - 700032, India

21/11/2023

Dr. Subhas Khajanchi
Assistant Professor
Department of Mathematics
Presidency University
86/1, College Street,
Kolkata - 700073, India

Dr. Santosh Biswas
Associate Professor
Department of Mathematics
Jadavpur University
Kolkata – 700 032, West Bengal

Assistant Professor
Department of Mathematics
Presidency University
Kolkata

ACKNOWLEDGEMENT

Kolkata - 700032
November, 2023

Mrinmoy Sardar
21/11/2023

Contents

vi

Chapter 1

Introduction

There were approximately 9.6 million cancer-related deaths worldwide in 2020 [8], according to the World Health Organization (WHO) report. Cancer is characterized by the uncontrolled growth and proliferation of cells, which poses a significant challenge to human health. The interaction between tumors and the immune system plays a crucial role in determining the outcome of this disease. The tumor-immune competitive system is a complex network of interactions involving tumor cells, immune cells and various signaling molecules. Understanding the dynamics of this complex system is essential for formulating effective therapeutic strategies and maximizing treatment results. Mathematical modeling provides a powerful tool for studying the tumor-immune competition, allowing researchers to gain insights into the underlying mechanisms and explore potential interventions. The preliminary focus of this thesis is to construct a mathematical model that captures the dynamics of the tumor-immune competitive system. The model will encompass crucial biological elements, such as tumor growth, infiltration of immune cells, activation of immune responses and the immune evasion mechanisms utilized by tumors. The mathematical model will be formulated using well-established principles of population dynamics, differential equations, mathematical epidemiology, etc. It will incorporate variables representing tumor cell populations, immune cell populations, cytokines, growth factors and other relevant factors. By simulating the interactions within the tumor-immune competitive system, the model will enable the investigation of important phenomena including tumor growth dynamics, immune surveillance, immune escape mechanisms and the impact of therapeutic interventions. The model will also allow for the exploration of various parameters and conditions that influence the outcomes of tumor development and immune response. The findings of this research will contribute to our understanding of the tumor-immune competitive system and provide valuable insights

into the underlying mechanisms of cancer progression and immune system interactions. Moreover, the developed mathematical model can serve as a platform for studying different treatment strategies and predicting their effectiveness. Ultimately, the results of this thesis will help in designing more personalized and targeted therapies for cancer patients. By optimizing treatment approaches based on mathematical predictions and simulations, the aim is to enhance the efficacy of immunotherapeutic interventions and improve patient outcomes. This thesis aims to develop a mathematical model of the tumor-immune competitive system to gain insights into the dynamics and interactions between tumor cells and the immune system. The model will provide a valuable tool for understanding the mechanisms of cancer progression, evaluating treatment strategies and guiding the development of novel therapeutic interventions.

1.1   Tumor cells

Cancer has become the leading cause of death worldwide in the 21st century. It is characterized by the uncontrolled growth of abnormal cells, leading to the rapid proliferation of new cells. There are three distinct types of tumor cells: benign tumors, premalignant tumors and malignant tumors. Benign tumors are non cancerous and do no harm to the body. They do not spread to other tissues or organs and are generally considered harmless. Premalignant tumors, although not initially cancerous, have the potential to develop into cancer over time. Some premalignant tumors progress and transform into malignant tumors, which can spread to neighboring cells, glands and other parts of the body. Cancer encompasses a variety of specific types that affect different organs and tissues. Examples include glioma cancer, which originates in the brain; leukemia cancer, which affects the blood-forming tissue in the bone marrow; lymphoma, involving T-lymphocytes or B cells; multiple myeloma cancer, impacting plasma cells; melanoma, a type of skin cancer; pancreatic cancer, occurring in the stomach and colorectal cancer, affecting the rectum. The impact of cancer on global mortality rates underscores the need for extensive research, prevention efforts, early detection methods and effective treatments. Advancements of these areas are crucial for improving patient outcomes, raising awareness and addressing the significant challenges posed by cancer worldwide.

1.2 Immune system

The immune system is a complex network, comprising various cells and cytokines, which play a crucial role in defending our body against foreign invaders, including tumor cells. The key components of the immune system are B cells, T cells (CD8+T cells or CD4+T cells), natural killer (NK) cells, macrophages and different types of cytokines. These components collaborate to establish a defense against harmful pathogens. Immune-effector cells such as cytotoxic T-lymphocytes (CD8+T cells), macrophages and natural killer cells are instrumental in combating threats [61]. They possess the ability to directly eliminate targeted cells, including tumor cells. On the other hand, dendritic cells act as antigen-presenting cells and they are messengers between the adaptive and innate immune systems. Dendritic cells play a vital role in activating immuno-stimulatory cytokines and CD8+T cells, which are essential for reducing tumor cells and enhancing an effective immune response against them. By orchestrating the activation and interaction of these immune components, dendritic cells contribute to the recognition and elimination of tumor cells.

The immune system and cytokines both have a vital role in maintaining a robust defense, safeguarding us not only from tumor cells but also from various other potential harms to our body. The tumor-immune interaction system heavily relies on cytokines, which play a pivotal role in the process. Regulatory T-cells (Tregs) serve as immuno-suppressive agents by inhibiting the activation of CD8+T cells [97]. On the other hand, macrophages are affected by various cytokines in the system. Interleukin-10 (IL-10), an anti-inflammatory cytokine, downregulates Type 1 T-helper cell cytokines (Th1 cytokines) and co-stimulatory molecules on macrophages [67]. Transforming growth factor-beta (TGF-β) is produced by all white blood cells and inhibits the activation of macrophages [4]. IL-12 is a pro-inflammatory cytokine generated by antigen-presenting cells, such as dendritic cells and macrophages [66]. IL-12 plays a vital role in activating effector cells to effectively eliminate tumor cells. Interferon-gamma (IFN-γ) is another important cytokine produced by natural killer cells and CD8+T cells [63]. IFN-γ not only promotes the proliferation of macrophages but also enhances their ability to destroy tumor cells. Overall, cytokines significantly impact the tumor-immune interaction system by modulating immune responses, regulating immune cell activity and influencing the balance between immune activation and suppression.

The immune system starts its response when it detects the presence of

3

cancer cells. Although the immune system can identify cancer cells in many cases, the response may not be robust enough to eliminate the tumor cells. In such cases, patients are administered various therapeutic interventions, including radiation therapy, chemotherapy, hormone therapy, immunotherapy, etc. These treatments aim to enhance the immune system's ability to eradicate the cancer cells, providing patients with additional support in their fight against the disease.

1.3 Some basic mathematical definitions and theorems

In this section, we will explore fundamental mathematical concepts and tools utilized to analyze the behavior of dynamical system. These mathematical definitions and theorems will be applied to investigate the various models proposed in this thesis.

1.3.1 Nonlinear system

A dynamical system focuses on the evolution of variables or states over time. It involves determining what will change over time and establishing the rules governing this evolution. Essentially, a dynamical system serves as a model that describes how a system evolves over time. To study a dynamical system, it is crucial to employ a differential equation, which captures the continuous dynamics of a nonlinear system. By utilizing a differential equation, we can mathematically express the relationship between the variables and their rates of change, enabling us to analyze the system's behavior and understand its evolution. A nonlinear dynamical system is of the form

$$\frac{dx(t)}{dt} \;=\; g(x(t)), \tag{1.1}$$

where g is a nonlinear vector valued function and each element operates the corresponding state vector

$$x(t) = [x_1, x_2, ..., x_m]^T. \tag{1.2}$$

In a dynamical system, the elements of the state vector x_i $(i = 1, 2, ..., m)$; exhibit changes over time, which are essential for the presence of dynamics within the system. To construct a mathematical model for a dynamical system, various types of differential equations can be employed, including ordinary differential equations (ODEs), delay differential equations (DDEs), and stochastic differential equations (SDEs), etc.

1.3.2 Positivity

The positivity of the solution in the system (1.1) guarantees that for non-negative initial conditions, the variables will remain nonnegative for all finite time t, providing confidence in the validity and meaningfulness of the model's predictions. A set $M \subset \mathbb{R}^n$ is said to be positive invariant set if

$$M = \{x \in \mathbb{R}^n : \psi(x) = 0\}, \tag{1.3}$$

where $x(0) = x_0 \in M$ implies $x(t, x_0) \in M$ for all $t \geq 0$ and ψ is a real-valued function.

1.3.3 Existence and uniqueness theorem

Theorem 1.3.1. *Let us assume that $g \in C^1(E)$, where E be an open subset of $\mathbb{R}^n$ containing a point x_0, then there exists a real number $k > 0$ such that the dynamical system (1.1) with initial condition $x(0) = x_0$ has a unique solution in the interval $[-k,\ k]$.*

1.3.4 Boundedness and uniform persistent

Biologically, boundedness of the system means that the population cannot be grow infinitely or unboundedly. On the other hand, to investigate the long-term behavior of the system, we need to study the uniform persistence.

Definition 1.3.1. *The nonlinear dynamical system (1.1) is said to be a bounded if there exists a positive k such that $\limsup\limits_{t \to \infty} x(t) \leq k$, where $x(t)$ is a solution of the system (1.1).*

Definition 1.3.2. *The nonlinear dynamical system (1.1) is said to be a uniform persistent if $\liminf\limits_{t \to \infty} x(t) > 0$, where $x(t)$ is a solution of the system (1.1).*

1.3.5 Equilibrium point

An equilibrium point in a dynamical system refers to a solution that remains unchanged over time and is derived from a differential equation. Equilibrium point is also known as singular point, fixed point, stationary point, etc.

Definition 1.3.3. *A point x_1 is said to be equilibrium point of the given system (1.1) if $\frac{dx_1}{dt} = g(x_1) = 0$.*

1.3.6   Local stability

The following section presents an overview of stability analysis. This is an important topic in various branches of applied mathematics.

Definition 1.3.4. *A fixed point x_1 of the system (1.1) is said to be locally stable, if for each $\epsilon > 0$ there exists a positive δ such that every solution $x(t)$ of the system (1.1) with initial condition $x(0) = x_0$, $||x_0 - x_1|| \leq \delta$ $\Rightarrow ||x(t) - x_1|| < \epsilon \; \forall \, t \geq 0$, where $||.||$ is the Euclidean norm.*

Definition 1.3.5. *A fixed point x_1 of the system (1.1) is said to be locally asymptotically stable, if x_1 is locally stable and there exists a positive μ such that $||x_0 - x_1|| < \mu \Rightarrow \lim\limits_{t \to \infty} ||x(t) - x_1|| = 0.$*

Definition 1.3.6. *A fixed point x_1 of the system (1.1) is said to be unstable if it is not stable.*

1.3.7   Routh-Hurwitz criteria

Let us assume that M be a square matrix and I_n be the identity matrix of order n and $m_i \in \mathbb{R}$ for $i = 1, 2, 3, ...n$, $m_n \neq 0$, then the characteristic polynomial of the matrix M is given by

$$M(\lambda) = det(M - \lambda I_n) = \lambda^n + m_1 \lambda^{n-1} + m_2 \lambda^{n-2} + ... + m_n \lambda + m_n. \quad (1.4)$$

The eigenvalues of the matrix M is negative or have negative real parts if and only if

$$M_k = \begin{vmatrix} m_1 & m_3 & m_5 & ..... & 0 \\ 1 & m_2 & m_4 & ..... & 0 \\ 0 & m_1 & m_3 & ..... & 0 \\ . & . & . & ..... & . \\ . & . & . & ..... & . \\ 0 & 0 & 0 & ..... & m_k \end{vmatrix} > 0, \quad \text{for k = 1, 2, 3,.....n.}$$

Followings are the Routh-Hurwitz criteria for $n = 2, \; 3$ and 4.

    For $n = 2 \;\; : \;\; m_1 > 0, \; m_2 > 0.$

    For $n = 3 \;\; : \;\; m_1 > 0, \; m_3 > 0, \; m_1 m_2 - m_3 > 0.$

    For $n = 4 \;\; : \;\; m_1 > 0, \; m_3 > 0, \; m_4 > 0, \; (m_1 m_2 - m_3)m_3 - m_1^2 m_4 > 0.$

1.3.8   Bifurcation theory

In mathematics, bifurcation theory studies how the behavior of a system changes as certain value of parameters are varied. It examines the points at which a system transitions from one state to another or exhibits different types of behavior. Bifurcation theory often involves the analysis of nonlinear system, such as differential equations and describes how small changes in parameters can lead to significant qualitative changes in the behavior of system.

- **Transcritical bifurcation**

  Transcritical bifurcation is a specific type of bifurcation that occurs in dynamical systems when a parameter reaches a critical value. It involves the exchange of stability between two fixed points or equilibrium points. The term "transcritical" indicates that the equilibrium points pass through each other and change their stability characteristics. During a transcritical bifurcation, the behavior of the system changes qualitatively. As the control parameter varies, the stability of these equilibrium points changes.

Let us assume that

$$\frac{dx}{dt} = g(x, \mu) \tag{1.5}$$

be a system of ordinary differential equation, where $x \in \mathbb{R}^n$, $\mu \in \mathbb{R}$ and the above system (1.5) has an equilibrium point x_0.

Theorem 1.3.2. *(Sotomayor's theorem). Suppose that $g(x_0, \mu_0) = 0$ and that the $m \times n$ order matrix $\Lambda \equiv g(x_0, \mu_0)$ has a simple eigenvalue $\lambda = 0$ with eigenvector v and that Λ^T has an eigenvector w corresponding to the eigenvalue $\lambda = 0$. If the following conditions are satisfied:*

$$w^T \Lambda(x_0; \mu_0) = 0; \qquad w^T [D\Lambda(x_0; \mu_0)v] \neq 0; \qquad w^T [D^2\Lambda(x_0; \mu_0)(v, v)] \neq 0,$$

then the system experiences a transcritical bifurcation at the steady state x_0 as the parameter passes through the bifurcation value $\mu = \mu_0$.

- **Hopf bifurcation**

  Hopf bifurcation is named after the mathematician Eberhard Hopf, who made significant contributions to the field of dynamical system

theory. Hopf bifurcation is mainly associated with the system of ordinary differential equations. Hopf bifurcation is a type of bifurcation that occurs in dynamical systems when a parameter reaches a critical value, then arises a stable limit cycle. It occurs when a stable equilibrium point loses stability as the control parameter varies and a limit cycle arises.

Theorem 1.3.3. *Let*

$$\frac{dx}{dt} = g(x, \ \tau) \tag{1.6}$$

be a system of continuous differentiable equation in $\mathbb{R}^n$ and $\tau \in \mathbb{R}$ be a parameter. The Jacobian matrix derived at equilibrium point E has one pair of complex conjugate eigenvalues

$$\lambda = a(\tau) \pm ib(\tau), (where a, \ b \in \mathbb{R})$$

such that for some critical value $\tau = \tau_1$, it becomes purely imaginary, that is, $[Re(\lambda)]_{\tau=\tau_1} = 0$.

Then, the eigenvalues cross the imaginary axis if transversality condition holds, that is,

$$\left[\frac{dRe(\lambda)}{d\tau}\right]_{\tau=\tau_1} \neq 0.$$

Then, the given system (1.6) experiences a Hopf bifurcation at the critical vale $\tau = \tau_1$ around the equilibrium point E. The parameter τ is called bifurcation parameter and τ_1 is called bifurcation point.

1.4   Optimal control theory

Optimal control theory, a significant field in mathematics, focuses on optimizing an objective function within a specified time interval of a dynamical system to determine an optimal control. This theory finds diverse applications in physics, engineering, science, operations research and more. Suppose an ordinary differential equation is of the following form

$$\begin{aligned}
\frac{dz(t)}{dt} &= g(z(t)), \quad (t > 0) \\
z(0) &= z_0.
\end{aligned} \tag{1.7}$$

Here, g is defined as $g : \mathbb{R}^n \to \mathbb{R}^n$ and $z_0 \in \mathbb{R}^n$ is given as initial condition. The unknown curve $z : [0, \infty) \to \mathbb{R}^n$ demonstrates the dynamical evolution of the state of a mathematical system.

Let us assume that the function g is dependent on some control parameters $U = (u_1, u_2, u_3, ...u_k)$ which belongs to the set $U \subset \mathbb{R}^k$, such that $g : \mathbb{R}^n \times U \to \mathbb{R}^n$. We choose some $u \in U$ and consider the corresponding dynamical system as

$$\frac{dz(t)}{dt} = g(z(t), u(t)), \qquad (1.8)$$

$$z(0) = z_0.$$

We can find out the evolution of our system by choosing the suitable value of u. Now, we consider a function $v : [0, \infty) \to U$ is following as

$$v(t) = \begin{cases} u_1 & , & 0 \leq t \leq t_1 \\ u_2 & , & t_1 \leq t \leq t_2 \\ u_3 & , & t_2 \leq t \leq t_3 \end{cases}$$

and so on.

For time windows $0 < t_1 < t_2 < .....$ and the values of control parameters $u_1, u_2, u_3, ... \in U$, we can solve the following dynamical system (1.8). The trajectory $z(.)$ is the response of the above system (1.8) corresponding to each control parameters $u(t)$. Let us define $\mathbb{L}$ as the collection of all admissible controls; then $\mathbb{L}$ is defined as follows:

$$\mathbb{L} = \{v : [0, \infty) \to U | \; v(.) \text{ is Lebesgue measurable function}\}.$$

We observe that the solution $z(.)$ of the system (1.8) depends on $v(.)$ and the given initial condition. Then, we can write that $z(.) = z(., v(.), z_0)$. For the admissible control set $\mathbb{L}$, we define an objective function J such that

$$J(v(.)) = \int_0^{t_f} [\lambda(z(t), v(t))]dt + f(z(t)), \qquad (1.9)$$

where $z(.)$ is the solution of the system (1.8) for the control $v(.)$. Here, $\lambda : \mathbb{R}^n \times U \to \mathbb{R}$ and $f : \mathbb{R}^n \to \mathbb{R}$ are called as a running objective and terminal objective functions, respectively. The finishing time is denoted as $t_f > 0$. We want to find a control $v^*(.)$, which minimizes or maximizes the objective function $J(v(.))$, resulting in $J(v^*(.)) \leq$ or $\geq J(v(.))$ for all controls $v(.) \in \mathbb{L}$. The control $v^*(.)$ is called an optimal control.

9

1.5 Literature review

In the past few decades, cancer has emerged as the leading cause of death worldwide. The interplay between our immune system and malignant tumor cells can be likened to a predator-prey relationship. To comprehend the dynamics of this interaction, various approaches have been employed in cancer research. Mathematical models offer a unique perspective, enabling us to gain insights into diverse dynamics associated with cancer. Numerous researchers have utilized mathematical models for both analytical and numerical analysis, deriving valuable findings from their investigations. These models encompass a wide range of assumptions and generate diverse results, ultimately enhancing our understanding of the underlying dynamical systems. Mathematical modeling has became an essential approach in the study of the relationship between tumor cells and the immune system. It plays a crucial role in the pursuit of new knowledge and potential treatments for cancer.

Over the past few years, a significant volume of research articles has emerged, focusing on comprehending the complex dynamics of the tumor-immune competitive system. From the perspective of mathematical biology, the theoretical exploration of the interaction between tumors and the immune system has a rich and extensive background. Many mathematical models for the growth of tumor cells are delineated in the review article by Eftimie et al [25]. The concept of mathematical modeling for tumor-immune interplay was initiated by Thomlinson & Gray [98] in the year 1955. The details of the mathematical models developed by numerous researchers for comprehending the interactive dynamics of tumor-immune competitive system can be found in the references [1, 4, 5, 12, 18, 24, 51, 56–58, 61, 63, 65–68, 80, 96, 108]. A good result of the tumor-immune interaction system was written in a book by Adam & Bellomo [1]. Kuznestov et al. [65] presented a mathematical model by taking the effector cell, which interacts of an immunogenic tumor. Their system was explored as immune stimulation of tumor growth, "sneaking through" mechanisms of the tumor and progression of tumor "dormant state". Kirschner & Panetta [61] first introduced adoptive cellular immunotherapy (cytokine IL-2) into their mathematical model to study the dynamics of the tumor-immune interaction system. Their mathematical model explored both short-term cancer oscillations in cancer sizes and long-run cancer relapse. Also, they described under what circumstances tumor cells can be destroyed in the presence of cytokine IL-2. Diefenbach et al. [22] proposed that ectopic expression of murine NKG2D ligands in some cancer cell lines followed the rejection of cancers by syngeneic mice

and that this rejection was moderated by both natural killer cells (NK cells) and cytotoxic T-lymphocytes. Based on the results of their experimental work, de Pillis et al. [16] introduced a mathematical model that focused on the interplays of the cytotoxic T-lymphocytes or CD8+T cells and natural killer cells with various types of tumor cells utilizing a system of coupled nonlinear ordinary differential equations. Moore et al. [70] proposed and analyzed a blood cancer, that is, chronic myelogenous leukaemia (CML) based mathematical model of interaction among naive T cells, effector cells and CML cancer cells using a system of nonlinear ordinary differential equations. The primary objective of this research was to identify the key parameters that contribute significantly to the regression of tumor cells in their proposed model. Dunn et al. [24] explored into the concept of cancer immunoediting and its evolutionary dynamics. The authors discussed three main stages of this process, namely equilibrium, escape and elimination, which are also known as cancer immunosurveillance. The study provided insights into how the immune system and cancer cells interact and evolve over time, shedding light on the mechanisms behind tumor growth, evasion and potential elimination by the immune response. de Pillis et al. [17] presented a tumor-immune interaction system of differential equations focusing on the role of effector cells (CD8+T cells and natural killer cells) to understand the dynamics of immune-mediated tumor rejection. Banerjee et al. [4] considered a set of nonlinear ordinary differential equations representing the dynamics of brain tumors (specifically glioma cells) and the immune system incorporating the immunotherapeutic drug T11 target structure. This research article aimed to devise a potent therapy for brain tumors by focusing on the design of an efficient treatment strategy. Mahasa et al. [68] formulated a deterministic model for the tumor growth mediated by NK cells and activated by CD8+T cells through a system of ordinary differential equations. Their model includes multiple tumor cell population and the tumor cells escape from immune surveillance according to this model.

In most cases, our immune system can not kill the tumor cell instantaneously, it depends on the its past history. Time lags play an important role in the dynamics of the tumor-immune interaction system. The delayed responses cannot be neglected for the interaction between tumor-immune system and most often the discrete time delays should be considered to describe the time necessary for the development of molecules, cell productions, cell differentiations and transport and so on [34, 35, 43–45, 52, 53, 55, 103]. The delays can be categorized into two types: discrete time delay and continuously distributed time delay. Numerous research papers have been published on the dynamics of tumor-immune

11

interactions, focusing specifically on discrete time delay. Baker et al. [2] explored the importance of discrete time lag and compared their model with related models. Also, the authors calculated the parameter values by using the least square method. Banerjee et al. [3] introduced a time lag τ in a kinetics of tumor-immune interaction system which was proposed by Kirschner et al. [61]. Galach [34] studied a cancer-immune interplays system mainly established by Kuznestov et al. [65] with considering the discrete time lag. A discrete delay induced in three nonlinear coupled ordinary differential equations taking tumor cells, resting immune cells and hunting immune cells was presented by Sarkar & Banerjee [91]. In this work, authors revealed that the proliferation of tumor cells can be influenced by manipulating the activation rate of immune cells and the deactivation rate of tumor cells, both of which have a threshold value that plays a crucial role. Khajanchi & Banerjee [43] studied the immune activation discrete time lag τ into the dynamics of tumor-immune competitive system, which was proposed by Kuznetsov et al. [65]. To understand the complexity of tumor-immune interactive dynamics, authors derived a single parameter bifurcation diagram as well as a two-parameter bifurcation diagram. A three nonlinear coupled differential equations of tumor cells, effector cells and host cells was described by Khajanchi et al. [49]. In this manuscript, authors studied how tumor cells developed and survived against our immune system. Mainly, they focused on the existence of Hopf bifurcation, whereby the time lag parameter is used as a bifurcation parameter. A tumor growth mathematical model incorporating the immune system interplays and phase-specific therapeutics was investigated by Villasana et al. [103]. Kronik et al. [63] described a simple mathematical model of tumor cells, cytotoxic T-lymphocytes (CD8+T cells), major histocompatibility complex (MHC) class I and MHC class II molecules and cytokines TGF-β and IFN-γ. The mathematical model effectively reproduced the outcomes of clinical trials demonstrating the efficacy of immunotherapy in treating recurrent anaplastic oligodendroglioma and anaplastic astrocytoma, both classified as WHO grade III tumors. Piotrowska et al. [77] modified this research article by introducing three discrete time delays. They showed that in case of fast growing of tumor cells, the intrinsic growth rate of the tumor cell is most important parameter in their mathematical model. Khajanchi & Banerjee [50] introduced four discrete time lags into their tumor-immune interaction system. Main work of this paper is how the multiple delays effected to their mathematical model in presence of immunotherapeutic drug T11 target structure. Ghosh et al. [35] described a mathematical model of interaction between host cells, effector cells and tumor cells with presence of two different delays. Authors find out the parameters value for producing a chaotic attrac-

tor with a system of without delay utilizing the technique of global attractor.

However, the number of research papers focusing on the tumor-immune interaction system incorporating continuously distributed time delay is limited. Caravagna et al. [10] studied a hybrid tumor-immune interaction system by incorporating distributed delays. By utilizing simulations and parametric sensitivity analysis, the authors measured the strength of the immune surveillance in terms of probability distribution of the eradication times. Yu et al. [110] introduced a distributed delay to study the interaction between tumor cells and immune system. The article provides evidence that the presence of distributed delay plays a significant role in regulating tumor proliferation. Piotrowska et al. [78] considered continuously distributed time delay in a generalization of tumor-immune interaction model and numerically solved the system with Erlang probability densities by applying the classic linear chain trick [64]. Yu et al. [111] proposed a special form of distributed delay with kernel to study the tumor-immune interaction system. Authors combine two different types of delay kernels, namely a monotonic delay kernel demonstrating a fading memory and a non-monotonic delay kernel representing a peaking memory. The non-monotonic delay kernel changes the stability of the interior steady state. Impact of continuously distributed delay into a system of tumor-immune interactive dynamics was investigated by Sardar et al. [88]. In this paper, authors reveal that the activation rate of CD8+T cells can prevent the oscillation of tumor-presence equilibria as well as tumor-free equilibria of the system.

Despite development of medical treatments, there are so many challenges remain against the treatment of cancer. Chemotherapy, hormone therapy, radiation therapy and surgery are the most effective treatments for cancer patients [7]. Appropriate treatment methods are utilized to identify the nature, location and stage of the cancer. Immunotherapy is employed to stimulate the immune system and impede the proliferation of cancer cell populations, thereby enhancing immune responses and suppressing cancer growth. This type of treatment is effective for enhancing the immune response and obstructing the growth of cancer cell population [44]. Chemotherapy has many harmful side effects, which can results the patient becoming induced to infection as well as it reduces the immune system's power to fight against cancer cell. Therefore, an optimal control problem has an important role in tumor-immune competitive system for the minimizing the total drug [19]. Swan [93] studied a mathematical model for tumor-immune interplays with cancer immunotherapy by applying optimal control problem. In this study, the author applied both experimental and

13

clinical outcomes for tumor cell population. Burden et al. [7] investigated a tumor-immune interactive dynamics among tumor cells, effector cells and cytokine interleukin-2 (IL-2), which was described by Kirschner and Panetta [61]. Authors implemented the optimal control theory in their paper to know under what circumstances tumor cells can be eradicated. Engelhart et al. [26] investigated four different mathematical models of chemotherapy with respect to optimal control of drug treatment schedules. They solved optimal control problem numerically with Bock's direct multiple shooting method. de Pillis et al. [19] explained a dynamics of tumor-immune interaction system captured by tumor cells, effector-immune cells, circulating lymphocyte cells and chemotherapy drug concentration. Authors established the existence of optimal control and solved for both linear and quadratic controls. An interesting fact of this paper is that the graphical region on which the singular control is optimal. In [28], authors applied optimal control strategy to develop optimal control technique for chemotherapeutic drug. They applied chemotherapy to study the qualitative behavior of three different cell-kill models. In each of the cases, authors minimized the drug amount and tumor cell burden. Fister & Donnelly [29] implemented an optimal control theory in a tumor-immune interaction system to eliminate the tumor cells. To minimize the tumor cells and maximize the immune cells, authors introduced the two types of objective functionals, the first having one control and second having two controls. In each of the cases, bang-bang optimal control exists. Also, the numerical results of this paper proved that the cancer cells have a cyclic nature at the maximum level of drug therapy. Khajanchi & Ghosh [44] introduced an optimal control strategy in nonlinear dynamics of tumor-immune interaction system which was described by Kuznestov et al. [65]. Authors implemented two types of external treatment strategies: adoptive cellular immunotherapy (ACI) and interleukin-2 (IL-2). An interaction of brain tumor (glioma) and immune cells has been described with immune-therapeutic drug T11 target structure (T11TS) in the research article [52]. In this work, authors introduced an optimal control strategy in their mathematical model to minimize the glioma burden and to maximized the immune cells (CD8+T cells and macrophages).

Based on the above discussions, it becomes evident that while several studies have explored the tumor-immune interaction system, certain aspects remain unexplored. Specifically, the influence of delay and optimal control theory in tumor-immune interaction models has yet to be thoroughly examined. The gaps in knowledge from previous studies present an opportunity for new ideas and advancements in research on tumor-immune competitive system. Therefore, the primary objective of this thesis is to investigate discrete

delay, continuously distributed delay and optimal control theory involving ordinary differential equations in order to contribute to the development of this field.

1.6 Outline of the thesis

The aim of the present thesis is to study the dynamics of tumor-immune interplays with different factors/mechanisms responsible for complex behavior in multi-species mathematical models. This is an attempt to analyze models with discrete time delays, distributed time delay, environmental fluctuations, and the theory of optimal control. An effort has been made to stabilize the complex behavior in the models. Numerical illustrations are carried out to explore the possibility of rich dynamics in the nonlinear models. The thesis is organized in the following way:

- In the present chapter, we give a brief introduction to the dynamics of tumor-immune interactions. The important concepts are overviewed here. Brief discussion on tools/techniques used in this thesis is also included. A brief literature review related work in this area has also been presented.

- **In chapter 2,** we propose and analyze a conceptual mathematical model that captures the dynamics of tumor-immune interactions, considering the effect of discrete time delay. The model consists of three coupled nonlinear ordinary differential equations (ODEs), representing tumor cells, effector cells and the cytokine Interleukin-2 (IL-2). Although the model is simple, it exhibits complex dynamical behaviors. We explore the qualitative properties of the mathematical model including the existence and positivity of solutions. We identify a tumor-free singular point and interior steady states in the model. Additionally, we conduct local stability analysis for both delayed system and non delayed system, focusing on biologically feasible steady states. To further investigate the system dynamics, we analyze Hopf bifurcation by considering the time delay parameter τ as a bifurcation parameter and employing the transversality condition. We have estimated the length of time delay parameter applying Laplace transformation for preserving the stability of period-1 limit cycle that provides the idea about the mode of action in controlling oscillations in the growth of tumor cells. We performed numerical simulations and

explored their biological implications to validate our theoretical analysis. We have also drawn bifurcation diagram of delayed model with reference to the intrinsic growth rate α of tumor cell, deactivation rate d_1 of tumor cell, activation rate c_2 of effector cell and death rate d_2 of effector cell. Theoretical and numerical analysis show that in presence of IL-2, the effector cells can cause the tumor cell population to regress.

- **In chapter 3,** we have examined the impact of continuously distributed delay on the intricate interaction between tumor cells, tumor-specific CD8+T cells, Helper T cells and the immuno-stimulatory cytokine interleukin-2 (IL-2). This interaction is described by a system of coupled nonlinear ordinary differential equations. Firstly, we conduct an analysis of the qualitative properties of the model including the positivity of solutions and the existence of biologically feasible equilibrium points. Next, we explore and analyze the local asymptotic stability of both the delayed system and non delayed system in depth. Our model system experiences Hopf bifurcation with respect to the activation rate λ_1 of tumor-specific CD8+T cells. The effect of continuously distributed delay involved in immune-activation on the system dynamics of the tumor is demonstrated. Our study reveals that the activation rate of CD8+T cells can prevent the oscillation of tumor-presence equilibria as well as tumor-free equilibria of the system. Then, we performed some numerical results and interpret their biological implications to validate our analytical findings.

- **In chapter 4,** We put forward a mathematical model to explore the progression of tumor cells and the influence of multiple discrete delays. The suggested model comprises nine nonlinear coupled ordinary differential equations (ODEs) representing various components, including tumor cells, tumor-specific CD8+T cells, dendritic cells, macrophages, regulatory T-cells (Tregs), interleukin-10 (IL-10), interleukin-12 (IL-12), transforming growth factor-β (TGF-β) and interferon-γ (IFN-γ). Employing the quasi-steady-state approximation, we formulate a system of four nonlinear coupled ordinary differential equations (ODEs). This system captures the intricate interplay between tumor cells, CD8+T cells, macrophages and dendritic cells. Additionally, we incorporate three distinct discrete time delays into our deterministic system. We thoroughly explore fundamental characteristics of the

system, encompassing aspects such as existence, uniqueness, positivity, boundedness and uniform persistence. The fixed points of the system are also evaluated. The stability analysis of both the delayed system and non delayed system has been performed and conditions for stability and direction of Hopf bifurcation have been determined. Furthermore, we assess the length of the time delay required to maintain the stability of the period-1 limit cycle. Furthermore, the techniques of parameter estimation are discussed and numerical simulations are provided to substantiate and support our theoretical analysis. Notably, for the existing set of parameter values, we observe that time delays have no significant influence on the system behavior.

- **In chapter 5,** we explore a mathematical model that outlines the nonlinear dynamics of the interplay between tumors and the immune system, incorporating the effects of immunotherapy and chemotherapy. The proposed model explored a system of coupled nine nonlinear ordinary differential equations, which involves tumor cell, cytotoxic T-lymphocytes (CD8+T cells), macrophages, dendritic cells, regulatory T-cells (Tregs), IL-10, TGF-β, IL-12, IFN-γ and the concentration of chemotherapeutic drug. We employ the optimal control theory to understand the dynamics of under what conditions the tumor cells can be eradicated by the immune system. We solved the control problem with an objective functional that minimizing the tumor cell population while simultaneously maximizing the immune components. The existence property of optimal control theory is established by boundedness of solutions for each state variables. We characterized our optimal control theory in which the state variables are coupled with costates. Also, our study investigates the uniqueness property of optimal control problem in a small time window. Finally, we demonstrate numerically that the optimal control strategy minimizes the tumor cells burden and maximizes the immune cells under different scenarios. Also, our study investigates the uniqueness property of optimal control problem in a small time window. Finally, we demonstrate numerically that the optimal control strategy minimizes the tumor cells burden and maximizes the immune cells under the different scenarios. Moreover, the corresponding biological implications are given.

- **In chapter 6,** we included conclusion with the overall concluding ob-

servations of this study along with a brief discussion on the scope for
future research work.

Chapter 2

Exploring the dynamics of a tumor-immune interplay with time delay †

2.1 Introduction

Cancer is a worldwide problem in all populations, irrespective of wealth or social status. The worldwide response to cancer has been intermittent and inequitable. Due to the report by World Health Organization (WHO), cancer is the second major cause of death throughout the world, accounting nearly 9.8 millions of deaths or one among six deaths, in the year 2018 [106]. The most general types of tumor in men are prostate, stomach, lung, colorectal and liver, while in women are thyroid, cervical, breast, lung and colorectal, etc. Cancer primarily occurred by uncontrolled proliferation of normal tissues which spread nearby organs of our body and invade to other parts. Mainly, there are three different types of tumors, namely benign, premalignant and malignant. Benign tumors are not cancerous. Most of the benign tumors are not dangerous and they are unlikely to influence other organs of our body. Premalignant tumors are not cancerous yet, but they have the capability to become malignant ones. These types of cells proliferate and extent to other parts of our body. But some of the benign tumors can become premalignant and then malignant one. It is not surprising the researchers are working with cancers and trying to control the cancers to ameliorate the patient's daily life. Cancer is a heterogeneous groups of neoplasms and it has unpredictable growth.

Immune system is the natural defence mechanism in our body, aids in fighting against cancer cell. Nowadays, a very important things in cancer biology is to how the body's immune system responds cancer progression [18]. Despite medical improvements, some challenges stay in the prognosis and treatment of this disease from last 10-15 years. Different types of cytokines, lymphoid tissues and cells have made our immune system that save our body from different types of pathogens or foreign antigens including cancer cells. Several kinds of immune cells like T-lymphocytes, B-lymphocytes, natural killer cells, macrophages are considered as immune effector cells [61]. Our immune system begins when the cancer cells are identified by the body's immune system. In most of the cases, cancer cells are recognized by immune system, but responds of immune system may not be strong and can not destroy tumor cells. Proliferation of effector cells are activated due to the presence of cancer cells. Mainly, cancer cells and effector cells are play as pre, predator role in our body. CD4+T cells produce the main cytokine interleukin-2 (IL-2) which stimulates the growth of immune cells to destroy or eliminate more cancerous cells [3, 61].

In the real world, the dynamic behavior of the system does not occur instantly; instead, it is depended by the system's past history. Hence, it is crucial to integrate time delays into the model formulation to reflect real-world situations. As we comprehend, the immune response to tumor proliferation is highly intricate and frequently subject to delays. Therefore, it becomes imperative to include the influence of time delay in our mathematical model for an accurate portrayal of the dynamics of system. In the present chapter, we have studied a three dimensional model of cancer cells, immune effector cells and immuno-stimulatory cytokine IL-2. Due to the clinical observations of [15, 36, 41], we can say that there is a stimulation of immune effector cells by the immuno-stimulatory cytokine IL-2 and there is a time delay among the recruitment of IL-2 by cytotoxic T-lymphocytes and the immune cell proliferation due to IL-2 [3]. Thus, we have incorporated a discrete time lag τ in our mathematical model. In this chapter, we have explored the complicated dynamics of tumor-immune interplays arising through Hopf bifurcation by altering time lag τ and other system parameters.

The remaining part of this chapter is arranged as follows. In the Section 2.2, we propose a mathematical model for the cancer-immune interplays with time lag and its dimensionalization. Section 2.3 investigates qualitative behavior of system (2.2) includes the existence and positivity of the solutions. Also, we have investigated the biologically relevant steady states and their local stability analysis both in presence of time lag and in exclusion

of time lag τ. Section 2.4 is devoted to the bifurcation analysis. Herein we provide the conditions for the existence of Hopf bifurcation. The Section 2.5 described the estimation of the length of time lag to maintain stability of the Hopf bifurcating limit cycle. Then, we carry out numerical simulations with different system parameters including time lag τ for different set of parameters in the Section 2.6. Numerical results fully demonstrate the complexity of the dynamic behavior, which includes Hopf bifurcation and appearance of limit cycles. These can be applied to illustrate some clinical phenomena and the corresponding biological implications are explained. This chapter concludes with a brief summary and conclusion in the Section 2.7.

2.2 The model

In the last few years, cancer-immune interaction mathematical models have been developed in different types. For small sizes tumor cells, growth is exponential but it slows for large sizes population. In many cases for non-exponential growth, logistic or Gompertz equation is used for tumor cell. Effector cells are the vital parts of the immune system that deactivate the tumor cells. Our immune system can not destroy the tumor cells instantaneously, so there is a time lag between the recruitment of IL-2 due to cytotoxic T-lymphocytes and the immune cell activation in presence of IL-2. In this section, we have studied a three dimensional tumor-immune interaction model through a coupled system of nonlinear ordinary differential equations. The model delineates the densities of cancer cells, effector cells such as CD8+T cells, macrophages or natural killer cells and immuno-stimulatory cytokine interleukin-2 (IL-2) are follows:

$$
\begin{aligned}
\frac{dT}{d\bar{t}} &= \alpha T(\bar{t})(1 - \beta T(\bar{t})) - \delta_1 T(\bar{t})E(\bar{t}), \\
\frac{dE}{d\bar{t}} &= s_2 + k_2 E(\bar{t} - \tau)I(\bar{t} - \tau) - \delta_2 E(\bar{t}), \\
\frac{dI}{d\bar{t}} &= s_3 + k_3 T(\bar{t})E(\bar{t}) - \delta_3 I(\bar{t}),
\end{aligned}
\tag{2.1}
$$

where T, E and I indicate the density of cancer cells, effector cells and IL-2, respectively.

First equation of (2.1) delineates the dynamics of cancer cell population. We consider that the cancer cells can proliferate logistically due to non-existence of immune cells [18, 49, 65], where α represents the proliferation rate and β^{-1} designates the biotic capacity. The last term is the eradication of cancer cells due to interplays with immune cells at the rate δ_1.

Second equation of model (2.1) designates the dynamics of the effector cells. First term s_2 indicates the external source of the immune cells. Effector cells are activated by the interplays with effector cells and IL-2, where k_2 is the stimulation rate. Due clinical investigation [15, 36, 41] it is observed that the immune cells are stimulated by the cytokine IL-2 and there is a time lag among the recruitment of IL-2 due to cytotoxic T-lymphocytes and the immune cell activation in presence of IL-2 [3]. Hence, we introduce a time lag in the second term of the second equation of (2.1). Herein τ represents time lag that has been incorporated due to the interaction delay. End term marks the natural decay rate δ_2 of immune cells.

The third equation of (2.1) designates the kinetics of the immunostimulatory cytokine IL-2. s_3 is the source term of IL-2. Next term of the final equation of (2.1) indicates the activation of IL-2 by the effector cells. Here, k_3 is the activation rate of IL-2 by effector cells and last term δ_3 is degrade rate of IL-2.

The system (2.1) is normalized using the following scales: $[x(t), y(t), z(t)] = \left(\frac{T}{T_0}, \frac{E}{T_0}, \frac{I}{T_0} \right)$, with $\bar{t} = \frac{t}{T_0}$, and obtain the following new parameters

$$\alpha = \alpha T_0, \quad \beta = \frac{\beta}{T_0}, \quad d_1 = \delta_1,$$

$$c_2 = \frac{s_2}{T_0^2}, \quad p_2 = k_2, \quad d_2 = \frac{\delta_2}{T_0},$$

$$c_3 = \frac{s_3}{T_0^2}, \quad p_3 = k_3, \quad d_3 = \frac{\delta_3}{T_0}.$$

Now, the system (2.1) becomes $(T, E, I) \mapsto (x, y, z)$, where $x(t)$, $y(t)$ and $z(t)$ represent normalized tumor cells, effector cells and cytokine IL-2, respectively, as

$$
\begin{aligned}
\frac{dx}{dt} &= \alpha x(1 - \beta x) - d_1 xy, \\
\frac{dy}{dt} &= c_2 + p_2 y(t - \tau) z(t - \tau) - d_2 y, \\
\frac{dz}{dt} &= c_3 + p_3 xy - d_3 z,
\end{aligned}
\tag{2.2}
$$

with initial conditions:

$$x(\omega) = \phi_1(\omega), \; y(\omega) = \phi_2(\omega), \; z(\omega) = \phi_3(\omega), \tag{2.3}$$

with $\phi_i(\omega) \geq 0$ for $i = 1$ to 3 and $\omega \in [-\tau, 0]$, where $\phi_i(\omega) \in \mathbf{R}_+^3$ are continuous functions on $[-\tau, 0]$ that may display jumps at $\omega = 0$.

2.3 Qualitative behavior of the model

2.3.1 Existence and positivity of the solutions

In this subsection, we will study the existence and positivity of the solutions of the delayed system (2.2). To do this, we consider the following lemma.

Lemma 2.3.1. *Every solution of (2.2) with initial values (2.3) exists and unique on $[0, \infty)$ with $x(t) > 0, y(t) > 0$ and $z(t) > 0, \forall\ t \geq 0$.*

Proof. The model (2.2) can be expressed into the vector form as $\dot{Y}(t) = H(Y)$, where $Y \equiv (x, y, z)^T$, and the mapping $H : C_+ \to \mathbf{R}^3_{+,0}$; with $H = (H_1, H_2, H_3)^T$, where $H_i \in C^\infty(\mathbf{R}_{+,0})$ for $i = 1, 2, 3$.

$$
\begin{aligned}
H_1 &= \alpha x(1 - \beta x) - d_1 xy, \\
H_2 &= c_2 + p_2 y(t - \tau)z(t - \tau) - d_2 y, \\
H_3 &= c_3 + p_3 xy - d_3 z.
\end{aligned}
$$

Let $Y(\omega) = (\phi_1(\omega), \phi_2(\omega), \phi_3(\omega)) \in C_+$ and $\phi_i(\omega) \geq 0, \forall\ i = 1$ to 3 with $\omega \in [-\tau, 0], \tau > 0$. The vector function H is locally Lipschitz and continuous function of the variables x, y, z in $\Phi = \{(x(t), y(t), z(t)) : x > 0, y > 0, z > 0\}$. Due to lemma [109], any solutions of (x, y, z) of (2.2) with initial values (2.3) exists and unique on $[0, \epsilon_0], \forall\ t\ \geq 0$, where $0 < \epsilon_0 < \infty$. $\qquad\square$

2.3.2 Biologically feasible steady states

In this subsection, we find the biologically meaningful singular points of the delayed system (2.2). To do this, we set $\frac{dx}{dt} = \frac{dy}{dt} = \frac{dz}{dt} = 0$ and take $\tau = 0$. Thus, we have

$$
\begin{aligned}
\alpha x(1 - \beta x) - d_1 xy &= 0, \\
c_2 + p_2 y(t - \tau)z(t - \tau) - d_2 y &= 0, \\
c_3 + p_3 xy - d_3 z &= 0.
\end{aligned}
$$

We find the tumor-free steady state $E^0(x^0, y^0, z^0)$ as

$$
E^0 \equiv (x^0, y^0, z^0) = \left(0, \frac{c_2 d_3}{d_2 d_3 - p_2 c_3}, \frac{c_3}{d_3}\right).
$$

If $d_2 > \frac{p_2 c_3}{d_3} \equiv \underline{d_2}$ *(say)*, then E^0 exists. For the existence of interior steady state E^*, we calculate for $x \neq 0$. Then, we get

$$
E^* \equiv (x^*, y^*, z^*) = \left(\frac{\alpha - d_1 y^*}{\alpha\beta}, y^*, \frac{\alpha\beta c_3 + (\alpha - d_1 y^*)p_3 y^*}{\alpha\beta d_3}\right),
$$

23

where y^* is the nonnegative root of the following equation

$$(y^*)^3 + \Sigma_1 (y^*)^2 + \Sigma_2 y^* + \Sigma_3 = 0, \qquad (2.4)$$

where

$$\begin{aligned}
\Sigma_1 &= -\frac{\alpha}{d_1}, \\
\Sigma_2 &= -\frac{\alpha\beta(p_2 c_3 - d_2 d_3)}{d_1 p_2 p_3}, \\
\Sigma_3 &= -\frac{\alpha\beta c_2 d_3}{d_1 p_2 p_3}.
\end{aligned}$$

It can be noted that $\Sigma_1 < 0$ and $\Sigma_3 < 0$. Thus, we can say that the number of positive roots of (2.4) either 1 or 3 according to the sign of the Σ_2. Now, we find the number of positive roots from the signs of Σ_2 and the terms ∇_1, ∇_2 and ∇_3 obtained from the Sturm's sequence, where

$$\begin{aligned}
\nabla_1 &= \Sigma_1 \Sigma_2 - 9\Sigma_3, \\
\nabla_2 &= 2\Sigma_1^2 - 6\Sigma_2, \\
\nabla_3 &= 2\Sigma_1 \frac{\nabla_1}{\nabla_2} - 2\left(\frac{\nabla_1}{\nabla_2}\right)^2 - \Sigma_2.
\end{aligned}$$

The criteria for obtaining the number of positive roots are given in the Table 2.1.

Table 2.1: Number of positive roots of the equation (2.4) based on the sign of the coefficients of Σ_1, Σ_2, Σ_3 and the terms of ∇_1, ∇_2 and ∇_3.

No. of positive roots	Σ_1	Σ_2	Σ_3	∇_1	∇_2	∇_3
1	-	+	-	+	+	+
				+	+	-
				+	-	+
				-	+	+
				-	-	+
				-	-	-
1	-	-	-	any sign	any sign	any sign
3	-	+	-	+	-	-
				-	+	-

2.3.3   Local stability analysis of the steady states

In this subsection, we investigate the asymptotic stability of the biologically meaningful singular points of the delayed system (2.2). To do this, we compute the variational matrix of (2.2) around the singular point $E(x, y, z)$ is

given by

$$
J(E) = \begin{pmatrix} j_{11} & j_{12} & j_{13} \\ j_{21} & j_{22} & j_{23} \\ j_{31} & j_{32} & j_{33} \end{pmatrix},
$$

with

$$
\begin{aligned}
j_{11} &= \alpha - 2\alpha\beta x - d_1 y, & j_{12} &= -d_1 x, & j_{13} &= 0, \\
j_{21} &= 0, & j_{22} &= p_2 z e^{-\lambda\tau} - d_2, & j_{23} &= p_2 y e^{-\lambda\tau}, \\
j_{31} &= p_3 y, & j_{32} &= p_3 x, & j_{33} &= -d_3.
\end{aligned}
$$

The eigenvalues corresponding to the tumor-free singular point E^0 without time lag $(\tau = 0)$ are

$$
\begin{aligned}
\lambda_1^0 &= \alpha - \frac{d_1 c_2 d_3}{d_2 d_3 - p_2 c_3}, \\
\lambda_2^0 &= \frac{p_2 c_3 - d_2 d_3}{d_3} < 0, & [\text{since } d_2 d_3 > p_2 c_3], \\
\lambda_3^0 &= -d_3 < 0.
\end{aligned}
$$

For $\lambda_1^0 < 0$, we get $d_2 < \frac{d_1 c_2 d_3 + \alpha p_2 c_3}{\alpha d_3} \equiv \overline{d_2}$ (say). Thus, we can write the following theorem.

Theorem 2.3.1. *In absence of time lag $(\tau = 0)$, the system (2.2) is asymptotically stable around the tumor-free steady state E^0 if $\underline{d_2} < d_2 < \overline{d_2}$.*

Now, our aim is to investigate the qualitative dynamics of (2.2) around the co-existing singular point $E^*(x^*, y^*, z^*)$ in presence of delay, that is, $\tau \neq 0$. In case of delay parameter τ, the characteristic equation around $E^*(x^*, y^*, z^*)$ can be expressed as

$$
A(\lambda) + B(\lambda)e^{-\lambda\tau} = 0, \tag{2.5}
$$

with

$$
\begin{aligned}
A(\lambda) &= \lambda^3 + a_1\lambda^2 + a_2\lambda + a_3, \\
B(\lambda) &= b_1\lambda^2 + b_2\lambda + b_3,
\end{aligned}
$$

where

$$
\begin{aligned}
a_1 &= -(\alpha - 2\alpha\beta x^* - d_1 y^* - d_2 - d_3), \\
a_2 &= d_2 d_3 - (\alpha - 2\alpha\beta x^* - d_1 y^*)(d_2 + d_3), \\
a_3 &= -d_2 d_3(\alpha - 2\alpha\beta x^* - d_1 y^*), \quad b_1 = -p_2 z^*, \\
b_2 &= p_2 z^*(\alpha - 2\alpha\beta x^* - d_1 y^*) - d_3 p_2 z^* - p_2 p_3 x^* y^*, \\
b_3 &= p_2(\alpha - 2\alpha\beta x^* - d_1 y^*)(p_3 x^* y^* + d_3 z^*) + d_1 p_2 p_3 x^* (y^*)^2.
\end{aligned}
$$

25

Around the co-existing steady state E^*, in the exclusion of delay ($\tau = 0$), the characteristic equation (2.5) leads to

$$\lambda^3 + (a_1 + b_1)\lambda^2 + (a_2 + b_2)\lambda + (a_3 + b_3) = 0. \qquad (2.6)$$

Using Routh-Hurwitz criteria, the roots of the characteristic equation (2.6) are negative or negative real parts if

$$
\begin{aligned}
S_1 &= (a_1 + b_1) = -(\alpha - 2\alpha\beta x^* - d_1 y^* - d_2 - d_3 + p_2 z^*) > 0, \\
S_2 &= (a_3 + b_3) \\
&= -d_2 d_3(\alpha - 2\alpha\beta x^* - d_1 y^*) + p_2(\alpha - 2\alpha\beta x^* - d_1 y^*)(p_3 x^* y^* + d_3 z^*) \\
&\quad + d_1 p_2 p_3 x^* (y^*)^2 > 0, \\
S_3 &= (a_1 + b_1)(a_2 + b_2) - (a_3 + b_3) \\
&= -(\alpha - 2\alpha\beta x^* - d_1 y^* - d_2 - d_3 + p_2 z^*)[\{d_2 d_3 \\
&\quad - (\alpha - 2\alpha\beta x^* - d_1 y^*)(d_2 + d_3)\} + \{p_2 z^*(\alpha - 2\alpha\beta x^* - d_1 y^*) \\
&\quad - p_2 d_3 z^* - p_2 p_3 x^* y^*\}] - S_2 > 0.
\end{aligned}
\qquad (2.7)
$$

We can encapsulate the outcomes in the theorem.

Theorem 2.3.2. *The necessary and sufficient condition of (2.2) (exclusion of delay, $\tau = 0$) to be locally asymptotically stable around co-existing steady state $E^*(x^*, y^*, z^*)$ is that S_1, S_2, $S_3 > 0$.*

Now, we will investigate how the stability is affected by time lag τ by utilizing τ as a threshold parameter. To obtain the periodic solutions of the system (2.2), we substitute $\lambda = i\theta(\theta > 0)$ into (2.5) and separating real and imaginary parts, we have

$$
\begin{aligned}
a_1 \theta^2 - a_3 &= (b_3 - b_1 \theta^2)\cos(\theta\tau) + b_2 \theta \sin(\theta\tau), \\
\theta^3 - a_2 \theta &= b_2 \theta \cos(\theta\tau) - (b_3 - b_1 \theta^2)\sin(\theta\tau).
\end{aligned}
\qquad (2.8)
$$

Squaring and adding above expressions, we have

$$(a_1 \theta^2 - a_3)^2 + (\theta^3 - a_2 \theta)^2 = (b_3 - b_1 \theta^2)^2 + (b_2 \theta)^2.$$

For simplicity, we can write

$$\theta^6 + A_1 \theta^4 + A_2 \theta^2 + A_3 = 0, \qquad (2.9)$$

where

$$
\begin{aligned}
A_1 &= a_1^2 - 2a_2 + b_1^2 \\
&= (\alpha - 2\alpha\beta x^* - d_1 y^* - d_2 - d_3)^2 - 2[d_2 d_3 \\
&\quad - (\alpha - 2\alpha\beta x^* - d_1 y^*)(d_2 + d_3)] + (p_2 z^*)^2, \\
A_2 &= a_2^2 - 2a_1 a_3 + 2b_1 b_3 - b_2^2 \\
&= [d_2 d_3 - (\alpha - 2\alpha\beta x^* - d_1 y^*)(d_2 + d_3)]^2 \\
&\quad - 2d_2 d_3(\alpha - 2\alpha\beta x^* - d_1 y^*)(\alpha - 2\alpha\beta x^* - d_1 y^* - d_2 - d_3) \\
&\quad - 2p_2 z^*[p_2(\alpha - 2\alpha\beta x^* - d_1 y^*)(p_3 x^* y^* + d_3 z^*) + d_1 p_2 p_3 x^*(y^*)^2] \\
&\quad - [p_2 z^*(\alpha - 2\alpha\beta x^* - d_1 y^*) - d_3 p_2 z^* - p_2 p_3 x^* y^*]^2, \\
A_3 &= a_3^2 - b_3^2 \\
&= [d_2 d_3(\alpha - 2\alpha\beta x^* - d_1 y^*)]^2 - [p_2(\alpha - 2\alpha\beta x^* - d_1 y^*)(p_3 x^* y^* + d_3 z^*) \\
&\quad + d_1 p_2 p_3 x^*(y^*)^2]^2.
\end{aligned}
$$

Equation (2.9) will have at least one positive root if

$$
A_1 > 0 \quad \text{and} \quad A_3 = a_3^2 - b_3^2 = (a_3 + b_3)(a_3 - b_3) < 0.
$$

From the above conditions, there is a positive root θ_0 obeying equation (2.9), that is, the characteristic polynomial (2.5) has a pair of complex roots in the form $\pm i\theta_0$. Simplifying both the equations of (2.8), we have

$$
\tan(\theta\tau) = \frac{b_2\theta(a_1\theta^2 - a_3) - (\theta^3 - a_2\theta)(b_3 - b_1\theta^2)}{(a_1\theta^2 - a_3)(b_3 - b_1\theta^2) + b_2\theta(\theta^3 - a_2\theta)}.
$$

Then, τ_n corresponding to θ_0 leads to

$$
\begin{aligned}
\tau_n &= \frac{1}{\theta_0} \arctan\left[\frac{b_2\theta_0(a_1\theta_0^2 - a_3) - (\theta_0^3 - a_2\theta_0)(b_3 - b_1\theta_0^2)}{(a_1\theta_0^2 - a_3)(b_3 - b_1\theta_0^2) + b_2\theta_0(\theta_0^3 - a_2\theta_0)}\right] \\
&\quad + \frac{2n\pi}{\theta_0}, \; n = 0, 1, 2, 3, ...
\end{aligned} \tag{2.10}
$$

For $\tau_n = 0$, E^* is stable, given the condition of Theorem (2.3.2) holds. According to Butler's lemma [31], E^* will be stable for $\tau_n < \tau_0$, where $\tau_n = \tau_0$ at $n = 0$.

2.4   Hopf bifurcation analysis

Now, we will prove that the transversality condition $\left[\frac{d(Re\lambda)}{d\tau}\right]_{\tau=\tau_n} > 0$ [48], which indicates that $\exists$ at least one eigenvalue with positive real part obeying

27

$\tau > \tau_n$. Firstly, we are interested in complex roots of the form $\lambda = i\theta_0$ of (2.5) indicates that $|P(i\theta_0)| = |Q(i\theta_0)|$, which determines the positive values of τ_n. Our goal is to investigate the direction of motion of λ as τ is altered. Now, we need to investigate that

$$\Theta = sign\left[\frac{d(Re\lambda)}{d\tau_n}\right]_{\lambda=i\theta_0} = sign\left[Re\left(\frac{d\lambda}{d\tau_n}\right)^{-1}\right]_{\lambda=i\theta_0}.$$

On differentiation of (2.5) with reference to τ gives

$$[(3\lambda^2 + 2a_1\lambda + a_2) + e^{-\lambda\tau}(2b_1\lambda + b_2) - \tau e^{-\lambda\tau}(b_1\lambda^2 + b_2\lambda + b_3)]\frac{d\lambda}{d\tau}$$
$$= (b_1\lambda^2 + b_2\lambda + b_3)\lambda e^{-\lambda\tau},$$

which implies that

$$\left(\frac{d\lambda}{d\tau}\right)^{-1} = \frac{3\lambda^2 + 2a_1\lambda + a_2}{\lambda e^{-\lambda\tau}(b_1\lambda^2 + b_2\lambda + b_3)} + \frac{2b_1\lambda + b_2}{\lambda(b_1\lambda^2 + b_2\lambda + b_3)} - \frac{\tau}{\lambda}$$

$$= \frac{3\lambda^2 + 2a_1\lambda + a_2}{-\lambda(\lambda^3 + a_1\lambda^2 + a_2\lambda + a_3)} + \frac{2b_1\lambda + b_2}{\lambda(b_1\lambda^2 + b_2\lambda + b_3)} - \frac{\tau}{\lambda}$$

$$= \frac{2\lambda^3 + a_1\lambda^2 - a_3}{-\lambda^2(\lambda^3 + a_1\lambda^2 + a_2\lambda + a_3)} + \frac{b_1\lambda^2 - b_3}{\lambda^2(b_1\lambda^2 + b_2\lambda + b_3)} - \frac{\tau}{\lambda}.$$

Therefore,

$$\Theta = sign\left[Re\left(\frac{2\lambda^3 + a_1\lambda^2 - a_3}{-\lambda^2(\lambda^3 + a_1\lambda^2 + a_2\lambda + a_3)}\right.\right.$$
$$\left.\left. + \frac{b_1\lambda^2 - b_3}{\lambda^2(b_1\lambda^2 + b_2\lambda + b_3)} - \frac{\tau}{\lambda}\right)\right]_{\lambda=i\theta_0}$$

$$= sign\left[Re\left(\frac{-2i\theta_0^3 - a_1\theta_0^2 - a_3}{-\theta_0^2(-i\theta_0^3 - a_1\theta_0^2 + ia_2\theta_0 + a_3)}\right.\right.$$
$$\left.\left. + \frac{-b_1\theta_0^2 - b_3}{-\theta_0^2(-b_1\theta_0^2 + ib_2\theta_0 + b_3)} - \frac{\tau}{i\theta_0}\right)\right]$$

$$= \frac{1}{\theta_0^2}sign\left\{Re\left[\frac{(a_1\theta_0^2 + a_3) + 2i\theta_0^3}{(a_1\theta_0^2 - a_3) + i(\theta_0^3 - a_2\theta_0)} + \frac{b_1\theta_0^2 + b_3}{(b_3 - b_1\theta_0^2) + i(b_2\theta_0)}\right]\right\},$$

which implies that

$$
\begin{aligned}
\Theta &= \frac{1}{\theta_0^2} sign\left[\frac{(a_1\theta_0^2 + a_3)(a_1\theta_0^2 - a_3) + 2\theta_0^3(\theta_0^3 - a_2\theta_0)}{(a_1\theta_0^2 - a_3)^2 + (\theta_0^3 - a_2\theta_0)^2}\right. \\
&+ \left.\frac{(b_1\theta_0^2 + b_3)(b_3 - b_1\theta_0^2)}{(b_3 - b_1\theta_0^2)^2 + (b_2\theta_0)^2}\right] \\
&= \frac{1}{\theta_0^2} sign\left[\frac{2\theta_0^6 + (a_1^2 - 2a_2 - b_1^2)\theta_0^4 + (b_3^2 - a_3^2)}{(b_3 - b_1\theta_0^2)^2 + (b_2\theta_0)^2}\right].
\end{aligned}
$$

Thus, the transversality condition $\frac{d(Re\lambda)}{d\tau}|_{\theta=\theta_0,\tau=\tau_n} > 0$ holds for $(a_1^2 - 2a_2 - b_1^2) > 0$ and $(b_3^2 - a_3^2) > 0$ by virtue of $A_1 > 0$ and $A_3 < 0$. Therefore, Hopf bifurcation experiences at $\theta = \theta_0, \tau = \tau_n$. We encapsulate the results as follows.

Theorem 2.4.1. *The delayed tumor model (2.2) with initial values (2.3) exists around interior steady state E^*. Thus,*
(i) if $\tau \in [0, \tau_n)$, then E^* is asymptotically stable,
(ii) E^* is unstable if $\tau > \tau_n$,
(iii) at $\tau_= \tau_n$, the system (2.2) undergoes Hopf bifurcation at E^*.

2.5   Estimation of the length of delay to preserve stability

In this section, we study the stability of bifurcating periodic oscillations and try to compute the length of time lag to maintain the stability of periodic limit cycle. The delayed model (2.2) with real valued continuous functions defined on $[-\tau, +\infty)$, satisfying the initial values on the interval $[-\tau, 0)$. We linearized the system (2.2) at the co-existing singular point $E^*(x^*, y^*, z^*)$ leads to

$$
\begin{aligned}
\frac{dx}{dt} &= -\alpha\beta x^* x - d_1 x^* y, \\
\frac{dy}{dt} &= -d_2 y + p_2 z^* y(t - \tau) + p_2 y^* z(t - \tau), \\
\frac{dz}{dt} &= p_3 y^* x + p_3 x^* y - d_3 z.
\end{aligned} \tag{2.11}
$$

Applying Laplace transformation of (2.11) leads to

$$
\begin{aligned}
(\rho + \alpha\beta x^*)L_x(\rho) &= -d_1 x^* L_y(\rho) + x(0), \\
(\rho + d_2)L_y(\rho) &= p_2 z^* e^{-\rho\tau}(L_y(\rho) + K_y(\rho)) \\
&+ p_2 y^* e^{-\rho\tau}(L_z(\rho) + K_z(\rho)) + y(0), \\
(\rho + d_3)L_z(\rho) &= p_3 y^* L_x(\rho) + p_3 x^* L_y(\rho) + z(0),
\end{aligned} \tag{2.12}
$$

with

$$K_y(\rho) = \int_{-\tau}^0 e^{-\rho\tau} y(t)dt \qquad \text{and} \qquad K_z(\rho) = \int_{-\tau}^0 e^{-\rho\tau} z(t)dt,$$

where $L_x(\rho)$, $L_y(\rho)$ and $L_z(\rho)$ are the corresponding Laplace transformations of $x(t)$, $y(t)$ and $z(t)$, respectively. By well-known results of Freedman et al. [31] and utilizing Nyquist criteria [72], we observed that the criterion for the locally asymptotically stability of $E^*(x^*,\ y^*,\ z^*)$ are stated as

$$Im[M(i\rho_0)] > 0, \qquad (2.13)$$

$$Re[M(i\rho_0)] = 0, \qquad (2.14)$$

with

$$M(\rho) = \rho^3 + a_1\rho^2 + a_2\rho + a_3 + e^{-\rho\tau}(b_1\rho^2 + b_2\rho + b_3),$$

and ρ_0 is the smallest nonnegative root of (2.14). We have investigated that E^* is stable in the exclusion of time lag ($\tau = 0$). Equations (2.13) and (2.14) can be explicitly written as

$$-\rho_0^3 + a_2\rho_0 \ > \ (b_3 - b_1\rho_0^2)\sin(\rho_0\tau) - b_2\rho_0\cos(\rho_0\tau), \qquad (2.15)$$

$$-a_1\rho_0^2 + a_3 \ = \ -b_2\rho_0\sin(\rho_0\tau) - (b_3 - b_1\rho_0^2)\cos(\rho_0\tau), \qquad (2.16)$$

that gives sufficient conditions for the stability of co-existing steady state E^* and we use them to obtain an estimate length of time lag τ. Our aim is to find an upper bound ρ_+ on ρ_0, that is, independent on time lag τ, and calculate length of τ. Thus, equation (2.15) holds $\forall$ values of ρ, $0 \le \rho \le \rho_+$ at $\rho = \rho_0$. We rewrite the equation (2.16) as

$$a_1\rho_0^2 = a_3 + b_3\cos(\rho_0\tau) + b_2\rho_0\sin(\rho_0\tau) - b_1\rho_0^2\cos(\rho_0\tau). \qquad (2.17)$$

We maximize the right side of (2.17), and leads to

$$a_3 + b_3\cos(\rho_0\tau) + b_2\rho_0\sin(\rho_0\tau) - b_1\rho_0^2\cos(\rho_0\tau),$$

subject to

$$|\cos(\rho_0\tau)| \le 1, \qquad |\sin(\rho_0\tau)| \le 1.$$

Therefore, from (2.17), we get

$$|a_1|\rho_0^2 \le |a_3| + |b_3| + |b_2|\rho_0 + |b_1|\rho_0^2.$$

30

Hence, it can be expressed as

$$(|a_1| - |b_1|)\rho_0^2 - |b_2|\rho_0 - (|a_3| + |b_3|) \leq 0.$$

From the above inequality, we have

$$\rho_+ \leq \frac{1}{2(|a_1|-|b_1|)}\left[|b_2| + \sqrt{|b_2|^2 + 4(|a_1| - |b_1|)(|a_3| + |b_3|)}\right]. \qquad (2.18)$$

Then, it is obvious from (2.18) that $\rho_0 \leq \rho_+$. Also, from the inequality (2.15), we have

$$\rho_0^2 < a_2 + b_2\cos(\rho_0\tau) + b_1\rho_0\sin(\rho_0\tau) - \frac{b_3\sin(\rho_0\tau)}{\rho_0}. \qquad (2.19)$$

As E^* is asymptotically stable without time lag, thus for enough small $\tau > 0$ the inequality (2.19) will satisfied. Putting (2.17) into (2.19) and rearrange leads to

$$(b_3 - b_1\rho_0^2 - a_1b_2)[\cos(\rho_0\tau) - 1] + \left\{(b_2 - a_1b_1)\rho_0 + \frac{a_1b_3}{\rho_0}\right\}\sin(\rho_0\tau)$$

$$< a_1a_2 - a_3 - b_3 + b_1\rho_0^2 + a_1b_2. \qquad (2.20)$$

Using the bounds, we have

$$(b_3 - b_1\rho_0^2 - a_1b_2)[\cos(\rho_0\tau) - 1] = 2(b_1\rho_0^2 + a_1b_2 - b_3)\sin^2\left(\frac{\rho_0\tau}{2}\right)$$

$$\leq \tfrac{1}{2}|(b_1\rho_+^2 + a_1b_2 - b_3)|\rho_+^2\tau^2,$$

and

$$\left\{(b_2 - a_1b_1)\rho_0 + \frac{a_1b_3}{\rho_0}\right\}\sin(\rho_0\tau) \leq \left\{|(b_2 - a_1b_1)|\rho_+^2 + |a_1||b_3|\right\}\tau.$$

After simplification of (2.20), we get

$$N_1\tau^2 + N_2\tau \leq N_3,$$

with

$$N_1 = \tfrac{1}{2}|(b_1\rho_+^2 + a_1b_2 - b_3)|\rho_+^2,$$
$$N_2 = \left\{|(b_2 - a_1b_1)|\rho_+^2 + |a_1||b_3|\right\},$$
$$N_3 = a_1a_2 - a_3 - b_3 + b_1\rho_+^2 + a_1b_2.$$

Hence, if

$$\tau_+ = \frac{1}{2N_1}[-N_2 + \sqrt{N_2^2 + 4N_1N_3}],$$

for $0 \leq \tau \leq \tau_+$, the Nyquist criteria satisfied and τ_+ estimates length of delay that maintain the stability of limit cycle.

31

2.6 Numerical illustrations

To complete the mathematical analysis of our system (2.2), it is important to discuss the suitable parameters and initial conditions of both delayed and non delayed ($\tau = 0$) version. We have chosen most of the parameters from previous published works [18, 88, 90]. To validate our theoretical analysis of the system (2.2), we perform some numerical simulations utilizing MATLAB and MATHEMATICA with set of system parameters are given in Table 2.2. At first, we have verified that the existence and stability condition of the tumor-free equilibrium state E^0 of (2.2) with no time lag ($\tau = 0$). For decay rate of effector cells $d_2 = 0.3743$ [110] and rest of the system parameters are given in Table 2.2, we compute $\underline{d_2} = 0.046111$. Also, for the same parameters set we have computed $\overline{d_2} = 0.511935$. Therefore, the existence criteria for the tumor-free steady state E^0 is verified, that is, $d_2(0.3743) > \underline{d_2}$. Due to absence of time lag, that is, $\tau = 0$ of (2.2) is locally asymptotically stable at the tumor-free steady state E^0, which is stated in the Theorem 2.3.1. For $d_2 = 0.3743$ and rest of system parameters are given in Table 2.2, we have $\underline{d_2} < d_2 < \overline{d_2}$. Numerically, we have calculated the tumor-free steady state $E^0(0, \ 0.359854, \ 0.37037)$ and corresponding eigenvalues are $-0.54, \ -0.180752, \ -0.328189$ and all the eigenvalues are negative. Thus, the cancer-free singular point E^0, the model (2.2) without delay parameter ($\tau = 0$) is asymptotically stable that has been drawn in Figure 2.1 with initial values $[x(0), y(0), z(0)] = [0, 0.3, 0.3]$.

We take initial values $[x(0), y(0), z(0)] = [4.5, 0.2, 2.6]$ and the set of system parameters are listed in Table 2.2. The model (2.2) has a unique co-existing steady state $E^*(4.52127, \ 0.253529, \ 2.68414)$ and the eigenvalues are $-0.977779, \ -0.0140229 \pm 0.2614791i$. Since all the eigenvalues are negative or negative real parts, then the co-existing singular point E^* is asymptotically stable. According to the Theorem 2.3.2, we obtained that $S_1 = 1.00582 > 0$, $S_2 = 0.0670441 > 0$ and $S_3 = 0.0295054 > 0$, which ensure that the stability of the co-existing steady state E^* of (2.2) (in absence of time lag, $\tau = 0$) (see the Figure 2.2).

For the specified set of system parameters in Table 2.2, we calculate $A_1 = 1.04327 > 0$ and $A_3 = -0.00449491 < 0$ that gives that the equation (2.9) has only one positive real root $\theta_0 = 0.228484$. Numerically, we compute $\tau_n \approx 0.67724$ from the equation (2.10). According to the Theorem 2.4.1, we noticed that the delayed model (2.2) is locally asymptotically stable at the co-existing equilibrium E^* for $\tau < \tau_n \approx 0.67724$. We have plotted the figure (See the Figure 2.3(A)) for $\tau = 0.12$. The figure 2.3(A) describes the lower

Figure 2.1: Time series evolution of (2.2) (without time delay $\tau = 0$) for tumor cells, effector cells and IL-2 at the tumor-free singular point $E^0 = (0, 0.359854, 0.37037)$ with initial values $[x(0), y(0), z(0)] = [0.0, 0.3, 0.3]$. We consider $d_2 = 0.3743$ and rest of system parameters are given in Table 2.2. The time series solutions represent the locally asymptotically stability of E^0.

critical value of τ_n of (2.2) goes a stable singular point in co-existing singular point E^*. For this condition, tumor cell populations are non-invasive and non spreadable which means that the cancerous cells are remain under control and can reach the cancer dormant or steady state [52]. Again, we observe that our delayed model (2.2) is unstable at interior singular point E^* for $\tau > \tau_n \approx 0.67724$, which has been shown in the Figure 2.3(B) for $\tau = 0.82$. Hence, the co-existing singular point E^* experiences a Hopf bifurcation (Figure 2.4) as time lag τ passes through its critical threshold $\tau > \tau_n$. We also calculate $\left[\frac{d(Re\lambda)}{d\tau} \right]_{\theta=\theta_0, \ \tau=\tau_n} = 0.538194 > 0$ that implies that transversality criteria of Hopf bifurcation is satisfied. The occurrence of the Hopf bifurcation in this scenario is that around the interior singular point E^*, a limit cycle is occurred at the bifurcation point and as a consequences a stable periodic oscillations [52]. The occurrence of periodic oscillations in the tumor cell populations describes that the cancer level may oscillate at a singular point without any drugs or therapeutics. Such type of scenario is

Table 2.2: The set of system parameters of tumor-immune interaction system used for numerical illustrations.

Par.	Description	Values	Source
α	Proliferation rate of cancer cells	0.431	[18]
β	Biotic capacity of cancer cells	0.2×10^{-6}	[3]
d_1	Deactivation rate of cancer cells due to effector cells	1.7	fit to data
c_2	Activation rate of effector cells	0.1181	[110]
p_2	Proliferation rate of CD8+T cells by IL-2	0.1245	[61]
d_2	Natural decay rate of effector cells	0.8	fit to data
c_3	Constant source rate of IL-2	0.2	[3]
p_3	Stimulation rate of IL-2 by cancer cells and effector cells	1.09	[88]
d_3	Degradation rate of IL-2	0.54	[88]

called Jeff's phenomena [99].

For various values of time lag τ we have drawn the 2-dimensional phase diagram (see the Figure 2.5) to better understand the kinetics of the cell interactions, namely tumor cells and immune cells, tumor cells and IL-2, immune cells and IL-2. For $\tau = 0.12$, the phase portrait of cancer cells and immune cells, cancer cells and IL-2, immune cells and IL-2 are shown in the first column of the Figure 2.5(A), which designates the stable solutions of the respective cells. Middle column of the Figure 2.5(B) indicates the phase portraits of cancer cells and immune cells, cancer cells and IL-2, immune cells and IL-2 for the time lag $\tau = 0.41$ that implies the stable oscillations with large periodic oscillations than the Figure 2.5(A). Right column of the Figure 2.5(C) designates the phase portrait of the cancer cells and immune cells, cancer cells and IL-2, immune cells and IL-2 for the time lag $\tau = 0.82$ that designates that the periodic solutions of the respective cells.

We have plotted the Hopf bifurcation diagram of (2.2) taking α (intrinsic growth rate of cancer population), d_1 (deactivation rate of cancer population due to immune cells), c_2 (influx rate of immune cells) and d_2 (death rate of immune cells) taking as the bifurcation parameters in the Figure 2.6, Figure 2.7, Figure 2.8 and Figure 2.9, respectively. From Figure 2.6, we noticed that when α crosses the critical level $\alpha^* = 0.425$, the equilibrium values for tumor
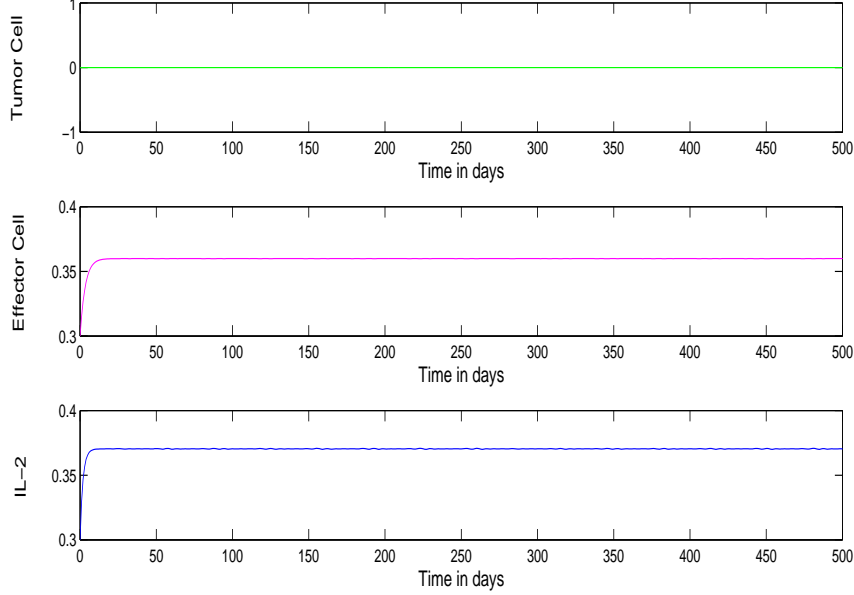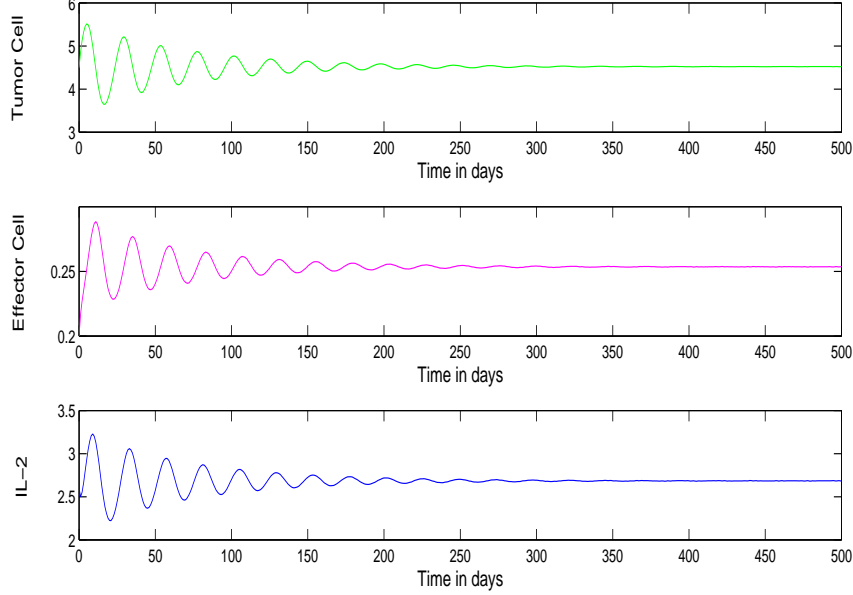
Figure 2.2: Time series evolution of (2.2) (without time lag $\tau = 0$) for tumor cells, effector cells and IL-2 around interior singular point $E^* = (4.52127, 0.253529, 2.68414)$ with initial values $[x(0), y(0), z(0)] = [4.5, 0.2, 2.6]$ and rest of system parameters are given in Table 2.2. The time series solutions represent the locally asymptotically stability of E^*.

cells, effector cells and IL-2 divided into minimum/maximum of the periodic solutions and interior singular point becomes unstable for $\tau = 0.12$ and rest of system parameters are listed in Table 2.2. From Figure 2.7, it is clear that for $\tau = 0.12$ and rest of system parameters given in Table 2.2, when d_1 passes through the critical value $d_1^* = 1.862$, then the minimum/maximum of the periodic solutions for cancer cells, immune cells and IL-2 are merged into the steady state value indicating the stability of interior singular point, that is, E^* is asymptotically stable. For the parameter c_2, the dynamics of (2.2) is shown using the bifurcation diagram (see the Figure 2.8). In this case, the bifurcation point is $c_2^* = 0.115$, that is, when c_2 passes through the threshold value $c_2^* = 0.115$, minimum/maximum of the periodic solutions for cancer populations, immune system and IL-2 are merged into the steady state value indicating the stability of interior equilibrium E^*, that is, E^* is asymptotically stable. We have drawn the bifurcation diagram (Figure 2.9) of (2.2) for cancer populations, immune system and IL-2 with respect to the d_2 by choosing $\tau = 0.12$ and rest of system parameters given in Table
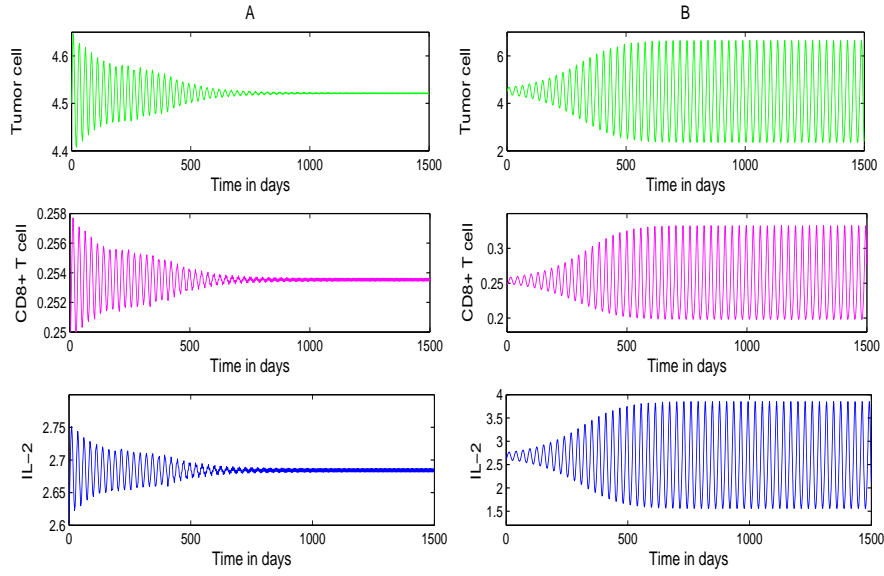
Figure 2.3: The left column (A) and the right column (B) shows that the time series solutions of (2.2) for $\tau = 0.12$ and $\tau = 0.82$, respectively, of cancer cells, immune cells and IL-2 around the interior equilibrium $E^* = (4.52127, 0.253529, 2.68414)$ with initial values $[x(0), y(0), z(0)] = [4.5, 0.2, 2.6]$ and rest of system parameters are listed in Table 2.2. The time series solutions of (2.2) represents the local asymptotic stability for $\tau = 0.12$ and periodic oscillations for $\tau = 0.82$.
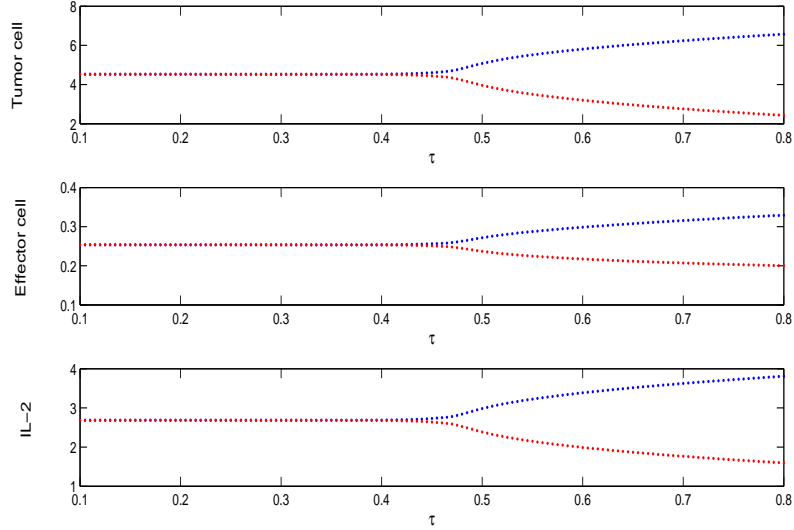
Figure 2.4: Bifurcation diagram of (2.2) for tumor cells, immune cells and IL-2 with reference to the discrete time lag τ and rest of system parameters are given in Table 2.2.

2.2. We have seen that when d_2 crosses threshold level $d_2^* = 0.778$, then the equilibrium values of every cells are divided into minimum/maximum of the periodic solutions and the interior steady state becomes unstable.

2.7 Conclusion

In this chapter, we have studied a conceptual mathematical model of tumor-immune dynamics by incorporating the effect of time lag. Our simple mathematical model plays a crucial role to delineates the cancer-immune interaction system with and without discrete time delay τ. The results from theoretic analysis not only show the role of time lag on the dynamical behaviors but also help to exhibit some complex dynamical phenomena through numerical simulations. On the other hand, the numerical simulations provide some important information, including the complexity of the dynamic behavior of the model, the diversity of its dependence on antigenicity, and the explanation of some clinical phenomena that incorporate observed in [61, 65]. The obtained results in this chapter exhibits the significance of discrete time delay in controlling the proliferation of cancer cells. The aim of this chapter is how the time delay
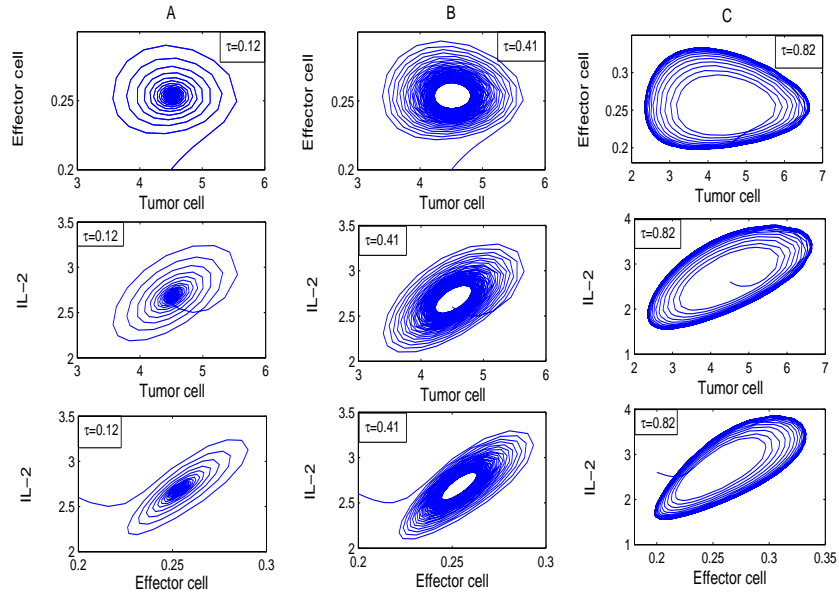
Figure 2.5: Numerical illustration shows the stable phase portraits of (2.2) at the interior equilibrium $E^* = (4.52127, 0.253529, 2.68414)$ with initial values $[x(0), y(0), z(0)] = [4.5, 0.2, 2.6]$ and rest of system parameters are given in Table 2.2. The left column (A) represents phase diagram for $\tau = 0.12$, the middle column (B) represents phase diagram for $\tau = 0.41$ and the right column (C) represents phase diagram for $\tau = 0.82$.
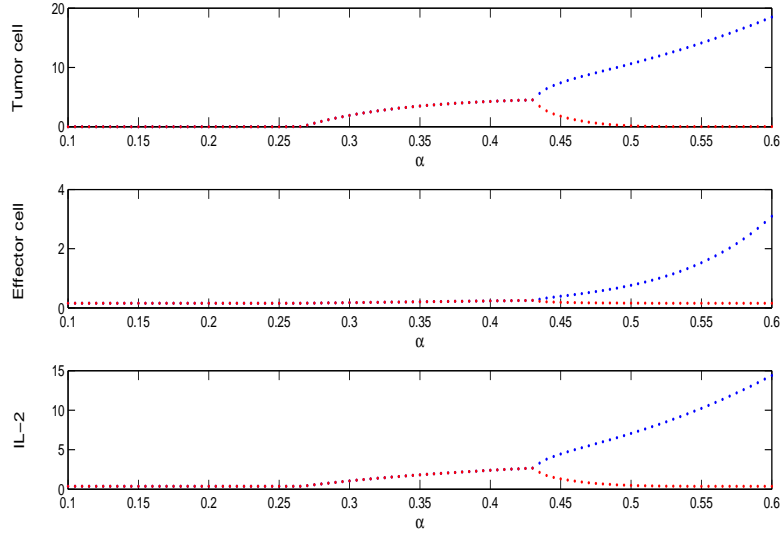
Figure 2.6: The figure shows the bifurcation diagram of (2.2) for tumor cells, effector cells and IL-2 with reference to the intrinsic growth rate α of tumor cell. Taking $\tau = 0.12$ and rest of system parameters are listed in Table 2.2.
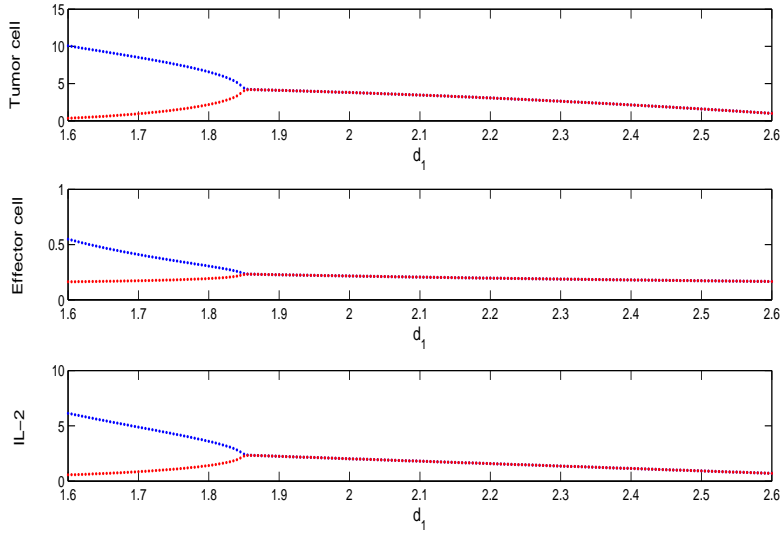
Figure 2.7: The figure represents the bifurcation diagram of (2.2) for tumor cells, immune cells and IL-2 with reference to the deactivation rate d_1 of tumor cell. Taking $\tau = 0.12$ and rest of system parameters are given in Table 2.2.
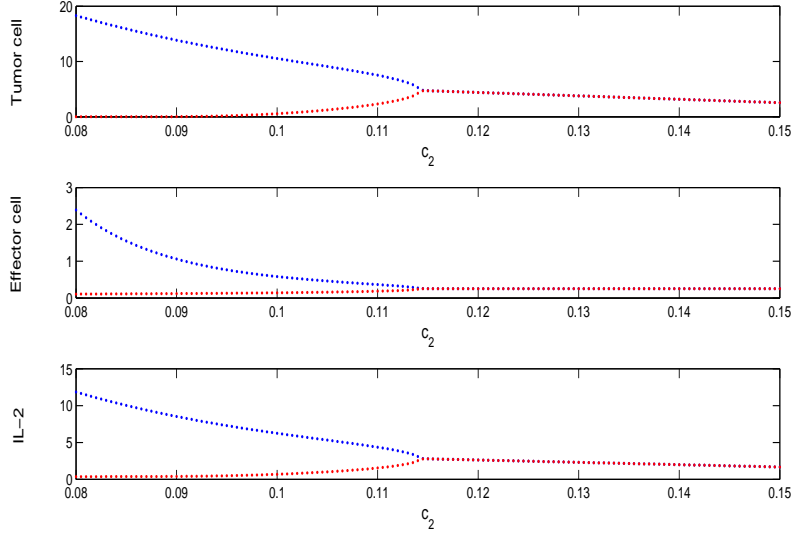
Figure 2.8: The figure represents the bifurcation diagram of (2.2) for tumor cells, effector cells and IL-2 with reference to activation rate c_2 of effector cell. Taking $\tau = 0.12$ and rest of system parameters are listed in Table 2.2.

influence the dynamics of our system in presence of the cytokine IL-2. Our mathematical model interplays the kinetics of cancer population, immune cell populations and immuno-stimulatory cytokine IL-2. At first, we have examined existence and positivity of the solutions of our mathematical model. Also, we have investigated local stability analysis of the biologically feasible steady states both in presence and absence of discrete time lag τ. To analyze the Hopf bifurcation, we prove that the transversality condition $\left[\frac{d(Re\lambda)}{d\tau}\right]_{\theta=\theta_0, \ \tau=\tau_n} > 0$, utilizing time delay τ is a threshold parameter. Also, we have computed the length of time lag to maintain stability of bifurcating limit cycle. We have performed some numerical illustrations to validate the theoretical findings. Local asymptotic stability of the delayed and non delayed system has been investigated to better understand the dynamics of the tumor-immune competitive system by steady state analysis [46, 47].

We incorporate a discrete time lag in our mathematical model. At first, we find the tumor-free singular point E^0 and tumor-presence or interior singular point E^*. We get a condition $\underline{d_2} < d_2 < \overline{d_2}$, for our system (2.2) is asymptotically stable around E^0 without time lag ($\tau = 0$). In Figure 2.1, we have drawn the model (2.2) without delay parameter ($\tau = 0$) is asymptoti-
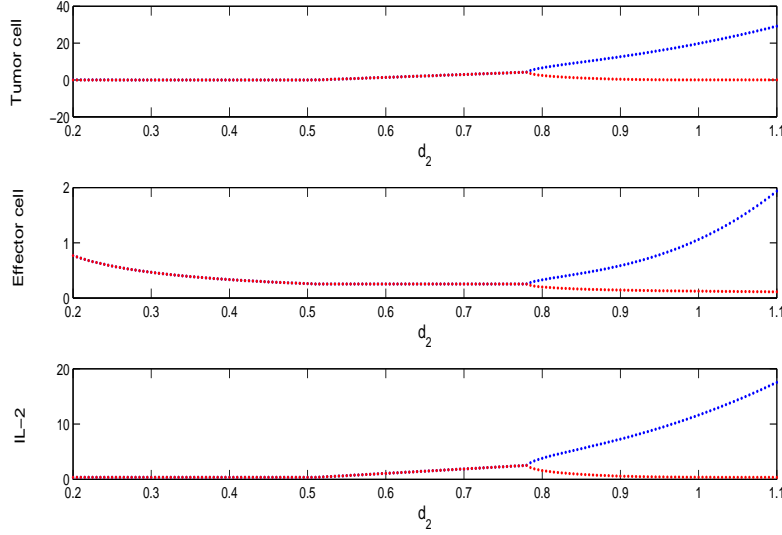
Figure 2.9: The figure shows bifurcation diagram of (2.2) for tumor cells, effector cells and IL-2 with reference to death rate d_2 of effector cell. Taking $\tau = 0.12$ and rest of system parameters are given in Table 2.2.

cally stable around the tumor-free singular point E^0. If S_1, S_2, $S_3 > 0$, then the model (2.2) is stable asymptotically at the co-existing singular point E^*, which has been shown in the Theorem 2.3.2. Time series evolution of model (2.2) (without time lag $\tau = 0$) represent the locally asymptotically stability around interior singular point E^*, which is shown in Figure 2.2. We explored numerical integration of our system in presence of time lag τ. If delay parameter τ is less than its corresponding critical value $\tau_n \approx 0.67724$, then our delayed system (2.2) is asymptotically stable around co-existing singular point E^* (in Figure 2.3(A), for $\tau = 0.12$). Again, around co-existing equilibrium point E^*, our system (2.2) is unstable if time lag τ is greater than the threshold value τ_n (in Figure 2.3(B), for $\tau = 0.82$). Hence, our co-existing equilibrium E^* experiences a Hopf bifurcation as the discrete time lag τ passes its critical level τ_n, which is plotted in Figure 2.4. The significance of the Hopf bifurcation is that a limit cycle is occurred at the bifurcation point around co-existing equilibrium E^* and thus, occurring a stable periodic oscillations. For $\tau = 0.12$, the phase portrait of tumor cells and immune cells, tumor cells and IL-2, immune cells and IL-2 are shown in the Figure 2.5(A), which designates the stable solutions of the respective cells. Figure 2.5(B) indicates the phase portraits of tumor cells and immune cells, tumor cells and IL-2, immune cells and IL-2 for the time lag $\tau = 0.41$

41

that implies the stable oscillations with large periodic oscillations than the Figure 2.5(A). Figure 2.5(C) represents the phase portrait of the tumor cells and immune cells, tumor cells and IL-2, immune cells and IL-2 for the time lag $\tau = 0.82$ that signals the periodic solutions of the respective cells. Our mathematical model shows complicated dynamics that has been noticed in the numerical part by altering parameters such that proliferation rate of tumor populations α, deactivation rate of tumor population due to immune system d_1, constant influx rate of immune system c_2 and decay rate of immune system d_2. If we increase α and d_2, then the co-existing singular point E^* of our mathematical model (2.2) goes from stable to unstable one in Figure 2.6 and Figure 2.9, respectively. On the other hand, for increasing the value of d_1 and c_2, our mathematical model (2.2) goes from unstable position to stable position in Figure 2.7 and Figure 2.8, respectively at co-existing singular point E^*.

In this chapter, we have analyzed Hopf bifurcation of our delayed model by transversality condition. We have studied that phase portrait of two dimensional cells, that is, tumor cells and immune cells, tumor cells and IL-2, immune cells and IL-2 for various values of delay parameter τ. We have investigated nature of solutions of respective cells for different values of τ. At last but not least, we have estimated length of time delay parameter τ for preserving the stability of period-1 limit cycle that provides the idea about the mode of action in controlling oscillations in the growth of tumor cells.

The result of this chapter provides an initial analytical skeleton in investigating tumor-immune interaction with time lag τ. Our simple tumor model explore how to the time lag effect in presence of the cytokine IL-2 in tumor-immune interaction system. However, we can investigate the role of other cytokines likelihood TGF-β, IL-10, IL-35, porstaglandin-E_2, IL-12, interferon-gamma (IFN-γ) that are related to cancer-immune interplays to cancer evolution and how these cytokines influence the kinetics of the system.

Chapter 3

The impact of distributed time delay in a tumor-immune interaction system [†]

3.1 Introduction

According to the World Health Organization (WHO) report, cancer is the second-leading cause of death globally and is responsible for an estimated 9.6 million deaths in 2019 [106]. Cancer is a generic term for a large group of diseases characterized by the abnormal growth of tissues beyond their usual boundaries, which can then invade nearby parts of the body and spread to the other organs. Other common terms can be used are malignant tumors and intracranial neoplasms. Cancer can affect any part of the body and has many anatomic and molecular subtypes that each requires specific management strategies. Despite medical advances, several challenges remain in the diagnosis and treatment of this disease. One great tool which has shown its potential to better understand of such a complicated biological system is mathematical modeling [4, 17, 18, 23, 47, 61, 65, 73]. Mathematical modeling gives realistic and quantitative representations of indispensable biological scenarios and biological elucidation of their outcomes can provide insight to make realistic predictions of the state of cancer under different situations [13, 45, 54, 62, 69, 74, 84].

One of the most important and challenging questions in immunology and cancer research is to understand how the immune system affects tumor

progression and development [4, 17, 18, 84]. The mechanisms underlying the interaction between tumor and immune system are critically important for understanding tumorigenesis and immunotherapy [62, 74]. The immune system is a very complicated network of cells and signals, which protect our body from pathogens or foreign antigens including tumor cells. The immune response begins when tumor cells are recognized by different kinds of immune cells like B-cells, cytotoxic T-lymphocytes or activated CD8+T cells considered as effector cells, Helper T cells, macrophages, etc. secreting different types of cytokines and hence, stimulating both B-cells and T-cells, and so on [1, 4]. In most of the cases, our immune system can recognize the tumor cells, but the responses are not sufficient to destroy the tumor cells [104]. Tumor cells are mainly the prey of the CD8+T cells, on the other hand, proliferation of CD8+T cells are stimulated due to the existence of tumor cells. However, tumor cells also cause a loss of CD8+T cells and intensity of an influx of CD8+T cells may rely on the size of the tumor cells [23]. Helper T cells are stimulated through antigen presenting cells (APCs), namely macrophages or dendritic cells and release the cytokines to stimulate proliferation of CD8+T cells to kill more and more tumor cells [23].

In reality, the duration of any process can never be constant and it usually fluctuates around some value. Therefore, it is believed that delay should be distributed around some average values instead of being concentrated in points. This approach, which allows to more closely mimic the reality, leads to integro-differential systems, where the integral part derives form taking into account the distributed nature of the delay. The density of the delay is called delay kernel. The constant delay case, thus may be considered a limit case of a distributed delay, where the delay kernel is a Dirac's delta function [64].

The organization of this chapter is as follows: In Section 3.2, we develop a mathematical model for tumor-immune interaction and its normalization. Section 3.3 contains some preliminary results of existence, non negativity and boundedness of solutions. The qualitative behavior of the model is described in the Section 3.4. Qualitative behavior includes nonnegativity of the solutions, existence of the biologically feasible equilibrium points and their local stability analysis. We introduce continuously distributed delay by considering kernel function as an additional compartment in the Section 3.5. We also investigate the existence of equilibrium points and their local stability analysis in the same section. Our model system experiences Hopf bifurcation with respect to activation rate λ_1 of CD8+T cells, which has been explored in the Section 3.6. Section 3.7 deals with the numerical results and their

biological interpretations for the analytical findings. Finally, we give a brief conclusion in the Section 3.8.

3.2 Model formulation

Our aim of this section is to formulate a mathematical model which allows sufficient complexity so that the model will qualitatively generate clinically observed in vivo tumor growth patterns, while it simultaneously maintains sufficient simplicity to perform model analysis. In this chapter, we examine the characteristics of shares in comparison to the tumor-immune interaction model introduced by de Pillis et al. [18], Khajanchi [44], Kirschner & Panetta [61] and Yu et al. [110]. A kernel function as immune activation continuous delay is introduced in the proliferation of CD8+T cells, which is activated by Helper T cells. The model describes the kinetics of CD8+T cells, Helper T cells, tumor cells and immuno-stimulatory cytokine IL-2, using a system of coupled nonlinear ordinary differential equations:

$$
\begin{aligned}
\frac{dT}{d\tau} &= a_1 T \left(1 - b_1 T\right) - i_1 T C_T, \\
\frac{dC_T}{d\tau} &= c_2 - m_2 C_T + n_2 C_T H + g_2 T C_T + f_2 C_T I_L, \\
\frac{dH}{d\tau} &= c_3 - m_3 H + n_3 T H, \\
\frac{dI_L}{d\tau} &= i_4 T C_T - m_4 I_L,
\end{aligned}
\tag{3.1}
$$

where T, C_T, H and I_L represent the number tumor cells, tumor specific CD8+T cells, Helper T cells and cytokine IL-2, respectively at any time t.

The first equation of (3.1) describes the rate of change of the density of tumor cells. We assume that the tumor cells can grow logistically without any immune intervention [18, 65], where a_1 is the intrinsic growth rate and $1/b_1$ is the maximum carrying capacity of the tumor cells. The second term corresponds to the elimination of tumor cells due to interaction with tumor-specific CD8+T cells. Elimination rate of tumor cells by CD8+T cells is i_1.

The second equation of the system (3.1) corresponds to the rate of change of tumor-specific CD8+T cells. The first term c_2 represents the constant source rate of CD8+T cells. CD8+T cells have a natural lifespan of an average $1/m_2$ days. n_2 is the activation rate of CD8+T cells due to interaction of Helper T cells. CD8+T cells are assumed to be activated to

the tumor site as a direct result for the presence of tumor cells. Here, g_2 is activation rate of CD8+T cells due to tumor cells. Tumor-specific CD8+T cells are stimulated by IL-2 and f_2 is the stimulating rate of CD8+T cells due to the cytokine IL-2.

The third equation of (3.1) stands for the rate of change for Helper T cells. Helper T cells are produce in the thymus with birth rate c_3. Helper T cells have a natural lifespan of an average $1/m_3$ days. n_3 is the stimulation rate of Helper T cells due to presence of tumor antigens.

The last equation of (3.1) gives the rate of change for the concentration of the immuno-stimulatory cytokine IL-2. Its source is the tumor-specific CD8+T cells that are stimulated by interaction with the tumor cells. i_4 represents the activation rate of the cytokine IL-2. The final term m_4 represents loss or degraded rate of the cytokine IL-2.

In order to consider a weak proliferation of tumor-specific CD8+T cells are stimulated by tumor cells, we can simplify this system (3.1) by omitting the CD8+T cells stimulating from Tumor cells (that is, ignoring the term g_2TC_T) [110], while keeping the essential dynamical properties of the original system. Then, we obtain the following simplified tumor-immune system:

$$
\begin{aligned}
\frac{dT}{d\tau} &= a_1 T \left(1 - b_1 T\right) - i_1 T C_T, \\
\frac{dC_T}{d\tau} &= c_2 - m_2 C_T + n_2 C_T H + f_2 C_T I_L, \\
\frac{dH}{d\tau} &= c_3 - m_3 H + n_3 T H, \\
\frac{dI_L}{d\tau} &= i_4 T C_T - m_4 I_L,
\end{aligned}
\tag{3.2}
$$

with initial conditions $T(0) = T_0 > 0$, $C_T(0) = (C_T)_0 \geq 0$, $H(0) = H_0 \geq 0$, $I_L(0) = (I_L)_0 \geq 0$.

To non dimensionalize the system (3.2), we introduce new variables

$$
x_1 = \frac{T}{T_0}, \quad y_1 = \frac{C_T}{T_0}, \quad z_1 = \frac{H}{T_0}, \quad u_1 = \frac{I_L}{T_0}, \quad \tau = \frac{t}{i_1 T_0};
$$

and the corresponding parameters are

$$
\alpha = \frac{a_1}{i_1 T_0}, \quad \beta = b_1 T_0, \quad \lambda_1 = \frac{c_2}{i_1 T_0^2}, \quad \theta_1 = \frac{m_2}{i_1 T_0}, \quad \rho_1 = \frac{n_2}{i_1}, \quad \mu_1 = \frac{f_2}{i_1},
$$

$$
\lambda_2 = \frac{c_3}{i_1 T_0^2}, \quad \theta_2 = \frac{m_3}{i_1 T_0}, \quad \rho_2 = \frac{n_3}{i_1}, \quad \mu_2 = \frac{i_4}{i_1}, \quad \theta_3 = \frac{m_4}{i_1 T_0}.
$$

Then, the model system (3.2) becomes the following form as

$$
\begin{aligned}
\frac{dx_1}{dt} &= \alpha x_1(1 - \beta x_1) - x_1 y_1, \\
\frac{dy_1}{dt} &= \lambda_1 - \theta_1 y_1 + \rho_1 y_1 z_1 + \mu_1 y_1 u_1, \\
\frac{dz_1}{dt} &= \lambda_2 - \theta_2 z_1 + \rho_2 x_1 z_1, \\
\frac{du_1}{dt} &= \mu_2 x_1 y_1 - \theta_3 u_1,
\end{aligned}
\tag{3.3}
$$

with the nonnegative initial conditions,

$$
x_1(0) = 1, \quad y_1(0) \geq 0, \quad z_1(0) \geq 0, \quad u_1(0) \geq 0,
$$

where $x_1(t)$, $y_1(t)$, $z_1(t)$ and $u_1(t)$ represent the non dimensionlize quantity of tumor cells, CD8+T cells, Helper T cells and IL-2, respectively.

3.3 Some preliminary results

3.3.1 Existence and uniqueness of the solution of the system

Proposition 3.3.1. *Every solution of the system (3.3) with respect to the nonnegative initial conditions exists and is unique.*

Proof. The system (3.3) can be written in vector form

$$
\dot{X} = G(X(t)),
$$

with $X(t) = (x_1, y_1, z_1, u_1)^T$ and $G(X) = (G_1(X), G_2(X), G_3(X), G_4(X))^T$ such that $G_1 = \alpha x_1(1 - \beta x_1) - x_1 y_1$, $G_2 = \lambda_1 - \theta_1 y_1 + \rho_1 y_1 z_1 + \mu_1 y_1 u_1$, $G_3 = \lambda_2 - \theta_2 z_1 + \rho_2 x_1 z_1$, $G_4 = \mu_2 x_1 y_1 - \theta_3 u_1$.

Then, G is the mapping from $\mathbb{R}_+^4$ to $\mathbb{R}^4$ with $G \in C^\infty(\mathbb{R}^4)$, $G_i(X) \mid_{X_i(t)=0, \, X \in \mathbb{R}_+^4} = G_i(0) \geq 0, \, \forall \, i = 1, 2, 3, 4$. Thus, vector function G is a locally Lipschitzian and completely continuous function of the variables x_1, y_1, z_1, u_1 in the nonnegative interior region of $\mathbb{R}_+^4 = \{(x_1, y_1, z_1, u_1) : x_1, y_1, z_1, u_1 > 0\}$. Applying the lemma in [109], we can say that any solution (x_1, y_1, z_1, u_1) of the system (3.3) with nonnegative initial values exists and is unique in the interval $[0, \, c]$, for all $t \geq 0$, where c is a finite positive real number. $\qquad \square$

3.3.2 Nonnegativity

In this subsection, we discuss the nonnegativity of the solution for the system (3.3) as the populations cannot be negative. We start with a theorem which assure that the system (3.3) is nonnegative in the interior of $\mathbb{R}_+^4$, where $\mathbb{R}_+^4$ is defined as

$$\mathbb{R}_+^4 = \{(x_1, y_1, z_1, u_1) : x_1, y_1, z_1, u_1 > 0\}.$$

Proposition 3.3.2. *Solution of (3.3) with respect to the nonnegative initial conditions is nonnegative in the interior of $\mathbb{R}_+^4$.*

Proof. The system (3.3) can be written in vector form in terms of $X(t) = (x_1, y_1, z_1, u_1)^T \in \mathbb{R}_+^4$ and $G(X) = (G_1(X), G_2(X), G_3(X), G_4(X))^T$ as

$$\dot{X} = G(X(t)),$$

where $. \equiv \frac{d}{dt}$, with initial conditions in vector form

$$X_0 = X(0) = (x_1(0), y_1(0), z_1(0), u_1(0)) \in \mathbb{R}_+^4.$$

Consider the mapping

$$G : \mathbb{R}_+^4 \longrightarrow \mathbb{R}^4 \quad \text{with} \quad G \in C^\infty(\mathbb{R}^4).$$

It is obvious that in the system (3.3),

$$G_i(X) \mid_{X_i(t)=0, \ X \in \mathbb{R}_+^4} = G_i(0) \geq 0, \ \forall \ i = 1, 2, 3, 4.$$

Due to the lemma in [109], the solution of the system (3.3) with initial conditions $X_0 \in \mathbb{R}_+^4$, in such a way that $X(t) = X(t, X_0)$, $X(t) \in \mathbb{R}_+^4 \ \forall \ t > 0$, that is, it remains nonnegative throughout the region $\mathbb{R}_+^4 \ \forall \ t > 0$. $\qquad \square$

3.3.3 Boundedness

Proposition 3.3.3. *All feasible solutions of the system (3.3) are uniformly bounded in the region $E_\varepsilon = \left\{ (x_1, y_1, z_1, u_1) \in R_+^4 : x_1 + u_1 \leq \frac{1}{\beta} + \varepsilon, y_1 \leq \frac{\beta \lambda_1}{\beta \theta_1 - \rho_1 k_1 \beta - \mu_1} + \varepsilon, z_1 \leq \frac{\beta \lambda_2}{\beta \theta_2 - \rho_2} + \varepsilon \right\}.$*

Proof. Let $V(x_1, u_1) = x_1 + u_1$, then we have
$\frac{dV}{dt} = \alpha x_1(1 - \beta x_1) - x_1 y_1 + \mu_2 x_1 y_1 - \theta_3 u_1$ (by using (3.3))
$\leq \alpha x_1(1 - \beta x_1) - (1 - \mu_2)x_1 y_1$

$\leq \alpha x_1 (1 - \beta x_1)$ (if $\mu_2 < 1$).

By using theory of differential inequality, we have

$$\limsup_{t \to \infty} [x_1(t) + u_1(t)] \leq \frac{1}{\beta}.$$

Thus, $x_1(t) + u_1(t)$ is bounded and defined on $[0, \infty)$ $\forall$ $t \geq 0$.

From third equation of the system (3.3), we have

$$\frac{dz_1}{dt} = \lambda_2 - \theta_2 z_1 + \rho_2 x_1 z_1,$$

$$\Rightarrow \frac{dz_1}{dt} \leq \lambda_2 - \theta_2 z_1 + \frac{\rho_2 z_1}{\beta},$$

$$\Rightarrow \frac{dz_1}{dt} + (\theta_2 - \frac{\rho_2}{\beta}) z_1 \leq \lambda_2.$$

Applying the standard theory of differential inequality, we get

$$z_1 \leq \frac{\lambda_2}{\theta_2 - \frac{\rho_2}{\beta}} \left(1 - e^{-(\theta_2 - \frac{\rho_2}{\beta})t} \right) + z_1(0) e^{-(\theta_2 - \frac{\rho_2}{\beta})t},$$

$$\Rightarrow \limsup_{t \to \infty} z_1(t) \leq \frac{\beta \lambda_2}{\beta \theta_2 - \rho_2} = k_1 (say), \ when \ \beta \theta_2 > \rho_2.$$

Therefore, $z_1(t)$ is bounded and defined on $[0, \infty)$ $\forall$ $t \geq 0$.

From second equation, we have

$$\frac{dy_1}{dt} = \lambda_1 - \theta_1 y_1 + \rho_1 y_1 z_1 + \mu_1 y_1 u_1,$$

$$\Rightarrow \frac{dy_1}{dt} + (\theta_1 - \rho_1 k_1 - \frac{\mu_1}{\beta}) y_1 \leq \lambda_1.$$

Again, applying the standard theory of differential inequality we obtain,

$\limsup_{t \to \infty} y_1(t) \leq \frac{\beta \lambda_1}{\beta \theta_1 - \rho_1 k_1 \beta - \mu_1}$, if $\beta \theta_1 > \rho_1 k_1 \beta + \mu_1$.

So all the solutions of (3.3) with nonnegative initial values are confined in the region

$$E_\varepsilon = \left\{ (x_1, y_1, z_1, u_1) \in R_+^4 : x_1 + u_1 \leq \frac{1}{\beta} + \varepsilon, y_1 \leq \frac{\beta \lambda_1}{\beta \theta_1 - \rho_1 k_1 \beta - \mu_1} + \varepsilon, \right.$$

$$\left. z_1 \leq \frac{\beta \lambda_2}{\beta \theta_2 - \rho_2} + \varepsilon \right\},$$

for any $\varepsilon > 0$. Hence, the result. $\qquad \square$

3.4 Qualitative behavior of the system

3.4.1 Equilibria

In order to investigate the steady states of the system (3.3), we write $\frac{dx_1}{dt} = \frac{dy_1}{dt} = \frac{dz_1}{dt} = \frac{du_1}{dt} = 0$. Then, we have

$$
\begin{aligned}
x_1[\alpha(1 - \beta x_1) - y_1] &= 0, \\
y_1(\theta_1 - \rho_1 z_1 - \mu_1 u_1) &= \lambda_1, \\
z_1(\theta_2 - \rho_2 x_1) &= \lambda_2, \\
\mu_2 x_1 y_1 - \theta_3 u_1 &= 0.
\end{aligned}
\tag{3.4}
$$

We obtain the tumor-free singular point E^0 is given by

$$
E^0 = (x_1^0, y_1^0, z_1^0, u_1^0) = \left(0, \frac{\lambda_1 \theta_2}{\theta_1 \theta_2 - \rho_1 \lambda_2}, \frac{\lambda_2}{\theta_2}, 0\right).
$$

E^0 exists, if $\rho_1 < \frac{\theta_1 \theta_2}{\lambda_2} \equiv \rho_1^0$ (say).

For the existence of tumor-presence singular point E^1, we set $x_1^1 \neq 0$. Then, we get

$$
E^1 = (x_1^1, y_1^1, z_1^1, u_1^1) = \left(x_1^1, \alpha(1 - \beta x_1^1), \frac{\lambda_2}{\theta_2 - \rho_2 x_1^1}, \frac{\alpha \mu_2 x_1^1(1 - \beta x_1^1)}{\theta_3}\right)
$$

and x_1^1 is the positive root of the given equation

$$
\begin{aligned}
F(x_1^1) &\equiv (x_1^1)^4 (\alpha^2 \beta^2 \mu_1 \mu_2 \rho_2) - \alpha^2 \mu_1 \mu_2 (\beta^2 \theta_2 + 2\beta \rho_2)(x_1^1)^3 \\
&+ (2\alpha^2 \beta \mu_1 \mu_2 \theta_2 + \alpha \beta \theta_1 \theta_3 \rho_2 + \alpha^2 \mu_1 \mu_2 \rho_2)(x_1^1)^2 \\
&+ (\alpha \beta \lambda_2 \theta_3 \rho_1 + \theta_3 \lambda_1 \rho_2 - \alpha \theta_1 \theta_3 \rho_2 - \alpha \beta \theta_1 \theta_2 \theta_3 - \alpha^2 \mu_1 \mu_2 \theta_2)(x_1^1) \\
&+ (\alpha \theta_1 \theta_2 \theta_3 - \lambda_1 \theta_2 \theta_3 - \alpha \lambda_2 \theta_3 \rho_1) = 0,
\end{aligned}
\tag{3.5}
$$

which is a fourth order equation and it has at most four positive roots. Analytically, it is quite difficult to find an explicit form of existence of tumor-presence singular point. We use numerical methods to explore the effect of target parameters upon tumor-presence different singular points and their stability analysis. By varying λ_1, we obtain one positive root for $\lambda_1 = 0.9$, two positive roots for $\lambda_1 = 0.052$, three positive roots for $\lambda_1 = 0.6$, and four positive roots for $\lambda_1 = 0.0052$ and other parameters value are taken from Table 3.2. This scenarios can be shown in the Figure 3.1.
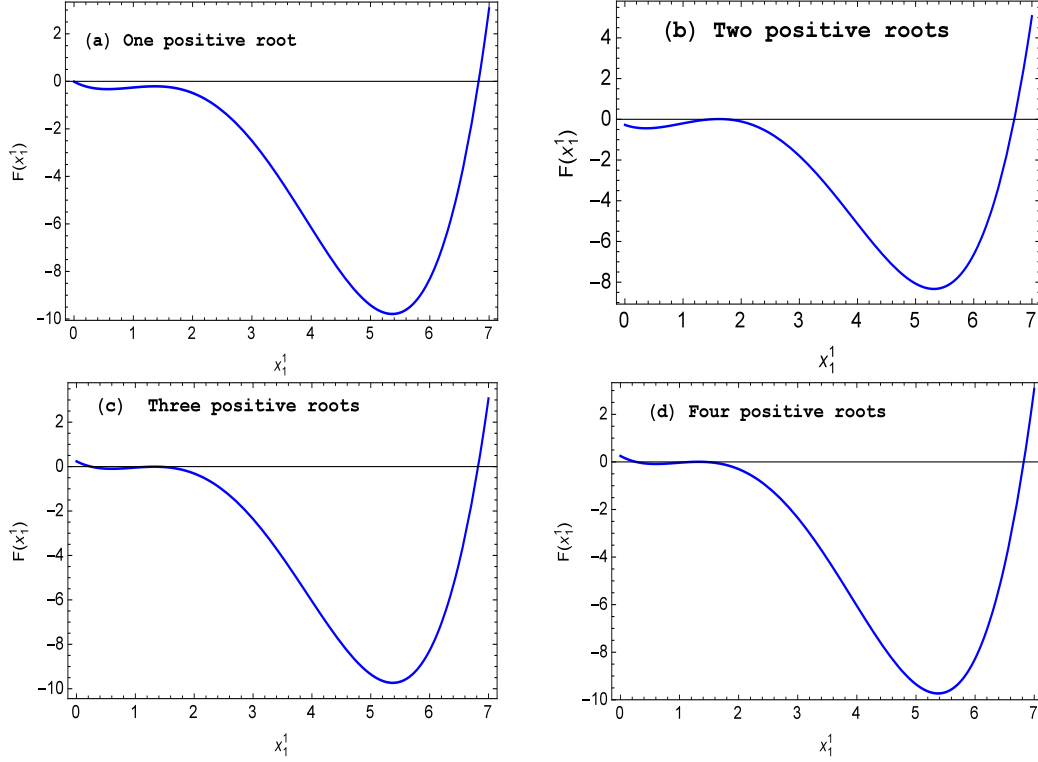
Figure 3.1: The figures represent the number of positive roots of the biquadratic equation (3.5). The figure (a) indicates the unique positive root $x_1^1(= 6.82384)$ for $\lambda_1 = 0.9$; (b) indicates two positive roots $x_1^1(= 0.244011, 6.82372)$ for $\lambda_1 = 0.052$; (c) indicates three positive roots $x_1^1(= 1.48454, 1.74751, 6.69677)$ for $\rho_1 = 0.6$; (d) indicates four positive roots $x_1^1(= 0.266121, 1.22575, 1.41656, 6.82372)$ for $\lambda_1 = 0.0052$ and other parameters value are specified in the Table 3.2.

3.4.2 Local stability analysis

In this subsection, we perform local asymptotically stability analysis (LAS) for the biologically feasible equilibrium points E^0 and E^1. In order to study the LAS, we compute the Jacobian matrix around the equilibrium point $E(x_1, y_1, z_1, u_1)$ is given by

$$
J(E) = \begin{bmatrix} \alpha - 2\alpha\beta x_1 - y_1 & -x_1 & 0 & 0 \\ 0 & -\theta_1 + \rho_1 z_1 + \mu_1 u_1 & \rho_1 y_1 & \mu_1 y_1 \\ \rho_2 z_1 & 0 & -\theta_2 + \rho_2 x_1 & 0 \\ \mu_2 y_1 & \mu_2 x_1 & 0 & -\theta_3 \end{bmatrix}.
$$

At the tumor free equilibrium point E^0, the Jacobian matrix $J(E^0)$ for the system (3.3) is given by

$$
J(E^0) = \begin{bmatrix} \alpha - \frac{\lambda_1 \theta_2}{\theta_1 \theta_2 - \rho_1 \lambda_2} & 0 & 0 & 0 \\ 0 & -\theta_1 + \rho_1 \frac{\lambda_2}{\theta_2} & \rho_1 \frac{\lambda_1 \theta_2}{\theta_1 \theta_2 - \rho_1 \lambda_2} & \mu_1 \frac{\lambda_1 \theta_2}{\theta_1 \theta_2 - \rho_1 \lambda_2} \\ \rho_2 \frac{\lambda_2}{\theta_2} & 0 & -\theta_2 & 0 \\ \mu_2 \frac{\lambda_1 \theta_2}{\theta_1 \theta_2 - \rho_1 \lambda_2} & 0 & 0 & -\theta_3 \end{bmatrix}.
$$

The eigenvalues corresponding to the Jacobian matrix $J(E^0)$ are given by

$$
\begin{aligned}
\epsilon_1 &= \alpha - \frac{\lambda_1 \theta_2}{\theta_1 \theta_2 - \rho_1 \lambda_2}, \\
\epsilon_2 &= -\theta_1 + \rho_1 \frac{\lambda_2}{\theta_2} = \frac{\rho_1 \lambda_2 - \theta_1 \theta_2}{\theta_2} < 0, \quad [\text{since } (\theta_1 \theta_2 - \rho_1 \lambda_2) > 0], \\
\epsilon_3 &= -\theta_2 < 0, \\
\epsilon_4 &= -\theta_3 < 0.
\end{aligned}
$$

If $\epsilon_1 < 0$, then we have $\rho_1 > \frac{\theta_1 \theta_2}{\lambda_2} - \frac{\lambda_1 \theta_2}{\alpha \lambda_2} \equiv \rho_1^1 (say)$. Thus, we have the following theorem.

Theorem 3.4.1. *The tumor-free singular point E^0 of the system (3.3) is locally asymptotically stable if $\rho_1^1 < \rho_1 < \rho_1^0$.*

Now, we compute the Jacobian matrix around the interior equilibrium point E^1 is given by

$$
J(E^1) = \begin{bmatrix} \alpha - 2\alpha\beta x_1^1 - y_1^1 & -x_1^1 & 0 & 0 \\ 0 & -\theta_1 + \rho_1 z_1^1 + \mu_1 u_1^1 & \rho_1 y_1^1 & \mu_1 y_1^1 \\ \rho_2 z_1^1 & 0 & -\theta_2 + \rho_2 x_1^1 & 0 \\ \mu_2 y_1^1 & \mu_2 x_1^1 & 0 & -\theta_3 \end{bmatrix}.
$$

The characteristic equation of $J(E^1)$ takes the following form

$$D(\epsilon) \equiv \epsilon^4 + b_1\epsilon^3 + b_2\epsilon^2 + b_3\epsilon + b_4 = 0, \tag{3.6}$$

where

$$b_1 = \left[\alpha\beta x_1^1 + \tfrac{\lambda_1}{y_1^1} + \tfrac{\lambda_2}{z_1^1} + \theta_3\right],$$

$$b_2 = \left[\alpha\beta x_1^1\tfrac{\lambda_1}{y_1^1} + \alpha\beta x_1^1\tfrac{\lambda_2}{z_1^1} + \tfrac{\lambda_1}{y_1^1}\tfrac{\lambda_2}{z_1^1} + (\alpha\beta x_1^1 + \tfrac{\lambda_1}{y_1^1} + \tfrac{\lambda_2}{z_1^1})\theta_3 - \mu_1\mu_2 x_1^1 y_1^1\right],$$

$$b_3 = \left[\alpha\beta x_1^1\tfrac{\lambda_1}{y_1^1}\tfrac{\lambda_2}{z_1^1} + \theta_3(\alpha\beta x_1^1\tfrac{\lambda_1}{y_1^1} + \alpha\beta x_1^1\tfrac{\lambda_2}{z_1^1} + \tfrac{\lambda_1}{y_1^1}\tfrac{\lambda_2}{z_1^1}) - \tfrac{\lambda_2}{z_1^1}\mu_1\mu_2 x_1^1 y_1^1\right.$$
$$\left. - \alpha\beta x_1^1\mu_1\mu_2 x_1^1 y_1^1 + \rho_1\rho_2 x_1^1 y_1^1 z_1^1 + \mu_1\mu_2 x_1^1(y_1^1)^2\right],$$

$$b_4 = \left[\alpha\beta x_1^1\tfrac{\lambda_1}{y_1^1}\tfrac{\lambda_2}{z_1^1}\theta_3 - \alpha\beta x_1^1\tfrac{\lambda_2}{z_1^1} + \tfrac{\lambda_1}{y_1^1}\tfrac{\lambda_2}{z_1^1}\mu_1\mu_2 x_1^1 y_1^1 + \rho_1\rho_2\theta_3 x_1^1 y_1^1 z_1^1\right.$$
$$\left. + \tfrac{\lambda_2}{z_1^1}\mu_1\mu_2 x_1^1(y_1^1)^2\right].$$

According to the Routh-Hurwitz criterion, we obtain a set of necessary conditions such that all roots of equation (3.6) are negative or have negative real parts if and only if $b_1 > 0$, $b_1b_2 - b_3 > 0$ and $(b_1b_2 - b_3)b_3 - b_1^2 b_4 > 0$.

From the expression, it is clear that $b_1 > 0$. Now, we consider that $b_1b_2 - b_3 = \Gamma - \Delta$,

where

$$\Gamma = \left(\alpha\beta x_1^1\right)^2\left(\tfrac{\lambda_1}{y_1^1} + \tfrac{\lambda_2}{z_1^1} + \theta_3\right) + \left(\tfrac{\lambda_1}{y_1^1}\right)^2\left(\alpha\beta x_1^1 + \tfrac{\lambda_2}{z_1^1} + \theta_3\right) + \left(\tfrac{\lambda_2}{z_1^1}\right)^2\left(\alpha\beta x_1^1 + \tfrac{\lambda_1}{y_1^1}\right)$$
$$+ \theta_3^2\left(\alpha\beta x_1^1 + \tfrac{\lambda_1}{y_1^1} + \tfrac{\lambda_2}{z_1^1}\right) + 2\alpha\beta x_1^1\tfrac{\lambda_1}{y_1^1}\tfrac{\lambda_2}{z_1^1} + 2\theta_3\left(\alpha\beta x_1^1\tfrac{\lambda_1}{y_1^1} + \alpha\beta x_1^1\tfrac{\lambda_2}{z_1^1} + \tfrac{\lambda_1}{y_1^1}\tfrac{\lambda_2}{z_1^1}\right),$$

and

$$\Delta = x_1^1 y_1^1\mu_1\mu_2\left(\tfrac{\lambda_1}{y_1^1} + \theta_3 + y_1^1\right) + \rho_1\rho_2 z_1^1.$$

So, we can say that $b_1b_2 - b_3 > 0$ for $\Gamma > \Delta$.

Thus, we have the following theorem.

Theorem 3.4.2. *The interior singular point E^1 of the system (3.3) is locally asymptotically stable if $\Gamma > \Delta$ and $(\Gamma - \Delta)b_3 > b_1^2 b_4$.*

3.5 Dynamics of delayed model

In reality, the dynamical behavior of the system does not happen instantaneously, but rather depends on the influence of the past history of the system.

Thus, it is very necessary to introduce time delays into model formulation to reflect the real scenarios. As we know that the activation of immune response against the progression of tumor development is very complicated and often delayed, such as, the immune activation delays of CD8+T cells by tumor cells and Helper T cells by tumor cells [34, 43, 110], and the immune activation delay of CD8+T cells by Helper T Cells [35, 44, 49, 52, 69] and so on.

The immune cells will take more time to give a suitable response after recognizing the tumor cells [50, 110], we only consider such delay in this study. Therefore, we need to take into account the effect of time delay to describe the proliferation of CD8+T cells stimulating by Helper T cells. The time delays can be classified into two types: discrete time delays (directly incorporate delay term, for example, $m_1 C(t-\tau)H(t-\tau)$ with $\tau > 0$) [44] and distributed delay (introducing a kernel function as an additional compartment) [40]. In this study, we are mainly interested in continuously distributed delay $M(t) = \int_{-\infty}^{t} b e^{-b(t-s)} z_1(s) ds$ to represent the immune activation delay, then we obtain the following system:

$$
\begin{aligned}
\frac{dx_1}{dt} &= \alpha x_1 (1 - \beta x_1) - x_1 y_1, \\
\frac{dy_1}{dt} &= \lambda_1 - \theta_1 y_1 + \rho_1 y_1 M + \mu_1 y_1 u_1, \\
\frac{dz_1}{dt} &= \lambda_2 - \theta_2 z_1 + \rho_2 x_1 z_1, \\
\frac{du_1}{dt} &= \mu_2 x_1 y_1 - \theta_3 u_1, \\
\frac{dM}{dt} &= l_1 z_1 - l_1 M,
\end{aligned}
\tag{3.7}
$$

where $l_1(t)$ (> 0) represents the strength of delay and a probability distribution function $z_1(t)$ is the distributed delay kernel. $l_1(t)$ is defined by

$$
l_1(t) = \frac{t^{j-1} b^j}{(j-1)!},
$$

with b is a constant, $(j - 1)$ is the order of the delay and j is a positive integer. We take $j = 1$, then we have

$$
l_1(t) = b.
$$

Then, the system (3.7) becomes

$$
\begin{aligned}
\frac{dx_1}{dt} &= \alpha x_1(1 - \beta x_1) - x_1 y_1, \\
\frac{dy_1}{dt} &= \lambda_1 - \theta_1 y_1 + \rho_1 y_1 M + \mu_1 y_1 u_1, \\
\frac{dz_1}{dt} &= \lambda_2 - \theta_2 z_1 + \rho_2 x_1 z_1, \qquad (3.8) \\
\frac{du_1}{dt} &= \mu_2 x_1 y_1 - \theta_3 u_1, \\
\frac{dM}{dt} &= b z_1 - bM.
\end{aligned}
$$

If we put $t - s = v$, then $M(t)$ can be written as

$$
M(t) = \int_0^\infty b e^{-bv} z_1(t - v) dv.
$$

It can be noted that the weight function of $z_1(t - v)$ is $b e^{-bv} = \frac{b}{e^{bv}}$ and monotonically decreasing with respect to v. The mean delay for the weight function $b e^{-bv}$ is

$$
\int_0^\infty v l_1(v) e^{-bv} dv = \frac{1}{b}.
$$

Thus, the immune activation depends on the density of Helper T cells at the present time t for large b. On the other hand, when b is sufficiently small, the activation depends also on the concentration of Helper T cells at the past time $t - v$.

3.5.1   Equilibria and their stability analysis

The system (3.8) has a tumor-free singular point

$$
E^\dagger = (x_1^\dagger, y_1^\dagger, z_1^\dagger, u_1^\dagger, M^\dagger) = \left(0, \frac{\lambda_1 \theta_2}{\theta_1 \theta_2 - \rho_1 \lambda_2}, \frac{\lambda_2}{\theta_2}, 0, \frac{\lambda_2}{\theta_2} \right).
$$

$E^\dagger$ exists when $\rho_1 < \rho_1^0$.
The system (3.8) has an interior singular point

$$
\begin{aligned}
E_1^\perp &= (x_1^\perp, y_1^\perp, z_1^\perp, u_1^\perp, M^\perp) \\
&= (x_1^\perp, y_1^\perp, z_1^\perp, u_1^\perp, z_1^\perp) \\
&= \left(x_1^\perp, \alpha(1 - \beta x_1^\perp), \frac{\lambda_2}{\theta_2 - \rho_2 x_1^\perp}, \frac{\alpha \mu_2 x_1^\perp (1 - \beta x_1^\perp)}{\theta_3}, \frac{\lambda_2}{\theta_2 - \rho_2 x_1^\perp} \right),
\end{aligned}
$$

55

and $x_1^\perp$ is the positive real root satisfying the equation

$$
\begin{aligned}
&(x_1^\perp)^4(\alpha^2\beta^2\mu_1\mu_2\rho_2) - \alpha^2\mu_1\mu_2(\beta^2\theta_2 + 2\beta\rho_2)(x_1^\perp)^3 + \\
&(2\alpha^2\beta\mu_1\mu_2\theta_2 + \alpha\beta\theta_1\theta_3\rho_2 + \alpha^2\mu_1\mu_2\rho_2)(x_1^\perp)^2 + \\
&(\alpha\beta\lambda_2\theta_3\rho_1 + \theta_3\lambda_1\rho_2 - \alpha\theta_1\theta_3\rho_2 - \alpha\beta\theta_1\theta_2\theta_3 - \alpha^2\mu_1\mu_2\theta_2)x_1^\perp + \\
&(\alpha\theta_1\theta_2\theta_3 - \lambda_1\theta_2\theta_3 - \alpha\lambda_2\theta_3\rho_1) = 0.
\end{aligned}
\tag{3.9}
$$

The nonnegative roots for the system (3.9) is already studied for equation (3.5). Now, we investigate the stability of the two biologically feasible singular points of $E^\dagger$ and $E^\perp$ for the system (3.8).

We compute Jacobian matrix $J(E)$ around the equilibrium point $E(x_1, y_1, z_1, u_1, M)$ for the system (3.8) is given by

$$
J(E) = \begin{bmatrix}
(\alpha - 2\alpha\beta x_1 - y_1) & -x_1 & 0 & 0 & 0 \\
0 & (-\theta_1 + \rho_1 M + \mu_1 u_1) & 0 & \mu_1 y_1 & \rho_1 y_1 \\
\rho_2 z_1 & 0 & (-\theta_2 + \rho_2 x_1) & 0 & 0 \\
\mu_2 y_1 & \mu_2 x_1 & 0 & -\theta_3 & 0 \\
0 & 0 & b & 0 & -b
\end{bmatrix}.
$$

Now, at the equilibrium point $E^\dagger\left(0, \frac{\lambda_1\theta_2}{\theta_1\theta_2 - \rho_1\lambda_2}, \frac{\lambda_2}{\theta_2}, 0, \frac{\lambda_2}{\theta_2}\right)$, the Jacobian matrix $J(E^\dagger)$ is given by

$$
J(E^\dagger) = \begin{bmatrix}
\alpha - \frac{\lambda_1\theta_2}{\theta_1\theta_2 - \rho_1\lambda_2} & 0 & 0 & 0 & 0 \\
0 & -\theta_1 + \rho_1\frac{\lambda_2}{\theta_2} & 0 & \mu_1\frac{\lambda_1\theta_2}{\theta_1\theta_2 - \rho_1\lambda_2} & \rho_1\frac{\lambda_1\theta_2}{\theta_1\theta_2 - \rho_1\lambda_2} \\
\rho_2\frac{\lambda_2}{\theta_2} & 0 & -\theta_2 & 0 & 0 \\
\mu_2\frac{\lambda_1\theta_2}{\theta_1\theta_2 - \rho_1\lambda_2} & 0 & 0 & -\theta_3 & 0 \\
0 & 0 & b & 0 & -b
\end{bmatrix}.
$$

The eigenvalues corresponding to the Jacobian matrix $J(E^\dagger)$ are given by

$$\epsilon_1^1 = \alpha - \frac{\lambda_1 \theta_2}{\theta_1 \theta_2 - \rho_1 \lambda_2},$$

$$\epsilon_2^1 = -\theta_1 + \rho_1 \frac{\lambda_2}{\theta_2} = \frac{\rho_1 \lambda_2 - \theta_1 \theta_2}{\theta_2} < 0, \quad [\text{since } (\theta_1 \theta_2 - \rho_1 \lambda_2) > 0],$$

$$\epsilon_3^1 = -\theta_2 < 0,$$

$$\epsilon_4^1 = -\theta_3 < 0,$$

$$\epsilon_5^1 = -b < 0.$$

For the system (3.8), it can be seen that all the eigenvalues are negative if and only if $\rho_1^1 < \rho_1 < \rho_1^0$. Thus, we have the following theorem.

Theorem 3.5.1. *The tumor-free singular point $E^\dagger$ of the system (3.8) is locally asymptotically stable if $\rho_1^1 < \rho_1 < \rho_1^0$.*

The Jacobian matrix of the system (3.8) at $E^\perp$ is given by

$$J(E^\perp) = \begin{bmatrix} \alpha - 2\alpha\beta x_1^\perp - y_1^\perp & -x_1^\perp & 0 & 0 & 0 \\ 0 & -\theta_1 + \rho_1 M^\perp + \mu_1 u_1^\perp & 0 & \mu_1 y_1^\perp & \rho_1 y_1^\perp \\ \rho_2 z_1^\perp & 0 & -\theta_2 + \rho_2 x_1^\perp & 0 & 0 \\ \mu_2 y_1^\perp & \mu_2 x_1^\perp & 0 & -\theta_3 & 0 \\ 0 & 0 & b & 0 & -b \end{bmatrix}.$$

The characteristic equation of $J(E^\perp)$ takes the form

$$\epsilon^5 + B_1 \epsilon^4 + B_2 \epsilon^3 + B_3 \epsilon^2 + B_4 \epsilon + B_5 = 0, \tag{3.10}$$

where

$$B_1 = b + b_1,$$

$$B_2 = b_2 + bb_1,$$

$$B_3 = bb_2 + b_3 - b_5, \quad (\text{where } b_5 = \rho_1 \rho_2 \delta_3 x_1^\perp y_1^\perp z_1^\perp)$$

$$B_4 = bb_3 + b_4 - b_5,$$

$$B_5 = bb_4.$$

According to the Routh-Hurwitz criterion, all the roots of equation (3.10) are negative or have negative real parts if and only if $B_i > 0$,

for i= 1 to 5, $B_1B_2 - B_3 > 0$, $(B_1B_2 - B_3)B_3 - B_1^2B_4 > 0$ and $(B_1B_2 - B_3)(B_3B_4 - B_2B_5) - (B_1B_4 - B_5)^2 > 0$.

From the expression, it is easy to verify that $B_1 > 0$.

Further, we can check that $B_1B_2 - B_3 > 0$. In fact, $B_1B_2 - B_3 = b^2b_1 + bb_1^2 + b_5 + (b_1b_2 - b_3) > 0$, since $b_1b_2 - b_3 > 0$ when $\Gamma > \Delta$. Thus, we have the following theorem.

Theorem 3.5.2. *The tumor-presence singular point $E^\perp$ of the system (3.8) is locally asymptotically stable if $\Gamma > \Delta$, $B_3 > 0$, $B_4 > 0$, $(B_1B_2 - B_3)B_3 - B_1^2B_4 > 0$ and $(B_1B_2 - B_3)(B_3B_4 - B_2B_5) - (B_1B_4 - B_5)^2 > 0$.*

We have also summarized the existence and stability criteria of the singular points of the systems (3.3) and (3.8) in Table 3.1.

Table 3.1: Community composition and the stability of singular points:

singular points	Non delay system (3.3)	Delay system (3.8)
Tumor-free singular point	Existence criterion: $\rho_1 < \rho_1^0$ Stability criterion: $\rho_1^1 < \rho_1 < \rho_1^0$	Existence criterion: $\rho_1 < \rho_1^0$ Stability criterion: $\rho_1^1 < \rho_1 < \rho_1^0$
Tumor-presence singular point	Existence criterion: Eq.(3.5) has a positive root with $x_1^1 < \min\{\frac{1}{\beta}, \frac{\theta_2}{\rho_2}\}$ Stability criterion: $\Gamma > \Delta$ and $(\Gamma - \Delta)b_3 > b_1^2b_4$	Existence criterion: Eq.(3.9) has a positive root with $x_1^\perp < \min\{\frac{1}{\beta}, \frac{\theta_2}{\rho_2}\}$ Stability criterion: $\Gamma > \Delta$, $B_3 > 0$, $B_4 > 0$, $(B_1B_2 - B_3)B_3 - B_1^2B_4 > 0$ and $(B_1B_2 - B_3)(B_3B_4 - B_2B_5) - (B_1B_4 - B_5)^2 > 0$

3.6   Hopf bifurcation analysis

In this section, we investigate Hopf bifurcation analysis for the model system (3.3), with respect to the recruitment rate λ_1 of activated CD8+ T cells.

Let us assume that $\sigma : (0, \infty) \to \mathbb{R}$ be a continuously differentiable function for λ_1, then we can write

$$\sigma(\lambda_1) = b_1(\lambda_1)b_2(\lambda_1)b_3(\lambda_1) - b_3^2(\lambda_1) - b_1^2(\lambda_1)b_4(\lambda_1). \qquad (3.11)$$

The assumptions for the occurrence of Hopf bifurcations are the usual ones and this is essential that $\sigma(\lambda_1) = \{\epsilon : D(\epsilon) = 0\}$ of the characteristic equation is such that :

(i) $\exists\, \lambda_1^* \in (0, \infty)$, at which a pair of imaginary eigenvalues $(\epsilon(\lambda_1^*),\ \bar{\epsilon}(\lambda_1^*)) \in \sigma(\lambda_1)$ are such that

$$Re\{\epsilon(\lambda_1^*)\} = 0, \qquad Im\{\epsilon(\lambda_1^*)\} = \omega_0 > 0,$$

and the transversality condition

$$\frac{d}{d\lambda_1}\left[Re\{\epsilon(\lambda_1)\}\right]\bigg|_{\lambda_1 = \lambda_1^*} \neq 0. \qquad (3.12)$$

(ii) All other elements of $\sigma(\lambda_1)$ have negative real parts. Mathematically, we can write the above two assumptions for Hopf bifurcation are as follows.

At an equilibrium point E^1, Hopf bifurcation occurs for $\lambda_1 = \lambda_1^* \in (0, \infty)$ if and only if

$$\sigma(\lambda_1^*) = 0, \qquad \frac{d}{d\lambda_1}\left[Re\{\epsilon(\lambda_1)\}\right]\bigg|_{\lambda_1 = \lambda_1^*} \neq 0, \qquad (3.13)$$

and all other eigenvalues are of negative real parts, where $\epsilon(\lambda_1)$ is purely imaginary at the threshold $\lambda_1 = \lambda_1^*$.

The existence of $\lambda_1^* \in (0, \infty)$ is ensured by solving the equation $\sigma(\lambda_1^*) = 0$. At $\lambda_1 = \lambda_1^*$, the characteristic equation (3.6) can be expressed as

$$\left(\epsilon^2 + \frac{b_3}{b_1}\right)\left(\epsilon^2 + b_1\epsilon + \frac{b_1 b_4}{b_3}\right) = 0.$$

The above equation has four roots, say ϵ_1, ϵ_2, ϵ_3, ϵ_4 with pair of purely complex roots at $\lambda_1 = \lambda_1^*$. Thus, we get

$$\epsilon_3 + \epsilon_4 = -b_1, \tag{3.14}$$

$$\omega_0^2 + \epsilon_3\epsilon_4 = b_2, \tag{3.15}$$

$$\omega_0^2(\epsilon_3 + \epsilon_4) = -b_3, \tag{3.16}$$

$$\omega_0^2\epsilon_3\epsilon_4 = b_4, \tag{3.17}$$

where $\omega_0 = Im\{\epsilon_1(\lambda_1^*)\}$. From the equations (3.14) and (3.16), we have

$$\omega_0^2 = \frac{b_3}{b_1}. \tag{3.18}$$

Since $\omega_0 > 0$, then we must have $b_3 > 0$ as $b_1 > 0$. Now, if ϵ_3 and ϵ_4 are complex conjugate, then from (3.14) it follows that $2Re\{\zeta_3\} = -b_1 < 0$. If they are real roots, then by equations (3.14) and (3.17), we have $\epsilon_3 < 0$, $\epsilon_4 < 0$ when $b_4 > 0$. To complete our discussion, we need to satisfy the transversality condition (3.12).

Since $\sigma(\lambda_1)$ is a continuously differentiable function of all its roots, then there exists an open interval $\lambda_1 \in (\lambda_1^* - \varepsilon, \lambda_1^* + \varepsilon)$, with $\epsilon > 0$. Let ϵ_1 and ϵ_2 are complex conjugate for λ_1. Suppose, their general forms in this neighborhood are

$$\epsilon_1(\lambda_1) = \beta_1(\lambda_1) + i\beta_2(\lambda_1), \tag{3.19}$$

$$\epsilon_2(\lambda_1) = \beta_1(\lambda_1) - i\beta_2(\lambda_1). \tag{3.20}$$

Now, we need to verify the transversality condition

$$\frac{d}{d\lambda_1}\left[Re\{\epsilon_j(\lambda_1)\}\right]\bigg|_{\lambda_1=\lambda_1^*} \neq 0; \text{ for } j = 1, 2. \tag{3.21}$$

Substituting $\epsilon_1(\lambda_1) = \beta_1(\lambda_1) + i\beta_2(\lambda_1)$ into the characteristic equation (3.6) and compute the differentiation, separating the real and imaginary parts, we have

$$A(\lambda_1)\beta_1' - B(\lambda_1)\beta_2' + C(\lambda_1) = 0,$$

$$B(\lambda_1)\beta_1' + A(\lambda_1)\beta_2' + D(\lambda_1) = 0,$$

where

$$
\begin{aligned}
A(\lambda_1) &= 4\beta_1^3 - 12\beta_1\beta_2^2 + 3b_1(\beta_1^2 - \beta_2^2) + 2b_2\beta_1 + b_3, \\
B(\lambda_1) &= 12\beta_1^2\beta_2 - 4\beta_2^3 + 6b_1\beta_1\beta_2 + 2b_2\beta_2, \\
C(\lambda_1) &= b_1\beta_1^3 - 3b_1'\beta_1\beta_2^2 + b_2'(\beta_1^2 - \beta_2^2) + b_3'\beta_1, \\
D(\lambda_1) &= 3b_1'\beta_1^2\beta_2 - b_1'\beta_2^3 + 2b_2'\beta_1\beta_2 + b_3'\beta_2.
\end{aligned}
$$

If $B(\lambda_1)D(\lambda_1) + A(\lambda_1)C(\lambda_1) \neq 0$ at the threshold $\lambda_1 = \lambda_1^*$, we have

$$
\frac{d}{d\lambda_1}\left[Re\{\epsilon_j(\lambda_1)\}\right]\Big|_{\lambda_1=\lambda_1^*} = \frac{B(\lambda_1^*)D(\lambda_1^*)+A(\lambda_1^*)C(\lambda_1^*)}{A^2(\lambda_1^*)+B^2(\lambda_1^*)} \neq 0.
$$

Therefore, the transversality condition holds for Hopf bifurcation is verified. We may summarized the above discussion in the form of the following theorem.

Theorem 3.6.1. *If the positive singular point E^1 of the system (3.3) exists, then the system around E^1 enters into the Hopf bifurcation at the critical value $\lambda_1 = \lambda_1^*$ provided $\sigma(\lambda_1^*) = 0$, $b_3\big|_{\lambda_1=\lambda_1^*} > 0$, $b_4\big|_{\lambda_1=\lambda_1^*} > 0$, $B(\lambda_1^*)D(\lambda_1^*) + A(\lambda_1^*)C(\lambda_1^*) \neq 0$.*

3.7 Numerical simulations

To check the feasibility of our analytical findings regarding stability conditions, we conduct some numerical computation using MATLAB and MATHEMATICA by choosing the parameters value specified in the Table 3.2. Here, recruitment rate λ_1 of CD8+T cells and the activation rate μ_1 of CD8+T cells due to IL-2 are two most important parameters under investigation. The main purpose of this section is to study the dynamical behavior of the systems [(3.3),(3.8)] for a wide range of above parameters value. For the parameter set in the Table 3.2, we have checked that the condition for the existence of the tumor-free singular point E^0 of system (3.3) is satisfied. For the CD8+T cells recruitment rate $\lambda_1 = 0.9$ and other parameters from Table 3.2, we have $\rho_1^1 = 0.169056$ and $\rho_1^0 = 0.388308$. Thus, the existence condition for tumor-free singular point E^0 is satisfied, that is, $\rho_1(= 0.18) < \rho_1^0$. In order to verify the stability condition for the tumor-free singular point E^0, we checked the statement of the Theorem 3.4.1. For $\lambda_1 = 0.9$ and other parameters value are in Table 3.2, we have $\rho_1^1 < \rho_1 < \rho_1^0$.

Table 3.2: Parameters for tumor-immune interaction model; their description and sources.

Par.	Description	Values	Source
α	Intrinsic growth rate of tumor cells	1.636	[110]
β	Maximum carrying capacity of tumor cells	0.7	[43]
λ_1	Recruitment rate of CD8+T cells	0.052	[46, 105]
θ_1	Natural death rate of CD8+T cells	0.9743	[69]
ρ_1	Activation rate of CD8+T cells by Helper T cells	0.18	fit to data
μ_1	Activation rate of CD8+T cells due to IL-2	0.7	fit to data
λ_2	Activation rate of Helper T cells	1.38	[18]
θ_2	Natural death rate of Helper T cells	0.55	[52]
ρ_2	Stimulation rate of Helper T cells due to tumor cells	0.08	[43]
μ_2	Production rate of IL-2 due to interaction between tumor cells and CD8+T cells	1.09	fit to data
θ_3	Degrade rate of IL-2	0.54	[61]
b	Nonnegative delay constant	1.04	fit to data

Numerically, we obtain the singular point $E^0(0,\ 1.72195,\ 2.50909,\ 0)$ and the corresponding eigenvalues are $-0.55,\ -0.54,\ -0.522664,\ -0.0859488$. It can be observed that all the eigenvalues of $J(E^0)$ are negative. Therefore, the tumor-free singular point E^0 for the system (3.3) is locally asymptotically stable (LAS).

For the existence of tumor-presence singular point E^1, we obtain a biquadratic equation (3.5) for tumor cells of the system (3.3). From the fourth-degree equation, it is clear that the equation (3.5) has at most four roots. For $\lambda_1 = 0.9$ and other parameters value are specified in Table 3.2, the equation (3.5) has a unique positive root $x_1^1 = 6.82384$ (See Figure 3.1(a)). For $\lambda_1 = 0.052$ and other parameters value are taken from Table 3.2, the equation (3.5) has two positive roots $x_1^1 = 0.244011$ and $x_1^2 = 6.82372$ (See Figure 3.1(b)). To get three positive roots $x_1^1 = 1.48454$, $x_1^2 = 1.74751$ and $x_1^3 = 6.69677$ (See the Figure 3.1(c)), we choose $\lambda_1 = 0.6$ and other

Figure 3.2: *The left panel (A) of the figures shows the time series evolution for the model system (3.3); the right panel (B) of the figures shows the time series evolution for the model system (3.8). For the left panel (A) parameters value are specified in the Table 3.2 and for right panel (B) $\rho_1 = 0.118$ and other parameters value are specified in the Table 3.2 with initial condition $x_1(0) = 0.3$, $y_1(0) = 1.37$, $z_1(0) = 2.61$, $u_1(0) = 0.67$ and $M(0) = 2.61$. The time series curves for the system (3.3) and (3.8) represent periodic oscillations.*

parameters value are specified in Table 3.2. If we choose $\lambda_1 = 0.0052$ and other parameters are specified in the Table 3.2, we get four positive roots $x_1^1 = 0.266121$, $x_1^2 = 1.22575$, $x_1^3 = 1.41656$ and $x_1^4 = 6.82372$ (See the Figure 3.1(d)).

3.7.1 Role of recruitment rate λ_1 of CD8+T cells

Now, we shall study the impact of one of the most important parameters, namely the recruitment rate λ_1 of CD8+T cells. At first, we set $\lambda_1 = 0.052$ and other parameters are specified in the Table 3.2, there exist a unique tumor-free E^0 and a unique tumor-presence E^1 singular point for the non delayed system (3.3) as well as a unique tumor-free $E^\dagger$ and a unique tumor-presence $E^\perp$ singular points for the delayed system (3.8). For the non delayed system (3.3), at $\lambda_1 = 0.052$, $E^0(0, 0.0994904, 2.50909, 0)$ has the following eigenvalues are 1.53651, -0.55, -0.54, -0.522664 and E^1
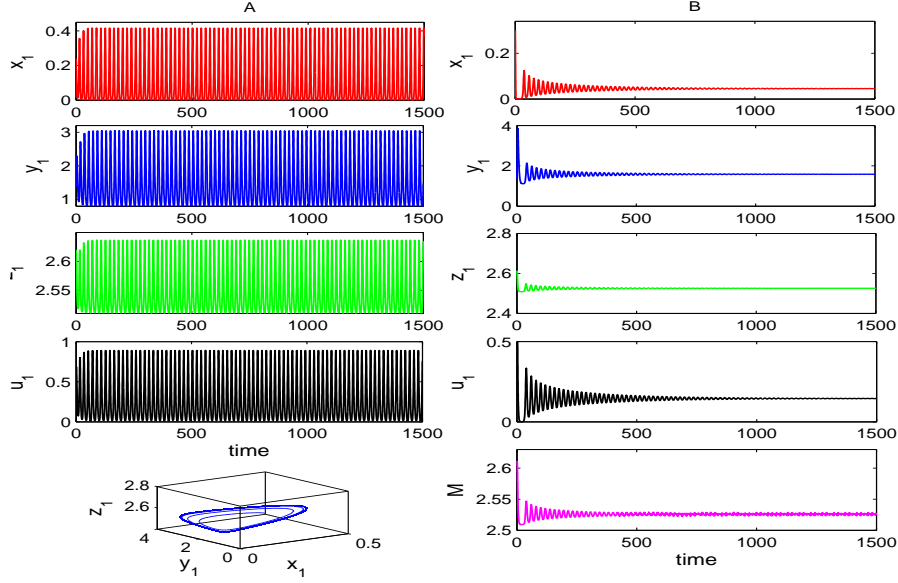
Figure 3.3: *The left panel (A) of the figures shows the time series evolution for the model system (3.3); the right panel (B) of the figures shows the time series evolution for the model system (3.8). $\lambda_1 = 0.39$ for left panel (A) and for right panel (B) $\lambda_1 = 0.39$, $\rho_1 = 0.248$ and other parameters value are specified in the Table 3.2, with initial condition $x_1(0) = 0.3$, $y_1(0) = 1.37$, $z_1(0) = 2.61$, $u_1(0) = 0.67$ and $M(0) = 2.61$. The time series curves for the system (3.3) represents periodic oscillations and (3.8) represents the locally asymptotically stability.*

(0.24401, 1.35656, 2.60142, 0.66816) has the following eigenvalues are -1.14178, -0.53076, 0.142144 ± 0.483779i. Also, for the delayed system (3.8), we set $\lambda_1 = 0.052$ and $\rho_1 = 0.118$, then $E^\dagger(0, 0.0766705, 2.50909, 0, 2.50909)$ has the following eigenvalues are 1.55933, -0.55, -0.54, -0.678227, -1.04 and $E^\perp(0.3575, 1.22659, 2.64672, 0.885133, 2.64672)$ has the following eigenvalues are -1.24128, -0.521843, -1.04, 0.124959 ± 0.4702591i. Thus, E^1 is periodic oscillation in nature which has been demonstrated in the left panel (A) of the Figure 3.2 and $E^\perp$ is also periodic oscillation in nature which has been shown in the right panel (B) of the Figure 3.2.

If we choose $\lambda_1 = 0.39$ and other parameters are in the Table 3.2, there exist one tumor-free E^0 and one tumor-presence E^1 equilibrium point for the non delayed system (3.3) as well as one tumor-free $E^\dagger$ and one tumor-presence $E^\perp$ equilibrium point for the delayed system (3.8). For the non delayed system (3.3), at $\lambda_1 = 0.39$, $E^0(0, 0.746178, 2.50909, 0)$
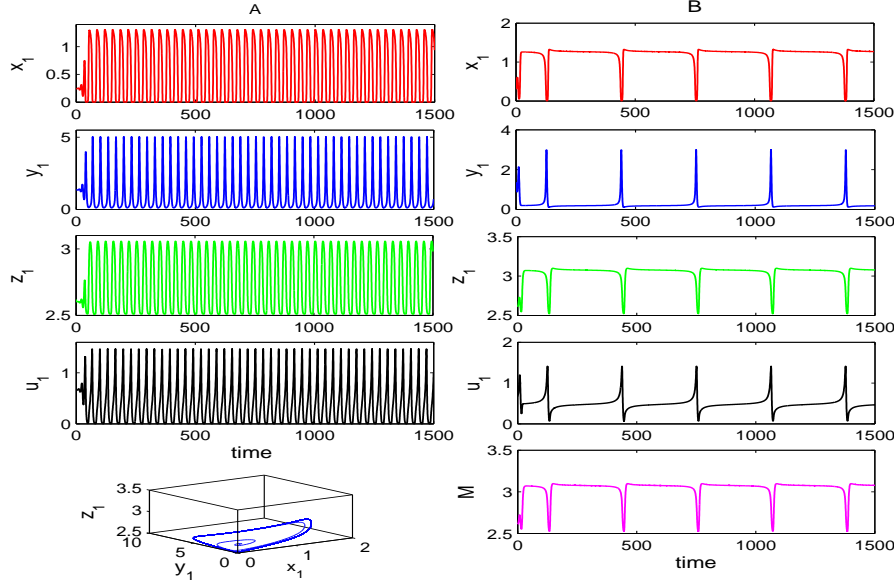
64
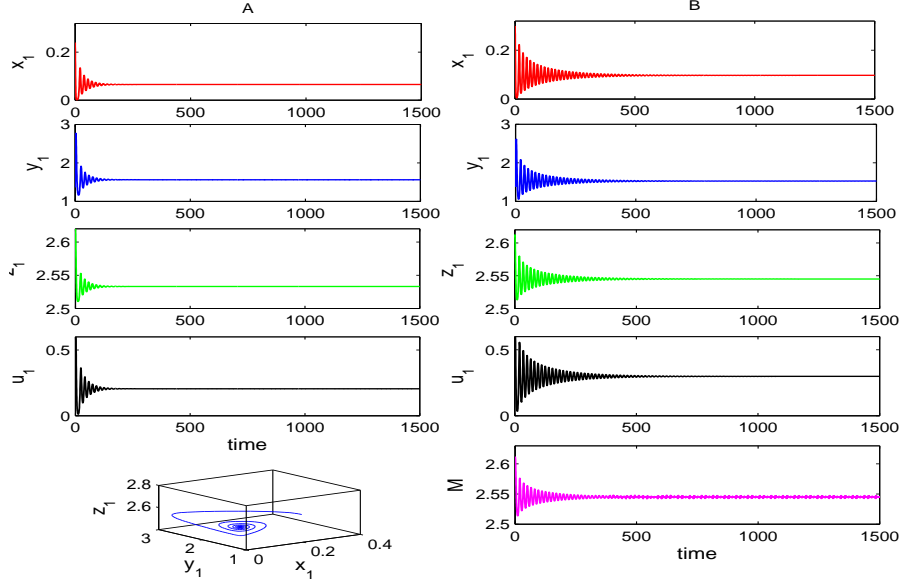
Figure 3.4: *The left panel (A) of the figures shows the time series evolution for the model system (3.3); the right panel (B) of the figures shows the time series evolution for the model system (3.8). $\lambda_1 = 0.585$ for left panel (A) and for right panel (B) $\lambda_1 = 0.585$, $\rho_1 = 0.15$ and other parameters value are specified in the Table 3.2, with initial condition $x_1(0) = 0.3$, $y_1(0) = 1.37$, $z_1(0) = 2.61$, $u_1(0) = 0.67$ and $M(0) = 2.61$. The time series curves for the system (3.3) and (3.8) represent the locally asymptotic stability.*

has the corresponding eigenvalues are 0.889822, -0.55, -0.54, -0.522664 and $E^1(0.120138, 1.49842, 2.55372, 0.363367)$ has the corresponding eigenvalues are -1.02884, -0.540379, $0.045488 \pm 0.452586i$. Also, for the delayed system (3.8), at $\lambda_1 = 0.39$ and $\rho_1 = 0.248$, $E^\dagger(0, 1.10781, 2.50909, 0, 2.50909)$ has the corresponding eigenvalues are 0.52819, -0.55, -0.54, -0.352046, -1.04 and $E^\perp(0.0454355, 1.58397, 2.52578, 0.145269, 2.52578)$ has the corresponding eigenvalues are -0.546169, -0.832104, -1.04, $-0.00317304 \pm 0.33723i$. Therefore, E^1 is unstable which has been plotted in the left panel (A) of the Figure 3.3 and $E^\perp$ is locally asymptotically stable which has been also plotted in the right panel (B) of the Figure 3.3.

If we set $\lambda_1 = 0.585$ and other parameters from Table 3.2, we obtain a tumor-free singular point $E^0 = (0, 1.11927, 2.50909, 0)$ and a unique interior singular point $E^1 = (0.0651269, 1.56142, 2.53309, 0.205264)$ and the corresponding eigenvalues for E^0 are given by $-0.55, -0.54, -0.522664,$ 0.51673. Also, the eigenvalues for the interior equilibrium point E^1 are given
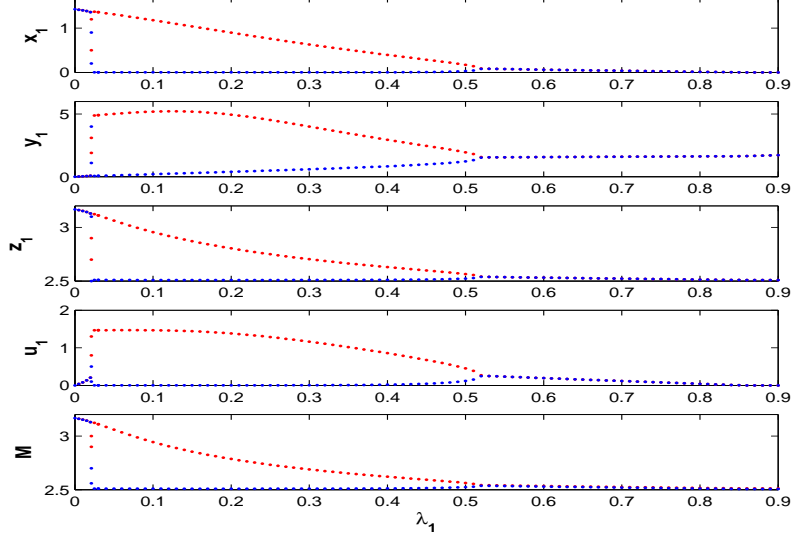
Figure 3.5: *Bifurcation diagram of the system (3.8) for tumor cells, CD8+T cells, Helper T cells, IL-2 with respect to the activation rate λ_1 of CD8+T cells and other parameters value are specified in the Table 3.2.*

by -0.93625, -0.544679, $-0.0265453 \pm 0.377604i$. Numerically, we have also checked the Routh-Hurwitz criteria $(b_1 b_2 - b_3) b_3 - b_1^2 b_4 = 0.0394294 > 0$. Numerically, We have also verified the Theorem 3.4.2 and obtained that $b_1 b_2 - b_3 = \Gamma - \Delta = 0.883444$ and $(\Gamma - \Delta) b_3 - b_1^2 b_4 = 0.0394294 > 0$ which ensure the asymptotic stability of the interior singular point E^1. From the eigenvalues of E^1 and the Theorem 3.4.2, it is clear that the tumor-presence singular point E^1 is locally asymptotically stable for $\lambda_1 = 0.585$. The left panel (A) of the Figure 3.4, shows that the tumor-presence singular point E^1 of the system (3.3) is locally asymptotically stable.

Now, we shall investigate the existence and local asymptotic stability for the delayed system (3.8). For $\lambda_1 = 0.585$, $\rho_1 = 0.15$ and other parameters from Table 3.2, the delayed system (3.8) has a unique tumor-free singular point $E^\dagger = (0, 0.978365, 2.50909, 0, 2.50909)$ and the corresponding eigenvalues are -0.55, -0.54, -0.597937, 0.657635, -1.04. Also, the delayed system (3.8) has a unique tumor-presence singular point $E^\perp = (0.0969665, 1.52495, 2.54499, 0.298477, 2.54499)$ with corresponding eigenvalues are -0.542198, -1.02123, -1.04, $-0.00673919 \pm 0.427909i$. In order to verify the Theorem 3.5.2 for the stability of $E^\perp$, we compute the followings for Routh-Hurwitz criteria: $B_1 = b + b_1 = 2.61691$, $B_2 = b_2 + bb_1 = 2.39792$, $B_3 = bb_2 + b_3 - b_5 = 1.07962$,

66

$B_4 = bb_3 + b_4 - b_5 = 0.404532$, $B_5 = bb_4 = 0.105468$. Also, we checked the expressions $B_1 B_2 - B_3 = 5.19551$, $(B_1 B_2 - B_3)B_3 - B_1^2 B_4 = 2.83885$ and $(B_1 B_2 - B_3)(B_3 B_4 - B_2 B_5) - (B_1 B_4 - B_5)^2 = 0.0466174$, which ensure the asymptotic stability of interior singular point $E^\perp$. The right panel (B) of Figure 3.4 demonstrates that the model system (3.8) is locally asymptotically stable around the positive interior singular point $E^\perp$.

If we gradually increase the recruitment rate λ_1 of CD8+T cells the tumor-presence singular point $E^\perp$ becomes stable to unstable (period-1 oscillation) around tumor-presence steady state, unstable to stable around tumor-presence steady state and finally, delayed system (3.8) becomes tumor-free $(E^\dagger)$ stable situation from the stable position around the tumor-presence steady state. Numerical simulation for the delayed system (3.8) shows that the tumor-presence singular point exists in stable nature for $\lambda_1 \in (0, 0.22]$. Tumor-presence system exhibits one periodic limit cycle oscillations in the range $0.023 \le \lambda_1 \le 0.522$ and the delayed system (3.8) becomes unstable round interior equilibrium point $E^\perp$. The delayed tumor-immune system (3.8) undergoes a stable situation around the positive interior steady-state $E^\perp$ for the interval $0.523 \le \lambda_1 < 0.856$. Finally, the delayed system (3.8) goes into the tumor-free stable situation from the stable situation around the interior equilibrium state for $\lambda_1 \ge 0.856$. Thus, there exist three threshold values for λ_1 which are denoted by $\lambda_1^0 \approx 0.023$, $\lambda_1^* \approx 0.523$ and $\lambda_1^c \approx 0.856$. Our numerical simulations suggest that the occurrence of oscillating behavior around tumor-presence singular point, a minimum threshold of recruitment rate $\lambda_1 (\approx 0.023)$ of CD8+T cell is required. The tumor-presence oscillations become stable when λ_1 crosses a critical value $\lambda_1^* \approx 0.523$. Thereafter, the tumor cannot present in the patient's body when λ_1 passing through the threshold λ_1^c. This result indicates that there is a maximum threshold of the recruitment rate λ_1^c (≈ 0.856) of CD8+T cells above which the tumor-presence situation cannot persist. Therefore, the recruitment rate can prevent the tumor-presence oscillations as well as makes tumor-free in the system. To make it more clear, we plot the bifurcation diagram (see the Figure 3.5) of the system (3.8) by considering λ_1 as a bifurcation parameter, we obtained that the delayed system (3.8) undergoes a Hopf bifurcation at the threshold value $\lambda_1^* = 0.523$. Analytically as well as numerical simulations, we obtain that $\frac{d}{d\lambda_1}[Re\{\zeta_j(\lambda_1)\}]\big|_{\lambda_1 = \lambda_1^*} = 0.146659 \ne 0$, which implies that the transversality condition for the Hopf bifurcation is satisfied.

It is clear from the bifurcation diagram that for lower threshold values for

λ_1 the system (3.8) is stable, but above the critical value of $\lambda_1 (= \lambda_1^0 \approx 0.023)$ the system losses its stability. If we further increase the magnitude of λ_1 and it crosses the critical value $\lambda_1^* \approx 0.523$ the system becomes stable through Hopf bifurcation. In the range of $0 < \lambda_1 < 0.856$, the growth of tumor cells are well controlled by our immune system, and the tumor is in benign state or non-invasive. For the range of $0.023 \leq \lambda_1 \leq 0.522$, the interaction between tumor and immune system leads to the periodic behavior of the model. For $0.523 \leq \lambda_1 \leq 0.856$, the model (3.8) has an exponential time domain behavior, reaching a stable critical point in the equilibrium state. This is similar to the spheroid tumor growth in the avascular phase, which is exponential and finally reaches the equilibrium state. We finally conclude that there is a critical value of recruitment rate λ_1 of CD8+T cells ($\lambda_1^{max} = \lambda_1^c \approx 0.856$), so that the tumor-presence interior steady-state switches from stable $E^\perp$ to stable tumor-free planar interior steady-state $E^\dagger$.

3.7.2 Effect of activation rate μ_1 of CD8+T cells due to IL-2 in both non delayed system (3.3) and delayed system (3.8)

Here, we shall study the impact of another most important parameter; the activation rate μ_1 of CD8+T cells due to IL-2. In order to check the stability, we vary the parameter μ_1 with fixed $\lambda_1 = 0.052$ and rest of the parameters are specified in the Table 3.2. If we consider $\mu_1 = 0.385$, then there exist a single tumor-free E^0 and a single tumor-presence E^1 singular point for non delayed system (3.3) as well as one tumor-free $E^\dagger$ and one tumor-presence $E^\perp$ equilibrium point for the delayed system (3.8). For the non delayed system (3.3) at $\mu_1 = 0.385$, $E^0(0, 0.0994904, 2.50909, 0)$ has the eigenvalues are 1.53651, -0.55, -0.54, -0.522664 and $E^1(0.553906, 1.00167, 2.72896, 1.11993)$ has the eigenvalues are -1.17093, -0.509026, $-0.0259931 \pm 0.326694i$. For delayed system (3.8) at $\mu_1 = 0.385$ and $\rho_1 = 0.197$, $E^\dagger(0, 0.108331, 2.50909, 0, 2.50909)$ has the eigenvalues are 0.55269, -0.55, -0.54, -1.04, -0.480009 and $E^\perp(0.462003, 1.10691, 2.68985, 1.03227, 2.68985)$ has the eigenvalues are -1.13228, -0.515322, -1.04, 0.00925187 $\pm 0.37525i$. Therefore, E^1 is stable and $E^\perp$ is unstable, which has been plotted the left panel (A) of the Figure 3.6 and right panel (B) of the Figure 3.6, respectively.

If we choose $\mu_1 = 0.49$ and other parameters are specified in the Table 3.2, there exist single tumor-presence singular point for non delayed
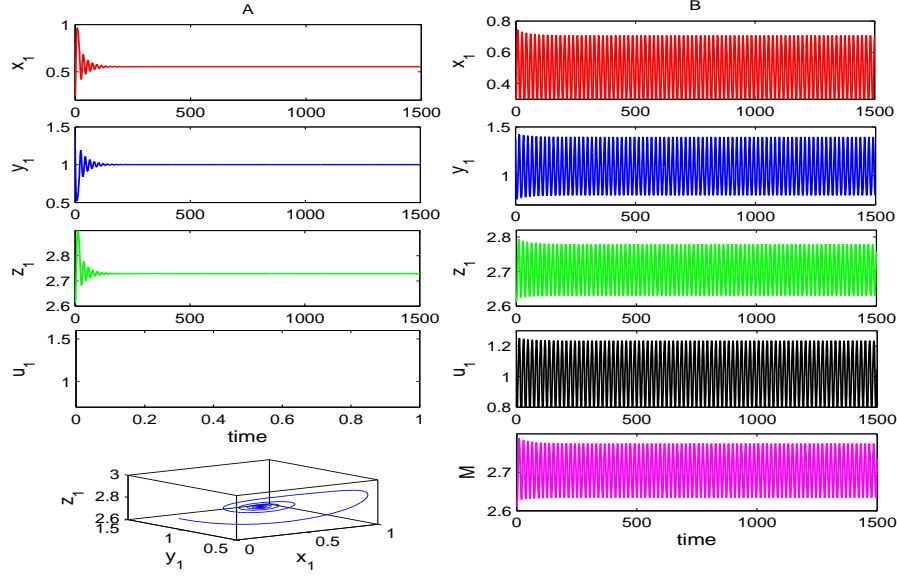
Figure 3.6: *The left panel (A) of the figures shows the time series evolution for the model system (3.3); the right panel (B) of the figures shows the time series evolution for the model system (3.8). $\mu_1 = 0.385$ for left panel (A) and for right panel (B) $\mu_1 = 0.385$, $\rho_1 = 0.197$ and other parameters value are specified in the Table 3.2, with initial condition $x_1(0) = 0.3$, $y_1(0) = 1.37$, $z_1(0) = 2.61$, $u_1(0) = 0.67$ and $M(0) = 2.61$. The time series curves for the system (3.3) represents the locally asymptotic stability and (3.8) represents the periodic oscillations.*

system (3.3) as well as a single tumor-presence $E^\perp$ equilibrium point for the delayed system (3.8). For the non delayed system (3.3) at $\mu_1 = 0.49$, $E^1(0.381849, 1.19871, 2.65665, 0.923926)$ has the eigenvalues are -1.15188, -0.520537, $-0.0661466 \pm 0.426065i$, which indicates the stable oscillating behavior. For delayed system (3.8) at $\mu_1 = 0.49$ and $\rho_1 = 0.117$, $E^\dagger(0, 0.0763879, 2.50909, 0, 2.50909)$ has the eigenvalues are 1.55961, -1.04, -0.680736, -0.55, -0.54. $E^\perp(1.3305, 0.112482, 3.1111, 0.302053, 3.1111)$ has the corresponding eigenvalues are -1.5366, -0.757572, -1.04, -0.437629, -0.237582. Thus, E^1 is unstable and $E^\perp$ is locally asymptotically stable, which has been demonstrated the left panel (A) of the Figure 3.7 and right panel (B) of the Figure 3.7, respectively. Here, we have also summarized some of the numerical results of the systems (3.3) and (3.8) in Table 3.3.

If we increase the activation rate μ_1 of CD8+T cells the tumor-presence singular point $E^\perp$ of the system (3.8) becomes stable to unstable state. In

69
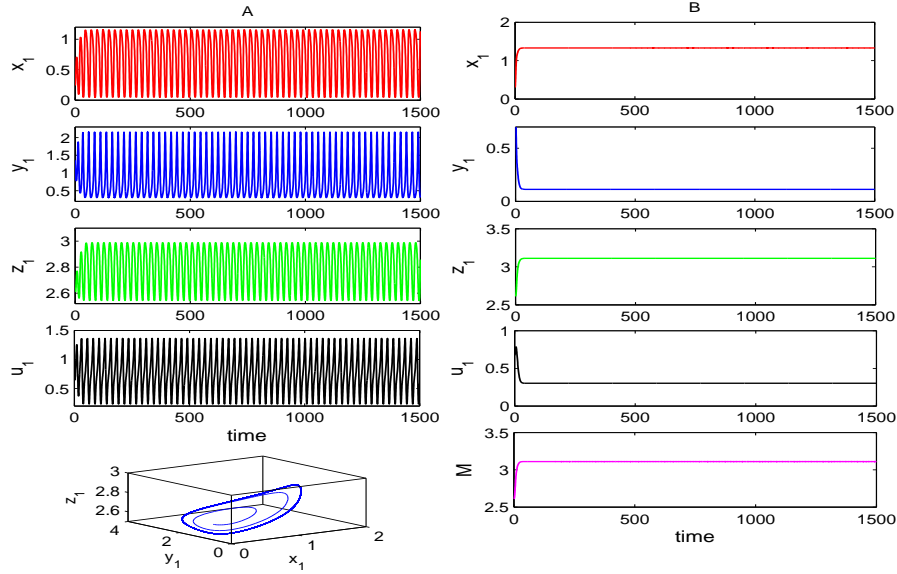
Figure 3.7: *The left panel (A) of the figures shows the time series evolution for the model system (3.3); the right panel (B) of the figures shows the time series evolution for the model system (3.8). $\mu_1 = 0.49$ for left panel (A) and for right panel (B) $\mu_1 = 0.49$, $\rho_1 = 0.117$ and other parameters value are specified in the Table 3.2, with initial condition $x_1(0) = 0.3$, $y_1(0) = 1.37$, $z_1(0) = 2.61$, $u_1(0) = 0.67$ and $M(0) = 2.61$. The time series curves for the system (3.3) represents periodic oscillations and (3.8) represents the locally asymptotically stability.*

order to understand this scenario, we plot the bifurcation diagram of the system (3.8) with respect to the parameter μ_1 (see the Figure 3.8). From the Figure 3.8, it is clear that the system (3.8) undergoes Hopf bifurcation at the threshold value $\mu_1 = 0.406$. From the bifurcation diagram, it can be observed that for lower values of μ_1 the system (3.8) is stable, but above the threshold value of $\mu_1 (= \mu_1^* = 0.406)$ the system losses its stability and periodic solution arises through Hopf bifurcation. In the range $0 < \mu_1 < 0.7$, the tumor cell growth is well controlled by the immune system, and the tumor is benign and non-invasive. For the range of $0 < \mu_1 < 0.406$, the system (3.8) has an exponential time domain behavior, acquiring a stable equilibrium point in the steady state. For the range of $0.406 < \mu_1 < 0.7$, the interplay between tumor and immune system leads to the periodic behavior of the model. The significance of Hopf bifurcations in this context is that at the bifurcation point, a limit cycle is formed around the singular point, thus resulting in stable periodic oscillations [103]. Existence of periodic solutions

70

Table 3.3: Dynamics of the systems (3.3) and (3.8) for different important parameters value and the other parameters are fixed as in Table 3.2:

Parameter value	Dynamics of Non delay system (3.3)	Dynamics of Delay system (3.8)
$\rho_1 = 0.118$	oscillatory behavior around E^1 (0.24401, 1.35656, 2.60142, 0.66816) with small period	oscillatory behavior around $E^\perp$(0.3575, 1.22659, 2.64672, 0.885133, 2.64672) with high enough period
$\lambda_1 = 0.39$, $\rho_1 = 0.248$	oscillatory behavior around E^1(0.120138, 1.49842, 2.55372, 0.363367)	stable nature at $E^\perp$(0.0454355, 1.58397, 2.52578, 0.145269, 2.52578)
$\lambda_1 = 0.585$, $\rho_1 = 0.15$	stable nature at E^1(0.0651269, 1.56142, 2.53309, 0.205264)	stable nature at $E^\perp$(0.0969665, 1.52495, 2.54499, 0.298477, 2.54499)
$\mu_1 = 0.385$, $\rho_1 = 0.197$	stable nature at E^1(0.553906, 1.00167, 2.72896, 1.11993)	oscillation nature around $E^\perp$(0.462003, 1.10691, 2.68985, 1.03227, 2.68985)
$\mu_1 = 0.49$, $\rho_1 = 0.117$	oscillation nature around E^1(0.381849, 1.19871, 2.65665, 0.923926)	stable nature at $E^\perp$(1.3305, 0.112482, 3.1111, 0.302053, 3.1111)

implies that tumor population may oscillate around the fixed point even in the absence of any treatment or drug. Such phenomena can be observed clinically and is known as Jeff's Phenomena [43, 103].

For better visualization of the stability dynamics of the delayed system (3.8), we draw the stability region of the singular points $E^\dagger$ and $E^\perp$. We draw the stability region of the delayed system (3.8) in $\mu_1 - \lambda_1$ parameter space (see the Figure 3.9). In Figure 3.9, the red shaded region (R_1) indicates the stability region of the tumor-presence singular point ($E^\perp$), the black region (R_2) indicates the limit cycle oscillation of the tumor-presence singular point ($E^\perp$) and the blue shaded region (R_3) indicates the stable region around the tumor-free singular point ($E^\dagger$). We observe that for the constant value of activation rate μ_1 of CD8+T cells, if the recruitment rate λ_1 of CD8+T cells is less than a maximum threshold value λ_1^c (≈ 0.856), the tumor-presence singular point stable or limit cycle oscillations nature

71
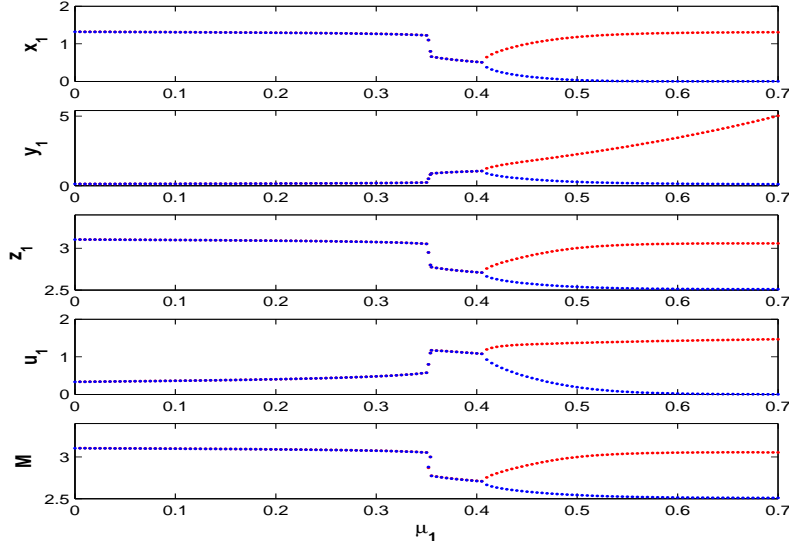
Figure 3.8: *Bifurcation diagram of the system (3.8) for tumor cells, CD8+T cells, Helper T cells, IL-2 with respect to the activation rate μ_1 of CD8+T cells due to IL-2 and other parameters value are specified in the Table 3.2.*

depending on sufficiently small (or higher) or moderate value of λ_1. If λ_1 is greater than a critical value of λ_1^c, then the system becomes tumor-free with stable nature. For the lower value of activation rate μ_1 of CD8+T cells, tumor cells exist within the system with stable nature when the recruitment rate λ_1 of CD8+T cells is less than λ_1^c. For $\lambda_1 < \lambda_1^c$, if the value of μ_1 is high enough, the system becomes tumor-presence with stable and oscillatory nature according to as the sufficiently small and large value of λ_1.

3.8 Conclusion

Nowadays, it is very important to take into account natural phenomena by introducing continuously distributed time delays in the description of the tumor-immune interaction model. A simple mathematical model can play an important role to describe the dynamics of tumor-immune interplays and help us for better understand the effect of distributed delay. The simple model is very interesting in the fact that it takes into account interplays of tumor cells, tumor-specific CD8+T cells, Helper T cells, immuno-stimulatory cytokine IL-2, and the continuously distributed time delay. We
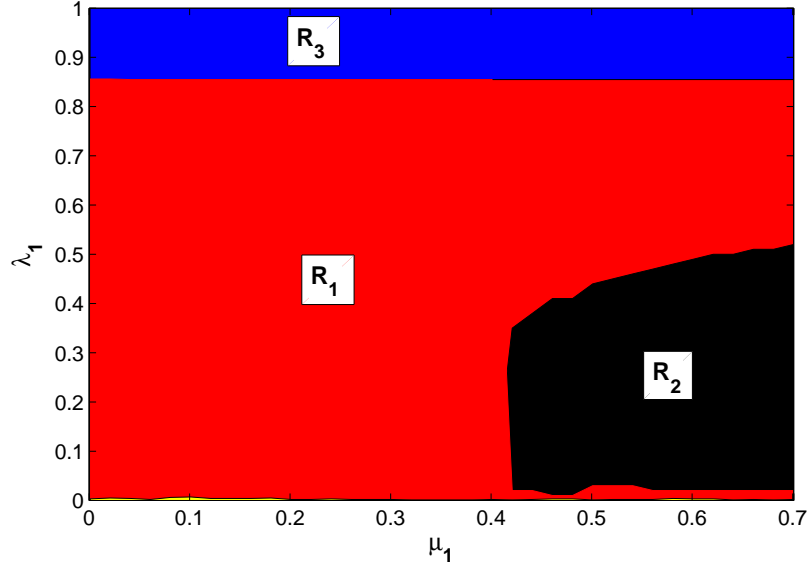
Figure 3.9: *Domain of stability and instability of the delayed system (3.8) in $\mu_1 - \lambda_1$ parameter space where other parameters value are specified in the Table 3.2. The horizontal axis represents the the activation rate μ_1 of CD8+T cells due to IL-2 and the vertical axis represents the recruitment rate λ_1 of CD8+T cells. The red region (R_1) depicts that the tumor-presence singular point $E^\perp$ is stable; the black region (R_2) depicts that the the tumor-presence singular point $E^\perp$ is one period oscillation in nature (unstable); on the other hand, the blue region (R_3) indicates the stability region of tumor-free singular point $E^\dagger$ is stable.*

prove preliminary results like existence, non negativity and boundedness of solutions for the system (3.3). We investigate the biologically feasible equilibrium points for the delayed and non delayed system. The novelty of this study is to incorporate a continuously distributed time delay by introducing a kernel function as an additional compartment, which can be regarded as the distributed immune activation delay. For understanding such complex biological scenarios, we performed extensive numerical simulations to validate the analytical findings.

In this study, we modified the system (3.3) by ignoring a weak immune activation of CD8+T cells due to interaction with tumor cells. Then, we incorporate a distributed time delay to the proliferation of CD8+T cells boosting by the Helper T cells, since the immune cells take more time to activate CD8+T cells [50, 110]. If we directly introduce the discrete

time delay term, it is difficult to compute the transcendent characteristic equation. Thus, we introduce a kernel function $M(t) = \int_0^\infty be^{-bv} z_1(t-v) dv$ as an additional compartment to model this immune activation delay effect. The immune activation depends on the density of Helper T cells at the present time t, when large b indicates a weak delay effect, meanwhile the system is more dependent on the past time $t - v$, while a small b indicates a strong delay effect. Then, we investigate the local asymptotic stability by establishing the well-known Routh-Hurwitz criterion. Our model system (3.8) undergoes Hopf bifurcation with respect to the recruitment rate λ_1 of CD8+T cells.

Next, we performed local asymptotic stability of the non delayed and delayed system (3.3) and (3.8), respectively. Numerically, we performed Hopf bifurcation analysis for two most important parameters λ_1 (recruitment rate of CD8+T cells) and μ_1 (CD8+T cells activation due to IL-2) for the model system (3.8) at the singular point $E^\perp$. If we increase the value of λ_1, then tumor-presence singular point $E^\perp$ becomes unstable from stable situation (one periodic oscillation), unstable to stable and finally, delayed system (3.8) goes into tumor-free $(E^\dagger)$ stable situation from the stable situation around the tumor-presence steady state. Thus, the recruitment rate can prevent the tumor-presence oscillation as well as makes tumor-free in the system. But, for increasing value of μ_1 the tumor-presence singular point $E^\perp$ of the system (3.8) goes from stable to unstable steady state. For better visualization of the stability dynamics of the delayed system (3.8), we draw the stability region of the delayed system (3.8) in $\mu_1 - \lambda_1$ parameter space. In order to make the model more useful in clinical applications, the parameters that have the most influence in the system dynamics under different situations, and their effects on the dynamics of the model were investigated in detail. We have shown that both the low and high tumor burden can have oscillatory dynamics. As the CD8+T cells recruitment rate λ_1 decreases, the interaction between tumor and their environment become more complex, and that leads to periodic oscillations. As the CD8+T cells activation rate μ_1 increases, the interaction between tumor and their environment become more complex, and that leads to periodic oscillations.

Our model system is very simple and does not take into account the biological complexity of tumor growth pattern such as genomic instability, expression for a given inhibition factor, etc. but focuses on the generic interplays between the different cell kinetics. The results of this work provide an initial analytical framework for studying tumor-immune interplays in combination with continuously distributed delay. In system (3.8), we

74

introduce the delay effect by a weak kernel, that is, $G(v) = be^{-bv}(b > 0)$. In future, we can incorporate the effect of delay by a non-monotone kernel, that is, $G(v) = b^r v e^{-bv}(b > 0)$ with $r > 0$.

Chapter 4

A mathematical model for tumor-immune competitive systems with multiple time delays †

4.1   Introduction

Cancer is increasingly becoming one of the leading causes of death throughout the world but our knowledge about its growth kinetics, prevention and eradication is still an enigma. According to the report by the Indian Council of Medical Research (ICMR), the estimated mortality due to cancer in India was 8.5 lakhs in 2020 [9]. This statistics emphasizes the ongoing significance of cancer as a major health issues in India. Cancer is characterized by the uncontrolled growth of cells, resulting in endless cell proliferation. There are three types of tumor cells like that benign, premalignant and malignant. Benign tumors are not cancerous and pose no harm, as they do not spread to other tissues or organs. Premalignant tumors, initially non-cancerous, can develop into cancer over time. Certain premalignant tumors may progress and evolve into malignant tumors, which can spread into neighboring cells.

The immune system is an intricate network composed of cells, tissues and organs that plays a significant role in defending the body against infections, diseases and foreign invaders. Its primary function is to identify and neutralize harmful substances such as bacteria, parasites, viruses and abnormal cells to maintain the body's health and integrity. Cytotoxic

---

†A considerable part of this chapter has been communicated.

T-lymphocytes (CD8+T cells), B-lymphocytes, natural killer cells (NK cells) and macrophages are referred as the effector cells [61] in the immune system. These specialized cells are play an important role in executing the immune response against pathogens, effectively neutralizing threats and maintaining the body's health and defense mechanisms. Dendritic cells, also known as antigen-presenting cells (APCs) are specialized immune cells that play a crucial role in initiating and modulating the immune response. By functioning as messengers between innate and adaptive immune responses, dendritic cells contribute significantly to the body's defense against infections and diseases, making them pivotal role in immune surveillance. After recognizing cancer cells, the immune system initiates its responses in human body. In many cases, the immune system can identify tumor cells; however, its response may not be sufficient to eliminate the tumor cells. This often results from the interaction between cancer cells and immune effector cells, which can be likened to a prey-predator relationship in the human body. The immune effector cells act as the predators targeting the cancer cells, while the cancer cells act as the prey. This dynamic interplay between the cancer cells and immune system highlights the complexity of cancer immunology and the challenges in developing effective immune-based therapies against cancer.

In the tumor-immune interaction model, cytokines play an important role. The present chapter describes the interaction among tumor cells, immune cells, as well as immuno-suppressive and immuno-stimulatory cytokines. IL-10 recognized as a Cytokine Synthesis Inhibitory Factor (CSIF), serves as an anti-inflammatory cytokine [27]. IL-10 is produced by several immune cells including macrophages, B cells and dendritic cells [67]. IL-12 serves as a pro-inflammatory cytokine generated by antigen-presenting cells, such as dendritic cells and macrophages [66]. When encountering foreign pathogens or antigens, dendritic cells and macrophages initiate an immune response by secreting IL-12. Then, this cytokine stimulates the activation of natural killer cells and T cells, promoting a robust immune defense against cancers. Regulatory T-cells, commonly known as Tregs play a vital role in immune regulation. One of their essential functions is to down-regulate CD8+T cell activation [97], which are responsible for targeting and eliminating infected or abnormal cells. Tregs achieve this by suppressing the proliferation and activation of CD8+T cells. The immuno-suppressive cytokine TGF-β is produced by white blood cells and tumor cells. TGF-β inhibits the activity of effector cells, particularly macrophages [4]. The cytokine IFN-γ is produced by several types of immune cells including cytotoxic T-lymphocytes, Helper T cells and natural killer cells [4, 63]. IFN-γ is a potent pro-inflammatory cytokine that plays a vital role

in enhancing the immune response against cancer cells and pathogens. It activates macrophages and enhances their ability to kill the cancer cells.

The immune activation against tumor proliferation involves a complex sequence of events and the response of immune cells may take time to reach its full potential after recognizing tumor cells. By incorporating time delays into our mathematical model, we can accurately represent the intricate and delayed nature of the immune response. Time delay plays an significant role in describing the interaction between immune cells, cytokines and tumor cells. The incorporation of time delays in our model is crucial for gaining a deeper understanding of the dynamics involved in tumor-immune interactions. There are mainly two types of time delays: distributed delay [88, 111] and discrete time delay [50, 89]. In this chapter, we are mainly interested in discrete time delay.

This chapter is structured as follows: Section 4.2 presents the development of a mathematical model that captures the interactions among tumor cells, immune cells, and cytokines. Additionally, we perform model simplification by considering the multiple time scales associated with tumor growth. Furthermore, we introduce three discrete time delays in our model. Section 4.3 discusses the basic properties of the system, which includes existence, uniqueness, positivity, boundedness and uniform persistence. Biologically feasible fixed points are obtained in this section. In Section 4.4, we performed stability analysis of the possible steady states for both the non delayed and delayed system. Furthermore, we establish the conditions for stability of Hopf bifurcation, investigate the direction of Hopf bifurcation and estimate the length of the time delay in this section. In Section 4.5, we discuss the parameter estimation techniques. In Section 4.6, we conduct numerical simulations of the proposed model in order to ensure our theoretical analysis. Finally, this chapter ends with a brief conclusion.

4.2   The mathematical model

A mathematical model for the tumor-immune interplays is formed in this section. Our mathematical model provides a structured framework for representing the complicated biological system, making it easier to understand the underlying mechanisms and their behavior. Our model comprises of a system of nine coupled ordinary differential equations (ODEs), namely tumor cells (T), CD8+T cells (T_8), macrophages (M), dendritic cells (D), regulatory T-cells or Tregs (T_g), interleukin-10 or IL-10 (I_{10}), transforming growth factor-β

or TGF-β (T_β), interleukin-12 or IL-12 (I_{12}) and interferon-γ or IFN-γ (I_γ). The proposed mathematical model for tumor-immune interplays is described by the following ODEs

$$
\begin{aligned}
\frac{dT}{dt} &= r_T T(1 - b_T T) - \frac{(\alpha_T' M + \gamma_T' T_8) T}{g_T' + I_{10}}, \\
\frac{dT_8}{dt} &= \frac{\alpha_8' I_{12}}{g_8' + T_g} - \delta_8 T_8, \\
\frac{dM}{dt} &= s_m + \frac{\alpha_m' I_\gamma}{(g_m' + I_\gamma)} \cdot \frac{1}{(g_{m1}' + T_\beta)} - \gamma_m MT - \delta_m M, \\
\frac{dD}{dt} &= s_d + \frac{\alpha_d T}{g_d + T} - \delta_d D, \\
\frac{dT_g}{dt} &= \alpha_g T_8 - \delta_g T_g, \\
\frac{dI_{10}}{dt} &= \alpha_{10} M - \delta_{10} I_{10}, \\
\frac{dT_\beta}{dt} &= s_\beta + \alpha_\beta T - \delta_\beta T_\beta, \\
\frac{dI_{12}}{dt} &= \alpha_{12} D - \delta_{12} I_{12}, \\
\frac{dI_\gamma}{dt} &= \alpha_\gamma T_8 - \delta_\gamma I_\gamma.
\end{aligned}
\tag{4.1}
$$

- The first equation in (4.1) describes the density of tumor cells at any time t. First term $r_T T(1 - b_T T)$ describes the logistic growth of tumor cells without any immune response [1], where r_T represents the intrinsic growth rate and the maximum carrying capacity of tumor cells is $\frac{1}{b_T}$. The second term designates the elimination of tumor cells due to interaction with macrophages [4] and CD8+T cells [65] with elimination rate α_T' and γ_T', respectively. The term g_T' represents the half saturation constant, where $\frac{1}{g_T' + I_{10}}$ serves as the major immuno-suppressive factor for both macrophages and CD8+T cells.

- Second equation of (4.1) describes the density of CD8+T cells, where the first term depicts the activation of CD8+T cells with activation rate α_8'. The activation of CD8+T cells relies on the presence of CD4+T cells, which are boosted by the cytokine IL-12 [66]. At the same time, the activation of CD8+T cells is suppressed by regulatory T-cells [97]. The natural death rate of CD8+T cells is δ_8.

- The density of macrophages is described in third equation of (4.1). s_m denotes the constant source rate of macrophages [67]. α_m' designates

the recruitment rate of macrophages due to the direct presence of IFN-γ, while $g_m^{'}$ denotes the half saturation constant [4, 67]. Meanwhile, the term $\frac{1}{g_{m1}^{'}+T_{\beta}}$ acts as a immuno-suppressive factor for macrophages, where $g_{m1}^{'}$ is the half-saturation constant. Third term delineates the inactivation of macrophages due to interaction with tumor cells at the rate γ_m [4] and δ_m is the natural death rate of macrophages.

- Fourth equation of (4.1) delineates the density of antigen-presenting dendritic cells. s_d is the constant source rate of dendritic cells [59]. The coefficient α_d incorporates the activation rate of dendritic cells due to the direct presence of tumor cells, where g_d is the half saturation constant followed by Michaelis-Menten kinetics [101]. Dendritic cell death rate is δ_d.

- Dynamics of Tregs is explained in the fifth equation of (4.1). Regulatory T-cells is produced from activated CD8+T cells [108] with activation term α_g and natural degradation rate of Tregs is δ_g.

- Sixth equation of the model (4.1) illustrates the density of anti-inflammatory cytokine IL-10. IL-10 is activated by macrophages [67] with activation rate α_{10} and δ_{10} is the decay rate of IL-10.

- Concentration of TGF-β is stated by the seventh equation of the model (4.1). s_{β} is the constant source rate of TGF-β [4]. The second term represents the source term, which is directly proportional to the size of the tumor cells, with α_{β} representing the release rate per tumor cell [63]. The last term accounts for the decay of immuno-suppressive cytokine TGF-β at a constant rate of δ_{β}.

- Density of IL-12 is expressed in eighth equation of (4.1). IL-12 is activated by dendritic cells, where α_{12} is the release rate per single antigen-specific dendritic cells [66]. The degradation rate of IL-12 is δ_{12}.

- The last equation of the system (4.1) is represented for the dynamics of IFN-γ. We assumed that IFN-γ is produced by CD8+T cells [4, 63] with production rate α_{γ}. The last term indicates the degradation of IFN-γ at a constant rate of δ_{γ}.

The system consists of nine coupled nonlinear ODEs with 29 parameters. To facilitate a comprehensive model analysis, we estimated these parameters from existing literatures.

4.2.1 Reduced model

Growth of tumor cells takes various time scale. Tumor cell proliferation happens over both long and short time scale, ranging from months to years and shorter time scales, ranging from weeks to months. The activation of CD8+T cells, macrophages and dendritic cells occurs over time span ranging from days to weeks. The secretion and degradation of both immuno-stimulatory and immuno-suppressive cytokines happen within a time frame of seconds to hours. To understand the interactive dynamics of the tumor-immune interaction system, we simplify our model by employing the quasi-steady-state approximations [92] for the concentrations of cytokines. According to the hypothesis, the cytokine equations, that is, from fifth to nine equation of (4.1) leads to

$$T_g = \frac{\alpha_g}{\delta_g}T_8, \ I_{10} = \frac{\alpha_{10}}{\delta_{10}}M, \ T_\beta = \frac{s_\beta}{\delta_\beta} + \frac{\alpha_\beta}{\delta_\beta}T,$$

$$I_{12} = \frac{\alpha_{12}}{\delta_{12}}D, \ I_\gamma = \frac{\alpha_\gamma}{\delta_\gamma}T_8.$$

After substituting these cytokine expressions into the first to fourth equation of (4.1), we derive the following four ODEs governing the tumor-immune interactive system

$$
\begin{aligned}
\frac{dT}{dt} &= r_T T(1 - b_T T) - \frac{(\alpha_T M + \gamma_T T_8)T}{g_T + M}, \\
\frac{dT_8}{dt} &= \frac{\alpha_8 D}{g_8 + T_8} - \delta_8 T_8, \\
\frac{dM}{dt} &= s_m + \frac{\alpha_m T_8}{(g_m + T_8)} \cdot \frac{1}{(g_{m1} + T)} - \gamma_m MT - \delta_m M, \\
\frac{dD}{dt} &= s_d + \frac{\alpha_d T}{g_d + T} - \delta_d D,
\end{aligned}
\tag{4.2}
$$

where

$$\alpha_T = \frac{\delta_{10}}{\alpha_{10}}\alpha_T', \quad \gamma_T = \frac{\delta_{10}}{\alpha_{10}}\gamma_T', \quad g_T = \frac{\delta_{10}}{\alpha_{10}}g_T', \quad \alpha_8 = \frac{\delta_g}{\alpha_g}\frac{\alpha_{12}}{\delta_{12}}\alpha_8',$$

$$g_8 = \frac{\delta_g}{\alpha_g}g_8', \quad \alpha_m = \frac{\delta_\beta}{\alpha_\beta}\alpha_m', \quad g_m = \frac{\delta_\gamma}{\alpha_\gamma}g_m', \quad g_{m1} = \frac{\delta_\beta}{\alpha_\beta}g_{m1}' + \frac{s_\beta}{\alpha_\beta}.$$

The system (4.2) has to be studied subject to the following positive initial

values:

$$T(0) = T_0 > 0, \quad T_8(0) = T_{80} > 0, \quad M(0) = M_0 > 0,$$

$$D(0) = D_0 > 0. \tag{4.3}$$

Our assumption considers all system parameters to be strictly positive.

4.2.2 Delayed model

In reality, the dynamical behavior of the system does not occur instantaneously; instead, it is influenced by the past history of the system. Therefore, it is essential to incorporate time delays into the model formulation to accurately reflect real-world scenarios. As we understand, the immune activation against tumor proliferation is very complicated and often delayed. After recognizing the tumor cells, our immune cells will require more time to provide a suitable response. Hence, it is necessary to incorporate the effect of time delay in our mathematical model to accurately describe the dynamics of the system. To enhance its compatibility with real-world scenarios, we have incorporated multiple discrete time delays into our model. Macrophages and CD8+T cells play an important role to eliminating tumor cells, but the activation of these effector cells is inhibited by the immuno-suppressive cytokine IL-10 [50]. These interactions do not occur instantaneously; instead, they are characterized by certain time lags. As a consequence, there is a delayed interaction between macrophages and CD8+T cells with tumor cells. Thus, we introduce discrete time delays τ_1 and τ_2, due to interaction delay between tumor cells and macrophages, tumor cells and CD8+T cells, respectively. During the interaction between tumor cells and macrophages, not only the tumor cells are destroyed, but macrophages are also inactivated by tumor cells. This process is not instantaneous but is instead followed by a time lag represented by τ_3 [50]. Therefore, we employ discrete time delays in our reduced model (4.2) and obtained the following system of coupled delay differential equations:

$$\frac{dT}{dt} = r_T T(1 - b_T T) - \frac{\alpha_T M(t - \tau_1)T(t - \tau_1)}{g_T + M(t - \tau_1)} - \frac{\gamma_T T_8(t - \tau_2)T(t - \tau_2)}{g_T + M(t - \tau_2)},$$

$$\frac{dT_8}{dt} = \frac{\alpha_8 D}{g_8 + T_8} - \delta_8 T_8, \qquad\qquad (4.4)$$

$$\frac{dM}{dt} = s_m + \frac{\alpha_m T_8}{(g_m + T_8)} \cdot \frac{1}{(g_{m1} + T)} - \gamma_m M(t - \tau_3)T(t - \tau_3) - \delta_m M,$$

$$\frac{dD}{dt} = s_d + \frac{\alpha_d T}{g_d + T} - \delta_d D.$$

The initial history of the delayed system (4.4) is satisfied within the interval $[-\max\{\tau_1,\ \tau_2,\ \tau_3\}, 0]$, as defined in the space

$$\mathcal{C}_+ = \{\varphi \in \mathcal{S}([-\tau_m, 0], \mathbb{R}_+^4) : \ T(\zeta) = \varphi_1(\zeta), \ T_8(\zeta) = \varphi_2(\zeta), \ M(\zeta) = \varphi_3(\zeta),$$
$$D(\zeta) = \varphi_4(\zeta)\}, \qquad\qquad (4.5)$$

where $\tau_m = \max_{i=1,2,3}\{\tau_i\}$ with $\varphi = (\varphi_1, \varphi_2, \varphi_3, \varphi_4) \in \mathcal{S}([-\tau_m, 0], \mathbb{R}_+^4)$, the Banach space of all continuous mapping in the interval $[-\tau_m, 0)$ to $\mathbb{R}_+^4$ for $\varphi_i(\zeta) \geq 0$ ($\zeta \in [-\tau_m, 0], i = 1, 2, 3$) and $(\varphi_1(0), \varphi_2(0), \varphi_3(0), \varphi_4(0)) > 0$, with $\mathbb{R}_+^4 = \{(T, T_8, M, D) : T > 0, T_8 > 0, M > 0, D > 0\}$.

4.3 Qualitative behavior of the delayed system

In this section, the existence and uniqueness property of the solution for the delayed model (4.4) will be studied. Additionally, an investigation will be carried out to determine whether the solution of the delayed model (4.4) remains positive and bounded. This aspect is crucial in a biological context, since the cell population must remain nonnegative and bounded to prevent uncontrolled growth.

4.3.1 Existence, uniqueness, positivity and boundedness

Proposition 4.3.1. *Every solution of (4.4) with initial history (4.5) exists, unique in $[0, \infty)$ and positive $\forall\ t \geq 0$.*

Proof. The delayed system (4.4) can be expressed in the vector form $G = (T, T_8, M, D)^T \in \mathbb{R}^4$ and

$$
G(Y) = \begin{pmatrix}
r_T T(1 - b_T T) - \frac{\alpha_T M(t-\tau_1)T(t-\tau_1)}{g_T + M(t-\tau_1)} - \frac{\gamma_T T_8(t-\tau_2)T(t-\tau_2)}{g_T + M(t-\tau_2)} \\
\frac{\alpha_8 D}{g_8 + T_8} - \delta_8 T_8 \\
s_m + \frac{\alpha_m T_8}{(g_m + T_8)} \cdot \frac{1}{(g_{m1} + T)} - \gamma_m M(t - \tau_3)T(t - \tau_3) - \delta_m M \\
s_d + \frac{\alpha_d T}{g_d + T} - \delta_d D
\end{pmatrix},
$$

where the mapping $G : \mathcal{C}_+ \to \mathbf{R}^4$ and $G \in C^\infty(\mathbf{R}^4)$, then our delayed system (4.4) reduces to

$$
\dot{Y} = G(Y), \tag{4.6}
$$

where $. \equiv \frac{d}{dt}$. Let $G(\zeta) = (\varphi_1(\zeta), \varphi_2(\zeta), \varphi_3(\zeta), \varphi_4(\zeta)) \in \mathcal{C}_+$ and $\varphi_i(\zeta) \geq 0, \forall$ $i = 1$ to 4 while $\zeta \in [-\tau_m, 0]$, where $\tau_m = \max_{i=1,2,3}\{\tau_i\}$. It is obvious that the vector function G is locally Lipschitz and continuous function of the variables T, T_8, M, D in the region $\Sigma = \{(T(t), T_8(t), M(t), D(t)) : T > 0, T_8 > 0, M > 0, D > 0\}$. Due to the Lemma [109], any solution of (T, T_8, M, D) of the delayed system (4.4) with initial history (4.5) exists and unique in the interval $[0, s_0], \forall\ t \geq 0$, where $0 < s_0 < \infty$. $\qquad\square$

Next, our objective is to demonstrate the boundedness of the solution for (4.4) concerning the initial history given in (4.5).

Proposition 4.3.2. *All solutions of (4.4) with respect to the initial history (4.5) is bounded $\forall\ t \geq 0$.*

Proof. From the first equation of (4.4), we have the following inequality

$$
\frac{dT}{dt} \leq r_T T(1 - b_T T).
$$

Using Kamke comparison theory [42], we obtain

$$
\limsup_{t \to \infty} T(t) \leq \frac{1}{b_T} = T_{\max}\ (say).
$$

Third equation of (4.4) can be written as

$$
\frac{dM}{dt} \leq s_m + \frac{\alpha_m T_8}{(g_m + T_8)} \cdot \frac{1}{(g_{m1} + T)} - \delta_m M
$$

$$
= s_m + \frac{\alpha_m}{(g_{m1} + T)} - \frac{\alpha_m g_m}{g_m + T_8} \cdot \frac{1}{(g_{m1} + T)} - \delta_m M
$$

$$
\Rightarrow \frac{dM}{dt} + \delta_m M \leq s_m + \frac{\alpha_m}{(g_{m1} + T)},
$$

84

which implies

$$\frac{dM}{dt} + \delta_m M \leq s_m + \frac{\alpha_m}{g_{m1}}, \quad \text{[by positiveness of } T\text{]}.$$

After some algebraic manipulation, we have

$$M \leq \frac{1}{\delta_m}\left(s_m + \frac{\alpha_m}{g_{m1}}\right) + c_m e^{-\delta_m t}, \quad [c_m \text{ is an arbitrary constant]}.$$

Thus, the maximum value of macrophages $M(t)$ is

$$\limsup_{t\to\infty} M(t) \leq \frac{1}{\delta_m}\left(s_m + \frac{\alpha_m}{g_{m1}}\right) = M_{\max} \; (say).$$

The last equation can be written as

$$\frac{dD}{dt} = s_d + \alpha_d - \frac{\alpha_d g_d}{g_d + T} - \delta_d D$$

$$\Rightarrow \frac{dD}{dt} + \delta_d D \leq s_d + \alpha_d.$$

Thus, the maximum value of dendritic cell $D(t)$ is

$$\limsup_{t\to\infty} D(t) \leq \frac{1}{\delta_d}(s_d + \alpha_d) = D_{\max} \; (say).$$

From second equation of (4.4), we have

$$\frac{dT_8}{dt} = \frac{\alpha_8 D}{g_8 + T_8} - \delta_8 T_8.$$

Above equation can be written as

$$\frac{dT_8}{dt} \leq \frac{\alpha_8 D_{\max}}{g_8 + T_8} - \delta_8 T_8.$$

Due to positiveness of T_8, we have

$$\frac{dT_8}{dt} + \delta_8 T_8 \leq \frac{\alpha_8 D_{\max}}{g_8}.$$

Then, the maximum value of CD8+T cells $T_8(t)$ is

$$\limsup_{t\to\infty} T_8(t) \leq \frac{\alpha_8 D_{\max}}{g_8 \delta_8} = T_{8\max} \; (say).$$

Therefore, the solution of our delayed system (4.4) is bounded in the region F defined as

$$F = \{(T(t), T_8(t), M(t), D(t)) \in \mathbb{R}_+^4 \; : \; 0 < T(t) \leq T_{\max}, \; 0 < T_8(t) \leq T_{8\max},$$
$$0 < M(t) \leq M_{\max}, \; 0 < D(t) \leq D_{\max}\}.$$

$\square$

4.3.2 Fixed points

The delayed system (4.4) has two biologically feasible steady states, namely (i) tumor-free fixed point

$$
\begin{aligned}
E^0 &\equiv (T^0,\ T_8^0,\ M^0,\ D^0) \\
&= \left(0,\ T_8^0,\ \frac{s_m g_{m1}(g_m + T_8^0) + \alpha_m T_8^0}{\delta_m g_{m1}(g_m + T_8^0)},\ \frac{s_d}{\delta_d}\right),
\end{aligned}
$$

where T_8^0 is the unique positive root of the given equation

$$
(T_8^0)^2 + g_8 T_8^0 - \frac{\alpha_8 s_d}{\delta_8 \delta_d} = 0, \tag{4.7}
$$

which implies

$$
T_8^0 = \frac{-g_8 + \sqrt{\left(g_8^2 + 4\frac{\alpha_8 s_d}{\delta_8 \delta_d}\right)}}{2}.
$$

(ii) Interior fixed point is $E^1(T^1, T_8^1, M^1, D^1)$. Finding the explicit form of the interior fixed point E^1 is a very difficult task. Hence, we find out its existence and stability by numerically.

4.3.3 Uniform persistence

In this subsection, we intend to show the uniform persistence of the system (4.4) without delay, that is, $\tau_1 = \tau_2 = \tau_3 = 0$.

Theorem 4.3.1. *The system (4.4) without delay, that is, $\tau_1 = \tau_2 = \tau_3 = 0$ is uniformly persistent if the interior fixed point exists and following sufficient conditions hold:*

$$
\begin{aligned}
(i)\ r_T &> \frac{\alpha_T M^0 + \gamma_T T_8^0}{G_T + M^0}, \quad (ii)\ \delta_8 = \frac{\alpha_8 D^0}{T_8^0(g_T + T_8^0)}, \\
(iii)\ \delta_m &= \frac{1}{M^0}\left(s_m + \frac{\alpha_m T_8^0}{g_{m1}(g_m + T_8^0)}\right), \quad (iv)\ \delta_d = \frac{s_d}{D^0}.
\end{aligned}
$$

Proof. To prove this theorem, we construct an average Lyapunov function $\Omega : \mathbb{R}_+^4 \to \mathbb{R}$ as follows:

$$
\Omega(T,\ T_8,\ M,\ D) = T^{\Omega_1} T_8^{\Omega_2} M^{\Omega_3} D^{\Omega_4},
$$

where $\Omega_1, \Omega_2, \Omega_3$ and Ω_4 are positive constants. We see that Ω is nonnegative function defined in $\mathbb{R}^4_+$. Then, we have

$$
\begin{aligned}
\Phi(T,\ T_8,\ M,\ D) \ &= \ \frac{\dot{\Omega}(T,\ T_8,\ M,\ D)}{\Omega(T,\ T_8,\ M,\ D)} = \Omega_1 \frac{\dot{T}}{T} + \Omega_2 \frac{\dot{T_8}}{T_8} + \Omega_3 \frac{\dot{M}}{M} + \Omega_4 \frac{\dot{D}}{D} \\
&= \ \Omega_1 \Big(r_T(1 - b_T T) - \frac{\alpha_T M + \gamma_T T_8}{g_T + M} \Big) + \Omega_2 \Big(\frac{\alpha_8 D}{T_8(g_8 + T_8)} - \delta_8 \Big) \\
&+ \ \Omega_3 \Big\{ \frac{1}{M} \Big(s_m + \frac{\alpha_m T_8}{(g_m + T_8)(g_{m1} + T)} \Big) - \gamma_m T - \delta_m \Big\} \\
&+ \ \Omega_4 \Big\{ \frac{1}{D} \Big(s_d + \frac{\alpha_d T}{g_d + T} \Big) - \delta_d \Big\}.
\end{aligned}
$$

It is enough to show that $\Phi(T,\ T_8,\ M,\ D) > 0$, to prove the uniform persistence of (4.4) without delay, that is, $\tau_1 = \tau_2 = \tau_3 = 0$, for a suitable choice of $\Omega_1,\ \Omega_2,\ \Omega_3,\ \Omega_4 > 0$. Then, we have following conditions

$$
\begin{aligned}
\Phi(E^0) \ &= \ \Phi(0,\ T_8^0,\ M^0,\ D^0) \\
&= \ \Omega_1 \Big(r_T - \frac{\alpha_T M^0 + \gamma_T T_8^0}{g_T + M^0} \Big) + \Omega_2 \Big(\frac{\alpha_8 D^0}{T_8^0(g_8 + T_8^0)} - \delta_8 \Big) \\
&+ \ \Omega_3 \Big\{ \frac{1}{M^0} \Big(s_m + \frac{\alpha_m T_8^0}{g_{m1}(g_m + T_8^0)} \Big) - \delta_m \Big\} + \Omega_4 \Big(\frac{s_d}{D^0} - \delta_d \Big) \\
&> \ 0.
\end{aligned}
$$

Above inequality holds, if the following sufficient conditions are satisfied

$$
(i)\ r_T \ > \ \frac{\alpha_T M^0 + \gamma_T T_8^0}{G_T + M^0}, \quad (ii)\ \delta_8 \ = \ \frac{\alpha_8 D^0}{T_8^0(g_T + T_8^0)},
$$

$$
(iii)\ \delta_m \ = \ \frac{1}{M^0} \Big(s_m + \frac{\alpha_m T_8^0}{g_{m1}(g_m + T_8^0)} \Big), \quad (iv)\ \delta_d \ = \ \frac{s_d}{D^0}.
$$

This completes the proof. $\qquad\qquad\qquad\qquad\qquad\qquad\qquad\qquad\qquad$ $\square$

4.4 Stability analysis and Hopf bifurcation

In this section, our goal is to determine the stability of the delayed system (4.4) at any point $E(T, T_8, M, D)$. We have linearized the delayed system (4.4) at the point E is given by

$$
\frac{dX}{dt} \ = \ A_1 X(t) + A_2 X(t - \tau_1) + A_3 X(t - \tau_2) + A_4 X(t - \tau_3), \quad (4.8)
$$

where

$$A_1 = \begin{pmatrix} r_T(1-2b_T T) & 0 & 0 & 0 \\ 0 & -\frac{\alpha_8 D}{(g_8+T_8)^2} - \delta_8 & 0 & \frac{\alpha_8}{g_8+T_8} \\ -\frac{\alpha_m T_8}{g_m+T_8} \cdot \frac{1}{(g_{m1}+T)^2} & \frac{\alpha_m g_m}{(g_m+T_8)^2} \cdot \frac{1}{g_{m1}+T} & -\delta_m & 0 \\ \frac{g_d \alpha_d}{(g_d+T)^2} & 0 & 0 & -\delta_d \end{pmatrix},$$

$$A_2 = \begin{pmatrix} -\frac{\alpha_T M}{g_T+M} & 0 & -\frac{\alpha_T g_T T}{(g_T+M)^2} & 0 \\ 0 & 0 & 0 & 0 \\ 0 & 0 & 0 & 0 \\ 0 & 0 & 0 & 0 \end{pmatrix},$$

$$A_3 = \begin{pmatrix} -\frac{\gamma_T T_8}{g_T+M} & -\frac{\gamma_T T}{g_T+M} & \frac{\gamma_T T_8 T}{(g_T+M)^2} & 0 \\ 0 & 0 & 0 & 0 \\ 0 & 0 & 0 & 0 \\ 0 & 0 & 0 & 0 \end{pmatrix},$$

$$A_4 = \begin{pmatrix} 0 & 0 & 0 & 0 \\ 0 & 0 & 0 & 0 \\ -\gamma_m M & 0 & -\gamma_m T & 0 \\ 0 & 0 & 0 & 0 \end{pmatrix},$$

and

$$X(.) = \begin{pmatrix} T(.) \\ T_8(.) \\ M(.) \\ D(.) \end{pmatrix}.$$

At the any point $E(T, T_8, M, D)$, the corresponding variational matrix of the linearized system (4.8) can be written as

$$J_E = \begin{pmatrix} j_1 + j_{11}e^{-\lambda \tau_1} + j_{111}e^{-\lambda \tau_2} & j_{12}e^{-\lambda \tau_2} & j_{13}e^{-\lambda \tau_1} + j_{131}e^{-\lambda \tau_2} & 0 \\ 0 & j_{22} & 0 & j_{24} \\ j_3 + j_{31}e^{-\lambda \tau_3} & j_{32} & j_{33} + j_{331}e^{-\lambda \tau_3} & 0 \\ j_{41} & 0 & 0 & j_{44} \end{pmatrix},$$

88

where

$$j_1 = r_T(1 - 2b_T T), \qquad j_{11} = -\frac{\alpha_T M}{g_T + M},$$

$$j_{111} = -\frac{\gamma_T T_8}{g_T + M}, \qquad j_{12} = -\frac{\gamma_T T}{g_T + M},$$

$$j_{13} = -\frac{\alpha_T g_T T}{(g_T + M)^2}, \qquad j_{131} = \frac{\gamma_T T_8 T}{(g_T + M)^2},$$

$$j_{22} = -\frac{\alpha_8 D}{(g_8 + T_8)^2} - \delta_8, \qquad j_{24} = \frac{\alpha_8}{g_8 + T_8},$$

$$j_3 = -\frac{\alpha_m T_8}{g_m + T_8} \cdot \frac{1}{(g_{m1} + T)^2}, \qquad j_{31} = -\gamma_m M,$$

$$j_{32} = \frac{\alpha_m g_m}{(g_m + T_8)^2} \cdot \frac{1}{g_{m1} + T}, \qquad j_{33} = -\delta_m,$$

$$j_{331} = -\gamma_m T, \qquad j_{41} = \frac{g_d \alpha_d}{(g_d + T)^2},$$

$$j_{44} = -\delta_d.$$

Then, the characteristic equation becomes

$$det(A_1 + A_2 e^{-\lambda \tau_1} + A_3 e^{-\lambda \tau_2} + A_4 e^{-\lambda \tau_3} - \lambda I_4) = 0,$$

where I_4 is the 4th order identity matrix. The above characteristic equation leads to

$$\Pi(\lambda, \tau_1, \tau_2, \tau_3) = a(\lambda) + b(\lambda)e^{-\lambda \tau_1} + c(\lambda)e^{-\lambda \tau_2} + d(\lambda)e^{-\lambda \tau_3}$$

$$+ \quad g(\lambda)e^{-\lambda(\tau_1+\tau_3)} + h(\lambda)e^{-\lambda(\tau_2+\tau_3)} = 0, \qquad (4.9)$$

where

$$a(\lambda) = \lambda^4 + a_1\lambda^3 + a_2\lambda^2 + a_3\lambda + a_4,$$
$$b(\lambda) = b_1\lambda^3 + b_2\lambda^2 + b_3\lambda + b_4,$$
$$c(\lambda) = c_1\lambda^3 + c_2\lambda^2 + c_3\lambda + c_4,$$
$$d(\lambda) = d_1\lambda^3 + d_2\lambda^2 + d_3\lambda + d_4,$$
$$g(\lambda) = g_1\lambda^2 + g_2\lambda + g_3,$$
$$h(\lambda) = h_1\lambda^2 + h_2\lambda + h_3,$$

with

$$a_1 = -j_1 - j_{22} - j_{33} - j_{44},$$

$$a_2 = j_1 j_{22} + j_1 j_{33} + j_1 j_{44} + j_{22} j_{33} + j_{22} j_{44} + j_{33} j_{44},$$

$$a_3 = -j_1 j_{33} j_{44} - j_1 j_{22} j_{33} - j_1 j_{22} j_{44} - j_{22} j_{33} j_{44},$$

$$a_4 = j_1 j_{22} j_{33} j_{44},$$

$$b_1 = -j_{11},$$

$$b_2 = j_{11} j_{22} + j_{11} j_{33} + j_{11} j_{44} - j_3 j_{13},$$

$$b_3 = -j_{11} j_{22} j_{33} - j_{11} j_{22} j_{44} - j_{11} j_{33} j_{44} + j_3 j_{13} j_{22} + j_3 j_{13} j_{44},$$

$$b_4 = j_{11} j_{22} j_{33} j_{44} - j_{13} j_{24} j_{32} j_{41},$$

$$c_1 = -j_{111},$$

$$c_2 = j_{22} j_{111} + j_{33} j_{111} + j_{44} j_{111} - j_3 j_{131},$$

$$c_3 = -j_{12} j_{24} j_{41} - j_{22} j_{33} j_{111} - j_{22} j_{44} j_{111} - j_{33} j_{44} j_{111} + j_3 j_{22} j_{131} + j_3 j_{44} j_{131},$$

$$c_4 = j_{12} j_{24} j_{33} j_{41} + j_{22} j_{33} j_{44} j_{111} - j_{24} j_{32} j_{41} j_{131},$$

$$d_1 = -j_{331},$$

$$d_2 = j_1 j_{331} + j_{22} j_{331} + j_{44} j_{331},$$

$$d_3 = -j_1 j_{22} j_{331} - j_1 j_{44} j_{331} - j_{22} j_{44} j_{331},$$

$$d_4 = j_1 j_{22} j_{44} j_{331},$$

$$g_1 = j_{11} j_{331} - j_{13} j_{31},$$

$$g_2 = -j_{11} j_{22} j_{331} - j_{11} j_{44} j_{331} + j_{13} j_{22} j_{31} + j_{13} j_{31} j_{44},$$

$$g_3 = j_{11} j_{22} j_{44} j_{331},$$

$$h_1 = j_{111} j_{331} - j_{31} j_{131},$$

$$h_2 = j_{22} j_{31} j_{131} + j_{31} j_{44} j_{131} - j_{22} j_{111} j_{331} - j_{44} j_{111} j_{331},$$

$$h_3 = j_{12} j_{24} j_{41} j_{331} + j_{22} j_{44} j_{111} j_{331}.$$

We observed that the equation (4.9) is transcendental in λ. We shall investigate the local stability analysis of the delayed and non-delayed system around the interior fixed point $E^1(T^1, T_8^1, M^1, D^1)$ by investigating the sign of real parts of the roots of (4.9). It is well-known that the interior fixed point E^1 will be locally asymptotically stable if and only if all the roots of (4.9) are negative or have negative real parts. The transcendental equation

governing our system will result in an infinite number of roots. Therefore, the Routh-Hurwitz criteria fails for local stability analysis of the delayed system.

Case 1: $\tau_1 = \tau_2 = \tau_3 = 0.$

If there are no delays, we can represent the characteristics equation (4.9) as follows

$$\lambda^4 + p_1\lambda^3 + p_2\lambda^2 + p_3\lambda + p_4 = 0, \tag{4.10}$$

with

$$
\begin{aligned}
p_1 &= a_1 + b_1 + c_1 + d_1, \\
p_2 &= a_2 + b_2 + c_2 + d_2 + g_1 + h_1, \\
p_3 &= a_3 + b_3 + c_3 + d_3 + g_2 + h_2, \\
p_4 &= a_4 + b_4 + c_4 + d_4 + g_3 + h_3.
\end{aligned}
$$

The classical Routh-Hurwitz criteria will be applied to determine the sign of the roots of the characteristic equation (4.10). Thus, we have following theorem.

Theorem 4.4.1. *At the interior fixed point $E^1(T^1, T_8^1, M^1, D^1)$, the system (4.4) (without delay) will be locally asymptotically stable, if the conditions $p_1 > 0$, $p_4 > 0$, $P_1 = p_1 p_2 - p_3 > 0$ and $P_2 = (p_1 p_2 - p_3)p_3 - p_1^2 p_4 > 0$ hold.*

Case 2: $\tau_1 > 0, \tau_2 = \tau_3 = 0.$

Let us consider, the time delay between tumor cells and macrophages, that is, $\tau_1 > 0$ and $\tau_2 = \tau_3 = 0$, then the characteristic equation (4.9) becomes

$$
\begin{aligned}
\Pi(\lambda, \tau_1, 0, 0) &= \lambda^4 + q_1\lambda^3 + q_2\lambda^2 + q_3\lambda + q_4 \\
&+ e^{-\lambda\tau_1}(l_1\lambda^3 + l_2\lambda^2 + l_3\lambda + l_4) = 0, \tag{4.11}
\end{aligned}
$$

where

$$q_1 = a_1 + c_1 + d_1,$$

$$q_2 = a_2 + c_2 + d_2 + h_1,$$

$$q_3 = a_3 + c_3 + d_3 + h_2,$$

$$q_4 = a_4 + c_4 + d_4 + h_3,$$

$$l_1 = b_1,$$

$$l_2 = b_2 + g_1,$$

$$l_3 = b_3 + g_2,$$

$$l_4 = b_4 + g_3.$$

The equation (4.11) reduces to the equation (4.10) for $\tau_1 = 0$ and the conditions of Theorem (4.4.1) hold for the local asymptotically stability at the fixed point $E^1(T^1, T_8^1, M^1, D^1)$. But, our aim is to investigate the system (4.11) in presence of time delay, that is, $\tau_1 > 0$. If the roots of the equation (4.11) crosses imaginary axis, then the stability around the fixed point $E(T, T_8, M, D)$ will change. Now, we substituting $\lambda = i\theta$ ($\theta > 0$), into the system (4.11) and separating real and imaginary parts, we get

$$\theta^4 - q_2\theta^2 + q_4 = (l_2\theta^2 - l_4)\cos(\theta\tau_1) + (l_1\theta^3 - l_3\theta)\sin(\theta\tau_1),$$

$$-q_1\theta^3 + q_3\theta = (l_1\theta^3 - l_3\theta)\cos(\theta\tau_1) - (l_2\theta^2 - l_4)\sin(\theta\tau_1). \quad (4.12)$$

Squaring and adding above equations, we have

$$\theta^8 + s_1\theta^6 + s_2\theta^4 + s_3\theta^2 + s_4 = 0, \quad (4.13)$$

with

$$s_1 = q_1^2 - 2q_2 - l_1^2,$$

$$s_2 = q_2^2 + 2q_4 - 2q_1q_3 - l_2^2 + 2l_1l_3,$$

$$s_3 = q_3^2 - 2q_2q_4 + 2l_2l_4 - l_3^2,$$

$$s_4 = q_4^2 - l_4^2.$$

Substituting $\theta^2 = \eta$ in the equation (4.13), then we get the following biquadratic equation

$$K(\eta) = \eta^4 + s_1\eta^3 + s_2\eta^2 + s_3\eta + s_4 = 0. \quad (4.14)$$

If $s_4 = q_4^2 - l_4^2 < 0$, then $K(0) < 0$ and $K(+\infty) = +\infty$, which means that the equation (4.14) has at least one positive root. Then, we can say that there is a unique positive root η_0 satisfying the equation (4.14). Consequently, the equation (4.13) has at least one positive root denoted by θ_0. Since θ_0 is a root of the system (4.13), then the characteristic equation (4.11) has a purely imaginary roots of the form $\pm i\theta_0$. Solving the both equations of (4.12), we get

$$\tan(\theta\tau_1) = \frac{(\theta^4 - q_2\theta^2 + q_4)(l_1\theta^3 - l_3\theta) - (q_3\theta - q_1\theta^3)(l_2\theta^2 - l_4)}{(\theta^4 - q_2\theta^2 + q_4)(l_2\theta^2 - l_4) + (q_3\theta - q_1\theta^3)(l_1\theta^3 - l_3\theta)}.$$

Then, τ_1^c corresponding to θ_0 is given by

$$\tau_1^c = \frac{1}{\theta_0} \arctan\left[\frac{(\theta_0^4 - q_2\theta_0^2 + q_4)(l_1\theta_0^3 - l_3\theta_0) - (q_3\theta_0 - q_1\theta_0^3)(l_2\theta_0^2 - l_4)}{(\theta_0^4 - q_2\theta_0^2 + q_4)(l_2\theta_0^2 - l_4) + (q_3\theta_0 - q_1\theta_0^3)(l_1\theta_0^3 - l_3\theta_0)}\right]$$

$$+ \frac{2\pi c}{\theta_0}, \quad c = 0, 1, 2, ... \tag{4.15}$$

For $\tau_1^c = 0$, the interior fixed point E^1 will be locally asymptotically stable, if the conditions of Theorem 4.4.1 hold. Due to Butler's lemma [31], we can say that E^1 will remain stable for $\tau_1 < \tau_1^c$. To study the Hopf bifurcation, we shall verify the transversality condition $\left[\frac{d(Re\lambda)}{d\tau_1}\right]_{\tau_1=\tau_1^c} > 0$. It implies the existence of at least one eigenvalue with a positive real part, fulfilling $\tau_1 > \tau_1^c$. It is necessary to verify the transversality condition

$$\Theta = sign\left[\frac{d(Re\lambda)}{d\tau_1^c}\right]_{\lambda=i\theta_0} = sign\left[Re\left(\frac{d\lambda}{d\tau_1^c}\right)^{-1}\right]_{\lambda=i\theta_0}.$$

Differentiate the equation (4.11) with respect to τ_1, we have

$$\left[(4\lambda^3 + 3q_1\lambda^2 + 2q_2\lambda + q_3) + e^{-\lambda\tau_1}(3l_1\lambda^2 + 2l_2\lambda + l_3)\right.$$

$$\left. - \tau_1 e^{-\lambda\tau_1}(l_1\lambda^3 + l_2\lambda^2 + l_3\lambda + l_4)\right]\frac{d\lambda}{d\tau_1}$$

$$= (l_1\lambda^3 + l_2\lambda^2 + l_3\lambda + l_4)\lambda e^{-\lambda\tau_1},$$

which implies that

$$\left(\frac{d\lambda}{d\tau_1}\right)^{-1} = \frac{4\lambda^3 + 3q_1\lambda^2 + 2q_2\lambda + q_3}{-\lambda(\lambda^4 + q_1\lambda^3 + q_2\lambda^2 + q_3\lambda + q_4)} + \frac{3l_1\lambda^2 + 2l_2\lambda + l_3}{\lambda(l_1\lambda^3 + l_2\lambda^2 + l_3\lambda + l_4)}$$

$$- \frac{\tau_1}{\lambda}.$$

93

At the point $\tau_1 = \tau_1^c$, (that is, $\lambda = i\theta_0$), we calculate

$$
\begin{aligned}
\Theta &= sign\left[Re\left(\frac{4\lambda^3 + 3q_1\lambda^2 + 2q_2\lambda + q_3}{-\lambda(\lambda^4 + q_1\lambda^3 + q_2\lambda^2 + q_3\lambda + q_4)}\right.\right.\\
&\quad + \left.\left.\frac{3l_1\lambda^2 + 2l_2\lambda + l_3}{\lambda(l_1\lambda^3 + l_2\lambda^2 + l_3\lambda + l_4)} - \frac{\tau_1}{\lambda}\right)\right]_{\lambda = i\theta_0}\\
&= \frac{1}{\theta_0}sign\left[Re\left(\frac{(-3q_1\theta_0^2 + q_3) + i(-4\theta_0^3 + 2q_2\theta_0)}{(-q_1\theta_0^3 + q_3\theta_0) - i(\theta_0^4 - q_2\theta_0^2 + q_4)}\right.\right.\\
&\quad + \left.\left.\frac{(-3l_1\theta_0^2 + l_3) + i.2l_2\theta_0}{(l_1\theta_0^3 - l_3\theta_0) + i(-l_2\theta_2^2 + l_4)} - \frac{\tau_1}{i\theta_0}\right)\right]\\
&= \frac{1}{\theta_0}sign\left[\left(\frac{(-3q_1\theta_0^2 + q_3)(-q_1\theta_0^3 + q_3\theta_0) - (-4\theta_0^3 + 2q_2\theta_0)(\theta_0^4 - q_2\theta_0^2 + q_4)}{(-q_1\theta_0^3 + q_3\theta_0)^2 + (\theta_0^4 - q_2\theta_0^2 + q_4)^2}\right.\right.\\
&\quad + \left.\left.\frac{(-3l_1\theta_0^2 + l_3)(l_1\theta_0^3 - l_3\theta_0) + 2l_2\theta_0(-l_2\theta_0^2 + l_4)}{(l_1\theta_0^3 - l_3\theta_0)^2 + (-l_2\theta_0^2 + l_4)^2}\right].
\end{aligned}
$$

After calculating both equations of (4.12), we get

$$
(-q_1\theta_0^3 + q_3\theta_0)^2 + (\theta_0^4 - q_2\theta_0^2 + q_4)^2 = (l_1\theta_0^3 - l_3\theta_0)^2 + (-l_2\theta_0^2 + l_4)^2.
$$

By using above condition and after some algebraic manipulation, we have

$$
\Theta = sign\left[\frac{4\theta_0^6 + 3s_1\theta_0^4 + 2s_2\theta_0^2 + s_3}{(l_1\theta_0^3 - l_3\theta_0)^2 + (-l_2\theta_0^2 + l_4)^2}\right], \quad (s_1, s_2 \text{ and } s_3 \text{ has been stated before}).
$$

Using equation (4.14), we obtain

$$
\Theta = \frac{sign\{K'(\theta_0^2)\}}{(l_1\theta_0^3 - l_3\theta_0)^2 + (-l_2\theta_0^2 + l_4)^2}.
$$

Therefore, the transversality condition $\left[\frac{d(Re\lambda)}{d\tau_1}\right]_{\tau_1 = \tau_1^c} > 0$ holds for $K'(\theta_0^2) > 0$. Thus, we can state the following theorem.

Theorem 4.4.2. *For $\tau_1 > 0$ and $\tau_2 = \tau_3 = 0$, the interior fixed point $E^1(T^1, T_8^1, M^1, D^1)$ will be locally asymptotically stable if $\tau_1 < \tau_1^c$. Moreover, our system (4.4) with $\tau_1 > 0$ and $\tau_2 = \tau_3 = 0$ experiences Hopf bifurcation around the fixed point E^1 at $\tau_1 = \tau_1^c$ if $K'(\theta_0^2) > 0$.*

4.4.1   Estimation of the length of time delay

Now, we shall estimate the time delay length to preserve the stability of period-1 limit cycle. We consider the characteristic equation (4.11) and the space of all continuous real-valued function defined on the interval $[-\tau_1, +\infty)$, which satisfy the initial history (4.5) on the interval $[-\tau_1, 0]$. At first, we linearize our delayed system (4.4) for $\tau_1 > 0$ and $\tau_2 = \tau_3 = 0$ around the interior fixed point $E^1(T^1, T_8^1, M^1, D^1)$. Then, we have

$$
\frac{dT}{dt} = \left[r_T(1 - 2b_T T^1) - \frac{\gamma_T T_8^1}{g_T + M^1} \right] T - \frac{\alpha_T M^1}{g_T + M^1} T(t - \tau_1)
$$

$$
- \frac{\alpha_T g_T T^1}{(g_T + M^1)^2} M(t - \tau_1) - \frac{\gamma_T T^1}{g_T + M^1} T_8 + \frac{\gamma_T T_8^1 T^1}{(g_T + M^1)^2} M,
$$

$$
\frac{dT_8}{dt} = -\left[\frac{\alpha_8 D^1}{(g_8 + T_8^1)^2} + \delta_8 \right] T_8 + \frac{\alpha_8}{g_8 + T_8^1} D, \tag{4.16}
$$

$$
\frac{dM}{dt} = -\left[\frac{\alpha_m T_8^1}{g_m + T_8^1} \cdot \frac{1}{(g_{m1} + T^1)^2} + \gamma_m M^1 \right] T + \frac{\alpha_m g_m}{(g_m + T_8^1)^2} \cdot \frac{1}{g_{m1} + T^1} T_8
$$

$$
- (\delta_m + \gamma_m T^1) M,
$$

$$
\frac{dD}{dt} = \frac{g_d \alpha_d}{(g_d + T^1)^2} T - \delta_d D.
$$

Taking Laplace transformation of the above linearized system, we get

$$
\left[\rho - r_T(1 - 2b_T T^1) + \frac{\gamma_T T_8^1}{g_T + M^1} \right] L_T(\rho) = -\frac{\alpha_T M^1}{g_T + M^1} e^{-\rho \tau_1} L_T(\rho)
$$

$$
- \frac{\alpha_T M^1}{g_T + M^1} e^{-\rho \tau_1} K_T(\rho)
$$

$$
- \frac{\alpha_T g_T T^1}{(g_T + M^1)^2} e^{-\rho \tau_1} K_M(\rho)
$$

$$
- \frac{\gamma_T T^1}{g_T + M^1} L_{T_8}(\rho)
$$

$$
+ \frac{\gamma_T T_8^1 T^1}{(g_T + M^1)^2} L_M(\rho) + \overline{T}(0),
$$

95

$$\left[\rho + \frac{\alpha_8 D^1}{(g_8 + T_8^1)^2} + \delta_8\right] L_{T_8}(\rho) = \frac{\alpha_8}{g_8 + T_8^1} L_D(\rho) + \overline{T}_8(0),$$

$$[\rho + (\delta_m + \gamma_T T^1)] L_M(\rho) = -\left[\frac{\alpha_m T_8^1}{g_m + T_8^1} \cdot \frac{1}{(g_{m1} + T^1)^2} + \gamma_m M^1\right] L_T(\rho)$$

$$+ \frac{\alpha_m g_m}{(g_m + T_8^1)^2} \cdot \frac{1}{g_{m1} + T^1} L_{T_8}(\rho)$$

$$+ \overline{M}(0),$$

$$[\rho + \delta_d] L_D(\rho) = \frac{g_d \alpha_d}{(g_d + T^1)^2} L_T(\rho) + \overline{D}(0),$$

where

$$K_T(\rho) = \int_{-\tau_1}^{0} e^{-\rho\tau_1} T(t) dt,$$

$$K_M(\rho) = \int_{-\tau_1}^{0} e^{-\rho\tau_1} M(t) dt.$$

$L_T(\rho)$, $L_{T_8}(\rho)$, $L_M(\rho)$ and $L_D(\rho)$ are the Laplace transformations of $T(t)$, $T_8(t)$, $M(t)$ and $D(t)$, respectively.

By well-known property of Freedman et al. [32] and using Nyquist criteria [72], we looked the conditions for the locally asymptotically stability of interior fixed point $E^1(T^1, T_8^1, M^1, D^1)$ are stated as

$$Re[Q(i\mu_0)] = 0, \tag{4.17}$$

and

$$Im[Q(i\mu_0)] > 0, \tag{4.18}$$

where

$$Q(\rho) = \rho^4 + q_1\rho^3 + q_2\rho^2 + q_3\rho + q_4 + e^{-\rho\tau_1}(l_1\rho^3 + l_2\rho^2 + l_3\rho + l_4),$$

and μ_0 is the smallest root of the expressions (4.17) and (4.18). We have investigated that E^1 remains stable in the absence of time delays ($\tau_1 = \tau_2 = \tau_3 = \tau_4 = 0$). Equations (4.17) and (4.18) can be explicitly written as

$$\mu_0^4 - q_2\mu_0^2 + q_4 = (l_2\mu_0^2 - l_4)\cos(\mu_0\tau_1) + (l_1\mu_0^3 - l_3\mu_0)\sin(\mu_0\tau_1), \tag{4.19}$$

and

$$-q_1\mu_0^3 + q_3\mu_0 > (l_1\mu_0^3 - l_3\mu_0)\cos(\mu_0\tau_1) - (l_2\mu_0^2 - l_4)\sin(\mu_0\tau_1), \quad (4.20)$$

that give sufficient conditions for the stability of the interior fixed point E^1 and we use them to estimate the length of time delay τ_1. Our goal is to calculate an upper bound μ_+ on μ_0, that is, not depends on time delay τ_1 and estimate the length of τ_1, then equation (4.20) holds for all values of μ, where $0 \le \mu \le \mu_+$ at the point $\mu = \mu_0$. We rewrite the equation (4.19) leads to

$$\begin{aligned}
\mu_0^4 &= q_2\mu_0^2 - q_4 + l_2\mu_0^2\cos(\mu_0\tau_1) - l_4\cos(\mu_0\tau_1) + l_1\mu_0^3\sin(\mu_0\tau_1) \\
&- l_3\mu_0\sin(\mu_0\tau_1).
\end{aligned} \quad (4.21)$$

The value of the time delay is estimated by maximizing the right-hand side of (4.21) and it is written as

$$q_2\mu_0^2 - q_4 + l_2\mu_0^2\cos(\mu_0\tau_1) - l_4\cos(\mu_0\tau_1) + l_1\mu_0^3\sin(\mu_0\tau_1) - l_3\mu_0\sin(\mu_0\tau_1),$$

subject to

$$|\cos(\mu_0\tau_1)| \le 1 \quad \text{and} \quad |\sin(\mu_0\tau_1)| \le 1.$$

Therefore, we obtain

$$\mu_0^4 \le |l_1|\mu_0^3 + |l_2|\mu_0^2 + (q_2 + |l_3|)\mu_0 + (|l_4| - q_4).$$

If μ_+ is the unique positive root of the equation

$$\mu_0^4 - |l_1|\mu_0^3 - |l_2|\mu_0^2 - (q_2 + |l_3|)\mu_0 + (q4 - |l_4|) = 0,$$

then $\mu_+ \ge \mu_0$. It is observed that μ_+ is independent of τ_1. Now, we shall estimate τ_1 from the inequality (4.20), holds for $0 \le \mu \le \mu_+$ using the bounds $|\sin(\mu_0\tau_1)| \le \mu_0\tau_1$ and $|1 - \cos(\mu_0\tau_1)| \le \frac{1}{2}\mu_0^2\tau_1^2$. Then, we rewrite the inequality (4.20) as

$$\frac{1}{2}(l_1\mu_0^2 - l_3)\mu_0^2\tau_1^2 + (l_4 - l_2\mu_0^2)\tau_1 < (q_3 - q_1\mu_0^2) + (l_3 - l_1\mu_0^2). \quad (4.22)$$

From equation (4.22), we can write that

$$L_1\tau_1^2 + L_2\tau_1 < L_3,$$

with

$$L_1 = \frac{1}{2}(l_1\mu_+^2 - l_3)\mu_+^2,$$

$$L_2 = (l_4 - l_2\mu_+^2),$$

$$L_3 = (q_3 - q_1\mu_+^2) + (l_3 - l_1\mu_+^2).$$

Then, for $0 \leq \tau_1 \leq \tau_1^+$, Nyquist criteria [72] holds, and we have

$$\tau_1^+ = \frac{1}{2L_1}(-L_2 + \sqrt{L_2^2 + 4L_1L_3}).$$

Then, the maximum length of discrete time delay τ_1^+ preserves the stability of period-1 limit cycle. Therefore, we have the following theorem.

Theorem 4.4.3. *If there exists $\tau_1 > 0$ in the interval $0 \leq \tau_1 \leq \tau_1^+$ such that $L_1\tau_1^2 + L_2\tau_1 < L_3$, then τ_1^+ is the maximum length of time delay τ_1 for which the interior fixed point $E^1(T^1, T_8^1, M^1, D^1)$ is locally asymptotically stable.*

4.4.2 Direction and stability of Hopf bifurcation

In the Theorem 4.4.2, we have proved that our delayed system (4.4) experiences Hopf bifurcation around the interior fixed point $E^1(T^1, T_8^1, M^1, D^1)$ at the threshold value $\tau_1 = \tau_1^c$ for $\tau_1 > 0$ and $\tau_2 = \tau_3 = 0$. Main goal of this subsection is to determine the direction of Hopf bifurcation and the stability of bifurcating periodic solutions around the interior fixed point $E^1(T^1, T_8^1, M^1, D^1)$ at $\tau_1 = \tau_1^c$ by using center manifold theory and the normal form method introduced by Hassard et al. [37]. We assume that
(i) characteristic equation (4.11) has a pair of imaginary roots $\pm i\theta_0$ at $\tau_1 = \tau_1^c$,

(ii) $K'(\theta_0^2) \neq 0$,

(iii) and the other roots of characteristic equation (4.11) have negative real parts.

To investigate the direction and stability of Hopf bifurcation, we first need to transformation $v_1(t) = T(\tau_1 t) - T^1(t)$, $v_2(t) = T_8(\tau_1 t) - T_8^1(t)$, $v_3(t) = M(\tau_1 t) - M^1(t)$, $v_4(t) = D(\tau_1 t) - D^1(t)$, $X(t) = (v_1(t), v_2(t), v_3(t), v_4(t))^T$, $\tau_1 = \tau_1^c + \mu$ and the delayed system (4.4) transformed into a functional differential equation (FDE) in $\mathcal{C} = \mathcal{C}([-1, 0], \mathbb{R}^4)$ as

$$X'(t) = S_\mu(X_t) + f(\mu, X_t), \qquad (4.23)$$

where $v_t(\psi) = v(t+\psi)$, for $\psi \in [-1,0)$, $\mathcal{C}^k[-\tau_1,0] = \{\eta|\eta : [-1,0) \to \mathbb{R}^4\}$, η has k-th order continuous derivative and $S_\mu : \mathcal{C} \to \mathbb{R}$, $f : \mathbb{R} \times \mathcal{C} \to \mathcal{C}$ are given by

$$
S_\mu(\eta) = (\tau_1^c + \mu)
$$

$$
\times \begin{pmatrix}
r_T(1 - 2b_T T^1) - \frac{\gamma_T T_8^1}{g_T + M^1} & -\frac{\gamma_T T^1}{g_T + M^1} & \frac{\gamma_T T_8^1 T^1}{(g_T + M^1)^2} & 0 \\
0 & -\frac{\alpha_8 D^1}{(g_8 + T_8^1)^2} - \delta_8 & 0 & \frac{\alpha_8}{g_8 + T_8^1} \\
-\frac{\alpha_m T_8^1}{(g_m + T_8^1)(g_{m1} + T^1)^2} - \gamma_m M^1 & \frac{\alpha_m g_m}{(g_m + T_8^1)^2(g_{m1} + T^1)} & -\delta_m - \gamma_m T^1 & 0 \\
\frac{\alpha_d g_d}{(g_d + T^1)^2} & 0 & 0 & -\delta_d
\end{pmatrix}
$$

$$
\times \begin{pmatrix} \eta_1(0) \\ \eta_2(0) \\ \eta_3(0) \\ \eta_4(0) \end{pmatrix} + (\tau_1^c + \mu) \begin{pmatrix}
-\frac{\alpha_T M^1}{g_T + M^1} & 0 & -\frac{\alpha_T g_T T^1}{(g_T + M^1)^2} & 0 \\
0 & 0 & 0 & 0 \\
0 & 0 & 0 & 0 \\
0 & 0 & 0 & 0
\end{pmatrix}
$$

$$
\times \begin{pmatrix} \eta_1(-1) \\ \eta_2(-1) \\ \eta_3(-1) \\ \eta_4(-1) \end{pmatrix},
\tag{4.24}
$$

and

$$
f(\mu, \eta) = (\tau_1^c + \mu) \begin{pmatrix}
-r_T b_T \eta_1^2(0) - \frac{\gamma_T \eta_1(0)\eta_2(0)}{g_T + M^1} + \frac{\gamma_T T^1 \eta_2(0)\eta_3(0)}{(g_T + M^1)^2} \\
+\frac{\gamma_T T_8^1 \eta_1(0)\eta_3(0)}{(g_T + M^1)^2} - \frac{\gamma_T T^1 T_8^1 \eta_3^2(0)}{(g_T + M^1)^3} \\
-\frac{\alpha_T g_T \eta_1(-1)\eta_3(-1)}{(g_T + M^1)^2} + \frac{\alpha_T T^1 \eta_3^2(-1)}{(g_T + M^1)^2} \\
\\
\frac{\alpha_8 D^1 \eta_2^2(0)}{(g_8 + T_8^1)^2} - \frac{\alpha_8 \eta_2(0)\eta_4(0)}{g_8 + T_8^1} \\
\\
\frac{\alpha_m T_8^1 \eta_1^2(0)}{(g_m + T_8^1)(g_{m1} + T^1)^3} - \frac{\alpha_m g_m \eta_2^2(0)}{(g_m + T_8^1)^3(g_{m1} + T^1)} \\
+\frac{\alpha_m g_m \eta_1(0)\eta_2(0)}{(g_m + T_8^1)^2(g_{m1} + T^1)^2} - \gamma_m \eta_1(0)\eta_3(0) \\
\\
-\frac{\alpha_d g_d \eta_1^2(0)}{(g_d + T_8^1)^2}
\end{pmatrix}.
\tag{4.25}
$$

By the Riesz representation theorem, there exists a 4×4 matrix-valued function $\epsilon(.,\mu) : [-1,0] \to \mathbb{R}^{4\times 4}$ defined as

$$
S_\mu \eta = \int_{-1}^0 d\epsilon(\psi, 0)\eta(0), \qquad \text{for } \eta \in \mathcal{C}^1[-1,0).
\tag{4.26}
$$

In fact, we can choose

$$
\epsilon(\psi,\mu) = (\tau_1^c + \mu)
$$

$$
\times \begin{pmatrix} r_T(1-2b_TT^1) - \frac{\gamma_T T_8^1}{g_T+M^1} & -\frac{\gamma_T T^1}{g_T+M^1} & \frac{\gamma_T T_8^1 T^1}{(g_T+M^1)^2} & 0 \\ 0 & -\frac{\alpha_8 D^1}{(g_8+T_8^1)^2} - \delta_8 & 0 & \frac{\alpha_8}{g_8+T_8^1} \\ -\frac{\alpha_m T_8^1}{(g_m+T_8^1)(g_{m1}+T^1)^2} & \frac{\alpha_m g_m}{(g_m+T_8^1)^2(g_{m1}+T^1)} & -\delta_m - \gamma_m T^1 & 0 \\ \frac{\alpha_d g_d}{(g_d+T^1)^2} & 0 & 0 & -\delta_d \end{pmatrix} \delta(\psi)
$$

$$
- (\tau_1^c + \mu) \begin{pmatrix} -\frac{\alpha_T M^1}{g_T+M^1} & 0 & -\frac{\alpha_T g_T T^1}{(g_T+M^1)^2} & 0 \\ 0 & 0 & 0 & 0 \\ 0 & 0 & 0 & 0 \\ 0 & 0 & 0 & 0 \end{pmatrix} \delta(\psi+1), \tag{4.27}
$$

where $\delta(\psi)$ is a Dirac delta function. For $\eta \in \mathcal{C}^1([-1,0),\mathbb{R}^4)$, we define

$$
I(\mu)\eta(\psi) = \left\{ \begin{array}{ll} \frac{d\eta(\psi)}{d\psi}, & \text{for} \quad \psi \in [-1,0) \\ \int_{-1}^0 d\epsilon(\psi,\mu)\eta(\theta), & \text{for} \quad \psi = 0 \end{array} \right\}, \tag{4.28}
$$

and

$$
J(\mu)\eta(\psi) = \left\{ \begin{array}{ll} 0, & \text{for} \quad \psi \in [-1,0) \\ f(\mu,\eta), & \text{for} \quad \psi = 0 \end{array} \right\}. \tag{4.29}
$$

Now, the system (4.23) is equivalent to the differential equation

$$
X_t' = I(\mu)X_t(\psi) + J(\mu)X_t(\psi), \tag{4.30}
$$

with $X_t(\psi) = X(t+\psi)$ for $\psi \in [-1,0)$.

Now, for $\pi \in \mathcal{C}^1([-1,0),(\mathbb{R}^4)^1)$, where $(\mathbb{R}^4)^1$ is a four dimensional space of row vectors and the adjoint of I, I^1 is defined as

$$
I^1(\mu)\pi(k) = \left\{ \begin{array}{ll} -\frac{d\pi}{dk}, & \text{for} \quad k \in (0,1] \\ \int_{-1}^0 d\epsilon^T(t,0)\pi(-t), & \text{for} \quad k = 0 \end{array} \right\}. \tag{4.31}
$$

A bilinear inner product, defined for $\eta \in [-1,0)$ and $\pi \in [0,1]$, takes the first term to be the conjugate linear and the second term to be linear in the following form

$$
< \pi(k), \eta(\psi) > = \overline{\pi}(0)\eta(0) - \int_{\psi=-1}^0 \int_{\sigma=0}^\psi \pi(\sigma-\psi)d\epsilon(\psi)\eta(\sigma)d\sigma, \tag{4.32}
$$

100

where $\epsilon(\psi) = \epsilon(\psi, 0)$. Then, $I(0)$ and I^1 are adjoint operators. From previous subsection, we know that $\pm i\theta_0\tau_1^c$ are the eigenvalues of $I(0)$ and $\mp i\theta_0\tau_1^c$ are the eigenvalues of I^1.

Proposition 4.4.1. *Let us consider $m(\psi) = (1, a, b, c)^T e^{i\theta_0\tau_1^c\psi}$ be the eigenvector of $I(0)$ corresponding to the eigenvalue $i\theta_0\tau_1^c$ and $m^1(\psi) = D(1, a^1, b^1, c^1)^T e^{i\theta_0\tau_1^c\psi}$ be the eigenvector of I^1 corresponds to eigenvalue $-i\theta_0\tau_1^c$. Then, $< m^1, m >= 1$, $< m^1, \overline{m} >= 0$, where $D = [(1 + \overline{a}a^1 + \overline{b}b^1 + \overline{c}c^1) + \left(\frac{\alpha_T M^1}{g_T + M^1} + \overline{b}\frac{\alpha_T g_T T^1}{(g_T + M^1)^2}\right)\tau_1^c e^{i\theta_0\tau_1^c}]^{-1}$.*

Proof. Since $m(\psi)$ is the eigenvector of $I(0)$ corresponding to eigenvalue $i\theta_0\tau_1^c$, then $I(0)m(\psi) = i\theta_0\tau_1^c m(\psi)$. Now, from equations (4.24), (4.26) and (4.27), we have

$$\tau_1^c \begin{pmatrix} a_{11} - i\theta_0 & a_{12} & a_{13} & 0 \\ 0 & a_{22} - i\theta_0 & 0 & a_{24} \\ a_{31} & a_{32} & a_{33} - i\theta_0 & 0 \\ a_{41} & 0 & 0 & a_{44} - i\theta_0 \end{pmatrix} m(0) = \begin{pmatrix} 0 \\ 0 \\ 0 \\ 0 \end{pmatrix},$$

with

$$a_{11} = r_T(1 - 2b_T T^1) - \frac{\gamma_T T_8^1}{g_T + M^1} - \frac{\alpha_T M^1}{g_T + M^1}e^{-i\theta_0\tau_1^c},$$

$$a_{12} = -\frac{\gamma_T T^1}{g_T + M^1},$$

$$a_{13} = \frac{\gamma_T T_8^1 T^1}{(g_T + M^1)^2} - \frac{\alpha_T g_T T^1}{(g_T + M^1)^2}e^{-i\theta_0\tau_1^c},$$

$$a_{22} = -\frac{\alpha_8 D^1}{(g_8 + T_8^1)^2} - \delta_8,$$

$$a_{24} = \frac{\alpha_8}{g_8 + T_8^1},$$

$$a_{31} = -\frac{\alpha_m T_8^1}{(g_m + T_8^1)(g_{m1} + T^1)^2} - g_m M^1,$$

$$a_{32} = \frac{\alpha_m g_m}{(g_m + T_8^1)^2(g_{m1} + T^1)},$$

$$a_{33} = -\delta_m - \gamma_m T^1,$$

$$a_{41} = \frac{\alpha_d g_d}{(g_d + T^1)^2},$$

$$a_{44} = -\delta_d.$$

After some simple calculations, we obtain

$$
\begin{aligned}
m(0) &= (1, a, b, c)^T \\
&= \left(1, -\frac{a_{24}c}{a_{22} - i\theta_0}, -\frac{a_{31} + aa_{32}}{a_{33} - i\theta_0}, -\frac{a_{41}}{a_{44} - i\theta_0}\right)^T.
\end{aligned}
$$

Since $m^1(k) = D(1, a^1, b^1, c^1)^T e^{i\theta_0 \tau_1^c \psi}$ is the eigenvector of A^1 corresponding to eigenvalue $-i\theta_0 \tau_1^c$, then we have

$$
\tau_1^c \begin{pmatrix}
a_{11} + i\theta_0 & 0 & a_{31} & a_{41} \\
a_{12} & a_{22} + i\theta_0 & a_{32} & 0 \\
a_{13} & 0 & a_{33} + i\theta_0 & 0 \\
0 & a_{24} & 0 & a_{44} + i\theta_0
\end{pmatrix} (m^1(0))^T = \begin{pmatrix} 0 \\ 0 \\ 0 \\ 0 \end{pmatrix},
$$

which implies

$$
\begin{aligned}
m^1(0) &= D(1, a^1, b^1, c^1) \\
&= \left(1, -\frac{a_{12} + b^1 a_{32}}{a_{22} + i\theta_0}, -\frac{a_{13}}{a_{33} + i\theta_0}, -\frac{(a_{11} + i\theta_0) + b^1 a_{31}}{a_{41}}\right).
\end{aligned}
$$

To determine the expression of D, we assume that $< m^1(k), m(\psi) >= 1$. Then, from equation (4.32), we get

$$
< m^1(k), m(\psi) >= \overline{D}(1, \overline{a}^1, \overline{b}^1, \overline{c}^1)(1, a, b, c)^T
$$

$$
- \int_{\psi=-1}^{0} \int_{\sigma=0}^{\psi} \overline{D}(1, \overline{a}^1, \overline{b}^1, \overline{c}^1) e^{-i\theta_0 \tau_1^c(\sigma-\psi)} d\epsilon(\psi)(1, a, b, c)^T e^{i\theta_0 \tau_1^c} \sigma d\sigma
$$

$$
= \overline{D}\left\{(1 + \overline{a}^1 a + \overline{b}^1 b + \overline{c}^1 c) - \int_{\psi=-1}^{0}(1, \overline{a}^1, \overline{b}^1, \overline{c}^1)\psi e^{i\theta_0 \tau_1^c \psi} d\epsilon(\psi)(1, a, b, c)^T\right\}
$$

$$
= \overline{D}\left\{(1 + \overline{a}^1 a + \overline{b}^1 b + \overline{c}^1 c) + \left(\frac{\alpha_T M^1}{g_T + M^1} + b\frac{\alpha_T g_T T^1}{(g_T + M^1)^2}\right)\tau_1^c e^{-i\theta_0 \tau_1^c}\right\}.
$$

Therefore, we can choose

$$
D = \frac{1}{(1 + \overline{a}a^1 + \overline{b}b^1 + \overline{c}c^1) + \left(\frac{\alpha_T M^1}{g_T + M^1} + \overline{b}\frac{\alpha_T g_T T^1}{(g_T + M^1)^2}\right)\tau_1^c e^{i\theta_0 \tau_1^c}}.
$$

By adjoint property, we can write

$$
< \pi, I\eta >=< I^1\pi, \eta > .
$$

102

Again, we have

$$-i\theta_0\tau_1^c < m^1, \overline{m} >=< m^1, I\overline{m} >=< I^1 m^1, \overline{m} > \quad = \quad < -i\theta_0\tau_1^c m^1, \overline{m} >$$
$$= \quad i\theta_0\tau_1^c < m^1, \overline{m} > .$$

Therefore, we get

$$< m^1, \overline{m} >= 0.$$

The proof of the proposition is completed. □

For the remaining portion of this subsection, we use the procedures as introduced by Hassard et al. [37]. At first, we obtain the coordinates to describe the center manifold $\mathcal{C}_0$ at $\mu = 0$. Let us assume that the equation (4.30) has a solution X_t for $\mu = 0$. We define

$$w(t) \quad = \quad < m^1, X_t >,$$
$$G(t, \psi) \quad = \quad X_t - w(t)m(\psi) - \overline{w}(t)\overline{m}(\psi)$$
$$= \quad X_t(\psi) - 2Re\{w(t)m(\psi)\}. \tag{4.33}$$

On the center manifold $\mathcal{C}_0$, we have $G(t, \psi) = G(w(t), \overline{w}(t), \theta)$ with

$$G(w, \overline{w}, \psi) \quad = \quad G_{20}(\psi)\frac{w^2}{2} + G_{11}(\psi)w\overline{w} + G_{02}(\psi)\frac{\overline{w}^2}{2}$$
$$+ \quad G_{30}(\psi)\frac{\overline{w}^3}{2} + ..., \tag{4.34}$$

where w, $\overline{w}$ are the local coordinates for center manifold $\mathcal{C}_0$ in the directions of $\overline{m}^1$, m^1. Observing that if X_t is real, then G is real. Here, we allow only real solutions. From equation (4.34), we have

$$< m^1, G > \quad = \quad < m^1, X_t - wm - \overline{wm} >$$
$$= \quad < m^1, X_t > -w < m^1, m > -\overline{w} < m^1, \overline{m} >= w - w = 0.$$

For the solution $X_t \in \mathcal{C}_0$ in equation (4.30), we have

$$\dot{w}(t) \quad = \quad < m^1, \dot{X}_t >$$
$$= \quad < I^1(0)m^1, X_t > +\overline{m}^1(0)f(0, X_t)$$
$$= \quad < -i\theta_0\tau_1^c m^1, X_t > +\overline{m}^1(0)f_0(w, \overline{w})$$
$$= \quad i\theta_0\tau_1^c w + \overline{m}^1(0)f_0(w, \overline{w})$$
$$= \quad i\theta_0\tau_1^c w(t) + g(w, \overline{w}),$$

103

where

$$g(w, \overline{w}) = \overline{g}^1(0) f_0(w, \overline{w})$$

$$= g_{20} \frac{w^2}{2} + g_{11} w \overline{w} + g_{02} \frac{\overline{w}^2}{2} + g_{21} \frac{w^2 \overline{w}}{2} + \dots \qquad (4.35)$$

From equations (4.33) and (4.34), we have

$$X_t(\psi) = (X_{1t}(\theta), X_{2t}(\theta), X_{3t}(\theta), X_{4t}(\theta))^T = G(t, \psi) + 2 Re\{w(t) m(t)\} \qquad (4.36)$$

Then, we have

$$X_t(\psi) = G(w(t), \overline{w}(t), \psi) + wm + \overline{wm}$$

$$= G_{20}(\psi) \frac{w^2}{2} + G_{11}(\psi) w \overline{w} + G_{02}(\psi) \frac{\overline{w}^2}{2} + w(1, a, b, c)^T e^{i\theta_0 \tau_1^c \psi}$$

$$+ \overline{w}(1, \overline{a}, \overline{b}, \overline{c})^T e^{-i\theta_0 \tau_1^c \psi} + \dots \qquad (4.37)$$

We can write this expression as

$$\begin{pmatrix} X_{1t}(\psi) \\ X_{2t}(\psi) \\ X_{3t}(\psi) \\ X_{4t}(\psi) \end{pmatrix} = \begin{pmatrix} G^1(\psi) \\ G^2(\psi) \\ G^3(\psi) \\ G^4(\psi) \end{pmatrix} + w \begin{pmatrix} 1 \\ a \\ b \\ c \end{pmatrix} e^{i\theta_0 \tau_1^c \psi} + \overline{w} \begin{pmatrix} 1 \\ \overline{a} \\ \overline{b} \\ \overline{c} \end{pmatrix} e^{-i\theta_0 \tau_1^c \psi} \equiv \begin{pmatrix} \Delta_1 \\ \Delta_2 \\ \Delta_3 \\ \Delta_4 \end{pmatrix},$$

where

$$\Delta_1 = w e^{i\theta_0 \tau_1^c \psi} + \overline{w} e^{-i\theta_0 \tau_1^c \psi} + G_{20}^1(\psi) \frac{w^2}{2} + G_{11}^1(\psi) w \overline{w} + G_{02}^1(\psi) \frac{\overline{w}^2}{2} + h.o.t.,$$

$$\Delta_2 = a w e^{i\theta_0 \tau_1^c \psi} + \overline{a} \overline{w} e^{-i\theta_0 \tau_1^c \psi} + G_{20}^2(\psi) \frac{w^2}{2} + G_{11}^2(\psi) w \overline{w} + G_{02}^2(\psi) \frac{\overline{w}^2}{2} + h.o.t.,$$

$$\Delta_3 = b w e^{i\theta_0 \tau_1^c \psi} + \overline{b} \overline{w} e^{-i\theta_0 \tau_1^c \psi} + G_{20}^3(\psi) \frac{w^2}{2} + G_{11}^3(\psi) w \overline{w} + G_{02}^3(\psi) \frac{\overline{w}^2}{2} + h.o.t.,$$

$$\Delta_4 = c w e^{i\theta_0 \tau_1^c \psi} + \overline{c} \overline{w} e^{-i\theta_0 \tau_1^c \psi} + G_{20}^4(\psi) \frac{w^2}{2} + G_{11}^4(\psi) w \overline{w} + G_{02}^4(\psi) \frac{\overline{w}^2}{2} + h.o.t..$$

It follows that

$$X_t(\psi) = \begin{pmatrix} X_{1t}(\psi) \\ X_{2t}(\psi) \\ X_{3t}(\psi) \\ X_{4t}(\psi) \end{pmatrix},$$

104

and

$$G(w, \overline{w}, \psi) = \begin{pmatrix} G^1(\psi) \\ G^2(\psi) \\ G^3(\psi) \\ G^4(\psi) \end{pmatrix}.$$

Then, we get

$$X_{1t}(0) = w + \overline{w} + G_{20}^1(0)\frac{w^2}{2} + G_{11}^1(0)w\overline{w} + G_{02}^1(0)\frac{\overline{w}^2}{2} + h.o.t.,$$

$$X_{2t}(0) = aw + \overline{a}\overline{w} + G_{20}^2(0)\frac{w^2}{2} + G_{11}^2(0)w\overline{w} + G_{02}^2(0)\frac{\overline{w}^2}{2} + h.o.t.,$$

$$X_{3t}(0) = bw + \overline{b}\overline{w} + G_{20}^3(0)\frac{w^2}{2} + G_{11}^3(0)w\overline{w} + G_{02}^3(0)\frac{\overline{w}^2}{2} + h.o.t.,$$

$$X_{4t}(0) = cw + \overline{c}\overline{w} + G_{20}^4(0)\frac{w^2}{2} + G_{11}^4(0)w\overline{w} + G_{02}^4(0)\frac{\overline{w}^2}{2} + h.o.t.,$$

$$X_{1t}(-1) = we^{-i\theta_0\tau_1^c} + \overline{w}e^{i\theta_0\tau_1^c} + G_{20}^1(-1)\frac{w^2}{2} + G_{11}^1(-1)w\overline{w}$$
$$+ G_{02}^1(-1)\frac{\overline{w}^2}{2} + h.o.t.,$$

$$X_{2t}(-1) = awe^{-i\theta_0\tau_1^c} + \overline{a}\overline{w}e^{i\theta_0\tau_1^c} + G_{20}^2(-1)\frac{w^2}{2} + G_{11}^2(-1)w\overline{w}$$
$$+ G_{02}^2(-1)\frac{\overline{w}^2}{2} + h.o.t.,$$

$$X_{3t}(-1) = bwe^{-i\theta_0\tau_1^c} + \overline{b}\overline{w}e^{i\theta_0\tau_1^c} + G_{20}^3(-1)\frac{w^2}{2} + G_{11}^3(-1)w\overline{w}$$
$$+ G_{02}^3(-1)\frac{\overline{w}^2}{2} + h.o.t.,$$

$$X_{4t}(-1) = cwe^{-i\theta_0\tau_1^c} + \overline{c}\overline{w}e^{i\theta_0\tau_1^c} + G_{20}^4(-1)\frac{w^2}{2} + G_{11}^4(-1)w\overline{w}$$
$$+ G_{02}^4(-1)\frac{\overline{w}^2}{2} + h.o.t.,$$

$$
\begin{aligned}
X_{1t}^2(0) &= w^2 + 2w\overline{w} + \overline{w}^2 + (G_{20}(0) + 2G_{11}(0))w^2\overline{w} + h.o.t., \\[2mm]
X_{2t}^2(0) &= a^2w^2 + 2|a|^2w\overline{w} + \overline{a}^2\overline{w}^2 \\[2mm]
&\quad + (\overline{a}G_{20}^2(0) + 2aG_{11}^2(0))w^2\overline{w} + h.o.t., \\[2mm]
X_{3t}^2(0) &= b^2w^2 + 2|b|^2w\overline{w} + \overline{b}^2\overline{w}^2 \\[2mm]
&\quad + (\overline{b}G_{20}^3(0) + 2bG_{11}^3(0))w^2\overline{w} + h.o.t., \\[2mm]
X_{4t}^2(0) &= c^2w^2 + 2|c|^2w\overline{w} + \overline{c}^2\overline{w}^2 \\[2mm]
&\quad + (\overline{c}G_{20}^4(0) + 2cG_{11}^4(0))w^2\overline{w} + h.o.t., \\[2mm]
X_{1t}(0)X_{2t}(0) &= aw^2 + (a+\overline{a})w\overline{w} + \overline{a}\,\overline{w}^2 \\[2mm]
&\quad + [G_{11}^3(0) + \tfrac{1}{2}G_{20}^3(0) + aG_{11}^1(0) + \left(\tfrac{\overline{a}}{2}\right)G_{20}^1(0)]w^2\overline{w} + h.o.t., \\[2mm]
X_{1t}(0)X_{3t}(0) &= bw^2 + (b+\overline{b})w\overline{w} + \overline{b}\,\overline{w}^2 \\[2mm]
&\quad + [G_{11}^3(0) + \tfrac{1}{2}G_{20}^3(0) + bG_{11}^1(0) + \left(\tfrac{\overline{b}}{2}\right)G_{20}^1(0)]w^2\overline{w} + h.o.t., \\[2mm]
X_{2t}(0)X_{3t}(0) &= abw^2 + (\overline{a}b + a\overline{b})w\overline{w} + \overline{a}\,\overline{b}\,\overline{w}^2 \\[2mm]
&\quad + [aG_{11}^3(0) + \tfrac{\overline{a}}{2}G_{20}^3(0) + bG_{11}^2(0) + \tfrac{\overline{b}}{2}G_{20}^2(0)]w^2\overline{w} + h.o.t., \\[2mm]
X_{2t}(0)X_{4t}(0) &= acw^2 + (\overline{a}c + a\overline{c})w\overline{w} + \overline{a}\,\overline{c}\,\overline{w}^2 \\[2mm]
&\quad + [aG_{11}^4(0) + \tfrac{\overline{a}}{2}G_{20}^4(0) + cG_{11}^2(0) + \tfrac{\overline{c}}{2}G_{20}^2(0)]w^2\overline{w} + h.o.t., \\[2mm]
X_{1t}(-1)X_{3t}(-1) &= bw^2 e^{-2i\theta_0\tau_1^c} + (b+\overline{b})w\overline{w} + \overline{b}^2\overline{w}^2 e^{2i\theta_0\tau_1^c} \\[2mm]
&\quad + [G_{11}^3(-1)e^{-i\theta_0\tau_1^c} + \tfrac{1}{2}G_{20}^3(-1)e^{i\theta_0\tau_1^c} + bG_{11}^1(-1)e^{-i\theta_0\tau_1^c} \\[2mm]
&\quad + \left(\tfrac{\overline{b}}{2}\right)G_{20}^1(0)e^{i\theta_0\tau_1^c}]w^2\overline{w} + h.o.t., \\[2mm]
X_{3t}^2(-1) &= bw^2 e^{-2i\theta_0\tau_1^c} + 2b\overline{b}w\overline{w} + \overline{b}^2\overline{w}^2 e^{2i\theta_0\tau_1^c} \\[2mm]
&\quad + [2bG_{11}^3(-1)e^{-i\theta_0\tau_1^c} + \overline{b}G_{20}^3(-1)e^{i\theta_0\tau_1^c}]w^2\overline{w} + h.o.t..
\end{aligned}
$$

106

From definition of q and equation (4.25), we have

$$
\begin{aligned}
q(w,\overline{w}) &= \overline{m}^1(0)f_0(w,\overline{w}) \\
&= \overline{m}^1(0)f(0,X_t) \\
&= \tau_1^c\overline{D}(1,\overline{a}^1,\overline{b}^1,\overline{c}^1)
\end{aligned}
$$

$$
\times
\begin{pmatrix}
-r_Tb_TX_{1t}^2(0) - \frac{\gamma_TX_{1t}(0)X_{2t}(0)}{g_T+M^1} + \frac{\gamma_TT^1X_{2t}(0)X_{3t}(0)}{(g_T+M^1)^2} \\
+\frac{\gamma_TT_8^1X_{1t}(0)X_{3t}(0)}{(g_T+M^1)^2} - \frac{\gamma_TT^1T_8^1X_{3t}^2(0)}{(g_T+M^1)^3} \\
-\frac{\alpha_Tg_TX_{1t}(-1)X_{3t}(-1)}{(g_T+M^1)^2} + \frac{\alpha_TT^1X_{3t}^2(-1)}{(g_T+M^1)^2} \\[2mm]
\frac{\alpha_8D^1X_{2t}^2(0)}{(g_8+T_8^1)^2} - \frac{\alpha_8X_{2t}(0)X_{4t}(0)}{g_8+T_8^1} \\[2mm]
\frac{\alpha_mT_8^1X_{1t}^2(0)}{(g_m+T_8^1)(g_{m1}+T^1)^3} - \frac{\alpha_mg_mX_{2t}^2(0)}{(g_m+T_8^1)^3(g_{m1}+T^1)} \\
+\frac{\alpha_mg_mX_{1t}(0)X_{2t}(0)}{(g_m+T_8^1)^2(g_{m1}+T^1)^2} - \gamma_mX_{1t}(0)X_{3t}(0) \\[2mm]
-\frac{\alpha_dg_dX_{1t}^2(0)}{(g_d+T_8^1)^2}
\end{pmatrix}.
$$

After simple calculation, we get

$$
\begin{aligned}
q(w,\overline{w}) &= \tau_1^c\overline{D}\Bigg[X_{1t}^2(0)\bigg(-r_Tb_T + \overline{b}^1\frac{\alpha_mT_8^1}{(g_m+T_8^1)(g_{m1}+T^1)^3} - \overline{c}^1\frac{\alpha_dg_d}{(g_d+T_8^1)^2}\bigg) \\
&+ X_{2t}^2(0)\bigg(\overline{a}^1\frac{\alpha_8D^1}{(g_8+T_8^1)^2} - \overline{b}^1\frac{\alpha_mg_m}{(g_m+T_8^1)^3(g_{m1}+T^1)}\bigg) \\
&+ X_{3t}^2(0)\bigg(-\frac{\gamma_TT^1T_8^1}{(g_T+M^1)^3}\bigg) \\
&+ X_{1t}(0)X_{2t}(0)\bigg(-\frac{\gamma_T}{g_T+M^1} + \overline{b}^1\frac{\alpha_mg_m}{(g_m+T_8^1)^2(g_{m1}+T^1)^2}\bigg) \\
&+ X_{2t}(0)X_{3t}(0)\bigg(\frac{\gamma_TT^1}{(g_T+M^1)^2}\bigg) + X_{1t}(0)X_{3t}(0)\bigg(\frac{\gamma_TT_8^1}{(g_T+M^1)^2} - \overline{b}^1\gamma_m\bigg) \\
&+ X_{2t}(0)X_{4t}(0)\bigg(-\overline{a}^1\frac{\alpha_8}{(g_T+T_8^1)}\bigg) + X_{3t}^2(-1)\bigg(\frac{\alpha_TT^1}{(g_T+M^1)^2}\bigg) \\
&+ X_{1t}(-1)X_{3t}(-1)\bigg(-\frac{\alpha_Tg_T}{(g_T+M^1)^2}\bigg)\Bigg].
\end{aligned}
$$

Above equation leads to

$$
\begin{aligned}
q(w,\overline{w}) &= \tau_1^c \overline{D}\Big[-r_T b_T + \overline{b}^1 \frac{\alpha_m T_8^1}{(g_m + T_8^1)(g_{m1} + T^1)^3} - \overline{c}^1 \frac{\alpha_d g_d}{(g_d + T_8^1)^2} \Big] \\
&\times\ [w^2 + 2w\overline{w} + \overline{w}^2 + (G_{20}(0) + 2G_{11}(0))w^2\overline{w} + h.o.t.] \\
&+\ \tau_1^c \overline{D}\Big[\overline{a}^1 \frac{\alpha_8 D^1}{(g_8 + T_8^1)^2} - \overline{b}^1 \frac{\alpha_m g_m}{(g_m + T_8^1)^3(g_{m1} + T^1)} \Big] \\
&\times\ [a^2 w^2 + 2|a|^2 w\overline{w} + \overline{a}^2\overline{w}^2 + (\overline{a}G_{20}^2(0) + 2aG_{11}^2(0))w^2\overline{w} + h.o.t.] \\
&+\ \tau_1^c \overline{D}\Big[-\frac{\gamma_T T^1 T_8^1}{(g_T + M^1)^3} \Big][b^2 w^2 + 2|b|^2 w\overline{w} + \overline{b}^2\overline{w}^2 \\
&+\ (\overline{b}G_{20}^3(0) + 2bG_{11}^3(0))w^2\overline{w} + h.o.t.] \\
&+\ \tau_1^c \overline{D}\Big[-\frac{\gamma_T}{g_T + M^1} + \overline{b}^1 \frac{\alpha_m g_m}{(g_m + T_8^1)^2(g_{m1} + T^1)^2} \Big] \\
&\times\ [aw^2 + (a + \overline{a})w\overline{w} + \overline{a}^2\overline{w}^2 \\
&+\ [G_{11}^3(0) + \frac{1}{2}G_{20}^3(0) + aG_{11}^1(0) + \frac{\overline{a}}{2}G_{20}^1(0)]w^2\overline{w} + h.o.t.] \\
&+\ \tau_1^c \overline{D}\Big[\frac{\gamma_T T^1}{(g_T + M^1)^2} \Big][abw^2 + (a\overline{b} + \overline{a}b)w\overline{w} + \overline{a}\overline{b}\overline{w}^2 \\
&+\ [aG_{11}^3(0) + \frac{\overline{a}}{2}G_{20}^3(0) + bG_{11}^2(0) + \frac{\overline{b}}{2}G_{20}^2(0)]w^2\overline{w} + h.o.t.] \\
&+\ \tau_1^c \overline{D}\Big[\frac{\gamma_T T_8^1}{(g_T + M^1)^2} - \overline{b}^1 \gamma_m \Big][bw^2 + (b + \overline{b})w\overline{w} + \overline{b}\overline{w}^2 \\
&+\ [G_{11}^3(0) + \frac{1}{2}G_{20}^3(0) + bG_{11}^1(0) + \frac{\overline{b}}{2}G_{20}^1(0)]w^2\overline{w} + h.o.t.] \\
&+\ \tau_1^c \overline{D}\Big[-\overline{a}^1 \frac{\alpha_8}{(g_T + T_8^1)} \Big][acw^2 + (a\overline{c} + \overline{a}c)w\overline{w} + \overline{a}\overline{c}\overline{w}^2 \\
&+\ [aG_{11}^4(0) + \frac{\overline{a}}{2}G_{20}^4(0) + cG_{11}^2(0) + \frac{\overline{c}}{2}G_{20}^2(0)]w^2\overline{w} + h.o.t.] \\
&+\ \tau_1^c \overline{D}\Big[\frac{\alpha_T T^1}{(g_T + M^1)^2} \Big][bw^2 e^{-2i\theta_0 \tau_1^c} + 2b\overline{b}w\overline{w} + \overline{b}^2\overline{w}^2 e^{2i\theta_0 \tau_1^c} \\
&+\ [2bG_{11}^3(-1)e^{-i\theta_0 \tau_1^c} + \overline{b}G_{20}^3(-1)e^{i\theta_0 \tau_1^c}]w^2\overline{w} + h.o.t.] \\
&+\ \tau_1^c \overline{D}\Big[-\frac{\alpha_T g_T}{(g_T + M^1)^2} \Big][bw^2 e^{-2i\theta_0 \tau_1^c} + (b + \overline{b})w\overline{w} + \overline{b}^2\overline{w}^2 e^{2i\theta_0 \tau_1^c} \\
&+\ [G_{11}^3(-1)e^{-i\theta_0 \tau_1^c} + \frac{1}{2}G_{20}^3(-1)e^{i\theta_0 \tau_1^c} + bG_{11}^1(-1)e^{-i\theta_0 \tau_1^c} \\
&+\ \frac{\overline{b}}{2}G_{20}^1(0)e^{i\theta_0 \tau_1^c}]w^2\overline{w} + h.o.t.].
\end{aligned} \tag{4.38}
$$

108

Comparing the coefficient of w^2, $w\overline{w}$, $\overline{w}^2$ and $w^2\overline{w}$ from the equations (4.35) and (4.38), we have

$$
\begin{aligned}
g_{20} \;=\; 2\tau_1^c\overline{D}\Big[&- r_T b_T + \overline{b}^1\frac{\alpha_m T_8^1}{(g_m + T_8^1)(g_{m1} + T^1)^3} - \overline{c}^1\frac{\alpha_d g_d}{(g_d + T_8^1)^2} \\
&+ a^2\overline{a}^1\frac{\alpha_8 D^1}{(g_8 + T_8^1)^2} - a^2\overline{b}^1\frac{\alpha_m g_m}{(g_m + T_8^1)^3(g_{m1} + T^1)} - b^2\frac{\gamma_T T^1 T_8^1}{(g_T + M^1)^3} \\
&- a\frac{\gamma_T}{g_T + M^1} + a\overline{b}^1\frac{\alpha_m g_m}{(g_m + T_8^1)^2(g_{m1} + T^1)^2} + ab\frac{\gamma_T T^1}{(g_T + M^1)^2} \\
&+ b\frac{\gamma_T T_8^1}{(g_T + M^1)^2} - b\overline{b}^1\gamma_m - ac\overline{a}^1\frac{\alpha_8}{g_8 + T_8^1} + be^{-2i\theta_0\tau_1^c}\frac{\alpha_T T^1}{(g_T + M^1)^2} \\
&- be^{-2i\theta_0\tau_1^c}\frac{\alpha_T g_T}{(g_T + M^1)^2}\Big],
\end{aligned}
$$

$$
\begin{aligned}
g_{11} \;=\; \tau_1^c\overline{D}\Big[&- 2r_T b_T + 2\overline{b}^1\frac{\alpha_m T_8^1}{(g_m + T_8^1)(g_{m1} + T^1)^3} - 2\overline{c}^1\frac{\alpha_d g_d}{(g_d + T_8^1)^2} \\
&+ 2|a|^2\overline{a}^1\frac{\alpha_8 D^1}{(g_8 + T_8^1)^2} - 2|a|^2\overline{b}^1\frac{\alpha_m g_m}{(g_m + T_8^1)^3(g_{m1} + T^1)} - 2|b|^2\frac{\gamma_T T^1 T_8^1}{(g_T + M^1)^3} \\
&- (a + \overline{a})\frac{\gamma_T}{g_T + M^1} + (a + \overline{a})\overline{b}^1\frac{\alpha_m g_m}{(g_m + T_8^1)^2(g_{m1} + T^1)^2} \\
&+ (a\overline{b} + \overline{a}b)\frac{\gamma_T T^1}{(g_T + M^1)^2} + (b + \overline{b})\frac{\gamma_T T_8^1}{(g_T + M^1)^2} - (b + \overline{b})\overline{b}^1\gamma_m \\
&- (a\overline{c} + \overline{a}c)\overline{a}^1\frac{\alpha_8}{g_8 + T_8^1} + 2b\overline{b}\frac{\alpha_T T^1}{(g_T + M^1)^2} - (b + \overline{b})\frac{\alpha_T g_T}{(g_T + M^1)^2}\Big],
\end{aligned}
$$

$$
\begin{aligned}
g_{02} \;=\; 2\tau_1^c\overline{D}\Big[&- r_T b_T + \overline{b}^1\frac{\alpha_m T_8^1}{(g_m + T_8^1)(g_{m1} + T^1)^3} - \overline{c}^1\frac{\alpha_d g_d}{(g_d + T_8^1)^2} \\
&+ \overline{a}^2\overline{a}^1\frac{\alpha_8 D^1}{(g_8 + T_8^1)^2} - \overline{a}^2\overline{b}^1\frac{\alpha_m g_m}{(g_m + T_8^1)^3(g_{m1} + T^1)} - \overline{b}^2\frac{\gamma_T T^1 T_8^1}{(g_T + M^1)^3} \\
&- \overline{a}^2\frac{\gamma_T}{g_T + M^1} + \overline{a}^2\overline{b}^1\frac{\alpha_m g_m}{(g_m + T_8^1)^2(g_{m1} + T^1)^2} + \overline{a}\overline{b}\frac{\gamma_T T^1}{(g_T + M^1)^2} \\
&- \overline{b}\frac{\gamma_T T_8^1}{(g_T + M^1)^2} - \overline{b}\overline{b}^1\gamma_m - \overline{a}c\overline{a}^1\frac{\alpha_8}{g_8 + T_8^1} + \overline{b}^2 e^{2i\theta_0\tau_1^c}\frac{\alpha_T T^1}{(g_T + M^1)^2} \\
&- \overline{b}^2 e^{2i\theta_0\tau_1^c}\frac{\alpha_T g_T}{(g_T + M^1)^2}\Big],
\end{aligned}
$$

$$
\begin{aligned}
g_{21} = {} & 2\tau_1^c \overline{D}\Big[(G_{20}(0) + 2G_{11}(0))\Big(-r_T b_T + \overline{b}^1 \frac{\alpha_m T_8^1}{(g_m + T_8^1)(g_{m1} + T^1)^3} \\
& - \overline{c}^1 \frac{\alpha_d g_d}{(g_d + T_8^1)^2}\Big) + (\overline{a}G_{20}^2(0) + 2aG_{11}^2(0))\Big(\overline{a}^1 \frac{\alpha_8 D^1}{(g_8 + T_8^1)^2} \\
& - \overline{b}^1 \frac{\alpha_m g_m}{(g_m + T_8^1)^3(g_{m1} + T^1)}\Big) - (\overline{b}G_{20}^3(0) + 2bG_{11}^3(0))\frac{\gamma_T T^{11} T_8^1}{(g_T + M^1)^3} \\
& + (G_{11}^3(0) + \frac{1}{2}G_{20}^3(0) + aG_{11}^1(0) + \frac{\overline{a}}{2}G_{20}^1(0))\Big(-\frac{\gamma_T}{g_T + M^1} \\
& + \overline{b}^1 \frac{\alpha_m g_m}{(g_m + T_8^1)^2(g_{m1} + T^1)^2}\Big) + (aG_{11}^3(0) + \frac{\overline{a}}{2}G_{20}^3(0) + bG_{11}^2(0) \\
& + \frac{\overline{b}}{2}G_{20}^2(0))\frac{\gamma_T T^1}{(g_T + M^1)^2} + (G_{11}^3(0) + \frac{1}{2}G_{20}^3(0) + bG_{11}^1(0) \\
& + \frac{\overline{b}}{2}G_{20}^1(0))\Big(\frac{\gamma_T T_8^1}{(g_T + M^1)^2} - \overline{b}^1 \gamma_m\Big) \\
& - (aG_{11}^4(0) + \frac{\overline{a}}{2}G_{20}^4(0) + cG_{11}^2(0) + \frac{\overline{c}}{2}G_{20}^2(0))\overline{a}^1 \frac{\alpha_8}{g_8 + T_8^1} \\
& + (2bG_{11}^3(-1)e^{-i\theta_0 \tau_1^c} + \overline{b}G_{20}^3(-1)e^{i\theta_0 \tau_1^c})\frac{\alpha_T T^1}{(g_T + M^1)^2} \\
& - (G_{11}^3(-1)e^{-i\theta_0 \tau_1^c} + \frac{1}{2}G_{20}^3(-1)e^{i\theta_0 \tau_1^c} + bG_{11}^1(-1)e^{-i\theta_0 \tau_1^c} \\
& + \frac{\overline{b}}{2}G_{20}^1(-1)e^{i\theta_0 \tau_1^c})\frac{\alpha_T g_T}{(g_T + M^1)^2}\Big].
\end{aligned}
$$

From the above expressions of g_{21}, it is clear that G_{11} and G_{20} involve in g_{21}. From equations (4.30) and (4.33), we have

$$
\begin{aligned}
\dot{G} = {} & \dot{X}_t - \dot{w}m - \dot{\overline{w}}\overline{m} \\
= {} & \begin{cases} I(0)G - 2Re\{\overline{m}^1 f_0 m(\psi)\}, & \text{for} \quad \psi \in [-1,0) \\ I(0)G - 2Re\{\overline{m}^1 f_0 m(\psi)\} + f_0(w,\overline{w}), & \text{for} \quad \theta = 0 \end{cases},
\end{aligned}
$$

which implies

$$
\dot{G} = I(0)G + L(w,\overline{w},\psi), \tag{4.39}
$$

where

$$
L(w,\overline{w},\psi) = L_{20}(\psi)\frac{w^2}{2} + L_{11}(\psi)w\overline{w} + L_{02}(\psi)\frac{\overline{w}^2}{2} + ... \tag{4.40}
$$

110

On the other way, the center manifold $\mathcal{C}_0$ around the origin is

$$\dot{G} = G_w \dot{w} + G_{\overline{w}} \dot{\overline{w}}. \qquad (4.41)$$

Together from equations (4.39) and (4.40), we obtain

$$(I(0) - 2i\theta_0 \tau_1^c) G_{20}(\psi) = -L_{20}(\psi), \quad I(0) G_{11}(\psi) = -L_{11}(\psi)... \quad (4.42)$$

For $\psi \in [-1, 0)$, from equations (4.35) and (4.39), we get

$$\begin{aligned}
L(w, \overline{w}, \psi) &= -2Re\{\overline{m}^1(0) f_0(w, \overline{w}) m(\psi)\} \\
&= -2Re\{q(w, \overline{w}) m(\psi)\} \\
&= -q(w, \overline{w}) m(\psi) - \overline{q}(w, \overline{w}) \overline{m}(\psi) \\
&= -\left(g_{20} \frac{w^2}{2} + g_{11} w\overline{w} + g_{02} \frac{\overline{w}^2}{2} + g_{21} \frac{w^2 \overline{w}}{2} + ... \right) \times m(\psi) \\
&\quad - \left(\overline{g}_{20} \frac{\overline{w}^2}{2} + \overline{g}_{11} w\overline{w} + \overline{g}_{02} \frac{w^2}{2} + \overline{g}_{21} \frac{\overline{w}^2 w}{2} + ... \right) \times \overline{m}(\psi) (4.43)
\end{aligned}$$

Comparing equations (4.40) and (4.43), we have

$$L_{20}(\psi) = -g_{20} m(\psi) - \overline{g}_{20} \overline{m}(\psi), \qquad (4.44)$$

and

$$L_{11}(\psi) = -g_{11} m(\psi) - \overline{g}_{11} \overline{m}(\psi). \qquad (4.45)$$

From equations (4.28), (4.42) and (4.44), we get

$$\begin{aligned}
\dot{G}_{20}(\psi) &= I(0) G_{20}(\psi) = 2i\theta_0 \tau_1^c G_{20}(\psi) - L_{20}(\psi) \\
&= 2i\theta_0 \tau_1^c G_{20}(\psi) + g_{20} m(\psi) + \overline{g}_{02} \overline{m}(\psi).
\end{aligned}$$

After using $m(\psi) = (1, a, b, c)^T e^{i\theta_0 \tau_1^c \psi}$, we have

$$\dot{G}_{20}(\psi) = 2i\theta_0 \tau_1^c G_{20}(\psi) + g_{20} m(0) e^{i\theta_0 \tau_1^c \psi} + \overline{g}_{02} \overline{m}(0) e^{-i\theta_0 \tau_1^c \psi}.$$

With respect to $G_{20}(\psi)$, the above equation is a first order linear differential equation. After solving, we have

$$G_{20}(\psi) = \frac{ig_{20}}{\theta_0 \tau_1^c} m(0) e^{i\theta_0 \tau_1^c \psi} + \frac{i\overline{g}_{02}}{3\theta_0 \tau_1^c} \overline{m}(0) e^{-i\theta_0 \tau_1^c \psi} + F_1 e^{2i\theta_0 \tau_1^c \psi}, \quad (4.46)$$

where $F_1 = (F_1^1, F_1^2, F_1^3, F_1^4) \in \mathbb{R}^4$ is a constant vector in $\mathbb{R}^4$. Similarly, we obtain

$$G_{11}(\psi) = -\frac{ig_{11}}{\theta_0 \tau_1^c} m(0) e^{i\theta_0 \tau_1^c \psi} + \frac{i\overline{g}_{11}}{\theta_0 \tau_1^c} \overline{m}(0) e^{-i\theta_0 \tau_1^c \psi} + F_2, \qquad (4.47)$$

where $F_2 = (F_2^1, F_2^2, F_2^3, F_2^4) \in \mathbb{R}^4$ is a constant vector in $\mathbb{R}^4$.

Now, our goal is to explain correct form of the constant vectors F_1 and F_2. Thus, from equations (4.28) and (4.42), we have

$$\int_{-1}^{0} d\epsilon(\psi) G_{20}(\psi) = 2i\theta_0 \tau_1^c G_{20}(\psi) - L_{20}(\psi), \qquad (4.48)$$

and

$$\int_{-1}^{0} d\epsilon(\psi) G_{11}(\psi) = -L_{11}(\psi), \qquad (4.49)$$

where $\psi = 0$, that is, $\epsilon(0, \psi) = \epsilon(\psi)$. Putting $\psi = 0$ in $L(w, \overline{w}, \psi)$, we have

$$
\begin{aligned}
L(w, \overline{w}, 0) = {}& -q(w, \overline{w})m(0) - \overline{q}(w, \overline{w})\overline{m}(0) + f_0(w, \overline{w}) \\
= {}& -\left(g_{20}\frac{w^2}{2} + g_{11}w\overline{w} + g_{02}\frac{\overline{w}^2}{2} + g_{21}\frac{w^2\overline{w}}{2} + \ldots\right) \times m(0) \\
& - \left(\overline{g}_{20}\frac{\overline{w}^2}{2} + \overline{g}_{11}w\overline{w} + \overline{g}_{02}\frac{w^2}{2} + \overline{g}_{21}\frac{\overline{w}^2 w}{2} + \ldots\right) \times \overline{m}(0) \\
& + \begin{pmatrix} \wedge_{11}w^2 + \wedge_{12}w\overline{w} + \wedge_{13}\overline{w}^2 + \wedge_{14}w^2\overline{w} + \ldots \\ \wedge_{21}w^2 + \wedge_{22}w\overline{w} + \wedge_{23}\overline{w}^2 + \wedge_{24}w^2\overline{w} + \ldots \\ \wedge_{31}w^2 + \wedge_{32}w\overline{w} + \wedge_{33}\overline{w}^2 + \wedge_{34}w^2\overline{w} + \ldots \\ \wedge_{41}w^2 + \wedge_{42}w\overline{w} + \wedge_{43}\overline{w}^2 + \wedge_{44}w^2\overline{w} + \ldots \end{pmatrix},
\end{aligned}
$$

where

$$
\begin{aligned}
\wedge_{11} = {}& -r_T b_T - \frac{a\gamma_T}{g_T + M^1} + \frac{b\gamma_T(aT^1 + T_8^1)}{(g_T + M^1)^2} - \frac{b^2\gamma_T T^1 T_8^1}{(g_T + M^1)^3} \\
& + \frac{b\alpha_T(T^1 - g_T)}{(g_T + M^1)^2}e^{-2i\theta_0\tau_1^c},
\end{aligned}
$$

$$
\begin{aligned}
\wedge_{12} = {}& -2r_T b_T - \frac{(a + \overline{a})\gamma_T}{g_T + M^1} + \frac{(\overline{a}b + a\overline{b})\gamma_T T^1 + (b + \overline{b})\gamma_T T_8^1}{(g_T + M^1)^2} \\
& - \frac{2|b|^2\gamma_T T^1 T_8^1}{(g_T + M^1)^3} + \frac{2b\overline{b}\alpha_T T^1 - (b + \overline{b})\alpha_T g_T}{(g_T + M^1)^2},
\end{aligned}
$$

112

$$\wedge_{13} \;=\; -r_T b_T - \frac{\overline{a}^2 \gamma_T}{g_T + M^1} + \frac{\overline{b}\gamma_T(\overline{a}T^1 + T^1_8)}{(g_T + M^1)^2} - \frac{\overline{b}^2 \gamma_T T^1 T^1_8}{(g_T + M^1)^3}$$

$$+ \;\; \frac{\overline{b}^2 \alpha_T (T^1 - g_T)}{(g_T + M^1)^2} e^{2i\theta_0 \tau^c_1},$$

$$\wedge_{14} \;=\; -rTb_T[G_{20}(0) + 2G_{11}(0)] - \frac{\gamma_T}{g_T + M^1}[G^3_{11}(0) + \frac{1}{2}G^3_{20}(0) + aG^1_{11}(0)$$

$$+ \;\; \frac{\overline{a}}{2}G^1_{20}(0)] + \frac{\gamma_T T^1}{(g_T + M^1)^2}[aG^3_{11}(0) + \frac{\overline{a}}{2}G^3_{20}(0) + bG^2_{11}(0) + \frac{\overline{b}}{2}G^1_{20}(0)]$$

$$+ \;\; \frac{\gamma_T T^1_8}{(g_T + M^1)^2}[G^3_{11}(0) + \frac{1}{2}G^3_{20}(0) + bG^1_{11}(0) + \frac{\overline{b}}{2}G^1_{20}(0)]$$

$$- \;\; \frac{\gamma_T T^1 T^1_8}{(g_T + M^1)^3}[\overline{b}G^3_{20}(0) + 2bG^3_{11}(0)] - \frac{\alpha_T g_T}{(g_T + M^1)^2}[G^3_{11}(-1)e^{-i\theta_0 \tau^c_1}$$

$$+ \;\; \frac{1}{2}G^3_{20}(-1)e^{i\theta_0 \tau^c_1} + bG^1_{11}(-1)e^{-i\theta_0 \tau^c_1} + \frac{\overline{b}}{2}G^1_{20}(0)e^{i\theta_0 \tau^c_1}]$$

$$+ \;\; \frac{\alpha_T T^1}{(g_T + M^1)^2}[2bG^3_{11}(-1)e^{-i\theta_0 \tau^c_1} + \overline{b}G^3_{20}(-1)e^{i\theta_0 \tau^c_1}],$$

$$\wedge_{21} \;=\; \frac{a^2 \alpha_8 D^1}{(g_8 + T^1_8)^2} - \frac{ac\alpha_8}{g_8 + T^1_8},$$

$$\wedge_{22} \;=\; 2|a|^2 \frac{\alpha_8 D^1}{(g_8 + T^1_8)^2} - \frac{\alpha_8(\overline{a}c + a\overline{c})}{g_8 + T^1_8},$$

$$\wedge_{23} \;=\; \overline{a}^2 \frac{\alpha_8 D^1}{(g_8 + T^1_8)^2} - \frac{\alpha_8 \overline{ac}}{g_8 + T^1_8},$$

$$\wedge_{24} \;=\; \frac{\alpha_8 D^1}{(g_8 + T^1_8)^2}[\overline{a}G^2_{20}(0) + 2aG^2_{11}(0)] - \frac{\alpha_8}{g_8 + T^1_8}[aG^4_{11}(0) + \frac{\overline{a}}{2}G^4_{20}(0)$$

$$+ \;\; cG^2_{11}(0) + \frac{\overline{c}}{2}G^2_{20}(0)],$$

$$\wedge_{31} \;=\; \frac{\alpha_m T^1_8}{(g_m + T^1_8)(g_{m1} + T^1)^3} - \frac{a^2 \alpha_m g_m}{(g_m + T^1_8)^3(g_{m1} + T^1)}$$

$$+ \;\; \frac{a\alpha_m g_m}{(g_m + T^1_8)^2(g_{m1} + T^1)^2} - b\gamma_m,$$

$$\Lambda_{32} = \frac{2\alpha_m T_8^1}{(g_m + T_8^1)(g_{m1} + T^1)^3} - \frac{2|a|^2\alpha_m g_m}{(g_m + T_8^1)^3(g_{m1} + T^1)}$$

$$+ \frac{(a + \bar{a})\alpha_m g_m}{(g_m + T_8^1)^2(g_{m1} + T^1)^2} - (b + \bar{b})\gamma_m,$$

$$\Lambda_{33} = \frac{\alpha_m T_8^1}{(g_m + T_8^1)(g_{m1} + T^1)^3} - \frac{\bar{a}^2\alpha_m g_m}{(g_m + T_8^1)^3(g_{m1} + T^1)}$$

$$+ \frac{\bar{a}^2\alpha_m g_m}{(g_m + T_8^1)^2(g_{m1} + T^1)^2} - \bar{b}\gamma_m,$$

$$\Lambda_{34} = \frac{\alpha_m T_8^1}{(g_m + T_8^1)(g_{m1} + T^1)^3}[G_{20}(0) + 2G_{11}(0)]$$

$$- \frac{\alpha_m g_m}{(g_m + T_8^1)^3(g_{m1} + T^1)}[\bar{a}G_{20}^2(0) + 2aG_{11}2(0)]$$

$$+ \frac{\alpha_m g_m}{(g_m + T_8^1)^2(g_{m1} + T^1)^2}[G_{11}^3(0) + \frac{1}{2}G_{20}^3(0) + aG_{11}^1(0) + \frac{\bar{a}}{2}G_{20}^1(0)]$$

$$- \gamma_m[G_{11}^3(0) + \frac{1}{2}G_{20}^3(0) + bG_{11}^1(0) + \frac{\bar{b}}{2}G_{20}^1(0)],$$

$$\Lambda_{41} = -\frac{\alpha_d g_d}{(g_d + T_8^1)^2},$$

$$\Lambda_{42} = -\frac{2\alpha_d g_d}{(g_d + T_8^1)^2},$$

$$\Lambda_{43} = -\frac{\alpha_d g_d}{(g_d + T_8^1)^2},$$

$$\Lambda_{44} = -\frac{\alpha_d g_d}{(g_d + T_8^1)^2}[G_{20}(0) + 2G_{11}(0)].$$

Comparing the corresponding coefficients of the above equation with equation (4.40) for $\psi = 0$, we have

$$L_{20}(0) = -g_{20}m(0) - \bar{g}_{20}\overline{m}(0) + 2\tau_1^c \begin{pmatrix} \Lambda_{11} \\ \Lambda_{21} \\ \Lambda_{31} \\ \Lambda_{41} \end{pmatrix}, \tag{4.50}$$

and

$$L_{11}(0) = -g_{11}m(0) - \bar{g}_{11}\overline{m}(0) + 2\tau_1^c \begin{pmatrix} \wedge_{12} \\ \wedge_{22} \\ \wedge_{32} \\ \wedge_{42} \end{pmatrix}. \qquad (4.51)$$

From definition of I and equations (4.28) and (4.42), we get

$$\left(i\theta_0 \tau_1^c I - \int_{-1}^0 e^{i\theta_0 \tau_1^c \psi} d\epsilon(\psi) \right) m(0) = 0,$$

$$\left(-i\theta_0 \tau_1^c I - \int_{-1}^0 e^{-i\theta_0 \tau_1^c \psi} d\epsilon(\psi) \right) \overline{m}(0) = 0.$$

After substituting equations (4.46) and (4.48) into the equation (4.50), we get

$$\left(2i\theta_0 \tau_1^c I - \int_{-1}^0 e^{2i\theta_0 \tau_1^c \psi} d\epsilon(\psi) \right) F_1 = 2\tau_1^c \begin{pmatrix} \wedge_{11} \\ \wedge_{21} \\ \wedge_{31} \\ \wedge_{41} \end{pmatrix},$$

which leads to

$$\begin{pmatrix} i\theta_0 - a_{11} & -a_{12} & -a_{13} & 0 \\ 0 & i\theta_0 - a_{22} & 0 & -a_{24} \\ -a_{31} & -a_{32} & i\theta_0 - a_{33} & 0 \\ -a_{41} & 0 & 0 & i\theta_0 - a_{44} \end{pmatrix} \begin{pmatrix} F_1^1 \\ F_1^2 \\ F_1^3 \\ F_1^4 \end{pmatrix} = 2 \begin{pmatrix} \wedge_{11} \\ \wedge_{21} \\ \wedge_{31} \\ \wedge_{41} \end{pmatrix}.$$

Solving F_1, we obtain

$$
F_1^1 = \frac{2}{\wedge}
\begin{vmatrix}
\wedge_{11} & -a_{12} & -a_{13} & 0 \\
\wedge_{21} & i\theta_0 - a_{22} & 0 & -a_{24} \\
\wedge_{31} & -a_{32} & i\theta_0 - a_{33} & 0 \\
\wedge_{41} & 0 & 0 & i\theta_0 - a_{44}
\end{vmatrix},
$$

$$
F_1^2 = \frac{2}{\wedge}
\begin{vmatrix}
i\theta_0 - a_{11} & \wedge_{11} & -a_{13} & 0 \\
0 & \wedge_{21} & 0 & -a_{24} \\
-a_{31} & \wedge_{31} & i\theta_0 - a_{33} & 0 \\
-a_{41} & \wedge_{41} & 0 & i\theta_0 - a_{44}
\end{vmatrix},
$$

$$
F_1^3 = \frac{2}{\wedge}
\begin{vmatrix}
i\theta_0 - a_{11} & -a_{12} & \wedge_{11} & 0 \\
0 & i\theta_0 - a_{22} & \wedge_{21} & -a_{24} \\
-a_{31} & -a_{32} & \wedge_{31} & 0 \\
-a_{41} & 0 & \wedge_{41} & i\theta_0 - a_{44}
\end{vmatrix},
$$

$$
F_1^4 = \frac{2}{\wedge}
\begin{vmatrix}
i\theta_0 - a_{11} & -a_{12} & -a_{13} & \wedge_{11} \\
0 & i\theta_0 - a_{22} & 0 & \wedge_{21} \\
-a_{31} & -a_{32} & i\theta_0 - a_{33} & \wedge_{31} \\
-a_{41} & 0 & 0 & \wedge_{41}
\end{vmatrix},
$$

with

$$
\wedge =
\begin{vmatrix}
i\theta_0 - a_{11} & -a_{12} & -a_{13} & 0 \\
0 & i\theta_0 - a_{22} & 0 & -a_{24} \\
-a_{31} & -a_{32} & i\theta_0 - a_{33} & 0 \\
-a_{41} & 0 & 0 & i\theta_0 - a_{44}
\end{vmatrix}.
$$

Similarly, substituting equations (4.47) and (4.49) into the equation (4.51), we get

$$
\begin{pmatrix}
a_{11} & a_{12} & a_{13} & 0 \\
0 & a_{22} & 0 & a_{24} \\
a_{31} & a_{32} & a_{33} & 0 \\
a_{41} & 0 & 0 & a_{44}
\end{pmatrix}
\begin{pmatrix}
F_2^1 \\
F_2^2 \\
F_2^3 \\
F_2^4
\end{pmatrix}
=
\begin{pmatrix}
\wedge_{12} \\
\wedge_{22} \\
\wedge_{32} \\
\wedge_{42}
\end{pmatrix}.
$$

116

Solving F_2, we have

$$F_2^1 = \frac{2}{\Sigma} \begin{vmatrix} \wedge_{12} & a_{12} & a_{13} & 0 \\ \wedge_{22} & a_{22} & 0 & a_{24} \\ \wedge_{32} & a_{32} & a_{33} & 0 \\ \wedge_{42} & 0 & 0 & a_{44} \end{vmatrix},$$

$$F_2^2 = \frac{2}{\Sigma} \begin{vmatrix} a_{11} & \wedge_{12} & a_{13} & 0 \\ 0 & \wedge_{22} & 0 & a_{24} \\ a_{31} & \wedge_{32} & a_{33} & 0 \\ a_{41} & \wedge_{42} & 0 & a_{44} \end{vmatrix},$$

$$F_2^3 = \frac{2}{\Sigma} \begin{vmatrix} a_{11} & a_{12} & \wedge_{12} & 0 \\ 0 & a_{22} & \wedge_{22} & a_{24} \\ a_{31} & a_{32} & \wedge_{32} & 0 \\ a_{41} & 0 & \wedge_{42} & a_{44} \end{vmatrix},$$

$$F_2^4 = \frac{2}{\Sigma} \begin{vmatrix} a_{11} & a_{12} & a_{13} & \wedge_{12} \\ 0 & a_{22} & 0 & \wedge_{22} \\ a_{31} & a_{32} & a_{33} & \wedge_{32} \\ a_{41} & 0 & 0 & \wedge_{42} \end{vmatrix},$$

with

$$\Sigma = \begin{vmatrix} a_{11} & a_{12} & a_{13} & 0 \\ 0 & a_{22} & 0 & a_{24} \\ a_{31} & a_{32} & a_{33} & 0 \\ a_{41} & 0 & 0 & a_{44} \end{vmatrix}.$$

We can find out $G_{20}(\psi)$ and $G_{11}(\psi)$ from the equations (4.46) and (4.47). With respect to parameters and delay of our system, we can be find out g_{21}. Therefore, we can obtain each g_{ij} in terms of discrete time delay and different

117

parameters of our system. Then, we have the following results

$$
\begin{aligned}
c_1(0) &= \frac{i}{2\tau_1^c\theta_0}\left(g_{20}g_{11} - 2|g_{11}|^2 - \frac{|g_{20}|^2}{3}\right) + \frac{g_{21}}{2}, \\
\mu_2(0) &= -\frac{Re\{c_1(0)\}}{Re\{\lambda'(\tau_1^c)\}}, \\
\beta_2 &= 2Re\{c_1(0)\}, \\
T_2 &= -\frac{Im\{c_1(0)\} + \mu_2 Im\{\lambda'(\tau_1^c)\}}{\theta_0\tau_1^c}.
\end{aligned}
\tag{4.52}
$$

The sign of μ_2 refers the direction of Hopf bifurcation, the sign of β_2 refers the stability of Hopf bifurcating periodic solutions and T_2 refers the period of bifurcating periodic solutions at the threshold value $\tau_1 = \tau_1^c$ for center manifold. Therefore, results from Hassard et al. [37], we can assure the properties of Hopf bifurcation at the threshold value $\tau_1 = \tau_1^c$ in the following theorem.

Theorem 4.4.4. *In the expression of equation (4.52), the following results hold by Hassard et al. [37]:*

(i) The Hopf bifurcation is subcritical or supercritical if $\mu_2 < 0$ or $\mu_2 > 0$.

(ii) The bifurcating periodic solutions are stable or unstable if $\beta_2 < 0$ or $\beta_2 > 0$.

(ii) The period of the bifurcated periodic solution decreases or increases if $T_2 < 0$ or $T_2 > 0$.

Case 3: $\tau_1 > 0$, $\tau_3 > 0$, $\tau_2 = 0$.

Now, our aim is to investigate the dynamics of delayed system (4.4) in presence of two discrete time delays τ_1 and τ_3. In this scenario, we consider two positive interaction delays τ_1 and τ_3 while $\tau_2 = 0$. Then, the characteristics equation (4.9) becomes

$$
\begin{aligned}
\Pi(\lambda, \tau_1, 0, \tau_3) &= \lambda^4 + [(a_1 + c_1) + b_1 e^{-\lambda\tau_1} + d_1 e^{-\lambda\tau_3}]\lambda^3 + [(a_2 + c_2) + b_2 e^{-\lambda\tau_1} \\
&+ (d_2 + h_1)e^{-\lambda\tau_3} + g_1 e^{-\lambda(\tau_1+\tau_3)}]\lambda^2 + [(a_3 + c_3) + b_3 e^{-\lambda\tau_1} \\
&+ (d_3 + h_2)e^{-\lambda\tau_3} + g_2 e^{-\lambda(\tau_1+\tau_3)}]\lambda \\
&+ [(a_4 + c_4) + b_4 e^{-\lambda\tau_1} + (d_4 + h_3)e^{-\lambda\tau_3} + g_3 e^{-\lambda(\tau_1+\tau_3)}] \\
&= 0.
\end{aligned}
\tag{4.53}
$$

118

We shall study the local asymptotic stability of the interior fixed point $E^1(T^1, T_8^1, M^1, D^1)$ of the delayed system (4.4). To do this, we investigate the sign of the real parts of the characteristic equation (4.53). Now, we have the following theorem.

Theorem 4.4.5. *[83] For $\tau_1 > 0$, if all the roots of the characteristic equation (4.11), that is, $\Pi(\lambda, \tau_1, 0, 0) = 0$ have negative real parts, then all the roots of the polynomial (4.53), that is, $\Pi(\lambda, \tau_1, 0, \tau_3) = 0$ have negative real parts and there exists a positive $\tau_3^c(\tau_1)$, (τ_3^c depends on τ_1) such that $\tau_3 < \tau_3^c(\tau_1)$.*

Proof. Let us assume that the equation (4.11), $\Pi(\lambda, \tau_1, 0, 0) = 0$ has no root with positive real part. If $\tau_1 > 0$ and $\tau_3 = 0$, then from equation (4.53), we have $\Pi(\lambda, \tau_1, 0, \tau_3) = 0$ has no root with positive real part. Now, we assume that τ_3 is a parameter. Then, the equation (4.53) is analytic in λ and τ_3. For τ_1 varies, sum of the multiplicity of zeroes of the left hand side of the equation (4.53) in the right half plane can only alter if a root crosses the imaginary axis. Since all the roots of (4.53) have negative real parts for $\tau_3 = 0$, then there exists a positive $\tau_3^c(\tau_1)$, (τ_3^c depends on τ_1) such that all the roots of the characteristic equation (4.53) have negative real parts with $\tau_3 < \tau_3^c(\tau_1)$. $\square$

Case 4: $\tau_1 = 0, \tau_2 > 0, \tau_3 > 0$.

Theorem 4.4.6. *[83] For $\tau_3 > 0$, if all the roots of the characteristic equation $\Pi(\lambda, 0, 0, \tau_3) = 0$ have negative real parts, then all the roots of the polynomial $\Pi(\lambda, 0, \tau_2, \tau_3) = 0$ have negative real parts and there exists a positive $\tau_2^c(\tau_3)$, (τ_2^c depends on τ_3) such that $\tau_2 < \tau_2^c(\tau_3)$.*

Proof. Proof is similar to the Theorem 4.4.5. $\square$

4.5 Parameter estimation

The behavior and analysis of the mathematical model is influenced by the system parameters. In this section, we estimate some of the parameters of our system (4.1) from the existing literature. We used following procedure to estimate the system parameters.

Natural death rate of CD8+T cells, δ_8: The approximate half-life of CD8+T cells (T_8) is 3.9 days [95]. We calculate the death rate δ_8 of CD8+T cells is given by

$$\frac{1}{2}T_8(0) = T_8(0)e^{(-\delta_8 t_{1/2}^{T_8})},$$

119

which leads to

$$\delta_8 \;=\; \frac{\ln 2}{3.9}\ \text{day}^{-1} \quad = 0.178\ \text{day}^{-1}.$$

Natural death rate of macrophages, δ_m: Wacker et al. [107] reported that the half-life of macrophages is 12.4 days. Thus, the death rate of macrophages is calculated as

$$\delta_m \;=\; \frac{\ln 2}{12.4\ \text{day}} \quad = 0.056\ \text{day}^{-1}.$$

Natural death rate of dendritic cell, δ_d: The half-life of dendritic cells is ranges $3-4$ days [38]. We assume that the median half-life of dendritic cells is 4 days. Consequently, the death rate δ_d is

$$\delta_d \;=\; \frac{\ln 2}{4\ \text{day}} \quad = 0.17\ \text{day}^{-1}.$$

Activation rate of dendritic cells production, α_d: The half-saturation constant for tumor cells is represented by g_d. Then, we have

$$\frac{T}{g_d + T} = \frac{1}{2}.$$

Coventry et al. [14] found that the density of dendritic cells in breast cancer patient is $D = 4 \times 10^{-4}$ cells. By considering the steady state of the fourth equation of (4.1), we have

$$\alpha_d \frac{T}{g_d + T} = \delta_d D,$$

which leads to

$$\alpha_d = 1.36 \times 10^{-4}\ \text{cell/day}.$$

Source rate of dendritic cells, s_d: In a healthy individual, the presence of tumor cells leads to the absence of dendritic cell production. Therefore, at steady state, we have

$$s_d \;=\; \delta_d D \quad \Rightarrow\ s_d = 0.68 \times 10^{-4}\ \text{cell/day}.$$

Natural degradation rate of Tregs, δ_g: According to the report of Q. Tang [94], the half-life of regulatory T-cells is 32 hours, that is, 1.3 days (approximately). Then, we have

$$\delta_g \;=\; \frac{\ln 2}{1.3}\ \text{day}^{-1} \quad = 0.53\ \text{day}^{-1}.$$

Activation rate of Tregs, α_g: The average estimated count of circulating regulatory T-cells in an adult human is around $0.25 \times 10^9 \ pg \cdot ml^{-1}$ [94]. Additionally, we assume that the density of CD8+T cells is 2×10^7 cells/ml. The steady state of the fifth equation of (4.1), we have

$$0 \ = \ \alpha_g T_8 - \delta_g T_g,$$

which implies that

$$\alpha_g \ = \ \frac{\delta_g T_g}{T_8}$$

$$= \ \frac{0.53 \times 0.25 \times 10^9}{2 \times 10^7} \ (\text{day}^{-1}.\text{pg.ml}^{-1})/(\text{cell.ml}^{-1})$$

$$= \ 6.62 \ \text{pg.day}^{-1}.\text{cell}^{-1}.$$

Degradation rate of interleukin-10, δ_{10}: The half-life of interleukin-10 (I_{10}) is 4.5 hours [39] ≈ 0.1875 days. Thus, the decay rate of interleukin-10 (I_{10}) is δ_{10} given by

$$\delta_{10} \ = \ \frac{\ln 2}{0.1875} \ \text{day}^{-1} \quad = 3.696 \ \text{day}^{-1}.$$

Activation rate of interleukin-10, α_{10}: Toossi et al. [100] found that 10^6 alveolar macrophages produce (in vitro) 3,200 pg/mL of interleukin-10 (I_{10}). Using the steady state of sixth equation of (4.1), we have

$$\alpha_{10} M - \delta_{10} I_{10} \ = \ 0,$$

which implies

$$\alpha_{10} \ = \ \frac{3.696 \ \times 3200}{10^6} \ (\text{day}^{-1}.\text{pg.ml}^{-1})/(\text{cell.ml}^{-1})$$

$$= \ 1.182 \times 10^{-2} \ \text{pg.day}^{-1}.\text{cell}^{-1}.$$

Decay rate of TGF-β, δ_β: The median half-life of TGF-β is estimated to be around 50 minutes, that is, 0.83 days [82]. Therefore, the decay rate of TGF-β is

$$\delta_\beta \ = \ \frac{\ln 2}{0.83} \ \text{day}^{-1} \quad = 0.832 \ \text{day}^{-1}.$$

Source rate of TGF-β, s_β: Peterson et al. [76] found that the density of TGF-β (T_β) is 609 pg/ml. We take the volume of cerebral spinal fluid

to be 150 ml. In the absence of cancer production of TGF-β, at the steady state, we observe that

$$
\begin{aligned}
s_\beta &= \delta_\beta T_\beta &&= 0.832 \text{ day}^{-1} \times 150 \text{ ml} \times 60.9 \text{ pg} \cdot \text{ml}^{-1} \\
&= 7.6 \times 10^3 \text{ pg} \cdot \text{day}^{-1}.
\end{aligned}
$$

Release rate of TGF-β by tumor cells, α_β: The mean level of the immuno-suppressive cytokine TGF-β (T_β) is 609 pg/ml $\times$ 150 ml = 91350 pg [76] for a high-grade glioblastoma patients. Using the seventh equation of the system (4.1) at an equilibrium state, we get

$$
\begin{aligned}
\alpha_\beta &= \frac{\delta_\beta T_\beta - s_\beta}{T} &&= \frac{91350 \text{ pg} \times 0.832 \text{ day}^{-1} - 7.6 \times 10^3 \text{ pg} \cdot \text{day}^{-1}}{10^6 \text{ cell}} \\
&= 6.84 \times 10^{-2} \text{ pg.day}^{-1}.\text{cell}^{-1}.
\end{aligned}
$$

Degradation rate of interleukin-12, δ_{12}: The half-life of the interleukin-12 (I_{12}) is 30 hours, that is, 1.25 days [11]. Then, the degradation rate of interleukin-12 (I_{12}) is

$$
\delta_{12} = \frac{0.693}{1.25 \text{ day}} \approx 0.55 \text{ day}^{-1}.
$$

Release rate of IL-12 by dendritic cells, α_{12}: For a breast cancer patient, concentration of interleukin-12 in the blood serum is 1.5×10^{-10} pg/ml [21]. Also, the concentration of dendritic cells is 4×10^{-4} cell/ml [14]. Therefore, steady state of the eighth equation of (4.1) implies that

$$
\begin{aligned}
\alpha_{12} &= \frac{\delta_{12} I_{12}}{D} &&= \frac{1.5 \times 10^{-10} \text{ pg} \cdot \text{ml}^{-1} \times 0.55 \text{ day}^{-1}}{4 \times 10^{-4} \text{ cell} \cdot \text{ml}^{-1}} \\
&= 2.06 \times 10^{-7} \text{pg.day}^{-1}.\text{cell}^{-1}.
\end{aligned}
$$

Decay rate of IFN-γ, δ_γ: The median half-life of IFN-γ is 6.8 hours $\approx$ 0.283 days [102]. Therefore, the decay rate of IFN-γ is

$$
\delta_\gamma = \frac{\ln 2}{0.283} \text{ day}^{-1} \approx 2.45 \text{ day}^{-1}.
$$

Production rate of IFN-γ by CD8+T cells, α_γ: In a specific experimental study, Kim et al. [60] reported that 200 pg/ml of IFN-γ is produced by CD8+ T cells. Based on this data, we made the assumption that the

concentration of CD8+ T cells is 2×10^7 cell/ml. Therefore, from steady state of ninth equation of (4.1), we get

$$
\begin{aligned}
\alpha_\gamma & = \frac{\delta_\gamma I_\gamma}{T_8} & = \frac{200 \text{ pg} \cdot \text{ml}^{-1} \times 2.45 \text{ day}^{-1}}{2 \times 10^7 \text{cell} \cdot \text{ml}^{-1}} \\
& = 2.45 \times 10^{-5} \text{ pg.day}^{-1}.\text{cell}^{-1}.
\end{aligned}
$$

Table 4.1 and Table 4.2 represent the summary of all the model parameters.

4.6 Numerical simulations

In this section, we proceed to validate the feasibility of stability criteria through numerical simulations. At first, we derive solutions for different cell population and investigate their behavior in the context of tumor-immune interplays without considering discrete time delay. Subsequently, we investigate the dynamics of tumor-immune interaction with time delay in the model, considering both analytical and numerical approaches. The model parameters used for the numerical illustrations are given in Table 4.1 and Table 4.2. For the numerical illustrations, several parameters are obtained from existing literature [4, 12, 33] and some parameters are estimated.

MATLAB and MATHEMATICA are used to solve numerically the delay differential equations with reference to the parameters are reported in Table 4.1 and Table 4.2. At first, we simulate our tumor model without time delay, that is, $\tau_1 = \tau_2 = \tau_3 = 0$ and obtained the tumor-free fixed point E^0 (0, 2.94586×10^{-11}, 9678.57, 0.0004). The corresponding eigenvalues of tumor-free fixed point E^0 are $-0.865106, \ -0.178, \ -0.17, \ -0.056$, which are all real and negative. Hence, the system (4.4) without time delay is locally asymptotically stable around the tumor-free fixed point E^0. There are two tumor-presence fixed points, with one being the low tumor-presence fixed point E_l^1(0.179273, 2.94586×10^{-11}, 3886.16, 0.0004) and the other being the high tumor-presence fixed point E_h^1(800000, 5.56441×10^{-11}, 0.00145511, 0.00075). The eigenvalues around E_l^1 are $-0.300816, -0.178, -0.17, \ 0.161346$, implying that our system (4.4) without delay is unstable around E_l^1. On the other hand, the eigenvalues around the high tumor-presence fixed point E_h^1 are $-372480, -0.5822, -0.178, \ -0.17$. It is noted that all of the eigenvalues are real and negative. Consequently, our system (4.4) without delay is locally asymptotically stable around the high-tumor presence fixed point E_h^1.

Figure 4.1: The figure shows that the dynamics of tumor cells and immune cells (CD8+T cells, macrophages and dendritic cells) with $\tau_1 \in \{0,\ 0.02,\ 0.07,\ 0.2,\ 0.7\}$ and $\tau_2 = \tau_3 = 0$. The parameters value are specified in the Table 4.1 and Table 4.2 with initial values (0.012, 2.9459 × 10^{-9}, 3000, 0.0002).

Now, we shall validate our theoretical analysis with the aid of numerical illustrations with discrete time delay(s). To better understand the tumor-immune interaction model with discrete time delays, we consider the following cases.

Strategy I: $\tau_1 \in \{0,\ 0.02,\ 0.07,\ 0.2,\ 0.7\}$, $\tau_2 = \tau_3 = 0$.

Equation (4.13) has no real roots for the specified parameters value in Table 4.1 and Table 4.2. In this situation, no Hopf bifurcation exists. In Figure 4.1, we present a comparison of our work for different values of the delay τ_1 and we fixed $\tau_2 = \tau_3 = 0$. In this figure, the density of tumor cells and immune components are represented by black, magenta, green, red and blue lines corresponding to $\tau_1 = 0$, 0.02, 0.07, 0.2, 0.7, respectively. The tumor cell population reaches their equilibrium state after 20 days for

different values of τ_1 (see Figure 4.1A). There is no significant changes in the cell count of immune components, namely CD8+T cells, macrophages and dendritic cells for both non delayed and delayed cases (see Figures 4.1B, 4.1C and 4.1D).
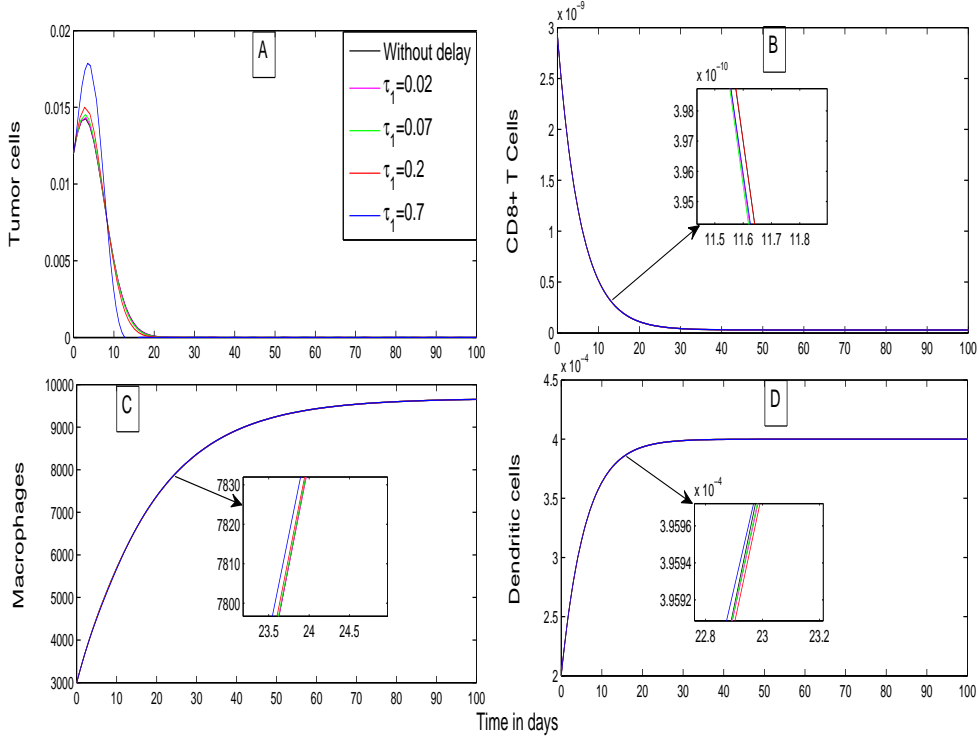

Figure 4.2: The figure shows that the dynamics of tumor cells and immune cells (CD8+T cells, macrophages and dendritic cells) with $\tau_1 = \tau_3 \in \{0,\ 0.02,\ 0.07,\ 0.2,\ 0.7\}$ and $\tau_2 = 0$. The parameters value are specified in the Table 4.1 and Table 4.2 with initial values $(0.012,\ 2.9459 \times 10^{-9},\ 3000,\ 0.0002)$.

Strategy II: $\tau_1 = \tau_3 \in \{0,\ 0.02,\ 0.07,\ 0.2,\ 0.7\}$, $\tau_2 = 0$.

We now taken into account two discrete time delays τ_1 and τ_3, while setting $\tau_2 = 0$ for the dynamics of tumor cells and the immune system. We take different values of τ_1 and τ_3, that is, $\tau_1 = \tau_3 = 0$ (black line), $\tau_1 = \tau_3 = 0.02$ (magenta line), $\tau_1 = \tau_3 = 0.07$ (green line), $\tau_1 = \tau_3 = 0.2$ (red line) and $\tau_1 = \tau_3 = 0.7$ (blue line). We observe that the time delays do not exert any effect on the dynamics of tumor cells. Moreover, there is no impact on the dynamics of immune components when varying the two

discrete time delays τ_1 and τ_3.

Figure 4.3: The figure shows that the dynamics of tumor cells and immune cells (CD8+T cells, macrophages and dendritic cells) with $\tau_2 = \tau_3 \in \{0, \ 0.02, \ 0.07, \ 0.2, \ 0.7\}$ and $\tau_1 = 0$. The parameters value are specified in the Table 4.1 and Table 4.2 with initial values (0.012, 2.9459 $\times$ 10^{-9}, 3000, 0.0002).

Strategy III: $\tau_2 = \tau_3 \in \{0, \ 0.02, \ 0.07, \ 0.2, \ 0.7\}$, $\tau_1 = 0$.

In the Figure 4.3, we consider $\tau_1 = 0$ and study the impact of different values of two delays τ_2 and τ_3 on the dynamics of tumor cells and the immune components (CD8+T cells, macrophages and dendritic cells). In this case, the interaction delays have no influence on the growth of tumor cells (see Figure 4.3A) and the immune components (see Figures 4.3B, 4.3C, 4.3D).

Strategy IV: $\tau_1 = \tau_2 \in \{0, \ 0.02, \ 0.07, \ 0.2, \ 0.7\}$, $\tau_3 = 0$.
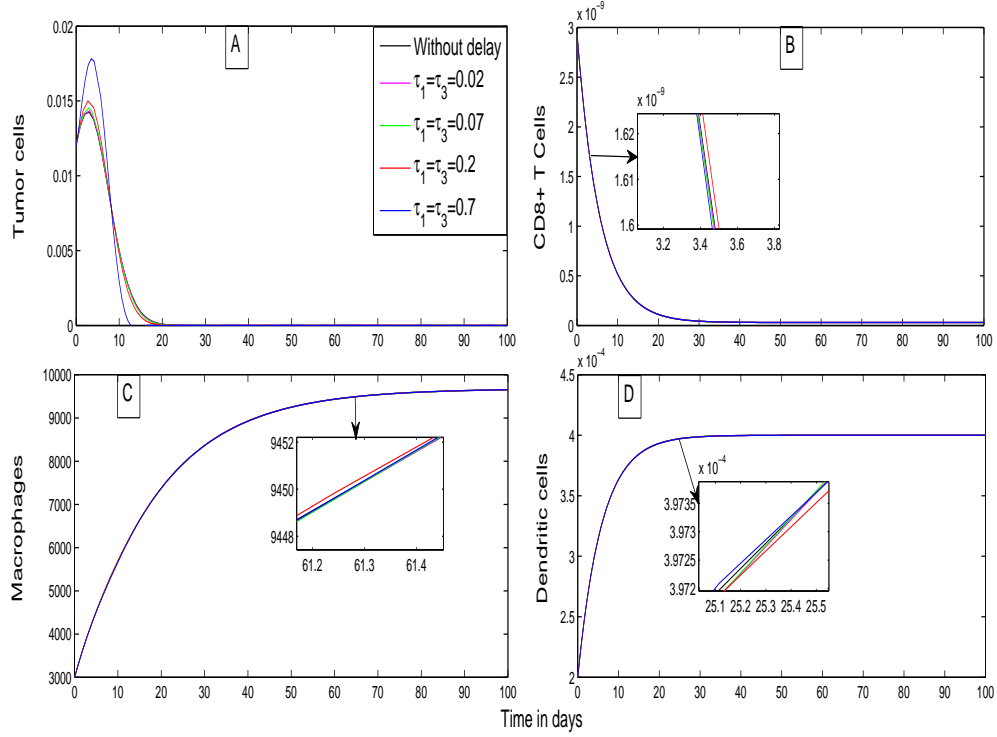
Figure 4.4: The figure shows that the dynamics of tumor cells and immune cells (CD8+T cells, macrophages and dendritic cells) with $\tau_1 = \tau_2 \in \{0, 0.02, 0.07, 0.2, 0.7\}$ and $\tau_3 = 0$. The parameters value are specified in the Table 4.1 and Table 4.2 with initial values (0.012, 2.9459 $\times$ 10^{-9}, 3000, 0.0002).

When we introduce two delays τ_1 and τ_2 into our delayed model, we find that the dynamics of tumor cells and immune system remain unchanged when compared with the without delay and with delays (see Figures 4.4A, 4.4B, 4.4C and 4.4D).

Strategy V: $\tau_1 = \tau_2 = \tau_3 \in \{0, 0.02, 0.07, 0.2, 0.7\}$.

In the previous strategies, we considered only two delays; however, in the current approach, we now taken into account all three discrete time delays in our delayed system. Figure 4.5 illustrates the dynamics of tumor cells, CD8+T cells, macrophages and dendritic cells for $\tau_1 = \tau_2 = \tau_3 \in \{0, 0.02, 0.07, 0.2, 0.7\}$. For all three delays, the dynamics of tumor cells and immune cells exhibit no significant changes (see Figures 4.5A, 4.5B, 4.5C and 4.5D).
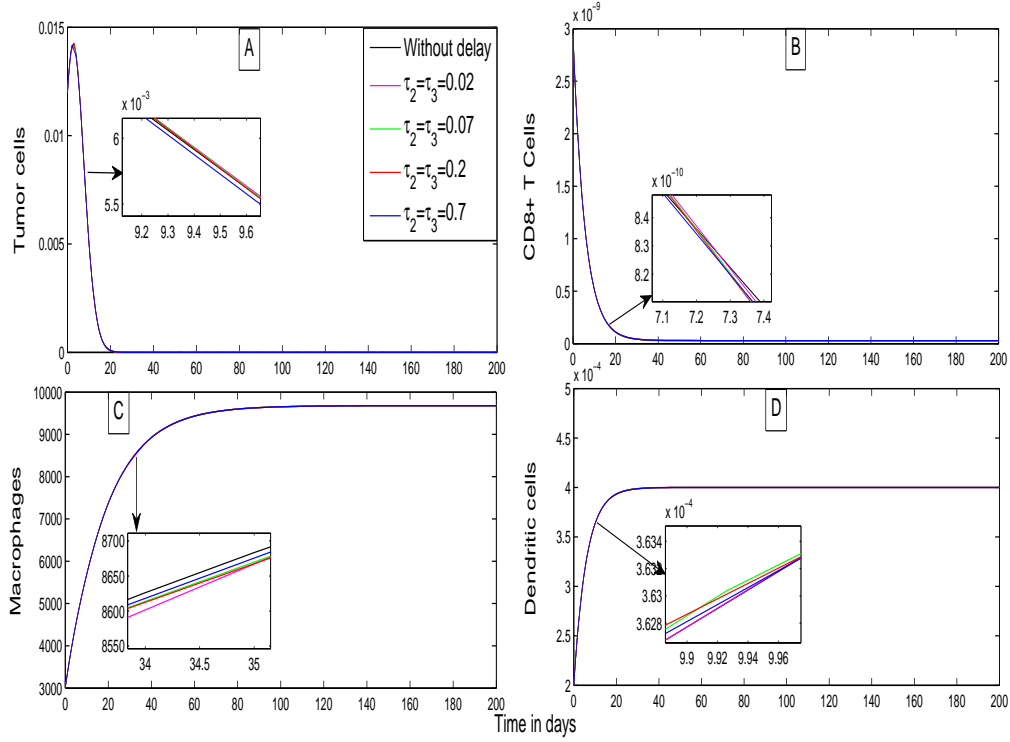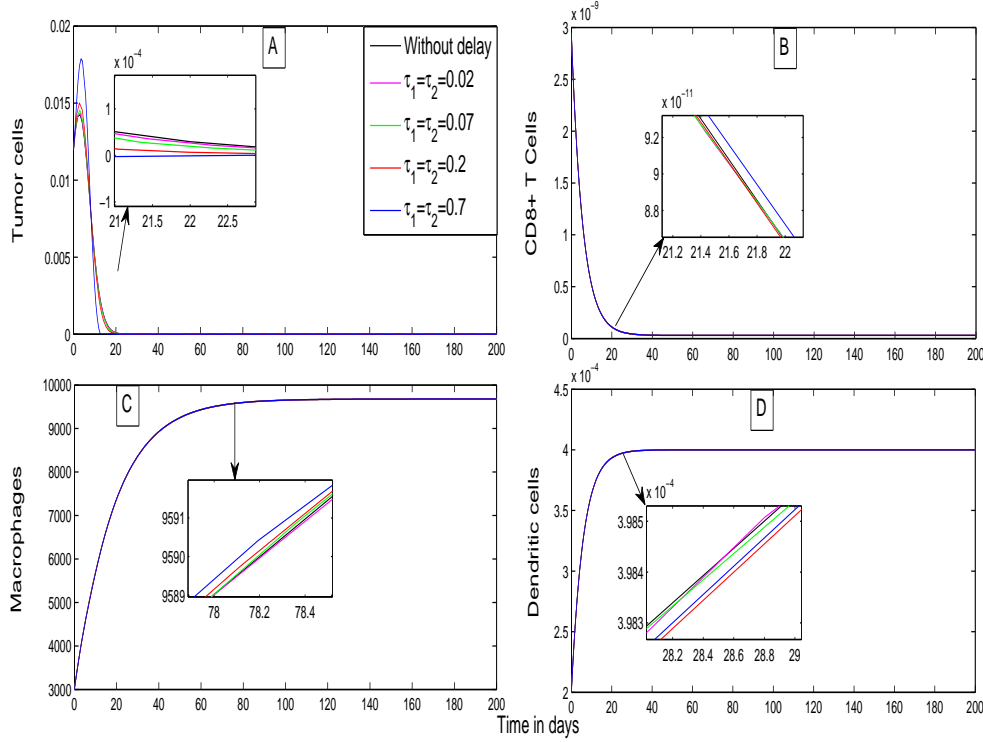
127
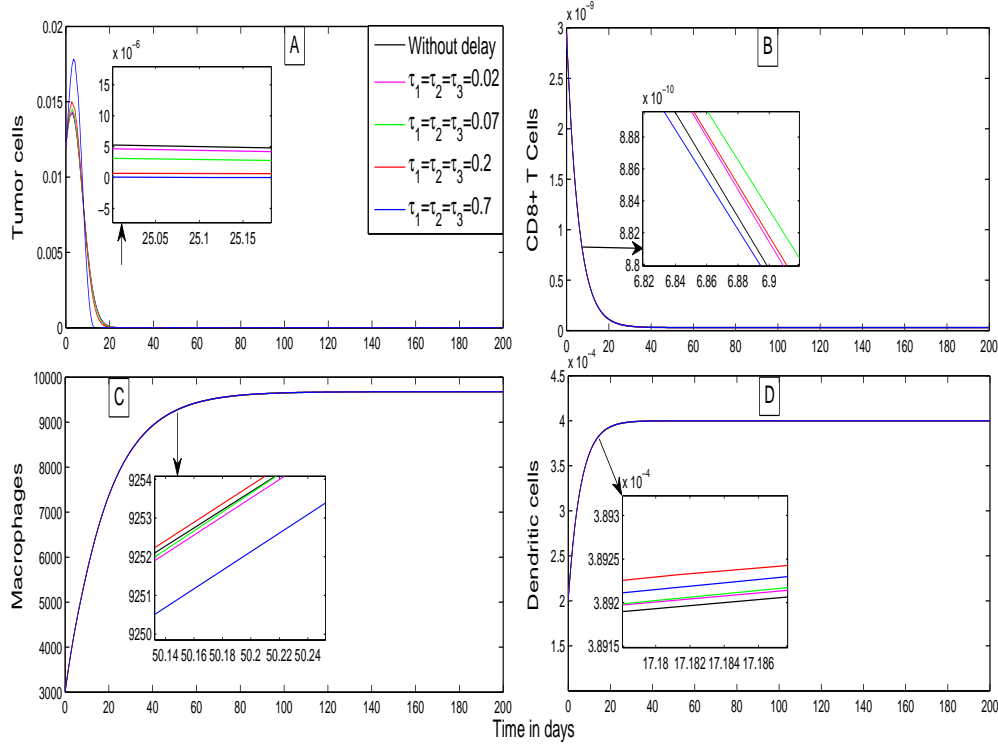
Figure 4.5: The figure shows that the dynamics of tumor cells and immune cells (CD8+T cells, macrophages and dendritic cells) with $\tau_1 = \tau_2 = \tau_3 \in \{0,\ 0.02,\ 0.07,\ 0.2,\ 0.7\}$. The parameters value are specified in the Table 4.1 and Table 4.2 with initial values $(0.012,\ 2.9459 \times 10^{-9},\ 3000,\ 0.0002)$.

4.7 Conclusion

This section summarizes the key findings of the research and highlights the contributions to the field of cancer-immune interaction model with multiple time delays. This study introduces a mathematical model, based on biological principles, to depict the interaction between tumors and the immune system. A coupled system of ordinary differential equations is utilized to construct the model, which incorporates different cells such as tumor cells, CD8+T cells, macrophages, antigen-presenting dendritic cells and several cytokines including regulatory T-cells or Tregs, IL-12, TGF-β, IL-10 and IFN-γ. To get a better visualization of the tumor-immune interplays, we simplified our model by employing quasi-steady-state approximations for the cytokines concentration [92]. The reduced model provides a detailed representation of the interactions between tumor cells, CD8+T cells, macrophages and dendritic cells. Our immune cells need additional time to

provide an appropriate response after identifying the tumor cells. Therefore, incorporating time delays into our mathematical model is necessary to accurately describe the dynamics of tumor-immune competitive system. To better understand the tumor-immune dynamics, we introduced multiple time delays in our model. In this chapter, we have demonstrated that the incorporating of delays does not impact the tumor-immune system significantly, and it may not always result in regular or irregular periodic oscillations. This observation is based on the analysis of a realistic set of parameters value presented in this chapter. Analytically, we established the conditions for existence, uniqueness, positivity and boundedness property of the solution for the delayed model. These mathematical analyses ensure that the solutions of the model are well-defined, nonnegative and remain within certain bounds for studying the behavior and properties of the tumor-immune competitive system. In order to conduct the fixed point analysis, we have found the biologically feasible equilibrium points. We derive some conditions to study the uniform persistence of the system (4.4) without delay. We provide analytical results concerning local stability analysis for both the tumor-immune interaction model without delays and the model incorporating delays. This study also examines the existence of Hopf bifurcation and determines the maximum length of discrete time delay to preserve the stability of period-1 limit cycle. Additionally, we investigate the direction of Hopf bifurcation and evaluate the stability of bifurcating periodic solutions of the delayed model. Using the skill presented by Khajanchi et al. [50], we performed an analysis of our delayed system considering two distinct discrete time delays.

This chapter distinguishes itself from existing literature in this direction through the introduction of three discrete time delays and its subsequent analysis. However, it is observed that despite the incorporation of multiple time delays, their influence on the dynamics of tumor-immune interaction system (4.4) is limited. In contrast to the typical expectation of delays leading to the destabilization of the stable steady state, our findings indicate that such destabilization does not occur in our proposed tumor-immune system. For the biologically relevant parameters value, multiple time delays had a negligible impact on the model dynamics. This observation suggests that delays can be considered as a supplementary elements with minor impact on the overall dynamics of the tumor model. This unique finding underscores the robustness of the model and suggests that other factors may play an important role in governing the behavior of the tumor-immune competitive system. This study contributes valuable insights to our understanding of the impact of multiple time delays on the tumor-immune interactions and

provides a foundation for further investigations in this field.

Table 4.1: Parameter values utilized in the simulations for the tumor-immune interaction model

Par.	Description	Value	Units	Source
r_T	Intrinsic growth rate of tumor cells	0.5822	day^{-1}	[68]
b_T	$1/b_T$ is carrying capacity of tumor cells	1.25×10^{-6}	$cell^{-1}$	Fit to data
α'_T	Tumor cells elimination rate by macrophages	1.5	$pg.day^{-1}.cell^{-1}$	[4]
γ'_T	Tumor cells elimination rate by CD8+T cells	2.4	$pg.day^{-1}.cell^{-1}$	[12]
g'_T	Half-saturation constant	10^4	pg	[80]
α'_8	CD8+T cells activation due IL-12	3.5	$cell.day^{-1}$	[33]
g'_8	Tregs reduce parameter for CD8+T cell production	10^2	pg	[81]
δ_8	CD8+T cells death rate	0.178	day^{-1}	Est.
s_m	Constant source rate of macrophages	5.42×10^2	$cell.day^{-1}$	[86]
α'_m	Recruitment rate of macrophage by IFN-γ	0.69	$pg.cell.day^{-1}$	[87]
g'_m	Half-saturation constant of IFN-γ	1.05×10^4	pg	[4]
g'_{m1}	TGF-β reduce parameter for macrophages	10^4	pg	[4, 76]
γ_m	Macrophages inactivation rate due to tumor cells	0.4656	$cell^{-1}.day^{-1}$	[4]
δ_m	Natural death rate of macrophages	0.056	day^{-1}	Est.
s_d	Constant source rate of dendritic cells	0.68×10^{-4}	$cell.day^{-1}$	Est.
α_d	Dendritic cells activation rate	1.36×10^{-4}	$cell.day^{-1}$	Est.
g_d	Half-saturation constant	10^6	$cell$	[61, 65]
δ_d	Dendritic cells death rate	0.17	day^{-1}	Est.

Table 4.2: Parameter values utilized in the simulations for the tumor-immune interaction model

Par.	Description	Value	Units	Source
α_g	Activation rate of tregs due to CD8+T cells	6.62	$pg.day^{-1}.cell^{-1}$	Est.
δ_g	Tregs degradation rate	0.53	day^{-1}	Est.
α_{10}	Activation rate of IL-10 due to macrophages	1.182×10^{-2}	$pg.day^{-1}.cell^{-1}$	Est.
δ_{10}	IL-10 degradation rate	3.696	day^{-1}	Est.
s_β	Constant source rate of TGF-β	7.6×10^3	$pg.day^{-1}$	Est.
α_β	Release rate of TGF-β by tumor cells	6.84×10^{-2}	$pg.day^{-1}.cell^{-1}$	Est.
δ_β	TGF-β decay rate	0.832	day^{-1}	Est.
α_{12}	Release rate of IL-12 by dendritic cells	2.06×10^{-7}	$pg.day^{-1}.cell^{-1}$	Est.
δ_{12}	IL-12 degradation rate	0.55	day^{-1}	Est.
α_γ	Activation rate of IFN-γ due to CD8+T cells	2.45×10^{-5}	$pg.day^{-1}.cell^{-1}$	Est.
δ_γ	IFN-γ decay rate	2.45	day^{-1}	Est.

Chapter 5

Modeling the dynamics of mixed immunotherapy and chemotherapy for the treatment of immunogenic tumor [†]

5.1 Introduction

Tumors arise from the abnormal proliferation and differentiation of cells in our body. Many benign tumors are under the effective control of the immune system and hence they do not affect patients' life. However, some malignant tumors (such as lymphoma, meningioma, melanoma, mesothelioma, epithelial cancer, and so on) pose a serious threat to human life and can significantly impact patients' quality of life [17, 61]. As per report by the World Health Organization (WHO) [8], cancer is the second largest cause of death globally, estimated to account for around 1 crore deaths in 2020. Nowadays, the most significant and demanding questions in oncology are how the immune system prevents cancer growth and evolution [4, 17]. The interaction between tumor and the immune system is a complicated process. So far, the underlying mechanisms are still not fully understood and have been the focus of research in many disciplines including medicine and mathematics. Mathematical modeling has been proven to be an effective tool for understanding the interaction and providing guidelines on controlling the growth of tumor [17, 19, 61, 65].

[†]A considerable part of this chapter has been communicated.

Our immune system is also a very complicated network composed of many cells, signals and proteins that defend our body against tumor cells and foreign invaders or pathogens. Different kinds of B-cells, T-cells (CD8+T cells or CD4+T cells), macrophages, natural killer cells (NK cells), antigen-presenting dendritic cells (such as dendritic cells, macrophages and Langerhans cells) and cytokines (immuno-stimulatory) are primary componenets of our immune system. Macrophages, CD8+T cells and NK cells are generally considered as effector cells. They can either destroy the tumor cell population or inhibit their proliferation. Meanwhile, tumor cells can in turn neutralize immune-effector cells, leading to a competitive relationship among these two types of cells [71]. On the other hand, in the presence of a tumor, it can promote the production of effector cells by releasing tumor antigens. In other words, the tumor can promote the growth of effector cells to some extent. Thus, there is an interaction between the tumor and the immune system analogous to the predator-prey relationship, with tumor cells as prey and effector cells as predators. [6]. As a result, models on the tumor-immune system dynamics typically incorporate these relationships of competition and predation. To simplify the mechanism underlying tumor-immune interactions and facilitate mathematical analysis, some dynamical models with effector cells and tumor cells only are proposed [43, 65].

Despite medical improvements, many challenges remain in the prognosis and treatment of malignant tumors. The most effective treatments for cancer patients are chemotherapy, surgery, hormone therapy, radiation therapy and so on [7]. The primary method of treatment is used to determine the appropriate position, nature and stage of cancer. Immunotherapy stimulates our immune system against cancer cell population to eliminate them. This type of treatment is effective in promoting an immune response and obstructing the growth of the cancer cell population [44]. Chemotherapy has many harmful side effects, which can result in the patient becoming susceptible to infections and it also reduces the immune system's ability to fight against the cancer cell population. Therefore, an optimal control problem is used in the cancer growth model with chemotherapy to minimize the total drug dosage [19].

The remaining portion of this chapter is described follows. We describe the mathematical model with biological justification in the Section 5.2. In the Section 5.3, we investigate the stability analysis around biologically feasible singular points of the given system. We define the control problem in our

stated model in the Section 5.4. Section 5.5 describes the existence of the control problem. We use Pontryagin's Maximum Principle [79] to analyze the characteristics of the optimal control problem in Section 5.6. In the Section 5.7, we study the uniqueness property of the optimality system, in which the state variables are coupled with adjoint or costate variables. Section 5.8 deals with extensive numerical simulations for our optimal control problem. Finally, this chapter ends with a brief conclusion in Section 5.9.

5.2   Deterministic model

In this section, we studied a mathematical model for nine coupled system of ordinary differential equations (ODEs) that takes into account the role of various cells and cytokines, namely tumor cells ($T(t)$), cytotoxic T-lymphocytes ($T_8(t)$), macrophages ($M(t)$), dendritic cells ($D(t)$), tregs ($T_g(t)$), IL-10 ($I_{10}(t)$), TGF-β ($T_\beta(t)$), IL-12 ($I_{12}(t)$) and IFN-γ ($I_\gamma(t)$). The mathematical model is given by the following system of ODEs:

$$\frac{dT}{dt} = r_T T(1 - b_T T) - \frac{(\alpha'_T M + \gamma'_T T_8)T}{g'_T + I_{10}},$$

$$\frac{dT_8}{dt} = \frac{\alpha'_8 I_{12}}{g'_8 + T_g} - \delta_8 T_8,$$

$$\frac{dM}{dt} = s_m + \frac{\alpha'_m I_\gamma}{(g'_m + I_\gamma)} \cdot \frac{1}{(g'_{m1} + T_\beta)} - \gamma_m MT - \delta_m M,$$

$$\frac{dD}{dt} = s_d + \frac{\alpha_d T}{g_d + T} - \delta_d D, \tag{5.1}$$

$$\frac{dT_g}{dt} = \alpha_g T_8 - \delta_g T_g,$$

$$\frac{dI_{10}}{dt} = \alpha_{10} M - \delta_{10} I_{10},$$

$$\frac{dT_\beta}{dt} = s_\beta + \alpha_\beta T - \delta_\beta T_\beta,$$

$$\frac{dI_{12}}{dt} = \alpha_{12} D - \delta_{12} I_{12},$$

$$\frac{dI_\gamma}{dt} = \alpha_\gamma T_8 - \delta_\gamma I_\gamma.$$

To better understand the interactive dynamics of tumor-immune competitive system, we simplify our model system by utilizing the quasi-steady-state approximations [92] for the concentrations of cytokines. Based on the hypothesis, the cytokine equations, that is, from fifth to nine equations of (5.1) lead to

$$T_g = \frac{\alpha_g}{\delta_g}T_8, \ I_{10} = \frac{\alpha_{10}}{\delta_{10}}M, \ T_\beta = \frac{s_\beta}{\delta_\beta} + \frac{\alpha_\beta}{\delta_\beta}T,$$

$$I_{12} = \frac{\alpha_{12}}{\delta_{12}}D, \ I_\gamma = \frac{\alpha_\gamma}{\delta_\gamma}T_8.$$

After substituting these cytokine expressions into the first to fourth equations of (5.1), we obtain the following four ordinary differential equations for the tumor-immune interactive dynamics

$$
\begin{aligned}
\frac{dT}{dt} &= r_T T(1 - b_T T) - \frac{(\alpha_T M + \gamma_T T_8)T}{g_T + M}, \\
\frac{dT_8}{dt} &= \frac{\alpha_8 D}{g_8 + T_8} - \delta_8 T_8, \\
\frac{dM}{dt} &= s_m + \frac{\alpha_m T_8}{(g_m + T_8)} \cdot \frac{1}{(g_{m1} + T)} - \gamma_m MT - \delta_m M, \\
\frac{dD}{dt} &= s_d + \frac{\alpha_d T}{g_d + T} - \delta_d D,
\end{aligned}
\tag{5.2}
$$

where

$$\alpha_T = \frac{\delta_{10}}{\alpha_{10}}\alpha_T', \quad \gamma_T = \frac{\delta_{10}}{\alpha_{10}}\gamma_T', \quad g_T = \frac{\delta_{10}}{\alpha_{10}}g_T', \quad \alpha_8 = \frac{\delta_g}{\alpha_g}\frac{\alpha_{12}}{\delta_{12}}\alpha_8',$$

$$g_8 = \frac{\delta_g}{\alpha_g}g_8', \quad \alpha_m = \frac{\delta_\beta}{\alpha_\beta}\alpha_m', \quad g_m = \frac{\delta_\gamma}{\alpha_\gamma}g_m', \quad g_{m1} = \frac{\delta_\beta}{\alpha_\beta}g_{m1}' + \frac{s_\beta}{\alpha_\beta}.$$

By employing the role of chemotherapeutic drug and introduce the optimal control theory, we obtain the following system of ODEs:

$$
\begin{aligned}
\frac{dT}{dt} &= r_T T(1 - b_T T) - \frac{(\alpha_T M + \gamma_T T_8)T}{g_T + M} - k_T(1 - e^{-\eta_T C})T, \\
\frac{dT_8}{dt} &= \frac{\alpha_8 D}{g_8 + T_8} - \delta_8 T_8 + u_2(t) - k_8(1 - e^{-\eta_8 C})T_8, \\
\frac{dM}{dt} &= s_m + \frac{\alpha_m T_8}{(g_m + T_8)} \cdot \frac{1}{(g_{m1} + T)} - \gamma_m MT - \delta_m M + u_3(t) - k_m(1 - e^{-\eta_m C})M, \\
\frac{dD}{dt} &= s_d u_4(t) + \frac{\alpha_d T}{g_d + T} - \delta_d D - k_d(1 - e^{-\eta_d C})D, \\
\frac{dC}{dt} &= -\gamma C + v_c(t),
\end{aligned}
\tag{5.3}
$$

with the following initial values:

$$
\begin{aligned}
T(0) &= T_0 \geq 0, \quad T_8(0) = T_{80} > 0, \quad M(0) = M_0 > 0, \quad D(0) = D_0 > 0, \\
C(0) &= C_0 > 0. \tag{5.4}
\end{aligned}
$$

Here,

- the term $r_T T(1 - b_T T)$ represents the logistic growth of tumor cell population without any immune response, where r_T is intrinsic growth rate and $\frac{1}{b_T}$ is carrying capacity of tumor cells.

- The function $\frac{(\alpha_T M + \gamma_T T_8)T}{g_T + M}$ is the clearance term of tumor cells due to macrophages and CD8+T cells with clearance rates α_T and γ_T, respectively. Here, g_T is the Michaelis-Menten term and the term $\frac{1}{g_T + M}$ represents the major immuno-suppressive factor for both macrophages and CD8+T cells.

- Last term of the first equation of system (5.3) represents the tumor death induced by chemotherapy, where k_T is the rate of chemotherapy induced tumor death and η_T is the chemotherapy efficacy coefficient.

- $\frac{\alpha_8 D}{g_8 + T_8}$ is the activation term of cytotoxic T-lymphocytes (CD8+T cells) due to the direct presence of dendritic cells and the activation rate is α_8. g_8 is the half-saturation constant of CD8+T cells in Michaelis-Menten term.

- The natural death rate of CD8+T cells is δ_8.

- $u_2(t)$ serves as the control parameter regulating the CD8+T cell population. This parameter plays a pivotal role in implementing an immunotherapeutic strategy aimed at enhancing the immune response. It represents a crucial factor in the design and execution of immunotherapy. In this approach, the introduction of antigen-specific cytotoxic immune cells empowers the body's immune system to more effectively target and eliminate cancer cells.

- $k_8(1 - e^{-\eta_8 C})T_8$ is the CD8+T cells death induced by chemotherapy, where k_8 is the rate of chemotherapy induced CD8+T cell death and η_8 is the chemotherapy efficacy coefficient.

- s_m is the constant source rate of macrophages. The function $\frac{\alpha_m T_8}{(g_m + T_8)} \cdot \frac{1}{(g_{m1} + T)}$ is activation term of macrophages. α_m is the activation rate of macrophages due to the presence of CD8+T cells, where g_m is the

half-saturation constant in Michaelis-Menten dynamics. $\frac{1}{(g_{m1}+T)}$ is the immuno-suppressive factor of macrophages and g_{m1} is the suppressive parameter.

- γ_m represents the loss of macrophages due to interaction of tumor cells.

- Natural death rate of macrophages is δ_m.

- $u_3(t)$ acts as a control parameter for macrophages, regulating various aspects of macrophage behavior and function within the immune system. It plays a crucial role in directing the body's immune response to cancer cells. The function of $u_3(t)$ can vary depending on the specific biological context and the particular immune responses under consideration.

- $k_m(1 - e^{-\eta_m C})M$ is the macrophages death induced by chemotherapy, where k_m is the rate of chemotherapy induced macrophages death and η_m is the chemotherapy efficacy coefficient.

- The variable $u_4(t)$ represents a control input or a control function that can be applied to modulate or regulate the constant source rate of dendritic cells, s_d. This implies that the production or supply of dendritic cells can be influenced externally. This control input could be in the form of a signal, treatment, medication or any other intervention aimed at enhancing the immune response against tumor cells.

- The coefficient α_d incorporates the activation rate of dendritic cells due to the direct presence of tumor cells, where g_d is the half-saturation constant following Michaelis-Menten term.

- The loss of dendritic cells is given by δ_d.

- Last term of the fourth equation of (5.3) represents the decay of dendritic cells induced chemotherapy. η_d is the chemotherapy efficacy coefficient and k_d is the rate of chemotherapy induced dendritic cells decay.

- Chemotherapy decays at a rate (γ) is proportional to its concentration [20].

- $v_c(t)$ is a dynamic control parameter that regulates the administration of chemotherapeutic drugs in a tumor-immune interaction system. It is an important component of personalized cancer treatment strategies, aiming to strike a balance between effectively targeting the tumor and minimizing harm to healthy tissues while considering the individual characteristics of patient and the tumor's behavior over time.

- The chemotherapy interacts each of the cell T, T_8, M and D through a term of the form in [26]. This term indicates the fractional killing rate of the drug.

5.3   Dynamical overview

In this section, we shall study the stability analysis around the biologically feasible steady states to understand the dynamics of our control system (5.3). To do this, we assumed that $u_2(t) = u_2$, $u_3(t) = u_3$, $u_4(t) = u_4$, $v_c(t) = v_c$, where u_2, u_3, u_4 and v_c are all constants. The system has the following two steady states:

(i) Tumor-free singular point is $E^0(0, T_8^0, M^0, D^0, C^0)$, where

$$
M^0 = \frac{1}{\delta_m + k_m\left(1 - e^{-\frac{\eta_m v_c}{\gamma}}\right)}\left[s_m + u_3 + \frac{\alpha_m T_8^0}{g_{m1}(g_m + T_8^0)}\right],
$$

$$
D^0 = \frac{s_d u_4}{\delta_d + k_d\left(1 - e^{-\frac{\eta_d v_c}{\gamma}}\right)},
$$

$$
C^0 = \frac{v_c}{\gamma},
$$

and T_8^0 is defined in following quadratic form:

$$
n_1(T_8^0)^2 + n_2 T_8^0 + n_3 = 0, \tag{5.5}
$$

with

$$
n_1 = \delta_8 + k_8\left(1 - e^{-\frac{\eta_8 v_c}{\gamma}}\right),
$$

$$
n_2 = n_8 g_8 - u_2,
$$

$$
n_3 = -(u_2 g_8 + \alpha_8 D^0).
$$

Since $n_3 < 0$, then above second degree equation (5.5) has a unique positive root is given by

$$
T_8^0 = \frac{-n_2 + \sqrt{n_2^2 - 4n_1 n_3}}{2n_1}.
$$

To know the dynamical nature around the singular point $E(T, T_8, M, D, C)$, first we calculate the Jacobian matrix J_E is derived as

$$J_E = \begin{pmatrix} a_{11} & a_{12} & a_{13} & 0 & a_{15} \\ 0 & a_{22} & 0 & a_{24} & a_{25} \\ a_{31} & a_{32} & a_{33} & 0 & a_{35} \\ a_{41} & 0 & 0 & a_{44} & a_{45} \\ 0 & 0 & 0 & 0 & a_{55} \end{pmatrix},$$

where

$$a_{11} = r_T - 2r_T b_T T - \frac{(\alpha_T M + \gamma_T T_8)}{g_T + M} - k_T \left(1 - e^{-\eta_T C}\right),$$

$$a_{12} = -\frac{\gamma_T T}{g_T + M},$$

$$a_{13} = -\frac{(g_T \alpha_T - \gamma_T T_8)T}{(g_T + M)^2},$$

$$a_{15} = -\eta_T k_T T e^{-\eta_T C},$$

$$a_{22} = -\frac{\alpha_8 D}{(g_8 + T_8)^2} - \delta_8 - k_8 \left(1 - e^{-\eta_8 C}\right),$$

$$a_{24} = \frac{\alpha_8}{g_8 + T_8},$$

$$a_{25} = -\eta_8 k_8 T_8 e^{-\eta_8 C},$$

$$a_{31} = -\frac{\alpha_m T_8}{(g_m + T_8)(g_{m1} + T)^2} - \gamma_m M,$$

$$a_{32} = \frac{\alpha_m g_m}{(g_m + T_8)^2(g_{m1} + T)},$$

$$a_{33} = -\gamma_m T - \delta_m - k_m \left(1 - e^{-\eta_m C}\right),$$

$$a_{35} = -\eta_m k_m M e^{-\eta_m C},$$

$$a_{41} = \frac{g_d \alpha_d}{(g_d + T)^2},$$

$$a_{44} = -\delta_d - k_d \left(1 - e^{-\eta_d C}\right),$$

$$a_{45} = -\eta_d k_d D e^{-\eta_d C},$$

$$a_{55} = -\gamma.$$

140

At the tumor-free singular point E^0, the Jacobian matrix J_{E^0} has the following eigenvalues

$$
\begin{aligned}
e_1^0 &= r_T - \frac{\alpha_T M^0 + \gamma_T T_8^0}{g_T + M^0} - k_T\left(1 - e^{-\frac{\eta_T v_c}{\gamma}}\right), \\
e_2^0 &= -\frac{\alpha_8 D^0}{(g_8 + T_8^0)^2} - \delta_8 - k_8\left(1 - e^{-\frac{\eta_8 v_c}{\gamma}}\right), \\
e_3^0 &= -\delta_m - k_m\left(1 - e^{-\frac{\eta_m v_c}{\gamma}}\right), \\
e_4^0 &= -\delta_d - k_d\left(1 - e^{-\frac{\eta_d v_c}{\gamma}}\right), \\
e_5^0 &= -\gamma.
\end{aligned}
$$

All the eigenvalues are negative if $e_1^0 < 0$. Therefore, the tumor-free singular point E^0 is locally asymptotically stable (LAS) if

$$
r_T \quad < \quad \frac{\alpha_T M^0 + \gamma_T T_8^0}{g_T + M^0} + k_T\left(1 - e^{-\frac{\eta_T v_c}{\gamma}}\right).
$$

(ii) Let us assume the interior singular point to be $E^1(T^1,\, T_8^1,\, M^1,\, D^1,\, C^1)$. To determine this interior singular point, we analyze the conditions $\frac{dT}{dt} = \frac{dT_8}{dt} = \frac{dM}{dt} = \frac{dD}{dt} = \frac{dC}{dt} = 0$. Subsequently, we can express the values of $T^1,\, T_8^1,\, M^1,\, D^1$ and C^1 as follows

$$
C^1 = \frac{v_c}{\gamma},\quad D^1 = \frac{s_d u_4(g_d + T^1) + \alpha_d T^1}{(g_d + T^1)[\delta_d + k_d(1 - e^{\frac{-\eta_d v_c}{\gamma}})]},
$$

$$
M^1 = \frac{\gamma_T T_8^1 + k_T g_T(1 - e^{\frac{-\eta_T v_c}{\gamma}}) - g_T r_T(1 - b_T T^1)}{r_T(1 - b_T T^1) - \alpha_T - k_T(1 - e^{\frac{-\eta_T v_c}{\gamma}})},
$$

$$
\begin{aligned}
T_8^1 =\; & \frac{u_2 - \delta_8 g_8 - g_8 k_8(1 - e^{\frac{-\eta_8 v_c}{\gamma}})}{2[\delta_8 + k_8(1 - e^{\frac{-\eta_8 v_c}{\gamma}})]} \\[6pt]
& + \frac{\sqrt{[\delta_8 g_8 - u_2 + g_8 k_8(1 - e^{\frac{-\eta_8 v_c}{\gamma}})]^2 + 4(\alpha_8 D^1 + u_2 g_8)[\delta_8 + k_8(1 - e^{\frac{-\eta_8 v_c}{\gamma}})]}}{2[\delta_8 + k_8(1 - e^{\frac{-\eta_8 v_c}{\gamma}})]},
\end{aligned}
$$

and

$$
s_m + \frac{\alpha_m T_8^1}{(g_m + T_8^1)(g_{m1} + T^1)} + u_3 = [\gamma_m T^1 + \delta_m + k_m(1 - e^{\frac{-\eta_m v_c}{\gamma}})]M^1.
$$

Obtaining an analytical expression for the interior singular point E^1 from the given expressions presents a substantial analytical challenge. As a result, we determine the singular point through numerical simulation. To evaluate

the stability of the interior singular point E^1, we proceed by calculating the variational matrix around the interior singular point E^1, as defined below

$$J(E^1) = [j_{ij}] = \begin{bmatrix} j_{11} & j_{12} & j_{13} & j_{14} & j_{15} \\ j_{21} & j_{22} & j_{23} & j_{24} & j_{25} \\ j_{31} & j_{32} & j_{33} & j_{34} & j_{35} \\ j_{41} & j_{42} & j_{43} & j_{44} & j_{45} \\ j_{51} & j_{52} & j_{53} & j_{54} & j_{55} \end{bmatrix},$$

where

$$j_{11} = r_T - 2r_T b_T T^1 - \frac{(\alpha_T M^1 + \gamma_T T_8^1)}{g_T + M^1} - k_T(1 - e^{\frac{-\eta_T v_c}{\gamma}}),$$

$$j_{12} = -\frac{\gamma_T T^1}{g_T + M^1}, \quad j_{13} = -\frac{(g_T \alpha_T - \gamma_T T_8^1)T^1}{(g_T + M^1)^2},$$

$$j_{14} = 0, \quad j_{15} = -\eta_T k_T T^1 e^{\frac{-\eta_T v_c}{\gamma}},$$

$$j_{21} = 0, \quad j_{22} = -\frac{\alpha_8 D^1}{(g_8 + T_8^1)^2} - \delta_8 - k_8(1 - e^{\frac{-\eta_8 v_c}{\gamma}}),$$

$$j_{23} = 0, \quad j_{24} = \frac{\alpha_8}{g_8 + T_8^1}, \quad j_{25} = -\eta_8 k_8 T_8^1 e^{\frac{-\eta_8 v_c}{\gamma}},$$

$$j_{31} = -\frac{\alpha_m T_8^1}{(g_m + T_8^1)(g_{m1} + T^1)^2} - \gamma_m M^1,$$

$$j_{32} = \frac{\alpha_m g_m}{(g_m + T_8^1)^2(g_{m1} + T^1)}, \quad j_{33} = -\gamma_m T^1 - \delta_m - k_m(1 - e^{\frac{-\eta_m v_c}{\gamma}}),$$

$$j_{34} = 0, \quad j_{35} = -\eta_m k_m M^1 e^{\frac{-\eta_m v_c}{\gamma}},$$

$$j_{41} = \frac{g_d \alpha_d}{(g_d + T^1)^2}, \quad j_{42} = j_{43} = 0,$$

$$j_{44} = -\delta_d - k_d(1 - e^{\frac{-\eta_d v_c}{\gamma}}), \quad j_{45} = -\eta_d k_d D^1 e^{\frac{-\eta_d v_c}{\gamma}},$$

$$j_{51} = j_{52} = j_{53} = j_{54} = 0, \quad j_{55} = -\gamma.$$

The characteristic equation at the interior singular point $E^1(T^1, T_8^1, M^1, D^1, C^1)$ is

$$\phi^5 + B_1\phi^4 + B_2\phi^3 + B_3\phi^2 + B_4\phi + B_5 = 0,$$

where

$$B_1 = -\sum_{i=1}^{5} j_{ii}, \; B_2 = \sum_{i,j=1}^{5} j_{ii}j_{jj} - \sum_{i,j=1}^{5} j_{ij}j_{ji},$$

$$B_3 = \sum_{i,j,k=1}^{5} j_{ij}j_{ji}j_{kk} - \sum_{i,j,k=1}^{5} j_{ii}j_{jj}j_{kk} - \sum_{i,j,k=1}^{5} j_{ij}j_{jk}j_{ki},$$

$$B_4 = \sum_{i,j,k,l=1}^{5} j_{ii}j_{jj}j_{kk}j_{ll} + \sum_{i,j,k,l=1}^{5} j_{ij}j_{ji}j_{ki}j_{ll} - \sum_{i,j,k,l=1}^{5} j_{ij}j_{ji}j_{kl}j_{lk}$$

$$\quad - \sum_{i,j,k,l=1}^{5} j_{ij}j_{ji}j_{kk}j_{ll} - \sum_{i,j,k,l=1}^{5} j_{ij}j_{jk}j_{kl}j_{li},$$

$$B_5 = -det(J(E^1)).$$

For all of the expressions mentioned above, it holds that $i \neq j \neq k \neq l$. According to the Routh-Hurwitz conditions, all roots of the characteristic equation have negative or negative real parts if $B_1 > 0$, $B_5 > 0$, $B_1B_2 - B_3 > 0$, $(B_1B_2 - B_3)B_3 - B_1(B_1B_4 - B_5) > 0$ and $(B_1B_2 - B_3)(B_3B_4 - B_2B_5) + (B_1B_4 - B_5)(B_5 - B_1B_4) > 0$. If the eigenvalues have negative real parts, then the interior singular point is considered stable.

5.4   Optimal control problem

This section describes the control problem in our model (5.3) to minimize the tumor cell population and maximize the immune components. Thus, we assume our control set $\mathbb{U}$ as follows

$$\mathbb{U} = \{u_2(t), \; u_3(t), \; u_4(t), \; v_c(t) \text{ are piecewise continuous} :$$
$$0 \leq u_2(t), \; u_3(t), \; u_4(t), \; v_c(t), \; \forall \, t \in [0, t_f]\}.$$

We would like to maximize the immune components (CD8+T cells and macrophages) to eliminate the tumor cell population. Therefore, we define the following objective functional

$$J(u_2, \; u_3, \; u_4, \; v_c) = \int_0^{t_f} [T(t) + \frac{1}{2}\epsilon_2 u_2^2 + \frac{1}{2}\epsilon_3 u_3^2 + \frac{1}{2}\epsilon_4 u_4^2 + \frac{1}{2}\epsilon_c v_c^2]dt, \quad (5.6)$$

where ϵ_2, ϵ_3, ϵ_4 and ϵ_c are positive constants. We must have to show J is concave and its minimum value can be obtained. We suggest the objective

functional J is a function of u, then our main aim is to characterize the optimal control $u^*(t) = (u_2^*(t),\ u_3^*(t),\ u_4^*(t),\ v_c^*(t))$ in such a way that

$$J(u^*) = \max_{0 \le u}\{J(u_2,\ u_3,\ u_4,\ v_c)\}.$$

5.5   Existence of optimal control

In this section, we shall prove the existence property of optimal control for the given system with the control set $\mathbb{U}$ due to the method described by Fleming & Rishel [30]. For this, we need to show that in a finite time interval the solution of each state equations of the system is bounded. Thus, we calculate the upper bounds (super-solutions) of T, T_8, M, D and C for the system (5.3). The first equation of (5.3) can be written as

$$\frac{dT}{dt} \le r_T T(1 - b_T T),$$

which implies that

$$T \le \frac{m_1 \frac{1}{b_T}}{m_1 + e^{-r_T t}}, \qquad m_1 \text{ being an arbitrary constant.}$$

Then, we have

$$\limsup_{t \to \infty} T(t) \le \frac{1}{b_T} = T_{\max} \text{ (say).}$$

Third equation for the system (5.3) can be written as

$$\frac{dM}{dt} = s_m + \frac{\alpha_m}{g_{m1} + T} - \frac{\alpha_m g_m}{(g_m + T_8)(g_{m1} + T)} - \gamma_m MT - \delta_m M$$

$$+ \ u_3 - k_m(1 - e^{-\eta_m C})M$$

$$\le \ s_m + \frac{\alpha_m}{g_{m1}} - \delta_m M + u_3,$$

which implies that

$$\frac{dM}{dt} + \delta_m M \le \frac{(s_m + u_3)g_{m1} + \alpha_m}{g_{m1}}.$$

After solving above inequality, we have

$$M \le \frac{(s_m + u_3)g_{m1} + \alpha_m}{g_{m1}\delta_m} + m_3 e^{-\delta_m t}, \qquad m_3 \text{ being an arbitrary constant.}$$

For $t > 0$, we get

$$\limsup_{t \to \infty} M(t) \leq \frac{(s_m + u_3)g_{m1} + \alpha_m}{g_{m1}\delta_m} = M_{\max} \text{ (say)}.$$

Now, from the fourth equation of (5.3), we have

$$\frac{dD}{dt} = (s_d u_4 + \alpha_d) - \frac{\alpha_d g_d}{g_d + T} - \delta_d D,$$

which leads to

$$\frac{dD}{dt} + \delta_d D \leq (s_d u_4 + \alpha_d).$$

For $t > 0$, we get

$$\limsup_{t \to \infty} D(t) \leq \frac{s_d u_4 + \alpha_d}{\delta_d} = D_{\max} \text{ (say)}.$$

By using the upper bound of $D(t)$, we get the following inequality

$$\frac{dT_8}{dt} \leq \frac{\alpha_8 D_{\max}}{g_8 + T_8} - \delta_8 T_8 + u_2$$

$$\frac{dT_8}{dt} + \delta_8 T_8 \leq \frac{\alpha_8 D_{\max}}{g_8} + u_2.$$

Solving the above inequality for $t > 0$, we have

$$\limsup_{t \to \infty} T_8(t) \leq \frac{\alpha_8 D_{\max} + u_2 g_8}{g_8 \delta_8} = T_{8\max} \text{ (say)}.$$

Again, the last equation of (5.3) implies that

$$\frac{dC}{dt} + \gamma C = v_c$$

$$\Rightarrow \limsup_{t \to \infty} C(t) = \frac{v_c}{\gamma} = C_{\max} \text{ (say)}.$$

By using the bounds of $T_{\max}$, $T_{8\max}$, $M_{\max}$, $D_{\max}$, $C_{\max}$ we have a set of upper bound solutions for the system (5.3). By denoting these notations $\overline{T}$, $\overline{T_8}$, $\overline{M}$, $\overline{D}$ and $\overline{C}$, we have

$$
\begin{aligned}
\frac{d\overline{T}}{dt} &= r_T \overline{T}, \\
\frac{d\overline{T_8}}{dt} &= \alpha_8 \overline{D} + u_2, \\
\frac{d\overline{M}}{dt} &= s_m + \alpha_m \overline{T_8} + u_3, \\
\frac{d\overline{D}}{dt} &= s_d u_4 + \alpha_d \overline{T}, \\
\frac{d\overline{C}}{dt} &= v_c,
\end{aligned} \tag{5.7}
$$

145

are bounded in a finite time interval. The above system can be written as

$$
\begin{pmatrix} \overline{T} \\ \overline{T_8} \\ \overline{M} \\ \overline{D} \\ \overline{C} \end{pmatrix}' = \begin{pmatrix} r_T & 0 & 0 & 0 & 0 \\ 0 & 0 & 0 & \alpha_8 & 0 \\ 0 & \alpha_m & 0 & 0 & 0 \\ \alpha_d & 0 & 0 & 0 & 0 \\ 0 & 0 & 0 & 0 & 0 \end{pmatrix} \begin{pmatrix} \overline{T} \\ \overline{T_8} \\ \overline{M} \\ \overline{D} \\ \overline{C} \end{pmatrix} + \begin{pmatrix} 0 \\ u_2 \\ s_m + u_3 \\ s_d u_4 \\ v_c \end{pmatrix}.
$$

We found a linear system with bounded coefficients, then the super-solutions $\overline{T}$, $\overline{T_8}$, $\overline{M}$, $\overline{D}$, $\overline{C}$ are uniformly bounded. Now, we use the boundedness of solutions of each state variables for established the existence of an optimal control.

Theorem 5.5.1. *For the given optimal control problem and the objective functional $J(u_2,\ u_3\ ,u_4,\ v_c) = \int_0^{t_f}[T(t) + \frac{1}{2}\epsilon_2 u_2^2 + \frac{1}{2}\epsilon_3 u_3^2 + \frac{1}{2}\epsilon_4 u_4^2 + \frac{1}{2}\epsilon_c v_c^2]dt$, with the control set*

$$
\begin{aligned}
\mathbb{U} &= \{u_2(t),\ u_3(t),\ u_4(t),\ v_c(t) \text{ are piecewise continuous}: \\
&\quad 0 \le u_2(t),\ u_3(t),\ u_4(t),\ v_c(t),\ \forall\ t \in [0, t_f]\},
\end{aligned}
$$

subject to state equations with initial solutions $T(0) = T_0$, $T_8(0) = T_{80}$, $M(0) = M_0$, $D(0) = D_0$, $C(0) = C_0$, there exists an optimal control $u^*(t) \in \mathbb{U}$, which minimizes $J(u^*)$, that is,

$$
J(u^*) = \max_{0 \le u}\{J(u_2,\ u_3,\ u_4,\ v_c)\},
$$

given by the following conditions are satisfied:
(i) The admissible control set $\mathbb{U}$, the optimal control $u(t)$ with initial solutions along with each of the given state variables are non-empty.
(ii) The admissible optimal control set $\mathbb{U}$ is closed and convex.
(iii) By adding the sum of bounded control, right hand side of given system (5.3) is continuous and bounded above and state equations can be expressed as a linear function of u with coefficients depend on sufficient time interval and the state variables.
(iv) The integrand of objective functional $J(u)$ is concave on $\mathbb{U}$ and bounded by $c_1 + c_2|u_2|^2 + c_3|u_3|^2 + c_4|u_4|^2 + c_c|v_c|^2$, where c_1 is the upper bound of $T(t)$ and depends on $T(t)$, $T_8(t)$, $M(t)$, $D(t)$, $C(t)$ and $c_c = \frac{\epsilon_c}{2}$, $c_i = \frac{\epsilon_i}{2}$ for $i = 2,\ 3,\ 4$.

146

Proof. Due to the theory developed by Fleming and Rishel [30], we prove the above theorem.

(i) An optimal control set $\mathbb{U}$ is continuous and the coefficients of given model are bounded. Also in the finite time interval, solutions of the given system are bounded.

(ii) By definition, $\mathbb{U}$ is closed and convex.

(iii) The right hand side of given optimal control system is continuous. Let $\sigma(t, X)$ be the right hand side of (5.3) excluding terms of u_2, u_3, u_4, v_c. Then,

$$H(t, X, u_2, u_3, u_4, v_c) = \sigma(t, X) + \begin{pmatrix} 0 \\ u_2 \\ u_3 \\ s_d u_4 \\ v_c \end{pmatrix},$$

where $X = [T(t), T_8(t), M(t), D(t), C(t)]^T$. Considering the upper bounds of solutions, we get

$$|H(t, X, u_2, u_3, u_4, v_c)| \leq \left| \begin{pmatrix} r_T & 0 & 0 & 0 & 0 \\ 0 & 0 & 0 & \alpha_8 & 0 \\ 0 & \alpha_m & 0 & 0 & 0 \\ \alpha_d & 0 & 0 & 0 & 0 \\ 0 & 0 & 0 & 0 & 0 \end{pmatrix} \begin{pmatrix} T \\ T_8 \\ M \\ D \\ C \end{pmatrix} \right| + \left| \begin{matrix} 0 \\ u_2 \\ u_3 \\ s_d u_4 \\ v_c \end{matrix} \right|$$

$$\leq H_1(|X| + |u|),$$

with H_1 depends on the coefficients of the system.

(iv) It can be noted that in $\mathbb{U}$, the integrand of $J(u)$ is concave. Also, $T(t) + \frac{1}{2}\epsilon_2 u_2^2 + \frac{1}{2}\epsilon_3 u_3^2 + \frac{1}{2}\epsilon_4 u_4^2 + \frac{1}{2}\epsilon_c v_c^2 \leq c_1 + c_2 |u_2|^2 + c_3 |u_3|^2 + c_4 |u_4|^2 + c_c |v_c|^2$, where c_1 is the upper bound of $T(t)$ and depends on $T(t)$, $T_8(t)$, $M(t)$, $D(t)$, $C(t)$ and $c_c = \frac{\epsilon_c}{2}$, $c_i = \frac{\epsilon_i}{2}$ for $i = 2, 3, 4$.

Hence, all conditions of the theorem are proved. $\square$

5.6 Characterization of optimal control

We use the theory of calculus of variation for prove the necessary conditions of given optimal control problem. To determine the characterization of optimal

control, we employ the Pontryagin's Maximum Principle [79]. To perform the necessary conditions, at first we define the Hamiltonian as

$$
\begin{aligned}
\mathbb{H} &= T(t) + \frac{1}{2}\epsilon_c(v_c(t))^2 + \frac{1}{2}\epsilon_2(u_2(t))^2 + \frac{1}{2}\epsilon_3(u_3(t))^2 + \frac{1}{2}\epsilon_4(u_4(t))^2 \\
&+ A_1\Big[r_T T(1 - b_T T) - \frac{(\alpha_T M + \gamma_T T_8)T}{g_T + M} - k_T(1 - e^{-\eta_T C})T\Big] \\
&+ A_2\Big[\frac{\alpha_8 D}{g_8 + T_8} - \delta_8 T_8 + u_2(t) - k_8(1 - e^{-\eta_8 C})T_8\Big] \\
&+ A_3\Big[s_m + \frac{\alpha_m T_8}{(g_m + T_8)} \cdot \frac{1}{(g_{m1} + T)} - \gamma_m MT - \delta_m M \\
&+ u_3(t) - k_m(1 - e^{-\eta_m C})M\Big] \\
&+ A_4\Big[s_d u_4(t) + \frac{\alpha_d T}{g_d + T} - \delta_d D - k_d(1 - e^{-\eta_d C})D\Big] \\
&+ A_5[-\gamma C + v_c(t)],
\end{aligned}
$$

where $A_i(t)$ ($i = 1, 2, 3, 4, 5$) are adjoint variables. Since the controls $u_2(t)$, $u_3(t)$, $u_4(t)$ and $v_c(t)$ are bounded, we define the Lagrangian as

$$
\begin{aligned}
\mathbb{L} &= \mathbb{H} + Q_1(t)v_c(t) - Q_2(t)(1 - v_c(t)) + Q_3(t)u_2(t) - Q_4(t)(1 - u_2(t)) \\
&+ Q_5(t)u_3(t) - Q_6(t)(1 - u_3(t)) + Q_7(t)u_4(t) - Q_8(t)(1 - u_4(t)),
\end{aligned}
$$

with penalty multipliers $Q_i(t) \geq 0$ satisfy the equations

$$
Q_1(t)v_c(t) = 0,
$$
$$
Q_2(t)(1 - v_c(t)) = 0,
$$

at the optimal control $v_c^*(t)$;

$$
Q_3(t)u_2(t) = 0,
$$
$$
Q_4(t)(1 - u_2(t)) = 0,
$$

at the optimal control $u_2^*(t)$;

$$
Q_5(t)u_3(t) = 0,
$$
$$
Q_6(t)(1 - u_3(t)) = 0,
$$

at the optimal control $u_3^*(t)$ and

$$
Q_7(t)u_4(t) = 0,
$$
$$
Q_8(t)(1 - u_4(t)) = 0,
$$

at the optimal control $u_4^*(t)$.

Theorem 5.6.1. *For the control u^* with corresponding solutions of state variables at interior steady state $E^1(T^1,\ T_8^1,\ M^1,\ D^1,\ C^1)$ that minimizes the objective functional $J(u)$, there exists costates $A_i(t)$; ($i = 1$ to 5) satisfying the following equations*

$$
\begin{aligned}
A_1' &= -\Big[1 + A_1\Big\{r_T(1-2b_T T) - \tfrac{\alpha_T M + \gamma_T T_8}{g_T + M} - k_T(1-e^{-\eta_T C})\Big\} \\
&\quad - A_3\Big\{\tfrac{\alpha_m T_8}{(g_m+T_8)\cdot(g_{m1}+T)^2} + \gamma_m M\Big\} + A_4\tfrac{\alpha_d g_d}{(g_d+T)^2}\Big], \\
A_2' &= -\Big[-A_1\tfrac{\gamma_T T}{g_T+M} - A_2\Big\{\tfrac{\alpha_8 D}{(g_8+T_8)^2} + \delta_8 + k_8(1-e^{-\eta_8 C})\Big\} \\
&\quad + A_3\tfrac{\alpha_m g_m}{(g_m+T_8)^2(g_{m1}+T)}\Big], \\
A_3' &= -\Big[-A_1\tfrac{(\alpha_T g_T - \gamma_T T_8)T}{(g_T+M)^2} - A_3(\gamma_m T + \delta_m + k_m(1-e^{-\eta_m C}))\Big], \\
A_4' &= -\Big[A_2\tfrac{\alpha_8}{g_8+T_8} - A_4(\delta_d + k_d(1-e^{-\eta_d C}))\Big], \\
A_5' &= A_1\eta_T k_T T e^{-\eta_T C} + A_2\eta_8 k_8 T_8 e^{-\eta_8 C} + A_3\eta_m k_m M e^{-\eta_m C} \\
&\quad + A_4\eta_d k_d D e^{-\eta_d C} + A_5\gamma,
\end{aligned}
\tag{5.8}
$$

where $A_i(t_f) = 0$; ($i{=}1$ to 5) known as transversality terminal conditions. Also, v_c^*, u_2^*, u_3^*, u_4^* are represented by

$$
v_c^* = \min\Big(1, \Big(\tfrac{-A_5}{\epsilon_c}\Big)^+\Big),
$$

$$
u_2^* = \min\Big(1, \Big(\tfrac{-A_2}{\epsilon_2}\Big)^+\Big),
$$

$$
u_3^* = \min\Big(1, \Big(\tfrac{-A_3}{\epsilon_3}\Big)^+\Big),
$$

$$
u_4^* = \min\Big(1, \Big(\tfrac{-A_4 s_d}{\epsilon_4}\Big)^+\Big).
$$

Proof. We use Pontryagin's Maximum Principle [79], to obtain the costates and transversality conditions. By differentiating Lagrangian $\mathbb{L}$ with reference to given state equations, we get $A_1' = -\tfrac{\partial \mathbb{L}}{\partial T}$, $A_2' = -\tfrac{\partial \mathbb{L}}{\partial T_8}$, $A_3' = -\tfrac{\partial \mathbb{L}}{\partial M}$, $A_4' = -\tfrac{\partial \mathbb{L}}{\partial D}$, $A_5' = -\tfrac{\partial \mathbb{L}}{\partial C}$. To obtain the optimal controls of v_c^*, u_2^*, u_3^*, u_4^*; we set

$\frac{\partial \mathbb{L}}{\partial v_c} = \frac{\partial \mathbb{L}}{\partial u_2} = \frac{\partial \mathbb{L}}{\partial u_3} = \frac{\partial \mathbb{L}}{\partial u_4} = 0.$ Then, we have

$$\epsilon_c v_c + A_5 + Q_1(t) + Q_2(t) = 0,$$

$$\epsilon_2 u_2 + A_2 + Q_3(t) + Q_4(t) = 0,$$

$$\epsilon_3 u_3 + A_3 + Q_5(t) + Q_6(t) = 0,$$

$$\epsilon_4 u_4 + A_4 s_d + Q_7(t) + Q_8(t) = 0.$$

By using standard optimality condition, we have

$$v_c^* = \min\left(1, \left(\frac{-A_5}{\epsilon_c}\right)^+\right),$$

$$u_2^* = \min\left(1, \left(\frac{-A_2}{\epsilon_2}\right)^+\right),$$

$$u_3^* = \min\left(1, \left(\frac{-A_3}{\epsilon_3}\right)^+\right),$$

$$u_4^* = \min\left(1, \left(\frac{-A_4 s_d}{\epsilon_4}\right)^+\right),$$

where the notation is

$$s^+ = \begin{cases} s, & \text{if} \quad s \geq 0 \\ 0, & \text{if} \quad s < 0. \end{cases}$$

Hence, the proof. $\qquad\qquad\qquad\qquad\qquad\qquad\qquad\square$

After getting the explicit expression of the optimal controls u_2^*, u_3^*, u_4^*, v_c^*; the adjoint or costate equations coupled with the state system including

transversality conditions, we obtain optimality system as follows

$$\frac{dT}{dt} = r_T T(1 - b_T T) - \frac{(\alpha_T M + \gamma_T T_8)T}{g_T + M} - k_T(1 - e^{-\eta_T C})T,$$

$$\frac{dL}{dt} = \frac{\alpha_8 D}{g_8 + T_8} - \delta_8 T_8 + \min\left(1, \left(\frac{-A_2}{\epsilon_2}\right)^+\right) - k_8(1 - e^{-\eta_8 C})T_8,$$

$$\frac{dM}{dt} = s_m + \frac{\alpha_m T_8}{(g_m + T_8)} \cdot \frac{1}{(g_{m1} + T)} - \gamma_m MT - \delta_m M + \min\left(1, \left(\frac{-A_3}{\epsilon_3}\right)^+\right)$$
$$- k_m(1 - e^{-\eta_m C})M,$$

$$\frac{dD}{dt} = s_d\left(\min\left(1, \left(\frac{-A_4 s_d}{\epsilon_4}\right)^+\right)\right) + \frac{\alpha_d T}{g_d + T} - \delta_d D - k_d(1 - e^{-\eta_d C})D,$$

$$\frac{dC}{dt} = -\gamma C + \min\left(1, \left(\frac{-A_5}{\epsilon_c}\right)^+\right),$$

$$A_1' = -\left[1 + A_1\left\{r_T(1 - 2b_T T) - \frac{\alpha_T M + \gamma_T T_8}{g_T + M} - k_T(1 - e^{-\eta_T C})\right\}\right.$$
$$\left. - A_3\left\{\frac{\alpha_m T_8}{(g_m + T_8) \cdot (g_{m1} + T)^2} + \gamma_m M\right\} + A_4 \frac{\alpha_d g_d}{(g_d + T)^2}\right], \qquad (5.9)$$

$$A_2' = -\left[-A_1 \frac{\gamma_T T}{g_T + M} - A_2\left\{\frac{\alpha_8 D}{(g_8 + T_8)^2} + \delta_8 + k_8(1 - e^{-\eta_8 C})\right\}\right.$$
$$\left. + A_3 \frac{\alpha_m g_m}{(g_m + T_8)^2(g_{m1} + T)}\right],$$

$$A_3' = -\left[-A_1 \frac{(\alpha_T g_T - \gamma_T T_8)T}{(g_T + M)^2} - A_3(\gamma_m T + \delta_m + k_m(1 - e^{-\eta_m C}))\right],$$

$$A_4' = -\left[A_2 \frac{\alpha_8}{g_8 + T_8} - A_4(\delta_d + k_d(1 - e^{-\eta_d C}))\right],$$

$$A_5' = A_1 \eta_T k_T T e^{-\eta_T C} + A_2 \eta_8 k_8 T_8 e^{-\eta_8 C} + A_3 \eta_m k_m M e^{-\eta_m C}$$
$$+ A_4 \eta_d k_d D e^{-\eta_d C} + A_5 \gamma,$$

where $T(0) = T_0$, $T_8(0) = T_{80}$, $M(0) = M_0$, $D(0) = D_0$, $C(0) = C_0$ and $A_i(t_f) = 0$ for $i = 1$ to 5.

5.7 Uniqueness of optimal control

By the boundedness property of the given optimal control system, the state equations and adjoint or costate equations both have bounded coefficients. For the small time interval, we shall prove the uniqueness of solution of the optimal system (5.3).

Theorem 5.7.1. *The solution of the optimal control system is unique for sufficient small time interval t_f.*

Proof. Let us consider $(T, T_8, M, D, C, A_1, A_2, A_3, A_4, A_5)$ and $(\overline{T}, \overline{T}_8, \overline{M}, \overline{D}, \overline{C}, \overline{A}_1, \overline{A}_2, \overline{A}_3, \overline{A}_4, \overline{A}_5)$ are two distinct solutions of the

151

optimal system. Suppose, $\lambda > 0$ be such that $T = e^{\lambda t}p_1$, $T_8 = e^{\lambda t}p_2$, $M = e^{\lambda t}p_3$, $D = e^{\lambda t}p_4$, $C = e^{\lambda t}p_5$, $A_1 = e^{-\lambda t}q_1$, $A_2 = e^{-\lambda t}q_2$, $A_3 = e^{-\lambda t}q_3$, $A_4 = e^{-\lambda t}q_4$, $A_5 = e^{-\lambda t}q_5$, $\overline{T} = e^{\lambda t}\overline{p}_1$, $\overline{T}_8 = e^{\lambda t}\overline{p}_2$, $\overline{M} = e^{\lambda t}\overline{p}_3$, $\overline{D} = e^{\lambda t}\overline{p}_4$, $\overline{C} = e^{\lambda t}\overline{p}_5$, $\overline{A}_1 = e^{-\lambda t}\overline{q}_1$, $\overline{A}_2 = e^{-\lambda t}\overline{q}_2$, $\overline{A}_3 = e^{-\lambda t}\overline{q}_3$, $\overline{A}_4 = e^{-\lambda t}\overline{q}_4$, $\overline{A}_5 = e^{-\lambda t}\overline{q}_5$. Also, we consider

$$v_c^*(t) = \min\left(1, \left(\frac{-e^{-\lambda t}q_5}{\epsilon_c}\right)^+\right) \quad , \quad \overline{v}_c^*(t) = \min\left(1, \left(\frac{-e^{-\lambda t}\overline{q}_5}{\epsilon_c}\right)^+\right);$$

$$u_2^*(t) = \min\left(1, \left(\frac{-e^{-\lambda t}q_2}{\epsilon_2}\right)^+\right) \quad , \quad \overline{u}_2^*(t) = \min\left(1, \left(\frac{-e^{-\lambda t}\overline{q}_2}{\epsilon_2}\right)^+\right);$$

$$u_3^*(t) = \min\left(1, \left(\frac{-e^{-\lambda t}q_3}{\epsilon_3}\right)^+\right) \quad , \quad \overline{u}_3^*(t) = \min\left(1, \left(\frac{-e^{-\lambda t}\overline{q}_3}{\epsilon_3}\right)^+\right);$$

$$u_4^*(t) = \min\left(1, \left(\frac{-e^{-\lambda t}q_4 s_d}{\epsilon_4}\right)^+\right) \quad , \quad \overline{u}_4^*(t) = \min\left(1, \left(\frac{-e^{-\lambda t}\overline{q}_4 s_d}{\epsilon_4}\right)^+\right).$$

We use $T = e^{\lambda t}p_1$ in first equation of the optimality system (5.9), then the state equation leads to

$$\dot{p}_1 + (\lambda - r_T)p_1 = -r_T b_T e^{\lambda t} p_1^2 - \frac{\alpha_T p_1 p_3 e^{\lambda t}}{g_T + e^{\lambda t}p_3} - \frac{\gamma_T p_1 p_2 e^{\lambda t}}{g_T + e^{\lambda t}p_3}$$

$$- k_T p_1(1 - e^{-\eta_T p_5 e^{\lambda t}}),$$

with $\dot{p} \equiv \frac{dp}{dt}$. Similarly, after putting $A_1 = e^{-\lambda t}q_1$ in sixth equation of (5.9), we have

$$-\dot{q}_1 + \lambda q_1 = e^{\lambda t} + q_1 \left\{ r_T(1 - 2b_T e^{\lambda t}p_1) - \frac{(\alpha_T p_3 + \gamma_T p_2)e^{\lambda t}}{g_T + e^{\lambda t}p_3} \right.$$

$$- k_T(1 - e^{-\eta_T p_5 e^{\lambda t}}) \bigg\} - e^{\lambda t}q_3 \left\{ \frac{\alpha_m p_2}{(g_m + e^{\lambda t}p_2)(g_{m1} + e^{\lambda t}p_1)^2} + \gamma_m p_3 \right\}$$

$$+ \frac{q_4 \alpha_d g_d}{(g_d + e^{\lambda t}p_1)^2} \bigg].$$

At first, the equations of T and $\overline{T}$, T_8 and $\overline{T}_8$, M and $\overline{M}$, D and $\overline{D}$, C and $\overline{C}$, A_1 and $\overline{A}_1$, A_2 and $\overline{A}_2$, A_3 and $\overline{A}_3$, A_4 and $\overline{A}_4$, A_5 and $\overline{A}_5$ are subtracted. The resulting equations are multiplied by a suitable difference of functions and integrated from 0 to t_f. After that, we add all 10 integral equations and estimates to find the uniqueness of the optimality system. As for example,

some integrals are listed as

$$\frac{1}{2}(p_1 - \overline{p}_1)^2(t_f) + (\lambda - r_T + k_T)\int_0^{t_f}(p_1 - \overline{p}_1)^2 dt$$

$$\leq \quad r_T b_T \int_0^{t_f} e^{\lambda t}(p_1 + \overline{p}_1)(p_1 - \overline{p}_1)^2 dt$$

$$+ \quad \alpha_T \int_0^{t_f} e^{\lambda t}(p_1 - \overline{p}_1)\left[\frac{g_T(p_1 p_3 - \overline{p}_1 \overline{p}_3) + e^{\lambda t}p_3 \overline{p}_3(p_1 - \overline{p}_1)}{(g_T + e^{\lambda t}p_3)(g_T + e^{\lambda t}\overline{p}_3)}\right] dt$$

$$+ \quad \gamma_T \int_0^{t_f} e^{\lambda t}(p_1 - \overline{p}_1)\left[\frac{g_T(p_1 p_2 - \overline{p}_1 \overline{p}_2) + e^{\lambda t}(p_1 p_2 \overline{p}_3 - \overline{p}_1 \overline{p}_2 p_3)}{(g_T + e^{\lambda t}p_3)(g_T + e^{\lambda t}\overline{p}_3)}\right] dt$$

$$+ \quad k_T \int_0^{t_f} e^{-\eta_T p_5 e^{\lambda t}}(p_1 - \overline{p}_1)^2 dt.$$

Now, we shall obtain the bounds on the right-hand sides of the integral equations. Since p_i, $\overline{p}_i \geq 0$ ($i = 1$ to 5), we estimate

$$(g_T + e^{\lambda t}p_3) \quad \geq \quad g_T,$$

$$(g_T + e^{\lambda t}\overline{p}_3) \quad \geq \quad g_T.$$

Then, we obtain

$$\frac{1}{2}(p_1 - \overline{p}_1)^2(t_f) \quad + \quad (\lambda - r_T + k_T)\int_0^{t_f}(p_1 - \overline{p}_1)^2 dt$$

$$\leq \quad 2\mu_1 r_T b_T \int_0^{t_f} e^{\lambda t}(p_1 - \overline{p}_1)^2 dt$$

$$+ \quad \frac{\alpha_T}{g_T}\int_0^{t_f} e^{\lambda t}(p_1 - \overline{p}_1)(p_1 p_3 - \overline{p}_1 \overline{p}_3) dt$$

$$+ \quad \frac{\alpha_T \mu_3^2}{g_T^2}\int_0^{t_f} e^{2\lambda t}(p_1 - \overline{p}_1)^2 dt$$

$$+ \quad \frac{\gamma_T}{g_T}\int_0^{t_f} e^{\lambda t}(p_1 - \overline{p}_1)(p_1 p_2 - \overline{p}_1 \overline{p}_2) dt$$

$$+ \quad \frac{\gamma_T}{g_T^2}\int_0^{t_f} e^{2\lambda t}(p_1 p_2 \overline{p}_3 - \overline{p}_1 \overline{p}_2 p_3)(p_1 - \overline{p}_1) dt$$

$$+ \quad k_T \int_0^{t_f} e^{-\eta_T p_5 e^{\lambda t}}(p_1 - \overline{p}_1)^2 dt,$$

153

where μ_i are upper bound of both p_i and $\overline{p}_i$ ($i = 1, 2, 3, 4, 5$). Now, we shall analyze the term $\int_0^{t_f}(p_1 p_2 \overline{p}_3 - \overline{p}_1 \overline{p}_2 p_3)(p_1 - \overline{p}_1)dt$ explicitly. To evaluate this estimate, we apply the Cauchy-Schwarz inequality to separate linear terms from quadratic terms. It can be observed that

$$(p_1 p_2 \overline{p}_3 - \overline{p}_1 \overline{p}_2 p_3) = (p_1 p_2 - \overline{p}_1 \overline{p}_2)\overline{p}_3 - \overline{p}_1 \overline{p}_2 (p_3 - \overline{p}_3),$$

and we get

$$\int_0^{t_f}(p_1 p_2 \overline{p}_3 - \overline{p}_1 \overline{p}_2 p_3)(p_1 - \overline{p}_1)dt \leq \int_0^{t_f} \overline{p}_3(p_1 - \overline{p}_1)(p_1 p_2 - \overline{p}_1 \overline{p}_2)dt$$

$$+ \int_0^{t_f} \overline{p}_1 \overline{p}_2 (p_1 - \overline{p}_1)(p_3 - \overline{p}_3)dt$$

$$\leq \mu_3 \int_0^{t_f} (p_1 - \overline{p}_1)(p_1 p_2 - \overline{p}_1 \overline{p}_2)dt$$

$$+ \mu_1 \mu_2 \int_0^{t_f} (p_1 - \overline{p}_1)(p_3 - \overline{p}_3)dt$$

$$\leq \frac{\mu_1 \mu_2}{2} \int_0^{t_f} (p_3 - \overline{p}_3)^2 dt$$

$$+ \frac{\mu_1 \mu_3}{2} \int_0^{t_f} (p_2 - \overline{p}_2)^2 dt$$

$$+ \frac{\mu_1 \mu_2 + 2\mu_2 \mu_3 + \mu_1 \mu_3}{2} \int_0^{t_f} (p_1 - \overline{p}_1)^2 dt.$$

Again, we can write that

$$\frac{1}{2}(q_1 - \overline{q}_1)^2(t_f) + (\lambda - r_T + k_T) \int_0^{t_f} (q_1 - \overline{q}_1)^2 dt$$

$$\leq \int_0^{t_f} 2 r_T b_T e^{\lambda t}(p_1 q_1 - \overline{p}_1 \overline{q}_1)(q_1 - \overline{q}_1)dt$$

$$+ \int_0^{t_f} \alpha_T e^{\lambda t} \left\{ \frac{p_3 q_1}{g_T + e^{\lambda t}p_3} - \frac{\overline{p}_3 \overline{q}_1}{g_T + e^{\lambda t}\overline{p}_3} \right\}(q_1 - \overline{q}_1)dt$$

$$+ \int_0^{t_f} \gamma_T e^{\lambda t} \left\{ \frac{p_2 q_1}{g_T + e^{\lambda t}p_3} - \frac{\overline{p}_2 \overline{q}_1}{g_T + e^{\lambda t}\overline{p}_3} \right\}(q_1 - \overline{q}_1)dt$$

154

$$+ \quad \int_0^{t_f} \alpha_m e^{\lambda t} \left\{ \frac{p_2 q_3}{(g_m + e^{\lambda t} p_2)(g_{m1} + e^{\lambda t} p_1)^2} \right.$$

$$- \quad \left. \frac{\overline{p}_2 \overline{q}_3}{(g_m + e^{\lambda t} \overline{p}_2)(g_{m1} + e^{\lambda t} \overline{p}_1)^2} \right\} (q_1 - \overline{q}_1) dt$$

$$+ \quad \int_0^{t_f} \gamma_m e^{\lambda t} (p_3 q_3 - \overline{p}_3 \overline{q}_3)(q_1 - \overline{q}_1) dt$$

$$+ \quad \int_0^{t_f} \alpha_d g_d \left\{ \frac{q_4}{(g_d + e^{\lambda t} p_1)^2} - \frac{\overline{q}_4}{(g_d + e^{\lambda t} \overline{p}_1)^2} \right\} (q_1 - \overline{q}_1) dt$$

$$+ \quad k_T \int_0^{t_f} e^{-\eta_T p_5 e^{\lambda t}} (q_1 - \overline{q}_1)^2 dt.$$

It is to be noted that

$$\int_0^{t_f} \alpha_T e^{\lambda t} \left\{ \frac{p_3 q_1}{g_T + e^{\lambda t} p_3} - \frac{\overline{p}_3 \overline{q}_1}{g_T + e^{\lambda t} \overline{p}_3} \right\} (q_1 - \overline{q}_1) dt$$

$$\leq \quad \frac{\alpha_T}{g_T} \int_0^{t_f} e^{\lambda t} (p_3 q_1 - \overline{p}_3 \overline{q}_1)(q_1 - \overline{q}_1) dt$$

$$+ \quad \frac{\alpha_T}{g_T^2} \int_0^{t_f} e^{2\lambda t} p_3 \overline{p}_3 (q_1 - \overline{q}_1)^2 dt.$$

Again, we have

$$\int_0^{t_f} \alpha_m e^{\lambda t} \left\{ \frac{p_2 q_3}{(g_m + e^{\lambda t} p_2)(g_{m1} + e^{\lambda t} p_1)^2} \right.$$

$$- \quad \left. \frac{\overline{p}_2 \overline{q}_3}{(g_m + e^{\lambda t} \overline{p}_2)(g_{m1} + e^{\lambda t} \overline{p}_1)^2} \right\} (q_1 - \overline{q}_1) dt$$

$$\leq \quad \frac{\alpha_m}{g_m g_{m1}^2} \int_0^{t_f} e^{\lambda t} (p_2 q_3 - \overline{p}_2 \overline{q}_3)(q_1 - \overline{q}_1) dt$$

$$+ \quad \frac{2\alpha_m}{g_m g_{m1}^3} \int_0^{t_f} e^{2\lambda t} (p_2 q_3 \overline{p}_1 - \overline{p}_2 \overline{q}_3 p_1)(q_1 - \overline{q}_1) dt$$

$$+ \quad \frac{\alpha_m}{g_m g_{m1}^4} \int_0^{t_f} e^{3\lambda t} (p_2 q_3 \overline{p}_1^2 - \overline{p}_2 \overline{q}_3 p_1^2)(q_1 - \overline{q}_1) dt$$

$$+ \quad \frac{\alpha_m}{g_m^2 g_{m1}^2} \int_0^{t_f} e^{2\lambda t}(p_2 q_3 \bar{p}_2 - \bar{p}_2 \bar{q}_3 p_2)(q_1 - \bar{q}_1)dt$$

$$+ \quad \frac{2\alpha_m}{g_m^2 g_{m1}^3} \int_0^{t_f} e^{3\lambda t}(p_2 q_3 \bar{p}_1 \bar{p}_2 - \bar{p}_2 \bar{q}_3 p_1 p_2)(q_1 - \bar{q}_1)dt$$

$$+ \quad \frac{\alpha_m}{g_m^2 g_{m1}^4} \int_0^{t_f} e^{4\lambda t}(p_2 q_3 \bar{p}_1^2 \bar{p}_2 - \bar{p}_2 \bar{q}_3 p_1^2 p_2)(q_1 - \bar{q}_1)dt.$$

To obtain the specific expression, we consider

$$\int_0^{t_f} (p_2 q_3 \bar{p}_1^2 \bar{p}_2 - \bar{p}_2 \bar{q}_3 p_1^2 p_2)(q_1 - \bar{q}_1)dt$$

$$\leq \quad \int_0^{t_f} \bar{p}_1^2 \bar{p}_2(p_2 q_3 - \bar{p}_2 \bar{q}_3)(q_1 - \bar{q}_1)dt + \int_0^{t_f} \bar{p}_2 \bar{q}_3(p_1^2 p_2 - \bar{p}_1^2 \bar{p}_2)(q_1 - \bar{q}_1)dt$$

$$\leq \quad \mu_1 \mu_2^2 \nu_3 \int_0^{t_f} (p_1 - \bar{p}_1)^2 dt + \mu_1^2 \mu_2 \nu_3 \int_0^{t_f} (p_2 - \bar{p}_2)^2 dt$$

$$+ \quad \frac{2\mu_1^2 \mu_2 \nu_3 + \mu_1^2 \mu_2^2 + 2\mu_1 \mu_2^2 \nu_3}{2} \int_0^{t_f} (q_1 - \bar{q}_1)^2 dt + \frac{\mu_1^2 \mu_2^2}{2} \int_0^{t_f} (q_3 - \bar{q}_3)^2 dt,$$

where ν_i are the upper bounds of q_i and $\bar{q}_i$ ($i = 1, 2, 3, 4, 5$). We add all the integrals of $(p_i - \bar{p}_i)$ (for $i = 1$ to 5) and $(q_j - \bar{q}_j)$ (for $j = 1$ to 5) for proving uniqueness of optimal control system. Since maximum fraction of killing rate by chemotherapeutic drug is 1, then $|e^{-\eta_T p_5 e^{\lambda t}}| < 1$. Thus, we have the following inequality:

$$\frac{1}{2}(p_1 - \bar{p}_1)^2(t_f) + \frac{1}{2}(p_2 - \bar{p}_2)^2(t_f) + \frac{1}{2}(p_3 - \bar{p}_3)^2(t_f) + \frac{1}{2}(p_4 - \bar{p}_4)^2(t_f)$$

$$+ \quad \frac{1}{2}(p_5 - \bar{p}_5)^2(t_f) + \frac{1}{2}(q_1 - \bar{q}_1)^2(t_f) + \frac{1}{2}(q_2 - \bar{q}_2)^2(t_f) + \frac{1}{2}(q_3 - \bar{q}_3)^2(t_f)$$

$$+ \quad \frac{1}{2}(q_4 - \bar{q}_4)^2(t_f) + \frac{1}{2}(q_5 - \bar{q}_5)^2(t_f) + (\lambda - r_T + k_T) \int_0^{t_f} (p_1 - \bar{p}_1)^2 dt$$

$$+ \quad (\lambda + \delta_8 + k_8) \int_0^{t_f} (p_2 - \bar{p}_2)^2 dt + (\lambda + \delta_m + k_m) \int_0^{t_f} (p_3 - \bar{p}_3)^2 dt$$

$$+ \quad (\lambda + \delta_d + k_d) \int_0^{t_f} (p_4 - \bar{p}_4)^2 dt + (\lambda + \gamma) \int_0^{t_f} (p_5 - \bar{p}_5)^2 dt$$

$$+ \quad (\lambda - r_T + k_T) \int_0^{t_f} (q_1 - \overline{q}_1)^2 dt + (\lambda + \delta_8 + k_8) \int_0^{t_f} (q_2 - \overline{q}_2)^2 dt$$

$$+ \quad (\lambda + \delta_m + k_m) \int_0^{t_f} (q_3 - \overline{q}_3)^2 dt + (\lambda + \delta_d + k_d) \int_0^{t_f} (q_4 - \overline{q}_4)^2 dt$$

$$+ \quad (\lambda + \gamma) \int_0^{t_f} (q_5 - \overline{q}_5)^2 dt$$

$$\leq \quad \overline{C}_1 e^{4\lambda t} \int_0^{t_f} [(p_1 - \overline{p}_1)^2 + (p_2 - \overline{p}_2)^2 + (p_3 - \overline{p}_3)^2 + (p_4 - \overline{p}_4)^2 + (p_5 - \overline{p}_5)^2$$

$$+ \quad (q_1 - \overline{q}_1)^2 + (q_2 - \overline{q}_2)^2 + (q_3 - \overline{q}_3)^2 + (q_4 - \overline{q}_4)^2 + (q_5 - \overline{q}_5)^2] dt.$$

We use the nonnegativity of the variables at the initial and final time and simplifying, then the above inequality is reduced to the following expression:

$$(\lambda - \overline{C}_2 - \overline{C}_1 e^{4\lambda t}) \int_0^{t_f} [(p_1 - \overline{p}_1)^2 + (p_2 - \overline{p}_2)^2 + (p_3 - \overline{p}_3)^2 + (p_4 - \overline{p}_4)^2$$

$$+ \quad (p_5 - \overline{p}_5)^2 + (q_1 - \overline{q}_1)^2 + (q_2 - \overline{q}_2)^2 + (q_3 - \overline{q}_3)^2 + (q_4 - \overline{q}_4)^2 + (q_5 - \overline{q}_5)^2] dt$$

$$\leq \quad 0;$$

where $\overline{C}_1$, $\overline{C}_2$ depend on the coefficients and their bounds of the state variables. If we choose that $\lambda > \overline{C}_2 + \overline{C}_1$, then we have $\lambda - \overline{C}_2 - \overline{C}_1 e^{4\lambda t} > 0$. Since logarithm is increasing function, thus $t_f < \frac{1}{4\lambda} \ln\left(\frac{\lambda - \overline{C}_2}{\overline{C}_1}\right)$, then $p_i = \overline{p}_i$ (for $i = 1$ to 5) and $q_j = \overline{q}_j$ (for $j = 1$ to 5). Therefore, in the small time interval, the solution of (5.9) is unique.

From the mathematical perspective, we can assert that the uniqueness of the solution of the control system satisfied for a sufficiently small time interval, where the state system has initial solutions and the adjoint or costate system has the final time conditions. The given optimal controls u_2^*, u_3^*, u_4^* and v_c^* are characterized in terms of the unique solution of the optimal system. $\qquad \square$

5.8   Numerical results

This section described the extensive numerical illustrations to validate our theoretical analysis including stability and the implementation of different treatment strategies. We have plotted our optimal control model numerically using MATLAB by choosing suitable parameters value are obtained

from existing literature that are given in the Table 4.1, Table 4.2 and Table 5.1. To study the impact of treatment strategies, we compare the numerical illustrations without treatment strategy and with treatment strategies for proposed control model (5.3).

5.8.1 Numerical results without treatment strategy

In this subsection, we study numerical behavior of (5.3) without implementation treatment strategy. In view of this, at first we check the existence of biologically feasible singular point(s) in absence of control (that is, $u_2 = u_3 = u_4 = v_c = 0$). We calculate the tumor-free steady state E^0 $(0, 0, 9678.57, 0, 0)$ and the corresponding eigenvalues are -0.9, -0.865109, -0.178, -0.17, -0.056. Since all the eigenvalues are negative, then we can say that tumor-free singular point E^0 is locally asymptotically stable. It is quite difficult to find the explicit form of interior singular point $E^1(T^1, T_8^1, M^1, D^1, C^1)$. So, we calculate interior singular point by numerically using the parameters value given in the Table 4.1, Table 4.2 and Table 5.1. There are two types of tumor-presence singular point. One is low tumor-presence singular point and another is high tumor-presence singular point. From the parameters in Table 4.1, Table 4.2 and Table 5.1, the low tumor-presence steady state E^l is $(0.179273, 1.05623 \times 10^{-17}, 3886.15, 1.43419 \times 10^{-10}, 0)$ and the corresponding eigenvalues are -0.9, -0.300816, -0.178, -0.17, 0.161346, which shows that low tumor-presence singular point E^l is unstable in nature. On the other hand, high tumor-presence singular point E^h is $(800000, 2.61855 \times 10^{-11}, 0.00145511, 0.0003555, 0)$ and the corresponding eigenvalues are -372480, -0.9, -0.5822, -0.178, -0.17. Since all of the eigenvalues are negative, then we can say that high tumor-presence steady state E^h is asymptotically stable.

5.8.2 Numerical results with treatment strategy

In this subsection, we investigate our proposed model with the implementation of different treatment strategies. We have introduced four different treatment strategies, namely $u_2(t)$, $u_3(t)$, $u_4(t)$ and $v_c(t)$ to destroy the tumor cell population. We performed the numerical simulation for the state variables by using Runge-Kutta forward method and the equations for the adjoint or costate variables by using Runge-Kutta backward method. To perform the numerical illustrations, we consider the initial values $T(0) = 0.01$, $T_8(0) = 0.2 \times 10^{-7}$, $M(0) = 3000$, $D(0) = 0.0002$ and time-window 200 days with taking parameters value are specified in the Table 4.1, Table 4.2 and Table 5.1. To know the better treatment techniques,

Table 5.1: Parameters value for tumor-immune interaction model used in the simulations

Par.	Description	Value	Units	Source
k_T	Chemotherapy induced tumor death rate	0.8	Day^{-1}	[20, 75]
η_T	Chemotherapy efficacy coefficient	0.1	$Liter.mg^{-1}$	Fit to data
k_8	Chemotherapy induced CD8+T cell decay rate	0.6	Day^{-1}	[20, 75]
η_8	Chemotherapy efficacy coefficient	0.1	$Liter.mg^{-1}$	Fit to data
k_m	Chemotherapy induced macrophages decay rate	0.4	Day^{-1}	Fit to data
η_m	Chemotherapy efficacy coefficient	0.1	$Liter.mg^{-1}$	Fit to data
k_d	Chemotherapy induced dendritic cell decay rate	0.6	Day^{-1}	Fit to data
η_d	Chemotherapy efficacy coefficient	0.1	$Liter.mg^{-1}$	Fit to data
γ	Decay rate for chemotherapeutic drug	0.9	Day^{-1}	[20]

we consider the following control strategies.

Strategy I: Implementation of only one treatment strategy.

Strategy II: Implementation of two different treatment strategies.

Strategy III: Implementation of three different treatment strategies.

Strategy IV: Implementation of four different treatment strategies.

Figure 5.1 illustrates the impact of tumor cells, CD8+T cells, macrophages and dendritic cells in the presence of a single treatment strategy, denoted as $(u_2(t), u_3(t), u_4(t), v_c(t))$, as well as in the absence of any treatment strategy (that is, $u_2(t) = u_3(t) = u_4(t) = v_c(t) = 0$). In Figure 5.1, the red curve represents the state variables without any optimal control strategy, while the black curve describes the state variables with only one treatment strategy, specifically $u_2(t) = 0.8$. The blue, green and magenta curves correspond to each of the state variables when $u_3(t) = 0.8$, $u_4(t) = 0.8$ and $v_c(t) = 0.8$, respectively. From the time series plot (see

Figure 5.1), it is evident that without application of any control strategy in our proposed model, the reduction of tumor cells takes more time than when a single control strategy is employed. Additionally, we observe that effector cells initially increase but decrease as time progresses. The utilization of a single control strategy proves to be more effective than administering no control at all.
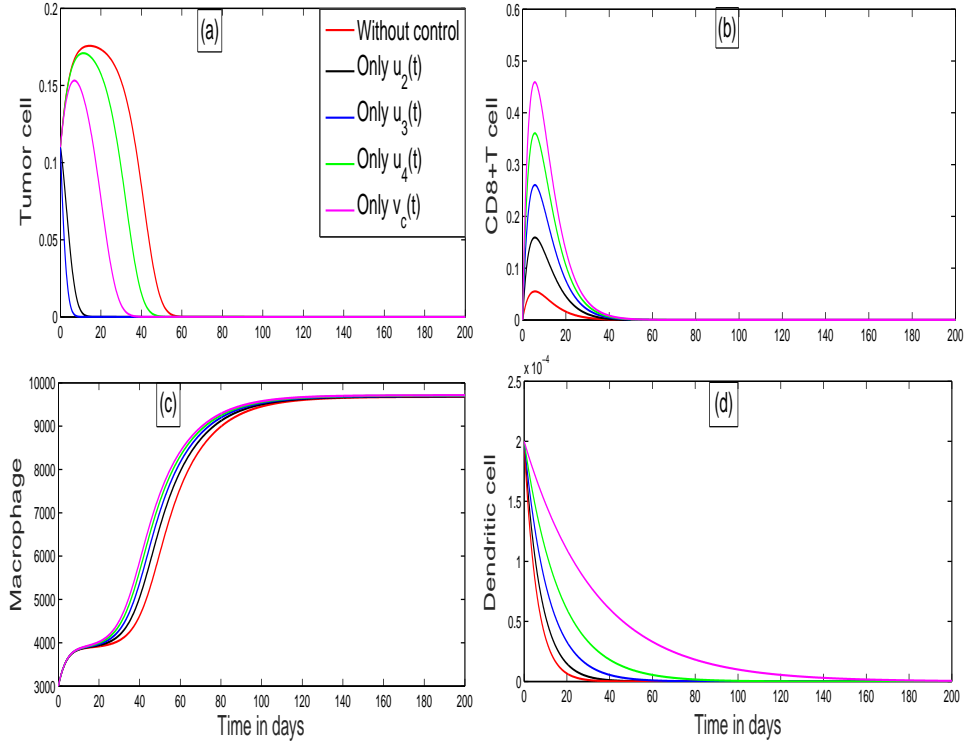

Figure 5.1: The figure shows that the comparison of the state variables without introduction of treatment strategy and with the implementation of single control.

Figure 5.2 illustrates the impact of various state variables under the influence of two optimal control strategies. These strategies are denoted as follows: $u_2(t)$, $v_c(t)$; $u_3(t)$, $v_c(t)$; $u_4(t)$, $v_c(t)$; $u_2(t)$, $u_3(t)$; $u_3(t)$, $u_4(t)$; $u_2(t)$, $u_4(t)$; and a scenario without any control strategy. In this visualization, the red curve represents the state variables when no control strategy is employed, while the black curve signifies the state variables when two control strategies are implemented, specifically $u_2(t) = v_c(t) = 0.8$. The blue curve illustrates the state variables with the application of two control strategies, namely $u_3(t) = v_c(t) = 0.8$. The green curve indicates the state

160

variables when two different controls are utilized, that is, $u_4(t) = v_c(t) = 0.8$. The magenta curve represents the state variables under the influence of two control strategies, where $u_2(t) = u_3(t) = 0.8$. The crayon curve depicts the state variables with two treatment strategies, specifically $u_3(t) = u_4(t) = 0.8$. Finally, the maroon curve explores the state variables with two treatment strategies, where $u_2(t) = u_4(t) = 0.8$. Analyzing the time series plot shown in Figure 5.2, it becomes obvious that when employing two different optimal control strategies, the tumor cells rapidly reach their equilibrium point. Meanwhile, the immune components initially experience an increase but eventually saturate over time. Consequently, We can conclude that employing two control strategies is more effective compared to a scenario with no treatment strategies.
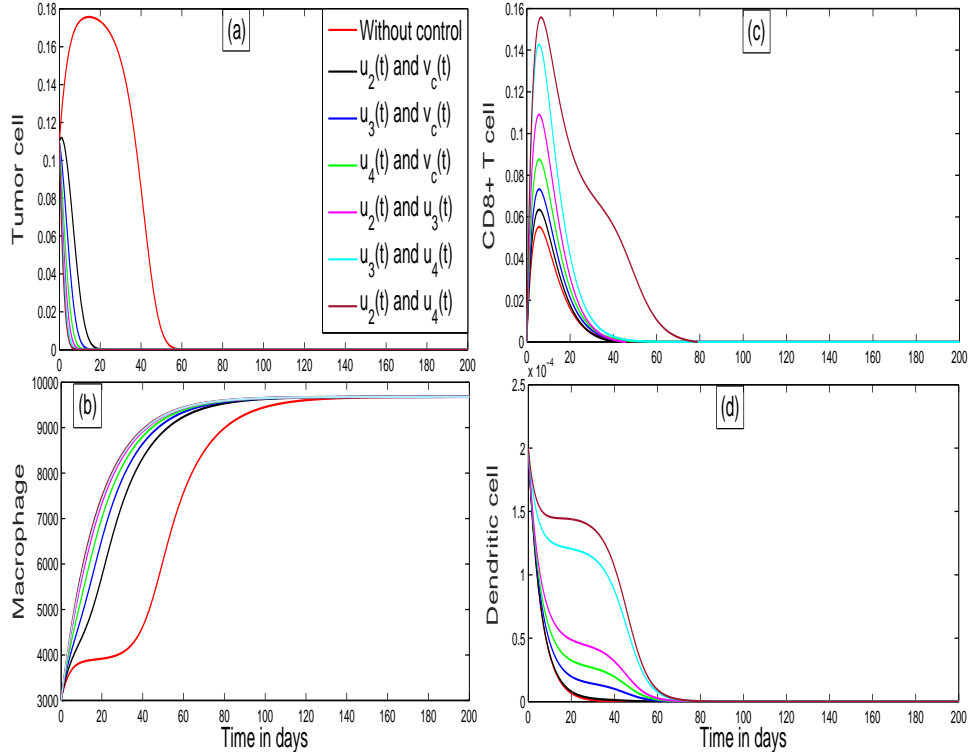

Figure 5.2: The figure describes that the comparison of the state variables without implementation of any treatment strategy and with the application of two treatment strategies.

The time series plot in Figure 5.3 illustrates the roles of tumor cells, CD8+T cells, macrophages and dendritic cells in the presence of three control strategies: $u_2(t)$, $u_3(t)$, $v_c(t)$; $u_3(t)$, $u_4(t)$, $v_c(t)$; $u_2(t)$, $u_3(t)$, $u_4(t)$ and

without the introduction of any control strategy. The red curve represents the state variables without any control strategy, while the black curve depicts the state variables under three different treatment strategies, specifically $u_2(t) = u_3(t) = v_c(t) = 0.8$. The blue curve shows the state variables under three distinct control strategies, where $u_3(t) = u_4(t) = v_c(t) = 0.8$. Finally, the green curve illustrates the state variables when three control strategies are introduced, with $u_2(t) = u_3(t) = u_4(t) = 0.8$. Figure 5.3 clearly demonstrates that employing a combination of three control strategies proves more effective when compared to the scenario with no treatment strategy.
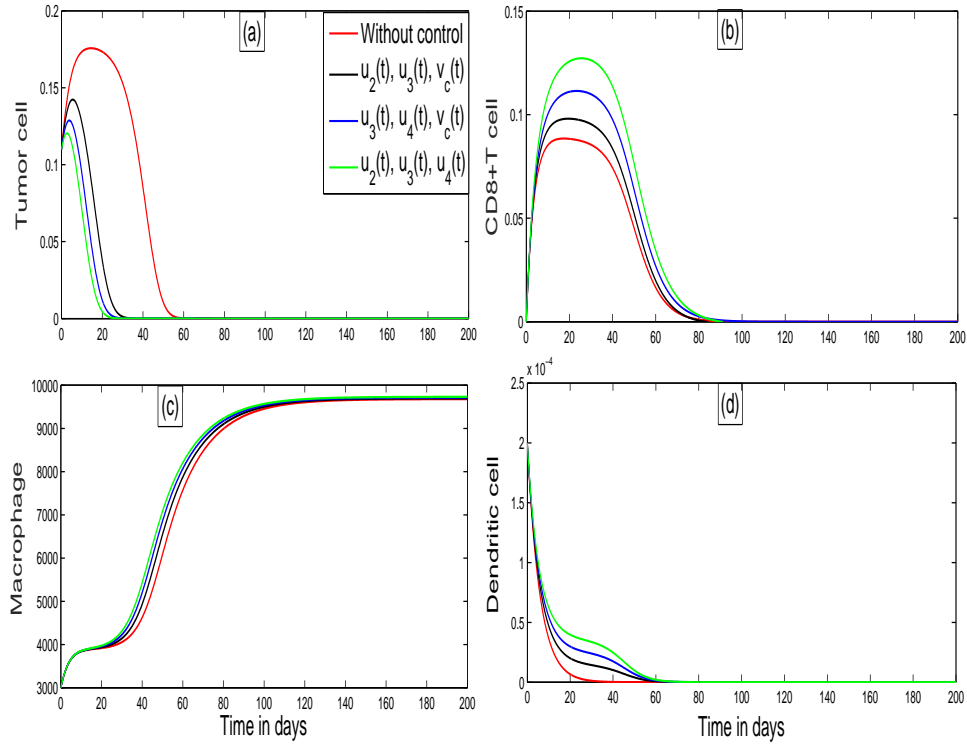

Figure 5.3: The figure indicates that the comparison of the state variables without introduction of any treatment strategy and with the application of three different control strategies.

The time series plot in Figure 5.4 depicts the application of four different control strategies alongside the scenario without any control strategy for the state variables. To visualize these four treatment strategies, we set the control variables as follows: $u_2(t) = u_3(t) = u_4(t) = v_c(t) = 0.8$. From the time series plot in Figure 5.4, it is evident that implementing four different

162

treatment strategies is more effective than using no treatment strategy, a single treatment strategy (Figure 5.1), two different treatment strategies (Figure 5.2) or three different treatment strategies (Figure 5.3). Additionally, in Figure 5.4, it is noticeable that tumor cells are rapidly eliminated and immune components are maximized upon the implementation of these four distinct control strategies.

To visualize the dynamics of the adjoint or costate variables A_1, A_2, A_3 and A_4 with the implementation of four different control strategies, we have drawn Figure 5.5. To do this, we consider the values of the control variables as follows: $u_2(t) = u_3(t) = u_4(t) = v_c(t) = 0.8$. The plot clearly illustrates that the costate variables are directly linked to changes in the values of the Lagrangian. The time derivatives of the costate variables are negative with respect to the corresponding partial derivatives of the Lagrangian.
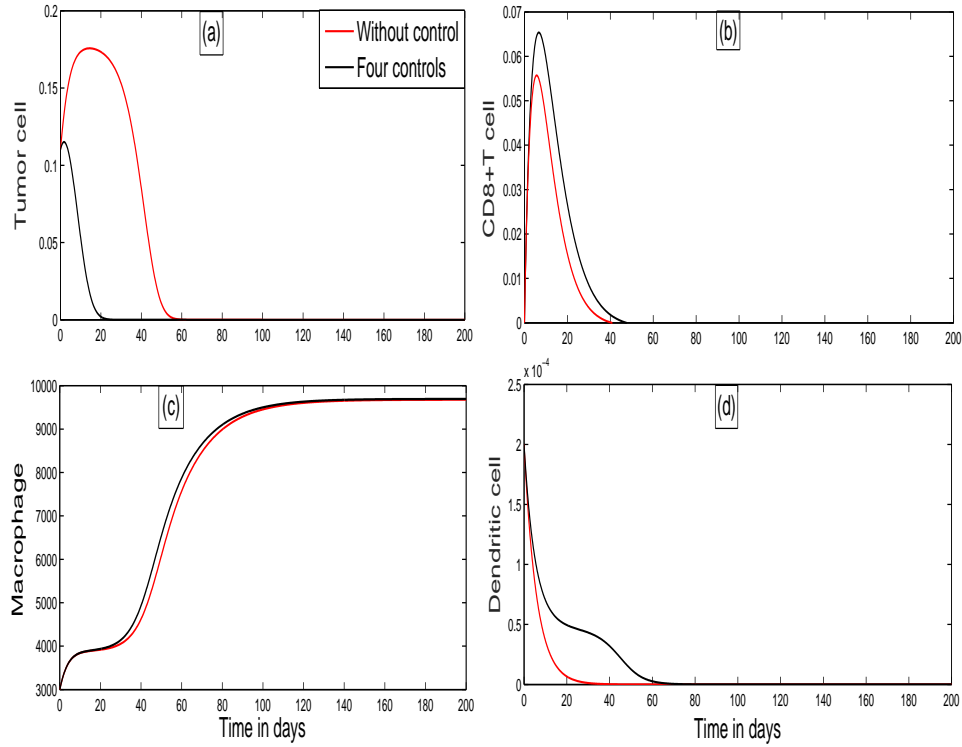

Figure 5.4: The figure shows that the comparison of the state variables without implementation of any treatment strategy and with the implementation four different treatment strategies.
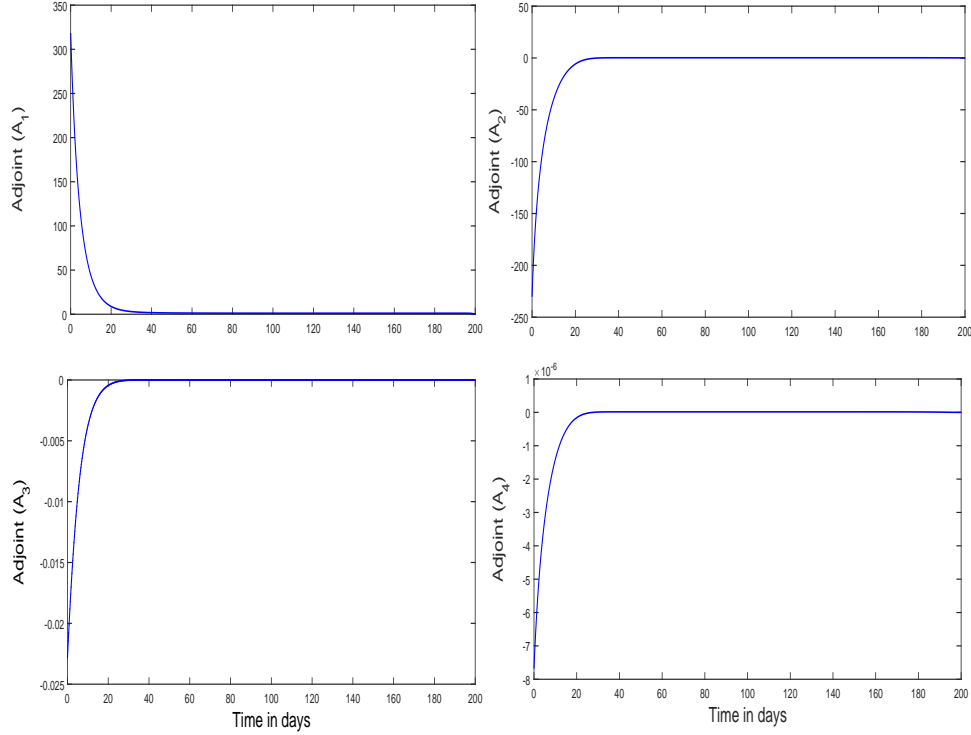
163

Figure 5.5: The figure shows that the nature of the adjoint or costate variables with the implementation of four different treatment strategies.

To visualize the dynamic behavior of the controls, we plot the control parameters in the Figure 5.6. The plot of the four graphs represents the optimal control functions with the implementation of four control strategies, namely $u_2(t) = u_3(t) = u_4(t) = v_c(t) = 0.8$. From the Figure 5.6, it can be noticed that control values decreased and eventually reach 0. The control parameters vanish before 40 days due to the fact that our adjoint or costate variables vanish.

The model is closely tied to the study of optimal control strategies within the context of tumor cell dynamics and the immune response. It explores into various control approaches, including the manipulation of tumor cell levels and key immune components (such as CD8+T cells, macrophages and dendritic cells), all with the aim of achieving specific biological outcomes. Our immune system, with its pivotal role in identifying and eliminating abnormal cells, including cancer cells, stands as a critical factor. Investigating how these control strategies impact the immune response can provide valuable insights into fortifying the body's inherent defenses against cancer. The signif-

icance of control parameters like $u_2(t)$, $u_3(t)$, $u_4(t)$ and $v_c(t)$ cannot be overstated, as they are intricately linked to immune components such as CD8+T cells, macrophages, dendritic cells and chemotherapeutic drugs. Their relevance lies in their potential to augment the immune response against cancer cells, thereby potentially enhancing the body's capacity to identify and eliminate cancer cells. Through comparisons of the efficacy of diverse control strategies (ranging from single to four treatments) in reducing tumor cell proliferation and maximizing the immune response, this model serves as a valuable tool for identifying the most promising avenues in cancer treatment. The control parameters represent the capacity to deploy multiple treatment strategies either individually or in combination. Moreover, the adaptability of these control parameters allows for a personalized approach to cancer treatment. Their biological significance is underscored by the ability of treatment strategies to individual patients, accounting for unique tumor characteristics and immune system profiles. Each of these parameters exerts a distinct influence on the dynamics of tumor cells and the immune response. Their biological significance lies in their potential to preserve precise control over tumor growth, ultimately suppressing the proliferation of cancer cells and potentially leading to tumor regression or even elimination.

5.9 Conclusion

Nowadays, it is very important and challenging question in immunology and oncology research is to understand how the immune system influences tumor progression and development. This study explores the dynamic behavior of a nonlinear tumor-immune interaction model using the theory of optimal control. Various scenarios for implementing different treatment strategies to eliminate the tumor cell population are considered. Here, we construct a mathematical model of nine nonlinear coupled ordinary differential equations (ODEs) by introducing different cells and cytokines, namely tumor cells, cytotoxic T-lymphocytes (CD8+T cells), macrophages, dendritic cells, tregs, IL-10, TGF-β, IL-12 and IFN-γ. Next, we simplify the proposed model into a system of four ODEs, which represent tumor cells, CD8+T cells, macrophages and dendritic cells, using the quasi-steady-state approximations method [92].

In this chapter, we analyzed a mathematical model for tumor-immune interaction with treatment strategies. Our goal is to provide an improved treatment strategy by eliminating the tumor cell population using both chemotherapeutic and immunotherapeutic drugs. To do this, we introduce
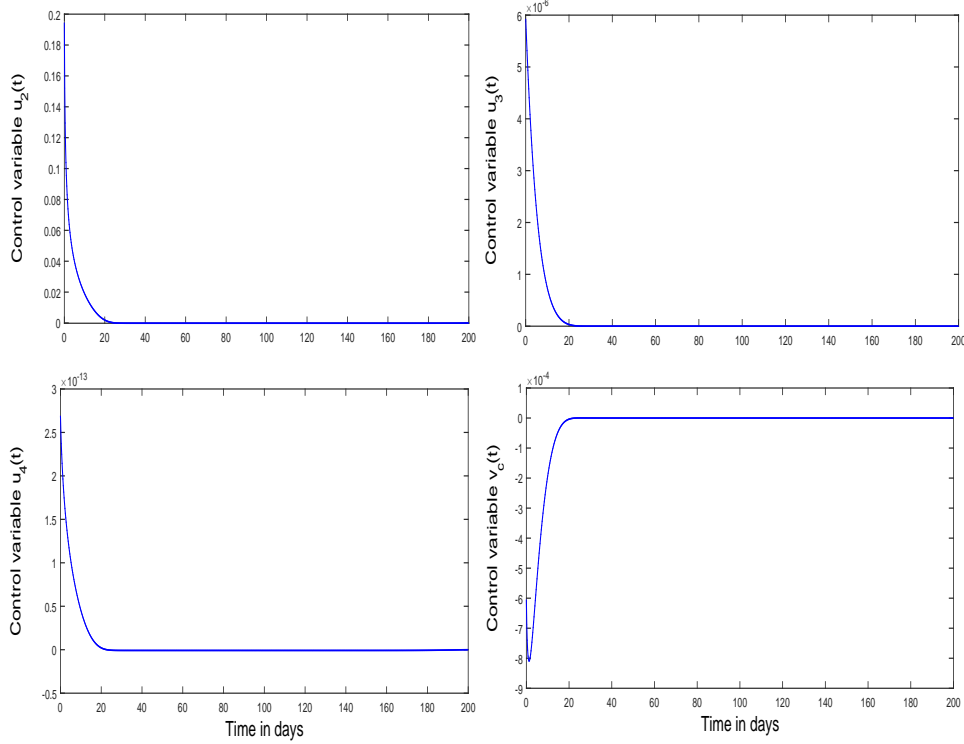
Figure 5.6: The figure shows the optimal controls as a function of time corresponding to the implementation of the single control $u_2(t)$, $u_3(t)$, $u_4(t)$ and $v_c(t)$.

four control parameters, namely $u_2(t)$, $u_3(t)$, $u_4(t)$ and $v_c(t)$. To minimize the tumor cells and maximize the immune cells, we define an objective functional $J(u^*)$. We prove the existence of control by applying the boundedness of super-solutions of the system. Additionally, we determine the characterization of the control by employing Pontryagin's Maximum Principle. We calculate the variation of the Lagrangian function to delineate the maximization of our optimal controls $u_2^*(t)$, $u_3^*(t)$, $u_4^*(t)$ and $v_c^*(t)$. Finally, we establish the uniqueness of the solution for the given optimal control system holds for a sufficient small time interval t_f.

We conducted a numerical study of our control system (5.3) under various conditions, including scenarios without a control strategy, with a single treatment strategy, with two treatment strategies, with three treatment strategies and with four treatment strategies. In Figure 5.1, we observed that a single control strategy proves more efficient than having no treatment strategy. Similarly, in Figure 5.2, the implementation of

two treatment strategies led to a rapid attainment of equilibrium in the tumor cell population compared to using a single treatment strategy or having no treatment strategy. Furthermore, the combination of three and four treatment strategies yielded remarkable results in minimizing the tumor cell burden, eventually leading to its complete elimination. This is demonstrated in Figure 5.3 and Figure 5.4, respectively. Simultaneously, the immune components, including CD8+T cells, macrophages and dendritic cells, reached their maximum levels, as shown in Figure 5.3 and Figure 5.4. In conclusion, our findings suggest that employing a combination of four different treatment strategies is highly effective in quickly reducing the tumor burden when compared to the other control strategies, including three, two or single control strategies, as well as having no treatment strategy. Additionally, this approach maximizes the presence of immune components, such as CD8+T cells, macrophages and dendritic cells, surpassing the results achieved by the alternative control strategies.

The innovative method we employ to understand and manage tumor-immune interactions is what sets our research apart. By systematically evaluating multiple treatment strategies and optimizing their effectiveness, we have provided a comprehensive framework for addressing a complex and pressing challenge in immunology and oncology. Our findings not only underscore the significance of having structured control strategies but also highlight the potential of combining multiple treatment strategies to achieve unprecedented results in tumor elimination. This novel perspective not only contributes to the theoretical foundations of the field but also holds great promise for practical applications in cancer treatment.

We expect that the outcomes from our mathematical model will prove valuable to future researchers engaged in the study of tumor-immune interaction system, particularly those applying optimal control theory. This study can offer significant assistance to researchers seeking to implement optimal control theory in various areas of research. Furthermore, we aspire to contribute to the improvement of cancer patient treatment by presenting a mathematical model that incorporates tumor cells and the immune system, potentially offering a more effective approach for the management of cancer patients.

Chapter 6

Conclusion and future directions

In this thesis, we studied tumor-immune competitive systems and incorporated the effect of discrete and distributed time delay, and the theory of optimal control. Discrete and distributed time delays has been added as the interaction in the cell populations is not an instantaneous process and followed by some time lag(s). We have also investigated the effect of drugs through optimal control theory. The summary of the results are given sequentially.

6.1 Conclusion

Our thesis focuses on developing a mathematical model to better understand the dynamics of the interaction between tumor cells and the immune system. Through the utilization of mathematical modeling techniques, the thesis investigates the interplay between tumor growth and the immune response. Considering various factors, including tumor growth and mortality rates, immune cell activity and death rates, the model provides a framework for simulating and analyzing the dynamic competition between the tumors and the immune system. The thesis highlights the significance of a comprehensive mathematical model in studying tumor-immune interactions, as it allows for a systematic exploration of various parameters and scenarios. By integrating experimental data and theoretical analysis, the model can be calibrated and validated, thus providing a realistic representation of the dynamics of tumor-immune interaction system. Overall, our thesis contributes to the field of cancer biology by providing a mathematical framework to understand the tumor-immune competitive system. It underscores

the importance of interdisciplinary approaches, combining mathematical modeling and experimental data to gain a deeper understanding of complex biological systems and improve cancer treatment strategies. Throughout the thesis, we have discussed the research contributions in a point-wise manner. The main contributions of the thesis can be summarized as follows:

- We have investigated the dynamics of the tumor-immune interaction system, considering the presence or absence of discrete time delay denoted as τ. The main objective is to understand the influence of time delay on the system dynamics, particularly in the presence of the cytokine IL-2. Initially, we examine the positivity and existence of the solutions for our mathematical model. We also conduct a local stability analysis of the biologically feasible steady states, both with and without the discrete time lag τ. This analysis provides insights into the stability of the system under different conditions. In addition to the local stability analysis, we investigate the local asymptotic stability of both the delayed and non delayed system. To analyze the Hopf bifurcation theorem, we establish that the transversality condition, utilizing the time delay τ as a threshold parameter, which plays a crucial role in our system. Furthermore, we calculate the length of the time lag required to maintain the stability of the bifurcating limit cycle of our delayed system. If we increase growth rate of tumor population α and decay rate of immune cell d_2, then the co-existing singular point E^* of our delayed model goes from stable to unstable. On the other hand, for increasing the value of deactivation rate of tumor population due to immune cell d_1 and constant source rate of immune system c_2, our mathematical model goes from unstable position to stable position at co-existing singular point E^*. Overall, our model contributes to the field by delineating the impact of discrete time delay on the proliferation of tumor cells in the presence of cytokine IL-2 of the dynamics of tumor-immune interaction system.

- In the study of tumor-immune interaction system, there is a growing recognition of the importance of incorporating continuously distributed time delays to capture natural phenomena accurately. By incorporating this type of delay, a simple mathematical model can effectively capture the dynamics of tumor-immune interplays and enhance our understanding of the effects of distributed time delay. It is a remarkable observation that the simple model captures the interplay

169

among tumor cells, tumor-specific CD8+T cells, Helper T cells, immuno-stimulatory cytokine IL-2 and the continuously distributed time delay. Preliminary results such that existence, nonnegativity and boundedness of solutions was established of the non delayed system. Moreover, the biologically feasible equilibrium points are investigated for both the delayed and non delayed system, providing valuable insights into the system's behavior under different conditions. A novel aspect of this study is the incorporation of a continuously distributed time delay through the introduction of a kernel function as an additional compartment. This compartment can be interpreted as the distributed immune activation delay, further enriching the model and capturing the complexity of biological scenarios. To validate the analytical findings of the dynamics of the system, a extensive numerical simulations have been performed. Numerically, we performed Hopf bifurcation analysis for two most important parameters λ_1 (recruitment rate of CD8+T cells) and μ_1 (CD8+T cells activation due to IL-2) for the delayed system at the singular point $E^{\perp}$. If we increase the value of λ_1, then tumor-presence singular point $E^{\perp}$ becomes unstable from stable situation (one periodic oscillation), unstable to stable and finally, delayed system goes into tumor-free ($E^{\dagger}$) stable situation around the tumor-presence steady state. Thus, the recruitment rate can prevent the tumor-presence oscillation as well as makes tumor-free in the system. But, for increasing value of μ_1, the tumor-presence singular point $E^{\perp}$ of the delayed system goes from stable to unstable steady state. For better visualization of the stability dynamics of the delayed system, we draw the stability region of the delayed system in $\mu_1 - \lambda_1$ parameter space.

- We have constructed a mathematical model for tumor-immune competitive system using a biologically inspired approach. The model is based on a coupled system of ordinary differential equations, incorporating various components such as tumor cells, CD8+T cells, macrophages, antigen presenting dendritic cells, regulatory T-cells (Tregs) and various cytokines including IL-10, TGF-β, IL-12 and IFN-γ. To better understand the tumor-immune interactive dynamics, we have simplified the model by employing quasi-steady-state approximations for the cytokine concentrations. Our immune system requires more time to give a suitable response after recognizing the tumor cells. Hence, it is crucial to incorporate time delays into our mathematical model to

170

accurately depict the interplay between the tumors and immune system. In order to gain deeper insights into this interaction, we introduce multiple time delays into our model. We have analytically defined the criteria for the existence, uniqueness, positivity and boundedness of solutions in the context of the delayed model. These mathematical results guarantee that solutions of the model are well-defined, nonnegative and remain within certain bounds for studying the tumor-immune competitive system. In order to conduct the fixed point analysis, we have found the biologically feasible equilibrium points. Furthermore, we deduce certain conditions to investigate the uniform persistence of the non delayed system. Our analytical findings encompass the local stability analysis for both the tumor-immune interaction model without delays and the model that incorporates delays. This study also examines the existence of Hopf bifurcation and determines the maximum length of discrete time delay to preserve the stability of period-1 limit cycle. Additionally, we investigate the direction of Hopf bifurcation and evaluate the stability of bifurcating periodic solutions of the delayed model. Our analysis encompasses the delayed system, considering two separate discrete time delays. We have shown that the introduction of delays does not markedly affect the tumor-immune interaction system; it may not invariably lead to regular or irregular periodic oscillations. This observation is based on the analysis of a realistic set of parameters value presented in this study. It is observed that despite the incorporation of multiple time delays, their influence on the dynamics of tumor-immune interaction system is limited. In contrast to the typical expectation of delays leading to the destabilization of the stable steady state, our results reveal that such destabilization does not occur in our proposed tumor-immune interaction system. Across biologically relevant parameter values, the influence of multiple time delays on model dynamics was found to be negligible. This observation implies that delays can be regarded as supplementary components with limited impact on the overall dynamics of the tumor-immune interaction system.

- We have utilized the theory of optimal control to investigate the dynamical behavior of a nonlinear tumor-immune interaction model. The focus is on exploring different treatment strategies to eliminate the tumor cell population. To achieve this, a mathematical model consisting of nine nonlinear coupled ordinary differential equations (ODEs) is constructed. To simplify the analysis, the proposed model is reduced to a system of four ODEs. These equations describe the dynamics of tumor cells, cytotoxic T-lymphocytes (CD8+T cells), macrophages,

171

dendritic cells and the concentration of chemotherapy. The reduction is achieved through the utilization of the quasi-steady-state approximations method. We conducted an analysis of a mathematical model that described the interaction between tumors and the immune system, specifically focusing on treatment strategies. Our primary objective was to propose an improved treatment approach for eliminating tumor cells by combining chemotherapeutic and immunotherapeutic drugs. To achieve this, we introduced four control strategies denoted as $u_2(t)$, $u_3(t)$, $u_4(t)$ and $v_c(t)$. In order to minimize the population of tumor cells and maximize the presence of immune cells, we formulate an objective functional denoted as $J(u^*)$. The existence of control is proven by utilizing the boundedness of super-solutions of the system. Moreover, the characterization of the optimal control is determined by applying Pontryagin's Maximum Principle. We take the variation of Lagrangian function for delineate the minimization of objective functional $J(u^*)$. Finally, we establish the uniqueness of the solution for the given optimal control system within a sufficiently small time interval t_f. We conducted numerical studies on our control system under various scenarios, including without control strategy, single treatment strategy, two treatment strategies, three treatment strategies and four treatment strategies. By exploring these different situations, we aimed to assess the effectiveness and impact of varying treatment strategies on the control system. Implementing control strategies, we observed a notable phenomenon that the tumor cell population reached an equilibrium point quickly, while the immune components were maximized. This finding suggests that the application of controls measure effectively controlled the tumor cell growth and enhanced the immune response. By effectively managing the dynamics of the system through control interventions, we were able to achieve a more favorable balance between tumor cells and immune components, contributing to better overall outcomes in terms of tumor control and immune system activation.

6.2   Future research

The scope of our future study will encompass, but is not limited to, the following topics:

- The use of stochasticity can help enhance our comprehension of the

intricate relationship between tumor cells and the immune system.

- Utilizing the Allee effect on a stochastic tumor model can provide valuable insights into comprehending the tumor extinction in a tumor-immune interaction system.

- Exploring the impact of impulsive therapy on enhancing treatment strategies in a tumor-immune interaction model.

- Undertaking a more comprehensive study of the tumor-immune interaction system by incorporating fractional order derivatives.

Publications from the content of the Thesis

Published:

1. **Mrinmoy Saradr**, Santosh Biswas, Subhas Khajanchi (2020): **The impact of distributed time delay in a tumor-immune interaction system**, Chaos, Solitons and Fractals,142, 110483, https://doi.org/10.1016/j.chaos.2020.110483.

2. **Mrinmoy Sardar**, Subhas Khajanchi, Santosh Biswas, Sayed F. Abdelwahab, Kottakkaran Sooppy Nisar (2021): **Exploring the dynamics of a tumor-immune interplay with time delay**, Alexandria Engineering Journal, 60(5), 4875–4888, https://doi.org/10.1016/j.aej.2021.03.041.

3. **Mrinmoy Sardar**, Subhas Khajanchi, Santosh Biswas: **A mathematical model for tumor-immune competitive systems with multiple time delays** (Revision submitted to Chaos, Solitons and Fractals journal).

Communicated:

1. **Mrinmoy Sardar**, Subhas Khajanchi, Santosh Biswas: **Modeling the dynamics of mixed immunotherapy and chemotherapy for the treatment of immunogenic tumor** (Communicated).

Bibliography

[1] Adam JA.: A survey of models for trumor immune system dynamics. Springer Science and Business Media. New York (1997).

[2] Baker CTH, Bocharov GA, Paul CAH, Rihan FA.: Modelling and analysis of time-lags in some basic patterns of cell proliferation. J. Math. Biol. 37 (1998) 341–371.

[3] Banerjee S.: Immunotherapy with interleukin-2: a study based on mathematical modelling. Int. J. Appl. Math. Comput. Sci. 18(3) (2008) 389–398.

[4] Banerjee S, Khajanchi S, Chaudhury S.: A mathematical model to elucidate brain tumor abrogration by immunotherapy with T11 target strunctture. PLoS ONE. 10(5) (2015) e0123611.

[5] Bunimovich-Mendrazitsky S, Gluckman JC, Chaskalovic J.: A mathematical model of combined bacillus calmette-guerin (BCG) and interleukin (IL)-2 immunotherapy of superficial bladder cancer. J. Theor. Biol. 277(1) (2011) 27–40.

[6] Brauer F, Castillo-Chavez C.: Mathematical models in population biology and epidemiology, 2nd ed. (New York: Springer) (2012).

[7] Burden T, Ernstberger J, Fister KR.: Optimal control applied to immunotherapy. Discrete Continuous Dyn. Syst. Ser. B. 4(1) (2004) 135–146.

[8] Cancer - World Health Organization. https://www.who.int.

[9] India Against Cancer. http://cancerindia.org.in.

[10] Caravagna G, Graudenzi A, d'Onofrio A.: A distributed delays in a hybrid model of tumor-immune system interplay. Math. Biosci. Eng. 10(1) (2013) 37–57.

[11] Carreno V, Zeuzem S, Hopf U, Marcellin P, Cooksley WG, Fevery J, Diago M, Reddy R, Peters M, Rittweger K, Rakhit A, Pardo M.: A phase I/II study of recombinant human interleukin-12 patients with chronic hepatitis B. J. Hepatology. 32(2) (2000) 317–324.

[12] Castiglione F, Piccoli B.: Optimal control in a model of dendritic cell transfection cancer immunotherapy. Bull. Math. Biol. 68 (2006) 255–274.

[13] Connor Y, Tekleab Y, Tekleab S, Nandakumar S, Bharat D, Sengupta S.: A mathematical model of tumor-endothelial interactions in a 3D co-culture. Sci. Rep. 9 (2019) 8429.

[14] Coventry BJ, Lee PL, Gibbs D, Hart DN.: Dendritic cell density and activation status in human breast cancer: CD1a, CMRF-44, CMRF-56 and CD-83 expression. Br. J. Cancer. 86(4) (2002) 546–551.

[15] Curti BD, Ochoa AC, Urba WJ, Alvord WG, Kopp WC, Powers G, Hawk C, Creekmore SP, Gause BL, Janik JE, Holmlund JT, Kremers P, Fenton RG, Miller L, Sznol M, Smith JW, Sharfman WH, Longo DL.: Influence of interleukin-2 regimens on circulating populations of lymphocytes after adoptive transfer of anti–CD3–stimulated T cells: Results from a phase i trial in cancer patients. J. Immunotherapy. 19(4) (1996) 296–308.

[16] de Pillis LG, Radunskaya AE.: A mathematical model of immune response to tumor invasion. Computational Fluid and Solid Mechanics. (2003) 1661–1668.

[17] de Pillis LG, Radunskaya AE, Wiseman CL.: A valiadated mathematical model of cell-mediated immune response to tumor growth. Cancer. Res. 65(17) (2005) 7950-7958 .

[18] de Pillis LG, Gu W, Radunskaya AE.: Mixed immunotherapy and chemotherapy of tumors: modeling, applications and biological interpretations. J. Theor. Biol. 238 (2006) 841–862.

[19] de Pillis LG, Gu W, Fister KR, Head T, Maples K, Murugan A, Neal T, Yoshida K.: Chemotherapy for tumors: An analysis of the dynamics and a study of quadratic and linear optimal controls. Math. Biosci. 209 (2007) 292–315.

[20] de Pillis LG, Fister KR, Gu W, Head T, Maples K, Neal T, Murugan A, Kozai K.: Optimal control of mixed immunotherapy and chemotherapy of tumors. J. Biol. Syst. 16(1) (2008) 51–80.

[21] Derin D, Soydinc HO, Guney N, Tas F, Camlica H, Duranyildiz D, Yasasever V, Topuz E.: Serum IL-8 and IL-12 levels in breast cancer. Med. Oncol. 24(2) (2007) 163–168.

[22] Diefenbach A, Jensen E, Jamieson A, Raulet D.: Rae1 and H60 ligands of the NKG2D receptor stimulate tumor immunity. Nature. 413(6852) (2001) 165–171.

[23] d'Onofrio A.: A general framework for modeling tumor-immune system competition and immunotherapy: Mathematical analysis and biomedical inferences. Physica D. 208 (2005) 220–235.

[24] Dunn GP, Old LJ, Schreiber RD.: The three Es of cancer immunoediting. Annu. Rev. Immunol. 22 (2004) 329–360.

[25] Eftimie R, Bramson JL, Earn DJD.: Interactions between the immune system and cancer: a brief review of non-spatial mathematical models. Bull. Math. Biol. 73 (2011) 2–32.

[26] Engelhart M, Lebiedz D, Sager S.: Optimal control for selected cancer chemotherapy ODE models: A view on the potential of optimal schedules and choice of objective function. Math. Biosci. 229 (2011) 123–134.

[27] Eskdale J, Kube D, Tesch H, Gallagher G.: Mapping of the human IL-10 gene and further characterization of the 5'flanking sequence. Immunogenetics. 46(2) (1997) 120–128.

[28] Fister KR, Panetta JC.: Optimal control applied to competing chemotheraputic cell-kill strategies. SIAM J. Appl. Math. 63(6) (2003) 1954–1971.

[29] Fister KR, Donnelly JH.: Immunotherapy: an optimal control theory approach. Math. Biosc. Engg. 2(3) (2005) 499–510.

[30] Fleming WH, Rishel RW.: Deterministic and stochastic optimal control. Springer-Verlag. New York (1975).

[31] Freedman HI, Rao VSH.: The trade-offbetween mutual interference and time lag in predator-prey systems. Bull. Math. Biol. 45(6) (1983) 991–1004.

[32] Freedman HI, Erbe L, Rao VSH.: Three species food chain models with mutual interference and time delays. Math. Biosci. 80(1) (1986) 57–80.

[33] Friedman A, Hao W.: The role of exosomes in pancreatic cancer microenvironment. Bull. Math. Biol. 80 (2018) 1111–1133.

[34] Galach M.: Dynamics of the tumor-immune system competition-the effect of time delay. Int. J. Appl. Math. Comput. Sci. 13 (2003) 395–406.

[35] Ghosh D, Khajanchi S, Mangiarotti S, Denis F, Dana SK, Letellier C.: How tumor growth can be influenced by delayed interactions between cancer cells and the microenvironment? BioSystems. 158 (2017) 17–30.

[36] Hara I, Hotta H, Sato N, Eto H, Arakawa S, Kamidono S.: Rejection of mouse renal cell carcinoma elicited by local secretion of interleukin-2. Jap. J. Cancer Res. 87(7) (1996) 724–729.

[37] Hassard BD, Kazarinoff ND, Wan YH.: Theory and application of Hopf bifurcation. Cambridge University Press, Cambridge (1981).

[38] Holt PG, Haining S, Nelson DJ, Sedgwick JD.: Origin and steady-state turnover of class II MHC-bearing dendritic cells in the epithelium of the conducting airways. J. Immunol. 153(1) (1994) 256–61.

[39] Huhn RD, Radwanski E, Gallo J, Affrime MB, Sabo R, Gonyo G, Monge A, Cutler DL.: Pharmacodynamics of subcutaneous recombinant human interleukin-10 in healthy volunteers. Clin. Pharmacol. Ther. 62 (1997) 171–180.

[40] Iannelli M, Pugliese A.: An introduction to mathematical population dynamics. Springer. 79(2014) 39-63.

[41] Kaempfer R, Gerez L, Farbstein H, Madar L, Hirschman O, Nussinovich R, Shapiro A.: Prediction of response to treatment in superficial bladder carcinoma through pattern of interleukin-2 gene expression. J. Clin. Oncol. 14(6) (1996) 1778–1786.

[42] Kamke E.: Zur theorie der systeme gewohnlicher differentialgleichungen II. Acta Math. 58 (1932) 57–85.

[43] Khajanchi S, Banerjee S.: Stability and bifurcation analysis of delay induced tumor immune interaction model. Appl. Math. Comput. 248 (2014) 652–71.

[44] Khajanchi S, Ghosh D.: The combined effects of optimal control in cancer remission. Appl. Math. Comp. 271 (2015) 375–388.

[45] Khajanchi S.: Bifurcations and oscillatory dynamics in a tumor immune interaction model. BIOMAT 2015: International Symposium on Mathematical and Computational Biology. (2016) 241-259.

[46] Khajanchi S, Banerjee S.: Quantifying the role of immunotherapeutic drug T11 target structure in progression of malignant gliomas: mathematical modeling and dynamical perspective. Math. Biosci. 289 (2017) 69–77.

[47] Khajanchi S.: Uniform persistence and global stability for a brain tumor and immune system interaction. Biophys. Rev. Lett. 12(4) (2017) 187–208.

[48] Khajanchi S.: Modeling the dynamics of stage-structure predator-prey system with Monod-Haldane type response function, Appl. Math. Comput. 302 (2017) 122–143.

[49] Khajanchi S, Perc M, Ghosh D.: The influence of time delay in a chaotic cancer model. Chaos. 28(10) (2018) 103101.

[50] Khajanchi S, Banerjee S.: Influence of multiple delays in brain tumor and immune system interaction with T11 target structure as a potent stimulator. Math. Biosci. 302 (2018) 116–130.

[51] Khajanchi S.: Modeling the dynamics of glioma-immune surveillance. Chaos Soliton Fract. 114 (2018) 110–118.

[52] Khajanchi S, Banrjee S.: A strategy of optimal efficacy of T11 target structure in the treatment of brain tumor. J. Biol. Syst. 27(2) (2019) 225–255.

[53] Khajanchi S, Nieto JJ.: Mathematical modeling of tumor-immune competitive system, considering the role of time delay. Appl. Math. Comput. 340 (2019) 180–205.

[54] Khajanchi S.: Stability analysis of a mathematical model for glioma-immune interaction under optimal therapy. Int. J. Nonlinear Sci. Numer. Simul. 20(3-4) (2019) 269–285.

[55] Khajanchi S.: Chaotic dynamics of a delayed tumorimmune interaction model. Int. J. Biomath. 13(2) (2020) 2050009.

[56] Khajanchi S, Nieto JJ.: Spatiotemporal dynamics of a glioma immune interaction model. Sci. Rep. 11 (2021) 22385.

[57] Khajanchi S.: The impact of immunotherapy on a glioma immune interaction model. Chaos Soliton Fract. 152 (2021) 111346.

[58] Khajanchi S, Sardar M, Nieto JJ.: Application of non-singular kernel in a tumor model with strong Allee effect. Differ. Equ. Dyn. Syst. (2022) https://doi.org/10.1007/s12591-022-00622-x.

[59] Khajanchi S, Mondal J, Tiwari PK. Optimal treatment strategies uding dendritic cell vaccination for a tumor model with parameter identifiability. J. Biol. Syst. (2022) 1–30 https://doi.org/10.1142/S0218339023500171.

[60] Kim JJ, Nottingham LK, Sin JI, Tsai A, Morrison L, Oh J, Dang K, Hu Y, Kazahaya K, Bennett M, Dentchev T, Wilson DM, Chalian AA, Boyer JD, Agadjanyan MG, Weiner DB.: CD8 positive T cells influence antigen-specific immune responses through the expression of chemokines. J Clin Invest. 102 (1998) 1112–1124.

[61] Kirschner D, Panetta JC.: Modeling immunotherapy of the tumor-immune interaction. J. Math. Biol. 37 (1998) 235-252 .

[62] Koebel CM, Vermi W, Swann JB, Zerafa N, Rodig SJ, Old LJ, Smyth MJ, Schreiber RD.: Adaptive immunity maintains occult cancer in an equilibrium state. Nature. 450(7171) (2007) 903–7.

[63] Kronik N, Kogan Y, Vainstein V, Agur Z.: Improving alloreactive CTL immunotherapy for malignant gliomas using a simulation model of their interactive dynamics. Cancer Immunol. Immunother. 57(3) (2008) 425–439.

[64] Kuang Y.: Delay differential equations with applications in population dynamics. Press Inc (1993).

[65] Kuznestov V, Makalkin I, Taylor M, Perelson A.: Non-linear dynamics of immunogenic tumors: parameter estimation and global bifurcation analysis. Bull. Math. Biol. 56(2) (1994) 295–321.

[66] Lai X, Friedman A.: Combination therapy of cancer with cancer vaccine and immune checkpoint inhibitors: a mathematical model. PLOS ONE. 12(5) (2017) e0178479.

[67] Louzoun Y, Xue C, Lesinski GB, Friedman A.: A mathematical model for pancreatic growth and treatments. J. Theor. Biol. 351 (2014) 74–82.

[68] Mahasa KJ, Ouifki R, Eladdadi A, de Pillis LG.: Mathematical model of tumor-immune surveilance. J. Theor. Biol. (2016) 312–330.

[69] Moghtadaei M, Golpayegani MRH, Malekzadeh R.: Periodic and chaotic dynamics in a map-based model of tumor-immune interaction. J. Theor. Biol. 334 (2013) 130–140.

[70] Moore H, Li NK.: A mathematical model for myelogenous leukemia (CML) and T cell interaction. J. Theor. Biol. 227(4) (2004) 513–523.

[71] Murray JD.: Mathematical Biology i. an introduction, 3rd ed., New York: Springer-Verlag (2002).

[72] Nyquist H.: Regeneration theory. Bell. Syst. Tech. J. 11(1) (1932) 126–147.

[73] Osojnik A, Gaffney EA, Davies M, Yates JWT, Byrne HM.: Identifying and characterising the impact of excitability in a mathematical model of tumour-immune interactions. J. Theor. Biol. 501 (2020) 110250.

[74] Pardoll D.: Does the immune system see tumors as foreign or self ? Annu. Rev. Immunol. 21 (2003) 807-39.

[75] Perry MC.: The chemotherapy source book, 3rd ed., Lippincott Williams & Wilkins (2001).

[76] Peterson PK, Chao CC, Hu S, Thielen K, Shaskan E.: Glioblastoma, transforming growth factor-beta, and candida meningitis: a potential link. Am. J. Med. 92 (1992) 262–264.

[77] Piotrowska MJ, Bodnar M, Poleszczuk J, Forys U.: Mathematical modelling of immune reaction against gliomas: Sensitivity analysis and influence of delays. Nonlinear Analysis: Real World Applications. 14 (2013) 1601–1620.

[78] Piotrowska MJ, Bodnar M.: Influence of distributed delays on the dynamics of a generalized immune system cancerous cells interactions model. Commun. Nonlinear. Sci. 54 (2018) 389-415.

[79] Pontryagin LS, Boltyanskii VG, Gamkrelidze RV, Mishchenko EF.: The mathematical theory of optimal processes. Wiley, New York (1962).

[80] Qomlaqi M, Bahrami F, Ajami M, Hajati J.: An extended mathematical model of tumor growth and its interaction with the immune system, to be used for developing an optimized immunotherapy treatment protocol. Math. Biosci. 292 (2017) 1–9.

[81] Radunskaya A, Hook S.: Modelling the kinetics of the immune response. Biomedicine. Springer-verlag. 267–282 (2012).

[82] Rollins BJ, O'Connell TM, Bennett G, Burton LE, Stiles CD, Rheinwald JG.: Environment-dependent growth inhibition of human epidermal keratinocytes by recombinant human transforming growth factor-Beta. J. Cell. Physiol. 139 (1989) 455–462.

[83] Ruan SG, Wei JJ.: On the zeros of transcendental functions with applications to stability of delay differential equations with two delays. Dyn. Contin. Discrete Impuls. Syst. Ser. A Math. Anal. 10 (2003) 863–874.

[84] Schreiber RD, Old LJ, Smyth MJ.: Cancer immunoediting: Integrating immunitys roles in cancer suppression and promotion. Science. 331 (2011) 1565-70.

[85] Schumacher TN, Schreiber RD.: Neoantigens in cancer immunotherapy. Science. 348 (2015) 69–74.

[86] Sherratt JA, Bianchin A, Painter KJ.: A mathematical model for lymphangiogenesis in normal and diabetic wounds. J. Theor. Biol. 383 (2014) 61–86.

[87] Siewe N, Yakubu A, Satoskar AR, Friedman A.: Immune response to infection by leishmania : a mathematical model. Math. Biosci. 276 (2016) 28–43.

[88] Sardar M, Biswas S, Khajanchi S.: The impact of distributed time delay in a tumor-immune interaction system. Chaos Soliton Fract. 142 (2021) 110483.

[89] Sardar M, Khajanchi S, Biswas S, Abdelwahab SF, Nisar KS.: Exploring the dynamics of a tumor-immune interplay with time delay. Alex. Eng. J. 60 (2021) 4875–4888.

[90] Sarkar RR, Banerjee S.: Cancer self remission and tumor stability-a stochastic approach. Math. Bio. 196 (2005) 65–81.

[91] Sarkar RR, Banerjee S.: A time delay model for control of malignant tumor growth, National conference on nonlinear sytems and dynamics. Riasm, University of Madras, Chennai. 1 (2006) 1–5.

[92] Segel LA, Slemrod M.: The quasi-steady-state assumption: a case study in peturbation. SIAM Rev. 31 (1989) 446–477.

[93] Swan GW.: Role of optimal control theory in cancer chemotherapy. Math. Biosci. 101(2) (1990) 237–284.

[94] Tang Q.: Pharmacokinetics of therapeutic Tregs. Am. J. Transplant. 14(12) (2014) 2679–2680.

[95] Taylor GP, Hall SE, Navarrete S, Michie CA, Davis R, Witkover AD, Rossor M, Nowak MA, Rudge P, Matutes E, Bangham CR, Weber JN.: Effect of lamivudine on human T-cell leukemia virus type 1(HTLV-1)bDNA copy number, T-cell phenotype, and anti-tax cytotoxic T-cell frequency in patients with HTLV-1-associated myelopathy. J. Virol. 73(12) (1999) 10289–10295.

[96] Tessi MR, Kareh AE, Goriely A.: A mathematical model of tumor-immune interactions. J. Theor. Biol. 294 (2012) 56–73.

[97] Thomas D, Massague J.: TGF-β directly targets cytotoxic T-cell functions during tumor evasion of immune surveillance. Cancer Cell. 8 (2005) 369–380.

[98] Thomlinson RH, Gray LJ.: The histological structure of some human lung cancers and the possible implications for radiotherapy. Br. J. Cancer. 9 (1995) 539–549.

[99] Thomlinson RH.: Measurement and management of carcinoma of the breast. Clin. Radiol. 33(5) (1982) 481–493.

[100] Toossi Z, Hirsch CS, Hamilton BD, Knuth CK, Friedlander MA, Rich EA.: Decreased production of TGF-beta 1 by human alveolar macrophages compared with blood monocytes. J. Immunol. 156(9) (1996) 3461–3468.

[101] Tsur N, Kogan Y, Rehm M, Agur Z.: Response of patients with melanoma to immune checkpoint blockade - insights gleaned from analysis of a new mathematical mechanistic model. J. Theor. Biol. 485 (2020) 110033.

[102] Turner PK, Houghton JA, Petak I, Tillman DM, Douglas L, Schwartzberg L, Billups CA, Panetta JC, Stewart CF.: Interferon-gamma pharmacokinetics and pharmacodynamics in patients with colorectal cancer. Cancer. Chemother. Pharmacol. 53 (2004) 253–260.

[103] Villasana M, Radunskaya AE.: A delay differential equation model for tumor growth. J. Math. Biol. 47 (2003) 270–294.

[104] Visser KE, Eichten A, Coussens LM.: Paradoxical roles of the immune system during cancer development. Nat. Rev. Cancer. 6(1) (2006) 24-37.

[105] Vivier E, Raulet DH, Moretta A, Caligiuri MA, Zitvogel L, Lanier LL, Yokoyama WM, Ugolini S.: Innate or adaptive immunity ? The example of natural killer cells. Science. 331 (2011) 44-49.

[106] World Health Organization (WHO) report https://www.who.int/health-topics/cancer#tab=tab_1.

[107] Wacker HH, Radzun RJ, Parwaresch MR.: Kinetics of Kupffer cells as shown by parabiosis and combined autoradiographic/immunohistochemical analysis. Virchows. Arch. B. Cell. Pathol. Incl. Mol. Pathol. 51(2) (1986) 71–78.

[108] Wilson S, Levy D.: A mathematical model of the enhancement of tumor vaccine efficacy by immunotherapy. Bull Math Biol. 74 (2012) 1485–1500.

[109] Yang X, Chen L, Chen J.: Permanence and positive periodic solution for the single-species nonautonomous delay diffusive model. Comput. Math. Appl. 32(4) (1996) 109–116.

[110] Yu M, Dong Y, Takeuchi Y.: Dual role of delay effects in a tumour-immune system. J. Biol. Dyn. 11(2) (2016) 1–14.

[111] Yu M, Huang G, Dong Y, Takeuchi Y.: Complicated dynamics of tumor-immune system interaction model with distributed time delay. Discrete Cont. Dyn-S, 25(7) (2020) 2391–2406.